Accelerated carbonation of waste incinerator bottom ash for trace metal immobilisation

Inaugural-Dissertation

zur

Erlangung des Doktorgrades

der Mathematisch-Naturwissenschaftlichen Fakultät

der Universität zu Köln

vorgelegt von

Felix Benjamin Brück

aus Lich

Köln 2019

Berichterstatter:	Prof. Dr. Tim Mansfeldt
	Prof. Dr. Harald Weigand
	Prof. Dr. Christina Bogner
Tag der mündlichen Prüfung:	24.07.2019

Summary

Bottom ash (BA) constitutes the dominant solid residue of municipal solid waste incineration and millions of tonnes are annually produced, worldwide. Fresh BA contains highly reactive constituents which are metastable under environmental conditions. Their transformation has been referred to as the ageing of BA. It has long since been recognized that ageing reduces the reactivity of BA and therewith the leachability of critical trace metals. Carbonation is a key process in the aging and is initiated by the access of CO_2. Passive ageing is commonly applied in many European countries prior to geotechnical utilization or landfilling of BA. However, it requires a large quantity of space, time, and lacks any process control. Carbonation of BA may be accelerated by contacting the material with CO_2-rich exhaust gas. Although this has long since been recognized, practical applications have remained beyond reach since reactor systems did not allow for the necessary throughput. Recent studies demonstrated that the material dynamics in rotating drum reactors favour the accelerated carbonation and that rotating drums may be suited for a process implementation at the industrial scale. Yet, knowledge regarding optimum drum operation for accelerated carbonation of BA is still scarce.

This thesis aimed at delineating both the technical set-up and the operation parameters suited for process integration of accelerated carbonation at incinerator sites. This included the development of a screening technique to evaluate the progress of carbonation as well as a stepwise transfer of the reactor system from a jar test into a continuously fed rotating drum reactor system. Effects of rotation speed and reactor fill level on the solid's motion were cinematographically analysed. Carbonation performance was assessed by thermogravimetric analyses and the leaching behaviour of the treated BA. The BA used in this study was sampled from a grate-type refuse derived fuel incinerator located in central Germany. Leachate values and particularly the high leachate concentrations of Pb characterized fresh BA as a hazardous waste.

Laboratory results demonstrated the serviceability and reproducibility of the developed method for the monitoring and quantification of the CO_2 uptake by BA in both static and dynamic reactor systems. The method is based on following the pressure drop in the gas phase induced by the CO_2 uptake of BA close to atmospheric pressure conditions.

The monitoring method was next applied to evaluate carbonation kinetics and the influence of fundamental parameters (CO_2 concentration, fill level, BA moisture) on accelerated carbonation of BA in a rotating drum batch reactor. Both the CO_2 uptake rate and the final level of carbonation increased as the CO_2 concentration was raised from 15 to 75 vol.-%. The optimum moisture content for the tested BA was found to be 21 wt.-%, which is roughly in the range of the typical moisture content of BA after temporary storage in a roofed pile. The fill level was not a limiting factor for BA carbonation within the tested range (7 - 45 vol.-%). The latter could be explained by findings obtained by the study of the solids' motion. The bed behaviour of BA strongly differed from that of standard materials and was more affected by fill level than by rotation speed. With increasing fill level, the bed motion changed from slipping to slumping thereby favouring the mixing process. Complementary logging of relative humidity and temperature showed constant moisture conditions and self-heating, induced by the exothermal carbonation reaction. A close relationship between CO_2 uptake and reactor temperature was confirmed by benchmarking a heat balance model against the carbonation enthalpy. Excellent agreement demonstrated that temperature monitoring may be an alternative way of evaluating the progress of carbonation.

As a next step carbonation of BA was studied with a continuous feed of the reactant gas and the effects of specific CO_2 supply, mixing tools, and reactor loadings on process performance were assessed. The reaction could be accelerated to around 100 minutes and was further enhanced by the use of mixing tools. Of the configurations tested, a perforated mixing cage performed best, even at fill levels of up to 50 %. This set-up was also least prone to the formation of BA incrustations.

Finally, a rotating drum reactor continuously fed with both, the reactant gas (60 L/min; 10 vol.-% CO_2) and the BA (9 - 18 kg/h), was developed and tested at varied BA residence times. Projected and experimental residence times were compared by mass balancing and by analysing the breakthrough curves of a tracer. Good agreement indicated adequate control of reactor loading and the BA feed rate. In one test, the gas was heated and humidified. Leachates and solid phase properties of the treated BA served to evaluate the carbonation performance. Overall, carbonation improved the leachate quality of BA as the leachate concentrations of critical trace metals (Pb, Zn, Cu) decreased by at least one order of magnitude. A residence time of 80 min was sufficient to reduce the BA leachability such as to characterize the carbonated material as a non-hazardous waste. This would allow for a disposal on a class 1 landfill or alternatively for a geotechnical reuse in accordance with the draft of the German Ordinance on Secondary Construction Materials. Other than the amphoteric metals, oxyanions like Cr, Mo and V became more mobile upon carbonation. This side effect did not outweigh the benefits since oxyanion concentrations remained below the specific limit values. Therefore, the accelerated carbonation of BA provides a material that is both suited for the cost-effective disposal on a lower landfill class and for geotechnical applications. In view of relatively short residence times and stable process performance, the rotating drum reactor seems promising for a full-scale implementation of BA carbonation.

Zusammenfassung

Rostaschen bilden den bedeutendsten festen Rückstand aus der Verbrennung von Restmüll und Ersatzbrennstoffen. Etablierte Entsorgungswege sind einerseits die Deponierung, andererseits die Verwertung als Ersatzbaustoff. Bedingt durch deren hohe Reaktivität durchlaufen Rostaschen während der Alterung eine Vielzahl von mineralogischen Phasenumwandlungsreaktionen. Besonders bedeutend ist die Carbonatisierung. Hierbei reagiert CO_2 mit alkalischen Mineralphasen, wodurch die Auslaugbarkeit vieler kritischer Spurenmetalle deutlich verringert wird. Gängige Praxis ist in vielen europäischen Ländern daher eine mindestens dreimonatige Lagerung, bei der die Alterung unter Umgebungsbedingungen in einem Haufwerk stattfindet. Problematisch hierbei ist neben dem hohen Zeit- und Platzbedarf die schlechte Kontrollierbarkeit des Prozesses. Bei der beschleunigten Carbonatisierung werden die unter natürlichen Bedingungen ablaufenden Alterungsprozesse durch technische Maßnahmen gezielt verstärkt. Vorteile sind der Wegfall einer Lagerhaltung und die Verkürzung des Zeitraumes zwischen Ascheanfall und -entsorgung. Trotz langjähriger Forschung auf diesem Gebiet wurden bisher nur wenige Ansätze zur beschleunigten Carbonatisierung unter vollmaßstäblichen Bedingungen getestet. Jüngere Veröffentlichungen weisen darauf hin, dass eine Umsetzung der Carbonatisierung in rotierenden Trommelreaktoren vielversprechend sein könnte; eine optimale Prozessauslegung fehlt jedoch bislang.

Das Ziel dieser Arbeit war es einen Verfahrensansatz für die beschleunigte Carbonatisierung von Rostasche zu entwickeln, welcher eine Prozessintegration in ein reales Aschemanagement erlaubt. Hierzu sollte zum einen die notwendige Reaktortechnik entwickelt sowie Reaktions- und Prozessbedingungen erprobt werden. Dies beinhaltete die Entwicklung eines Messsystems zur Erfassung der CO_2-Aufnahme sowie die schrittweise Reaktorentwicklung vom einfachen Glasgefäß bis hin zu einem kontinuierlich betriebenen Drehrohreaktor. Der Einfluss der Drehgeschwindigkeit und des Reaktorfüllgrades auf die Materialbewegung wurde mittels Videoanalyse untersucht. Die Beurteilung der Carbonatisierungsleistung erfolgte thermogravimetrisch sowie anhand des Auslaugverhaltes der behandelten Rostasche.

Die experimentellen Ergebnisse belegten die Eignung und Reproduzierbarkeit der entwickelten Methode zur Quantifizierung der CO_2-Aufnahme der Rostasche sowohl unter statischen als auch unter dynamischen Reaktionsbedingungen. Das Messsystem basiert auf einer Messung des systeminternen Druckabfalls, welcher aus der CO_2-Aufnahme der Rostasche resultiert. Die Methode wurde weiterhin verwendet, um die Carbonatisierungskinetik und den Einfluss wesentlicher Betriebsparameter auf die beschleunigte Carbonatisierung von Rostasche in einem Drehrohreaktor zu untersuchen. Die CO_2-Aufnahmerate sowie die innerhalb von 2 h erzielte Gesamtaufnahme erhöhte sich durch Anhebung der CO_2-Konzentration von 15 Vol.-% auf 75 Vol.-%. Die optimale Feuchte des Feststoffs lag bei ca. 21 Mass.-%, was in etwa dem typischen Wassergehalt einer zwischengelagerten Rostasche entspricht. Der Reaktorfüllgrad war innerhalb des geprüften Wertebereichs (7 - 45 Vol.-%) kein limitierender Faktor. Letzteres konnte anhand des Bewegungsverhaltens der Rostasche im Drehrohr erklärt werden. Mit zunehmendem Füllgrad änderte sich das Bewegungsmuster von ‚slipping' zu ‚slumping', woraus eine erhöhte Mischleistung resultierte. Während der Carbonatisierung stellte sich im Reaktor eine konstante Gasfeuchte ein und aufgrund der Exothermie der Reaktion kam es zu einer Selbsterwärmung. Im Bilanzmodell zeigte sich entsprechend ein enger Zusammenhang zwischen der beobachteten Wärmefreisetzung und der aufgenommenen CO_2 Menge. Die Reaktortemperatur wurde daher als ein möglicher Parameter zum Prozessmonitoring vorgeschlagen.

Im Anschluss an die Versuche zur Carbonatisierung im Batch-Modus wurde eine Durchflussbegasung realisiert und der Einfluss der spezifischen CO_2-Beschickung, von Mischwerkzeugen und des Reaktorfüllgrads auf die Carbonatisierungsleistung untersucht. Die nötige Reaktionszeit lag bei 100 Minuten und die Reaktion konnte durch den Einsatz von Mischwerkzeugen weiter forciert werden. Von den getesteten Mischwerkzeugen erwies sich ein perforierter Mischkorb als besonders günstig, da dieser einerseits die Durchmischung verbesserte, andererseits auch die geringste Anfälligkeit gegenüber Verkrustungsbildung zeigte. So konnte selbst bei hohen Füllständen (50 Vol.-%) noch eine gute Carbonatisierung erzielt werden.

Als letzter Schritt wurde ein Drehrohrreaktor zur kontinuierlichen Beaufschlagung sowohl mit Reaktionsgas (3600 L/h; 10 Vol.-% CO_2) als auch mit Rostasche (9 - 18 kg/h) konstruiert und getestet. Die vorgegebenen und experimentell ermittelten Verweilzeiten wurden basierend auf einer Massenbilanz und der Analyse des Tracerdurchbruchverhaltens verglichen und zeigten eine sehr gute Übereinstimmung. Entsprechend der Auslauguntersuchungen war eine Verweilzeit von 80 Min ausreichend, um eine deutliche Immobilisierung kritischer Spurenmetalle (Pb, Zn, Cu) zu erzielen. Insgesamt verbesserte sich das Auslaugverhalten soweit, dass die Zuordnungswerte der Deponieklasse I erfüllt wurden. Im Unterschied zu den genannten Metallen war für die Oxoanionenbildner (Cr, Mo, V) eine geringfügige Konzentrationszunahme festzustellen. Diese stellte jedoch weder eine Einschränkung für die kostengünstigere Deponierung noch die ersatzbaustoffliche Verwertung der carbonatisierten Rostasche dar. Die hier gezeigten Ergebnisse zeigen erstmalig, dass und wie die Carbonatisierung von Rostasche in einem dynamischen Reaktor bei kontinuierlicher Feststoff- und Reaktionsgasaufgabe gelingt. Damit ist eine wesentliche Voraussetzung für die Integration in das Aschemanagement von Müllverbrennungsanlagen und Aufbereitungsanlagen gegeben.

Acknowledgements

Completing a thesis is truly a long journey and would not be possible if it is an individual task. I hereby thank all of those who supported me along the way to complete this thesis.

At first, I want to express my gratitude to my advisor Prof. Dr. Tim Mansfeldt for giving me the opportunity to write my thesis at the University of Cologne (UC). He provided me with valuable advice and freedom to pursue my own ideas.

My special thanks go to Prof. Dr. Harald Weigand, my mentor. His guidance (stop signs and signposts) gave me a good guideline through my thesis. I am honoured to have gained Harald's trust over all this time since I became his first assistant student at THM. Through all this time his commitment and enthusiasm deeply inspired me scientifically and personally.

I also thank Prof. Dr. Christina Bogner (UC) being the third supervisor of this thesis and Prof. Dr. Bülent Tezkan (UC) is thanked for acting as commission head.

The CarbonAsh-project and thereby my thesis was expedited by the engagement and spirit of a great team. The task of bringing a process from lab-scale to large-scale would not have been possible without the contribution of a lot of people (Tim Hoberg, Tobias Bauch, and many more). I would particularly like to express my heartfelt thanks to Jürgen Henkel. Without his technical support and his passion, many ideas could not be implemented. I am delighted to have such a colleague.

Furthermore, I would like to thank Kevin Schnabel for valuable discussions and fruitful collaboration, Anna Wirtz and Markus Marschner for assistance with analytical work at the THM laboratories, Dr. Christine Fröhlich for establishing thermoanalysis in our working group which provided valuable input to my thesis, and the Department FTN (THM) for the follow-up financing to finish my work.

Outside the THM I also received valuable help to complete my work. I like to give special appreciation to Karin Greef for vast ICP-MS measurements, the working group Soil Geography / Soil Science (UC) for their warm welcome and support with administrative issues, and to Dr. Kristian Ufer from the Bundesanstalt für Geowissenschaften und Rohstoffe (BGR, Hannover) for the XRD measurements.

Next, I would like to extend my thanks to Dr. Rüdiger Borchardt for proofreading the manuscripts and the pleasant diversion during our musical sessions.

Finally, I would like to express my sincere thanks to my parents, Doris and Klaus Brück, for supporting me in all situations, and to my wife Tince and my daughters Mora and Matilda for their patience and the joy they bring into my life.

Contents

Chapter 1 Introduction

1.1 Waste incineration and bottom ash generation

Human activities have always been accompanied by the production of solid waste. Concomitant with the establishment of larger settlements dump sites emerged and until now dumping or landfilling (as the technically controlled form of dumping) are the most common forms of waste management. In the past century, the amount of municipal solid waste (MSW) increased by a factor of ten due to the exponential growth of population, improved living standards and increasing urbanisation (Karak et al., 2012). Growing piles of rubbish along with limited land capacities for dumping posed an ever enhanced problem to the waste management of most municipalities. Moreover, increasing ecological awareness of the general public and growing environmental concerns forced waste management practice to change and brought up new treatment methods, e.g. bio-mechanical treatment, incineration and recycling. The recent past showed that waste production is coupled to the wealth of societies but may also reach a limit (‘peak waste’) at a distinct level of affluence (Hoornweg et al., 2015). Unto that point municipal solid waste (MSW) generation can be expected to increase with increasing living standards. It was estimated that the total solid waste generation will reach 27 billion tons per year by 2050 (Karak et al., 2012) and that the peak time might not be achieved within this century, unless more efforts are made to reduce population growth and material consumption rates (Hoornweg et al., 2013). Hence, the management of MSW represents a major economic and environmental issue throughout the world (Makarichi et al., 2018).

Current waste management practice substantially differs across the world. On the one hand dumping and controlled landfilling still predominates in developing countries and countries that are less affected by land scarcity (e.g. USA, Canada, Russia, and Australia). On the other hand, some countries (e.g. European countries) have strictly limited or even fully prohibited landfilling of untreated MSW (Karak et al., 2012; Cucchiella et al., 2017; Seifert and Vehlow, 2017). Although those countries already achieved high rates in separation and recycling the potentials are still not fully utilized due to the limited economic incentives (Zacho et al., 2018). Thus, a considerable quantity of MSW still has to be handled and in the last 20 years waste incineration, possibly in conjunction with energy recovery, has become one of the key components of integrated waste management strategies (Chandler et al., 1997; Makarichi et al., 2018). From the very beginning of waste incineration in the late 19th century the technology underwent an intensive development. Nowadays, MSW incineration is performed in waste-to-energy (WtE) plants with intensified energy recovery and air pollution control. The commonly applied technologies for MSW combustion are fluidized bed boilers and moving grate firing systems. The latter are used in the vast majority of incineration plants in Europe (Lombardi et al., 2015). As opposed to disposal incineration has significant benefits such as

- Immediate reduction of the volume and mass of MSW (70 - 90% by volume, about 70% by mass);
- Reduced transportation costs when building incinerators closer to the sources of MSW (municipalities, industry);
- Efficient energy recovery ($\eta_{electric}$ 0.2 – 0.3, $\eta_{thermal}$ 0.8);
- Control of emissions in view of legal limits (Karak et al., 2012; Allegrini et al., 2015; Dou et al., 2017).

In Germany, about 16 million tons of MSW are treated in 69 WtE plants (Seifert and Vehlow, 2017) and worldwide approximately 2,150 incinerations plants are in operation (Döing, 2017). Installation of incineration capacities is steadily increasing, especially in Asia (Döing, 2017; Makarichi et al., 2018). Asides incineration in WtE plants MSW is also used as a substitute fuel in thermal processes which are not primarily designed for waste treatment, e.g. cement kilns (Seifert and Vehlow, 2017). In some countries (e.g. Germany, Italy) there is an increasing trend towards improving the energy recovery by processing MSW to refuse derived fuel (RDF) prior to incineration in order to increase its homogeneity and calorific value (Rocca et al., 2012; Dou et al., 2017).

During incineration, the organic fraction of MSW is almost completely oxidized leaving inorganic compounds and air pollution control residues as unavoidable by-products. The dominant solid residue generated in MSW incinerators and WtE plants is bottom ash (BA) which amounts to between 15 and 30 % of the original input (Chimenos et al., 1999; Sabbas et al., 2003; Caprai et al., 2019). Annually, about 18 million tonnes of BA are produced in Europe (CEWEP, 2017) and much more worldwide (Liu et al., 2015). Thus, incineration residues, in particular BA, have become a significant mass flux to be handled by integrated waste management systems. As incineration expands roughly at the pace of increasing MSW generation rates, also the BA quantity will increase further. As outlined in the following sections, BA is suited for geotechnical reuse and resource recovery as long as its environmental properties are carefully addressed or properly engineered.

1.2 Characteristics of BA

Bottom ash is a heterogeneous mixture mainly composed of fine materials (e.g. ash in the strict sense), melt components, small quantities of metallic components, synthetic ceramics and stones as well as traces of unburned organic matter (Chimenos et al., 1999; Speiser et al., 2000; Piantone et al., 2004; Wei et al., 2011; Williams, 2013). Figure 1.1 shows the average composition of BA. The specific proportion of the above components may vary depending on the incineration technology, incineration temperature and input materials (Pfrang-Stotz and Schneider, 1995; Fujimori et al., 2004; Song et al., 2004; Rendek et al., 2007; Saqib and

Bäckström, 2015). Typically, BA exhibits a broad particle size distribution with diameters ranging from powder (<0.063 mm) to coarse aggregates (>25 mm) (Inkaew et al., 2016; Chimenos et al., 1999). When the powder (<2 wt.-% Huber et al., 1996) and oversized grain (>2 or 63 mm) is excluded, BA conforms to a well-graded sand to gravel (Bendz et al., 2007; Costa et al., 2007; Lin et al., 2012; Tang et al., 2015; Le et al., 2018). Therefore, BA could potentially substitute natural aggregates in constructions and geotechnical applications (Lam et al., 2010).

Part of BA heterogeneity is inherited from the waste (MSW and RDF) which itself is a heterogeneous fuel. The ash and melt components differ by morphology and particle size. The ash fraction comprises glass rubbings, inorganic and organic residues as well as soot and dust with a mean particle size between <0.002 mm and 2 mm (Brett et al., 2018). By contrast, melt components are porous, irregular shaped grains or aggregates with a particle size of > 2 mm comprised of a siliceous matrix (glass) with newly formed mineral phases as a consequence of high combustion temperatures (Bayuseno and Schmahl, 2010).

From the physical perspective, BA can be considered a porous lightweight aggregate with specific surface areas ranging from 3 to 46 m^2/g dry weight (Dou et al., 2017). Compared to natural aggregates, BA has a more angular geometry and higher surface roughness (Chandler et al., 1997).

Bottom ash is usually wet since the majority of incinerators employ a quenching step. Depending on ash characteristics and quenching procedures, the moisture contents of BA can vary considerably (Costa et al., 2007). This is reflected in the disparity of moisture levels reported in the literature (5 - 25 wt.-% Tang et al., 2015; 3 - 15 wt.-% Heuss-Aßbichler et al., 2010; 14 - 25 wt.-% Nørgaard et al., 2019). Also, the moisture is unevenly distributed across the particles size fractions. The highest moisture contents are found in the fine fraction (<0.1 mm, 40 wt.-%) and the lowest in the coarse (>6 mm, 4 wt.-%) (Arickx et al., 2006).

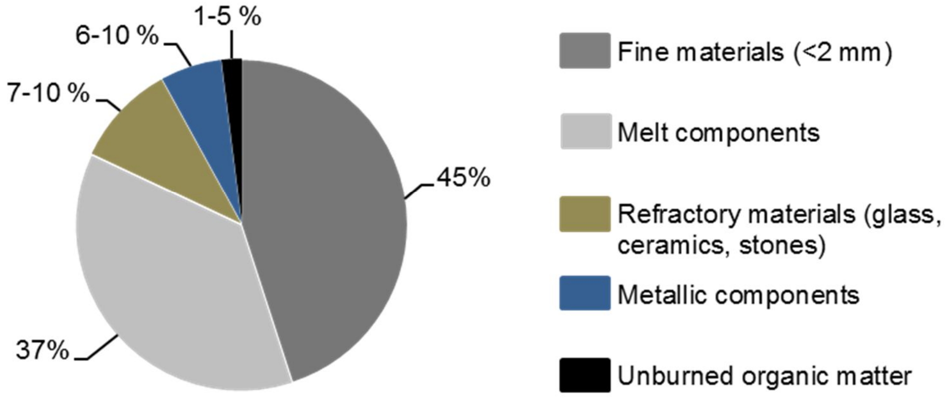

Figure 1.1. Average composition of bottom ash from municipal solid waste incineration according to (Knorr et al., 1999; Martens, 2011; Förstner, 2012).

Chemical properties

Due to their different volatility the individual elements present in the waste partition between the gas phase (ending up in air-pollution control residues) and the BA during the incineration process. Thus, relative to the fuel input they may be either depleted or enriched in the BA (Chandler et al., 1997; Williams, 2013). Depletion is typically observed for Cl, Cd, and Hg while Cu, Zn and S are often enriched in BA (Seifert and Vehlow, 2017). In terms of the abundance of major elements (O, Si, Ca, Al, Cl, Na, K, S and Fe) BA is similar to basaltic and other geologic materials (Kirby and Rimstidt, 1993; Huber et al., 1996; Wiles, 1996; Chandler et al., 1997). This does, however, not hold for minor elements and trace metals since, e.g. Pb, Cu, Zn, Cr, Mo, Sb, and V as well as Cl and S, are enriched in BA compared to natural rocks (Wiles, 1996; Chimenos et al., 2000; Bayuseno and Schmahl, 2010; Lam et al., 2010; Wei et al., 2011;). A large share of the trace metals is incorporated into melt components (glasses as well as oxide and silicate minerals) while other phases such as refractory components are of lesser significance (Wei et al., 2011). Several studies agree that the trace metals are concentrated in the finest particle fractions of BA (<2 mm) (Stegemann and Schneider, 1991; Chimenos et al., 1999). The enrichment of certain metals may be related to their melting behaviour as pure solids and the tendency to form smaller particle sizes (Chandler et al., 1997). As will be discussed later, the enrichment and leachability of trace metals is of high relevance for the utilisation or disposal of BA.

Morphologically, BA contains non-crystalline (amorphous) as well as crystalline to semi-crystalline (mineral) constituents. The amorphous fraction amounts to between 34 and 76 wt.-% of BA (Knorr et al., 1999; Bayuseno and Schmahl, 2010; Santos et al., 2013). It mostly consists of silicate-based glass phases (CaO-Al_2O_3-SiO_2), which are formed during partial melting and the following quenching of BA (Wei et al., 2011). Typical mineral groups identified in BA are spinels, carbonates, sulfates, silicates, oxides and hydroxides (Williams, 2013). Table 1.1 presents a literature overview of mineral phases identified by x-ray diffraction (XRD) of fresh and/or aged BA samples. To account for the fact that far more fresh BA samples have been investigated, the given frequency of identification is normalized to the total number of references for fresh and aged BA, respectively. It should be noted that the particle size fraction of samples used for analysis and the ageing conditions may vary among the underlying studies. The aim here is to provide an overview about the mineral diversity of BA and to pinpoint common mineral phases which are frequently identified in fresh and/or aged BA. While solid phases with high melting points (refractory minerals) are already contained in the original MSW and pass the incineration process unaltered, some new phases are during the combustion (Zevenbergen and Comans, 1994; Pfrang-Stotz and Schneider, 1995). Examples for the latter are melilite, magnetite and spinels, plagioclase feldspar, wollastonite and lime (Eusden et al., 1999; Wei et al., 2011).

Table 1.1 Mineral phases in fresh and aged bottom ash samples identified in the literature (n_{fresh} = 25; n_{aged} = 14) with scaled frequency of identification (- = not identified, + ≤ 25%, ++ = >25-50%, +++ = >50%). References: (Giordano et al., 1983; Kirby and Rimstidt, 1993; Knorr et al., 1999; Chimenos et al., 2000; Speiser et al., 2000; Chimenos et al., 2003; Fernández Bertos et al., 2004; Polettini and Pomi, 2004; Ohtsubo et al., 2004; Piantone et al., 2004; You et al., 2006; Han et al., 2009; Baciocchi et al., 2010; Bayuseno and Schmahl, 2010; Lin et al., 2015; Saffarzadeh et al., 2011; Wei et al., 2011; Rocca et al., 2012; Santos et al., 2013; Um et al., 2013; Tang et al., 2015; Yang et al., 2014; Yao et al., 2015; Inkaew et al., 2016; Blanc et al., 2018).

Mineral group / phase	Chemical formula	Frequency		Mineral group / phase	Chemical formula	Frequency	
		Fresh	Aged			Fresh	Aged
Spinels				**Hydroxides**			
Magnetite	Fe_3O_4	+	++	Portlandite	$Ca(OH)_2$	+++	+
Hercynite	$FeAl_2O_4$	+	+	Friedel's salt	$Ca_2Al(OH)_6(Cl,OH)\cdot 2H_2O$	++	+
Carbonates				Hydrocalumite	$Ca_2Al(OH)_6[Cl_{1-x}(OH)_x]\cdot 3H_2O$	++	+
Calcite	$CaCO_3$	+++	+++	Goethite	α-FeO(OH)	+	+
Hydrotalcite	$Mg_6Al_2CO_3(OH)_{16}\cdot 4H_2O$	+	+	Aluminium hydroxide	$Al(OH)_3$	+	+
Potash	K_2CO_3	+	+	**Silicates**			
Sulfates				Gehlenite	$Ca_2Al_2SiO_7$	+++	++
Anhydrite	$CaSO_4$	+++	++	Larnite	Ca_2SiO_4	+	-
Gypsum	$CaSO_4\cdot 2H_2O$	+	++	Anorthite	$CaAl_2Si_2O_8$	++	+
Ettringite	$Ca_6Al_2[(OH)_{12}\vert(SO_4)_3]\cdot 26H_2O$	++	+	Wollastonite	$CaSiO_3$	+	+
Thenardite	Na_2SO_4	+	-	Melilite	$(Ca,Na)_2(Mg,Fe,Al)(Si,Al)_2O_7$	+	+
Barite	$BaSO_4$	+	+	Kaolinite	$Al_4[(OH)_8\vert(Si_4O)_{10}]$	+	+
Oxides				Halloysite	$Al_2Si_2O_5(OH)_4$	-	+
Quartz	SiO_2	+++	+++	Forsterite	Mg_2SiO_4	+	+
Cristobalite	SiO_2	+	+	Diopside	$MgCaSi_2O_6$	+	+
Corundum	Al_2O_3	+	+	Muscovite/Illite	$KAl_2(AlSi_3O_{10})(OH)_2$	+	+
Hematite	Fe_2O_3	++	++	Feldspar_Alkali	$(Na,K)Si_3AlO_8$	+	+
Wüstite	FeO	+	+	**Zeolites**			
Lepidocrocite	$^{\gamma}$-FeO(OH)	-	+	Gismondine	$CaAl_2Si_2O_8\cdot 4(H_2O)$	+	+
Ferrous oxide	Fe(II)O	+	+	Laumontite	$CaAl_2Si_4O_{12}\cdot 4(H_2O)$	+	-
Rutile	TiO_2	+	+	Boggsite	$Ca_8Na_3(Si,Al)_{96}0_{192}\cdot 70H_2O$	+	-
Lime	CaO	+	-	**Others**			
Periclase	MgO	-	+	Apatite	$Ca_5(PO_4)_3(Cl,F,OH)$	+	-
Cuprite	Cu_2O	-	+	Halite	NaCl	+	+

Only a few studies have performed quantitative XRD analyses to identify the mineral composition. For fresh BA the following mineral phases were quantified as important constituents: quartz (9 - 57 wt.-%), calcite (0.5 - 27 wt.-%), anhydrite (0.3 - 15 wt.-%), portlandite (0 - 10 wt.-%), gehlenite, magnetite and hematite (all 0.4 - 6 wt.-%) (Knorr et al., 1999; Bayuseno and Schmahl, 2010; Santos et al., 2013). This is in qualitative agreement with high identification frequencies for same minerals reported in Table 1.1.

As already pointed out, several trace metals are found in BA. Among the latter Pb, Zn, Cu and Cr usually dominate (Lam et al., 2010; Dou et al., 2017) and are environmentally relevant in the context of landfilling or reutilization (Huber et al., 1998; Ecke and Aberg, 2006). However, the risk potential is not primarily determined by the total content of the individual contaminants but rather by their binding strengths and solubilities (Bruder-Hubscher et al., 2002; Köster and Vehlow, 2002). Therefore, the mineralogical characteristics of the BA play an important role in the leaching behaviour of BA.

Leaching behaviour

Bottom ash is not generally considered as a hazardous waste according to the European Waste Catalogue, yet its leaching behaviour has been an issue of controversial discussions for a long time (Chandler et al., 1997; Bilitewski and Härdtle, 2013). The leaching of trace metals is of particular importance since almost all regulations for the disposal or utilisation of BA are based on standardised leaching tests (Liu et al., 2015). The leaching of BA has been extensively examined in the literature, e.g. (Kim et al., 2002; Cornelis et al., 2008; Hyks et al., 2009). Major components of BA leachates are typically derived from the salts of alkali and earth alkali elements. These give rise to high aqueous concentrations of Ca, Na and K together with a few bulk anions (e.g. Cl^-, SO_4^{2-}), all readily available in the leaching tests (Wiles, 1996; Dou et al., 2017). Several studies demonstrated that the pH is one of the main factors controlling the release of major elements (Astrup et al., 2006; Dijkstra et al., 2006; Dijkstra et al., 2008). This is due to the pH-dependent solubility of many minerals (Meima and Comans, 1997; Rocca et al., 2012). Fresh BA exhibits a pH in the range of 10 to 12.6 (Huber et al., 1998; Chimenos et al., 2000; Speiser et al., 2001; Polettini and Pomi, 2004; Dijkstra et al., 2006) and buffering in this range can be attributed mainly to the presence of $Ca(OH)_2$ (Johnson et al., 1995; Chandler et al., 1997).

In terms of the pH-dependent leaching the trace metals can be roughly divided into two groups: i) metals with amphoteric character which react either as acid or base, like Pb, Cu and Zn; and ii) oxyanion forming metals, e.g. Cr, V, Sb and Mo.

The leachability of amphoterics like Pb, Cu and Zn is mainly controlled by precipitation/dissolution reactions (Zhang et al., 2008) and the following mineral phases have been suggested as mineral host phases: $Pb(OH)_2$, $PbCO_3$, ZnO, $Zn(OH)_2$, CuO, Cu_2O, $Cu_2(OH)_2CO_3$ (Meima et al., 1999; Köster and Vehlow, 2002; Polettini and Pomi, 2004; Dijkstra et al., 2006; Saffarzadeh et al., 2011). Their solubility is high under both alkaline (pH >11) and acidic conditions (pH < 4) and relatively low in the weakly alkaline range (pH 9 – 10) (Chimenos et al., 2000; Köster and Vehlow, 2002). In the leachates of fresh BA with a highly alkaline pH, amphoteric metals are usually present as free cations as well as hydroxo complexes and high concentrations are observed, in particular for Pb (Arickx et al., 2006; Seifert and Vehlow, 2017). This may cause the need to store BA on hazardous waste landfills but particularly hampers their geotechnical utilisation (Bayuseno and Schmahl, 2010).

Heaps of BA represents an alkaline and oxidizing (Meima and Comans, 1997; Dijkstra et al., 2006) environment where redox-sensitive elements like Cr, Mo, Sb, and V are predominantly present as chromate, molybdate, antimonate and vanadate, i.e. as oxyanions. Their concentration-vs.-pH characteristic differs greatly from that of the amphoteric metals. A leaching minimum is found at pH ≈ 12 and for some oxyanions a secondary minimum is found at pH <6 (Köster and Vehlow, 2002; Cornelis et al., 2008). Although the total contents of oxyanion-forming elements are typically lower than those of amphoteric metals they are often readily available for leaching. This is due to the high solubility of the corresponding host phases, e.g. $Cu_{11}(OH)_{14}(CrO_4)$, $PbCrO_4$, Na_2CrO_4, $CaMoO_4$ and $(Zn,Cu)PbVO_4(OH)$ (Zevenbergen and Comans, 1994; Chandler et al., 1997; Meima and Comans, 1999; Freyssinet et al., 2002; Piantone et al., 2004). Oxyanion leaching has been reported to be limited by sorption to Fe- and Al-(hydr)oxides (Kersten et al., 1997). Although the sorption is weak in the pH range of fresh BA (Johnson et al., 1999), it may become more important when the pH drops, i.e. during ageing of the material (see section 1.4). The role of metalloids substitution for other anions in minerals like ettringite, calcite and hydrocalumite and its effects on the oxyanions leaching has been highlighted by several researchers (Piantone et al., 2004; Cornelis et al., 2008).

1.3 Utilisation of BA

Bottom ash contains potentially valuable constituents (metals, glass) and bulk materials (aggregates and minerals) that may be recycled or used in geotechnical applications. In many countries the reuse of BA (“waste to materials”) is therefore preferred over landfilling (Liu et al., 2015; Dou et al., 2017).

From the geotechnical viewpoint, BA is a compactable material with high elasticity in the uncured state and good geotechnical properties (Chandler et al., 1997; Holm and Simon, 2016). Furthermore, several investigations also identified BA as a pozzolanic material (Abdulmatin et al., 2018; Shi et al., 2018). The reuse of BA as a secondary construction material has long since been promoted. Applications comprise the use as road subbases and sound barriers on highways, wind barriers, parking lot and bike path groundings (Schreurs et al., 2000; Fujimori et al., 2004; Hjelmar et al., 2007; Alwast and Riemann, 2010; Lynn et al., 2017). Also, the use in landfill construction and land reclamation in coastal areas have been reported (Wiles, 1996). These applications involve the benefit of substituting geogenic aggregates and thereby conserving natural resources (Brett et al., 2018).

Other attempts for recycling and reuse of specific BA fractions include glass recycling (Barberio et al., 2010; del Valle-Zermeño et al., 2017), the use as an aggregate and/or cement substitute in mortar or concrete applications (Wiles, 1996; Bertolini et al., 2004; Al-Rawas et al., 2005; Lam et al., 2010; Kuo et al., 2013; Keulen et al., 2016), or in bituminous pavements (Wiles, 1996). More exotic uses include the use as a sorbent for gas-purification (Mostbauer et al., 2008; Mostbauer et al., 2014; del Valle-Zermeño et al., 2015) or raw material in the ceramic industry (Fujimori et al., 2004; Bourtsalas et al., 2015). However, in consideration of the huge amount of BA produced, only geotechnical reuse and the use as an aggregate in cement mortar and concrete provides the necessary volume to avoid BA landfilling (Santos et al., 2013).

Prior to any reuse option, ferrous and non-ferrous metals should be separated from BA (Wiles, 1996; Xuan et al., 2018). Basic mechanic treatment methods include shredding for size reduction, ferrous and non-ferrous metal recovery by magnetic and eddy current separation, screening or windsifting to remove uncombusted material, and sometimes sensor based sorting (Chandler et al., 1997; Holm and Simon, 2016). Increasing raw material prices and a growing demand for non-ferrous metals have prompted German operators to intensify their efforts towards metal recovery (Vehlow and Seifert, 2012; Holm and Simon, 2016). Enhanced metal recycling often requires a shredding of the mineral fraction, which in turn lowers the suitability for geotechnical reuse, leaving landfilling as the only remaining option (Quicker, 2017).

Waste balances show that high BA utilisation rates are already achieved in some European countries, e.g. > 90% in Denmark and the Netherlands, 80% in Germany and 70% in France (Dou et al., 2017), while in other countries (e.g. Austria, Belgium, Sweden) landfilling is still the predominant disposal route due to the lack of suitable valorisation routes (Santos et al., 2013; Dou et al., 2017). For Germany, however, it should be noted that the major share of utilized BA goes into landfill construction (Holm and Simon, 2016). This is, however, quite a dead-end-path in view of the presumably low number of newly built landfills and the decreasing number of active landfill sites (Rettenberger, 2017). Therefore, more efforts have to be devoted to the reuse of BA in geotechnical applications.

For this purpose, engineering criteria and environmental performance guidelines have to be observed (Wiles, 1996), which can considerably vary between different countries (Liu et al., 2015). Indeed, due to länder-specific regulations in Germany the utilization rate exhibits high regional variability (Zwahr, 2005; Holm and Simon, 2016). Recently, a new German ordinance has been drafted (ErsatzbaustoffV), which determines quality standards for secondary construction materials including BA. The pertinent legislative process is still in progress.

Geotechnical reuse options for BA (as well as BA landfilling costs) depend on national guidelines especially regarding the leachability of trace elements (Liu et al., 2015). Reactive compounds present in fresh BA like CaO, $Ca(OH)_2$, and Al^0 (see section 1.2) are one of the major reasons for the high leachability of critical trace elements (e.g. Pb, Cu, Zn). Therefore, decreasing reactivity by natural ageing is one of the most common approaches to improve the leaching behaviour of BA and will be outlined in detail in the following section.

1.4 Ageing processes

It has long since been recognized that the ageing of BA is beneficial to its leaching behaviour (Wiles, 1996; Meima and Comans, 1999; Polettini and Pomi, 2004; Wei et al., 2011). Fresh BA contains highly reactive constituents (e.g. lime, anhydrite) which are metastable under environmental conditions (Bayuseno and Schmahl, 2010). Their transformation under ambient conditions has been referred to as ageing of BA. The majority of ageing reactions is driven by atmospheric agents (oxygen, carbon dioxide) and requires the presence of pore water (Costa et al., 2007). The ageing process includes dissolution/precipitation of salts, glass corrosion, oxidation, hydration, slaking of lime, carbonation, hardening and hydraulic cementation reactions, and neo-formation of clay-like minerals (Kirby and Rimstidt, 1993; Eighmy et al., 1994; Zevenbergen et al., 1996; Meima and Comans, 1997; Eusden et al., 1999; Wei et al., 2011; Wei et al., 2014).

As pointed out in section 1.2, the mineralogy of BA is quite versatile for fresh BA and becomes even more complex when the material ages since secondary mineral phases emerge (e.g. calcite, Fe oxides quartz, sulphates and/or ettringite, hydrocalumite and calcium-silicate-hydrates (C−S−H phases) (Piantone et al., 2004; Bayuseno and

Schmahl, 2010). To date, the understanding of the complex mineral alteration reactions induced by aging and weathering is still patchy (Costa et al., 2007; Bayuseno and Schmahl, 2010). However, the following processes are often outlined to be of particular importance:

1. Oxidation of metallic Al/Fe
2. Hydration of metal oxides
3. Carbonation

Freshly quenched BA contains metals in elemental form, mostly Fe^0 (9 − 15 %) and Al^0 (1 − 2 %) (Cornelis et al., 2008). Both metals have been reported to undergo corrosion both under anaerobic conditions (Hao et al., 2017) and under the aerobic conditions induced by the access of atmospheric oxygen. Corrosion results in the formation of Fe- and Al-(hydr)oxides, which have been recognized as prominent sorbents for environmentally relevant trace metals (Meima and Comans, 1997; Todorovic and Ecke, 2006; Chaspoul et al., 2008; Oehmig et al., 2015).

Hydration starts during the quenching process when BA comes into contact with water (Chimenos et al., 2000). Metal oxides of the alkali and earth-alkali element groups formed during the combustion react as bases and determine the alkalinity of BA. Calcium is one of the major elements of BA and CaO (lime) is an abundant mineral phase in unquenched BA (Inkaew et al., 2016). Thus, one of the most prominent hydration processes in BA is the hydration of CaO to $Ca(OH)_2$ according to the following equation (1.1):

$$CaO + H_2O \rightarrow Ca(OH)_2 \qquad (\Delta H = -65\ \frac{kJ}{mol}) \qquad \text{(Eq. 1.1)}$$

Portlandite ($Ca(OH)_2$) is one of the most frequently identified alkaline mineral phases in freshly quenched BA (see Table 1.1). Its presence is an important prerequisite for the carbonation reaction which is considered as the most relevant aging process for BA (Meima and Comans, 1997; Arickx et al., 2006; Costa et al., 2007).

Carbonation

Carbonation is an irreversible gas/solid reaction and involves the absorption of atmospheric CO_2 by an initially alkaline material. For the typically moist BA the reaction is mediated through the pore water. Bottom ash contains several alkaline compounds which are suitable for carbonation. For instance, olivine, feldspars, Ca-containing oxides and silicates (e.g. larnite and wollastonite, see Table 1.1) and C−S−H phases can react with CO_2 and produce $CaCO_3$ and a silica gel (Kirby and Rimstidt, 1993; Eusden et al., 1999; Fernández Bertos et al., 2004b; Pan, 2012). However, except the Ca-containing oxides most of the mentioned compounds are only trace constituents. Due to the abundance of CaO in unquenched BA its hydroxide $Ca(OH)_2$ is considered to be the main alkaline phase in fresh BA (Chimenos et al., 2000; Rendek et al., 2006) and the simplified carbonation reaction can be described according to equation (1.2):

$$Ca(OH)_2 + CO_2 \rightarrow CaCO_3 + H_2O, \quad (\Delta H = -113\ \frac{kJ}{mol}) \qquad \text{(Eq. 1.2)}$$

Figure 1.2 gives a schematic of the involved reaction steps. Initially, $Ca(OH)_2$ dissolves and Ca^{2+} and OH^- ions are released into the pore water with a rapid and strong increase of the pH (Pan, 2012). Due to the high pH of the pore water, carbonic acid evolved by the dissolution of atmospheric CO_2 dissociates almost completely to form carbonate (CO_3^{2-}) ions. The latter combine with the Ca^{2+} ions to $CaCO_3$ which precipitates at pH above 9 (Pan, 2012) forming a coating layer on the BA surface (Brett et al., 2018). For each carbonic acid ion two H^+ ions are released into the pore water and combine with OH^- (neutralisation), which results in a decrease of leachate pH to the circumneutral range (Wiles, 1996). This reaction sequence will proceed as long as the reactants, CO_2 and $Ca(OH)_2$, are available in the pore water.

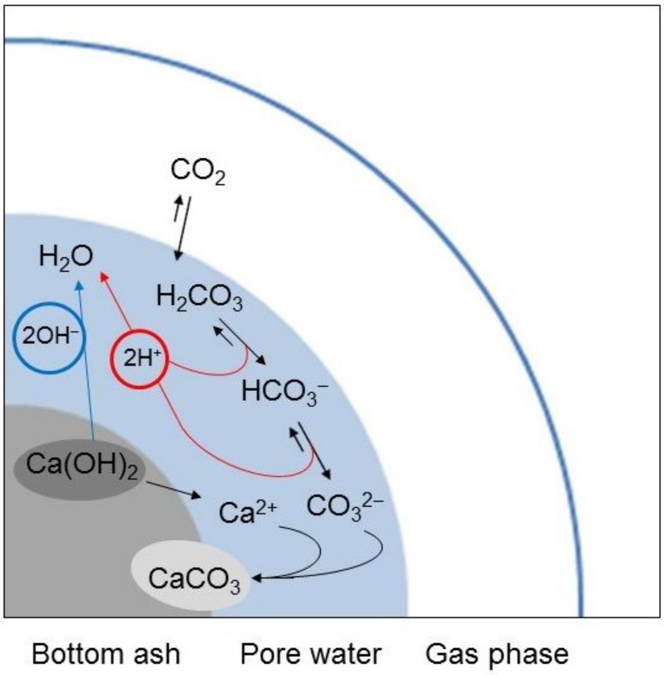

Figure 1.2 Schematic of the carbonation of portlandite {$Ca(OH)_{2(s)}$} by CO_2. Atmospheric $CO_{2(g)}$ dissolves in the alkaline pore water to form carbonic acid (H_2CO_3), bicarbonate (HCO_3^-) and carbonate (CO_3^{2-}). The latter combines with $Ca^{2+}(aq)$ and finally precipitates as calcite {$CaCO_3(s)$}. Adopted and modified from (Brett et al., 2018).

Calcite is, by far, the most commonly precipitated mineral during carbonation and its content can increase by up to 18 wt.-% (Fléhoc et al., 2006). Carbonates are thermodynamically stable under atmospheric conditions (Piantone et al., 2004). Generally, it would be a very long process (probably thousands of years) to decrease the leachate pH to the acid range merely by the acid precipitation because of the high acid neutralization capacity of BA (Hirner et al., 2000; Johnson and Furrer, 2002). Therefore, carbonation of BA is considered suitable for CO_2 storage under ambient conditions (Pan, 2012). However, compared to the total CO_2 emissions of a MSW incinerator plant the achievable CO_2 uptake by BA carbonation is almost negligible (Santos et al., 2013). Thus, the main benefit of BA carbonation rests with the improvement of leachate quality caused by the mobility decrease of certain regulated metals (Fernández Bertos et al., 2004b; Costa et al., 2007; Wei et al., 2011). A number of studies have focused on this effect and several processes have so far been identified:

a) Carbonation affects the solubility of different BA constituents due to pH decrease (Di Gianfilippo et al., 2016). This is especially the case for the amphoteric metals (Fernández Bertos et al., 2004a; Saffarzadeh et al., 2011; Wei et al., 2011), since leaching of Pb, Zn and Cu is generally high at the typical pH (>12) of fresh BA and is lowered when the pH decreases to values between 8 and 10 (Verbinnen et al., 2016).

b) Metal immobilization may be driven by the alterations of BA mineralogy (Bertos et al., 2004; van Gerven et al., 2004; Verbinnen et al., 2016). On the one hand carbonation my trigger the direct involvement of Pb, Zn, and Cu by the precipitation of sparingly soluble (hydroxy-) carbonates (e.g. $ZnCO_3$ and $Cu_2CO_3(OH)_2$ (Zhang et al., 2008) and $PbCO_3$). The carbonates' solubility depends on the involved cations and decreases in the order $Mg^{2+} > Ca^{2+} > Zn^{2+} > Cd^{2+} > Pb^{2+}$ (Salminen and Prausnitz, 2007), indicating that precipitation of trace metals is favoured. On the other hand, the formation of solid solutions may also contribute to the metal binding properties of BA, since Pb, Zn and Cd may substitute for calcium (as cations) and As, Cr, Mo, Sb, and V for sulfate (as oxyanions) in mineral phases like gypsum, ettringite, and hydrocalumite (Bayuseno and Schmahl, 2010; Cornelis et al., 2008; Piantone et al., 2004).

c) Carbonation also induces changes of the physical properties of BA (Chimenos et al., 2005). On the one hand, $CaCO_3$ was found to precipitate on the surface of BA particles forming a carbonate layer (coating), which may cover potential host phases of critical metals. This, so-called, physical containment may contribute to the benefits of BA carbonation (Um et al., 2013; Sakita and Nishimura, 2015). On the other hand, the formation of $CaCO_3$ in the microstructure of BA decreases porosity and increases tortuosity (Xuan et al., 2018), which in turn has beneficial effects on the retention of contaminants (Lange et al., 1996; Rendek et al., 2006).

d) The formation of secondary phases may also contribute to the immobilisation of oxyanions by sorption and surface precipitation (Cornelis et al., 2008). The sorption potential for oxyanions in Al- and Fe(hydr)oxides is well documented in the literature (Essington, 2004; Karamalidis and Dzombak, 2011). Sorption of most oxyanions is typically weak in the pH range of fresh BA (Johnson et al., 1999), but increases towards neutral pH (Cornelis et al., 2008) since most of the reactive minerals constitute variable charge surfaces. Thus, the pH decrease induced by carbonation may additionally enhance immobilisation by sorption (Meima and Comans, 1998). Furthermore, several secondary mineral phases, like calcite, can provide sorption sites for certain elements (Meima and Comans, 1999; Piantone et al., 2004).

The above-named processes associated with primary and secondary mineral reactions may overlap (Lin et al., 2015a). Irrespective of knowledge gaps regarding specific mechanisms, the beneficial effect of ageing reactions, especially carbonation, is beyond doubt (Meima and Comans, 1997; Zevenbergen et al., 1996; Marzi et al., 1998; Chimenos et al., 2005; van Gerven et al., 2005; Todorovic and Ecke, 2006; Gori et al., 2011; Saffarzadeh et al., 2011; Santos et al., 2013; Yin et al., 2017; Di Gianfilippo et al., 2018; Sormunen et al., 2018).

Current practice of BA ageing

As outlined in the previous section, ageing reduces the BA reactivity and the mobility of BA-borne contaminants. Furthermore, ageing may also improve the geotechnical properties of BA, e.g. by increasing the compressive strength, modulus of elasticity and structural durability (Wiles, 1996; Fernández Bertos et al., 2004b; Chimenos et al., 2005;). Therefore, ageing is commonly applied in many European countries prior to geotechnical utilization or landfilling of BA (e.g. German LAGA-guideline from 1994). For passive ageing (pile ageing), BA is usually stored in open stockpiles of up to 5,000 tons (Blanc et al., 2018; Nørgaard et al., 2019) for periods between 1 and 3 months (Chimenos et al., 2003; Sabbas et al., 2003; Arickx et al., 2010; Gori et al., 2011). However, this timeframe may not be sufficient to meet regulatory limit values and ageing periods have been extended to about 12 months in Denmark (Astrup, 2007). This, in turn, requires larger storage capacities which might not be available in densely populated areas (Lin et al., 2015a).

Based on the experience gathered over the last decades, ageing should be performed under controlled conditions (Wiles, 1996; Palitzsch et al., 1999). Under natural conditions carbonation is quite slow (Costa et al., 2007) and often limited to the upper layers of BA piles (Freyssinet et al., 2002). Marzi et al. (1998) and Arickx et al. (2006) showed that after 3 months of natural ageing only the upper 5 cm of a BA pile underwent significant carbonation as judged from the leachate pH and concentration of trace metals. Therefore, BA stockpiles should be periodically homogenized by turning, thereby also improving the access of CO_2 (Polettini and Pomi, 2004). For this purpose, machinery and manpower is required (Blanc et al., 2018).

Depending on whether BA is stored in roofed or open-air stockpiles, specific water management requirements need to be observed. Generally, the storage should be performed on concrete floors including adequate facilities to collect drainage and run-off water for treatment (Wiles, 1996). On the other hand, wetting of the stockpiles may be required if the moisture content falls below a certain level (Wiles, 1996). Indeed, water contents tend to decrease during storage mainly due to exothermic ageing reactions (see equation 1.1 and 1.2) (Chimenos et al., 2003; Nørgaard et al., 2019). Besides the risk of potential dust emissions, excessive drying may ultimately impede carbonation of BA.

Overall, passive ageing requires large quantity of space, time and appropriate measures to control the process. Thus, as will be shown in detail in the next section, a number of researchers have addressed the question of how the ageing of BA can be accelerated under controlled conditions.

1.5 Accelerated carbonation

The accelerated carbonation of alkaline materials, whether minerals or residues, is a controlled enhancement of their natural ageing (Fernández Bertos et al., 2004b; Pan, 2012). For several decades, enhanced carbonation has been applied to the hardening and curing of cement and concrete systems (Klemm and Berger, 1972; Kashef-Haghighi and Ghoshal, 2013). More recently, it has gained attention in the context of carbon capture and storage as well as in the treatment of contaminated soil, hazardous waste, and alkaline residues (e.g. BA, fly ash and other air pollution control residues, steel-making slags, etc.) (Bodor et al., 2013). The approaches can be differentiated into the indirect and direct carbonation routes. Indirect carbonation takes place in several stages, typically including extraction, reaction and extractants recycling (Bobicki et al., 2012). Since it is primarily applied in carbon capture and storage technologies, it will not be discussed here.

Alkaline residues of high temperature processes (waste incineration, steel making etc.) are suited for direct carbonation in a single reaction step. Direct carbonation of these materials leads to a CO_2 uptake by the solid and improves its leaching (Fernández Bertos et al., 2004b; Lim et al., 2010). Based on the reaction environment direct carbonation can be further divided into dry, moist and aqueous applications (Bodor et al., 2013).

Dry carbonation is the direct gas-solid reaction of alkaline minerals with CO_2 at temperatures above 300 °C. It is applicable when high-temperature CO_2 sources are available and when the material exhibits high levels of readily reactive calcium oxide or hydroxide compounds (Costa et al., 2007). For BA, the former is typically not the case, leaving moist and aqueous accelerated carbonation as the most adequate approaches (Costa et al., 2007; Fernández Bertos et al., 2004b). Both comprise a heterogeneous gas-liquid-solid reaction and thus require the presence of liquid water. While in moist carbonation the CO_2 is introduced into the available pore water at low liquid to solid ratios (L/S <1), aqueous carbonation handles slurries with L/S >2 (Pan, 2012; Bodor et al., 2013). Aqueous carbonation requires a subsequent liquid-solid separation, generates wastewater and thereby additional treatments costs. This can be circumvented by moist carbonation where the aqueous phase is provided by the pore water, alone. Relying on the inherent moisture content of the residues, only a slight adaption of the water content would be necessary to obtain the optimal CO_2-uptake. Since BA carries inherent moisture from the quenching step, moist carbonation is the favoured approach for this material (Costa et al., 2007).

The most straight forward way to accelerate the naturally slow carbonation reaction is to increase the CO_2 supply. This can be achieved by contacting BA with a CO_2-rich reaction gas at ambient pressure or by using overpressures of up to 17 bar. The latter approach has been investigated in pressurized stainless steel vessels with a thin layer of BA exposed to the reaction gas (Fernández Bertos et al., 2004a; Rendek et al., 2006; Baciocchi et al., 2010).

For carbonation at ambient pressure reactor systems with a continuous gas supply have been implemented in climate chambers, incubators, and columns where BA is exposed to a CO_2 rich reaction gas under flow-through conditions (van Gerven et al., 2005; Arickx et al., 2006; Nam et al., 2012; Um et al., 2013; Lin et al., 2015a; Sakita and Nishimura, 2015). Accelerated (moist) carbonation has proven successful to increase the chemical stability and improve leaching behaviour of BA within time frames ranging from minutes to hours. Yet a practical applicability of the above named systems remains beyond reach since static treatment do not allow for the necessary throughput.

Current developments

In recent years much research has focused on the principal carbonation mechanisms and controlling operating parameters, such as temperature, CO_2 partial pressure, water content, residence time as well as particle size (Costa et al., 2007). Despite the progress made in this context, commercial applications are still out-of-sight due to technical limitations and high costs (Fernández Bertos et al., 2004b). One of the major hurdles with regard to scale-up is the transfer the mostly static reactor systems studied so far to concepts applicable at the industrial scale. Marzi et al. (2004) were one of the first to explore the scale-up by loading 167 t of BA into a compost tunnel utilising its aeration system for CO_2 supply (synthetic reaction gas with 8 vol.-% CO_2). Carbonation of BA was achieved within a few days and the leaching of Pb, Cu and Mo clearly decreased. However, problems related to pile ageing (see section 1.4) remained and thus the approach was not pursued further.

To enhance carbonation efficiency, the penetration of CO_2 into the porous system needs to be favoured (Freyssinet et al., 2002). One of the key variables to be optimized is therefore the material exchange between the solid, liquid and gaseous phases. Therefore, dynamic reactor systems have been suggested (Fernández Bertos et al., 2004a,b). Initial attempts to provide agitation of BA were reported by Palitzsch et al. (1999) who used a vibrating feeder as dynamic reaction system. The necessary treatment time could be shortened to 10 minutes if pure CO_2 was used as reaction gas, but carbonation was insufficient when the CO_2 concentration was reduced to 10 vol.-%. Although the results were promising, some problems remained unsolved, e.g. the use of costly synthetic CO_2, the requirement of a gastight reactor and the control of sufficiently long residence times on the vibrating feeder.

Rotating drums have been suggested as an alternative reactor concept (Fernández Bertos et al., 2004b; Zingaretti et al., 2013). These simultaneously provide agitation and mixing (thereby enhancing the contact between BA and the reaction gas) and homogenize the solid with respect to moisture. Beyond BA, rotating drums have proven useful for the accelerated carbonation of other alkaline residues like fly ash, biomass ash, steel slag, and paper ash (Gunning et al., 2009; Łączny et al., 2015; Librandi et al., 2017; Librandi et al., 2019). Lombardi et al. (2016) studied the CO_2 uptake from synthetic landfill gas by BA. Under batch conditions, they found higher CO_2 uptake rates in their rotating drum reactor compared to static conditions.

The findings published so far suggest that rotating drum reactors are promising for the implementation of accelerated carbonation at the industrial scale. However, several issues need to be considered: Until now the accelerated carbonation of BA was only tested under batch conditions. To integrate the process into the management of BA at the industrial scale the system should be ideally operated under flow-through conditions in terms of both, gas and BA. Using waste gas as the CO_2 source for accelerated carbonation was suggested by Marzi et al. (2004) and Palitzsch et al. (1999). This would increase the economic efficiency of the treatment process and also reduce, albeit slightly, the amount of anthropogenic CO_2 emissions. Several exhaust gases have been suggested including syngas from gasification processes (Zingaretti et al., 2014), biogas (Baciocchi et al., 2013; del Valle-Zermeño et al., 2015) and landfill gas (Mostbauer et al., 2014). Their CO_2 concentration ranges from 5 to 70 vol.-%. One obvious option is to use the stack gas from waste incinerators (van Gerven et al., 2005; Nam et al., 2012). This normally contains around 10 vol.-% CO_2 (Song et al., 2004; Costa et al., 2007) and is available in large quantities at the origin of the BA. However, effects of gas temperature and moisture have not been extensively examined up to now.

1.6 Scope of the thesis

As previously outlined, accelerated carbonation under controlled conditions is a promising technology to reduce BA disposal costs while overcoming problems related to passive BA ageing. Although the scientific literature reveals substantial progress regarding carbonation conditions, the translation of the more fundamental findings into practicable processes is still sketchy. Recent studies demonstrated that the material dynamics in rotating drum reactors favour the accelerated carbonation. Yet, prior to the integration into the management of BA, optimum drum operating conditions need to be identified.

This thesis aimed at delineating both the technical set-up and the operation parameters suited for process integration at incinerator sites. This included the development of a screening technique to evaluate the progress of carbonation as well as a stepwise transfer of the reactor into a continuously fed system.

Process integration requires that the treatment should ideally be synchronized to timescales of the BA generation at the incineration plant or to typical residence times during BA treatment (metal recovery, sieving, crushing). As outlined in Figure 1.3, typical residence times of those processes are within the range of minutes to hours, while the timeframe of passive ageing is far beyond (between several months and one year). Shortening the necessary treatment time is therefore crucial for process integration.

One of the key issues of reactor design is therefore the enhancement of BA exposure to the reactant gas by agitation and mixing. Contrary to the bed behaviour of dry standard materials, little is known about the motion of wet BA in rotating drums and its implications for accelerated carbonation.

Depending on the patterns of bed motion, mixing tools may be required to speed up the carbonation process. These alter the geometry of the reactor interior and provide obstacles for the motion of BA induced by drum rotation. Adequate designs need to consider the rheology of wet BA to prevent the formation of incrustations on the drum mantle and the mixing tools.

Bed motion may also be affected by the reactor fill level and when a continuous reactor operation is aimed at, fill level is a critical design parameter itself. For a given feed rate (related to rate of BA generation) the fill level determines the BA residence time which in turn feeds back into the degree of carbonation when CO_2-uptake is rate-limited.

The carbonation of BA is known to reduce the leaching of amphoteric trace metals but may have the adverse side-effect of enhancing the mobility of oxyanions (see section 1.4). Therefore, process integration for a more economic disposal of BA requires an optimum degree of carbonation both with respect to its immobilizing and mobilizing effects.
The objectives of this thesis are as follows:

a) Develop a monitoring system to evaluate the progress of carbonation under static and dynamic conditions
b) Evaluate the benefits of mixing and agitation for the accelerated carbonation
c) Study the bed behaviour of BA in rotating drum reactors
d) Investigate the effect of process conditions and reactor design on carbonation performance
e) Develop a continuous-fed operating reactor with adjustable BA residence time

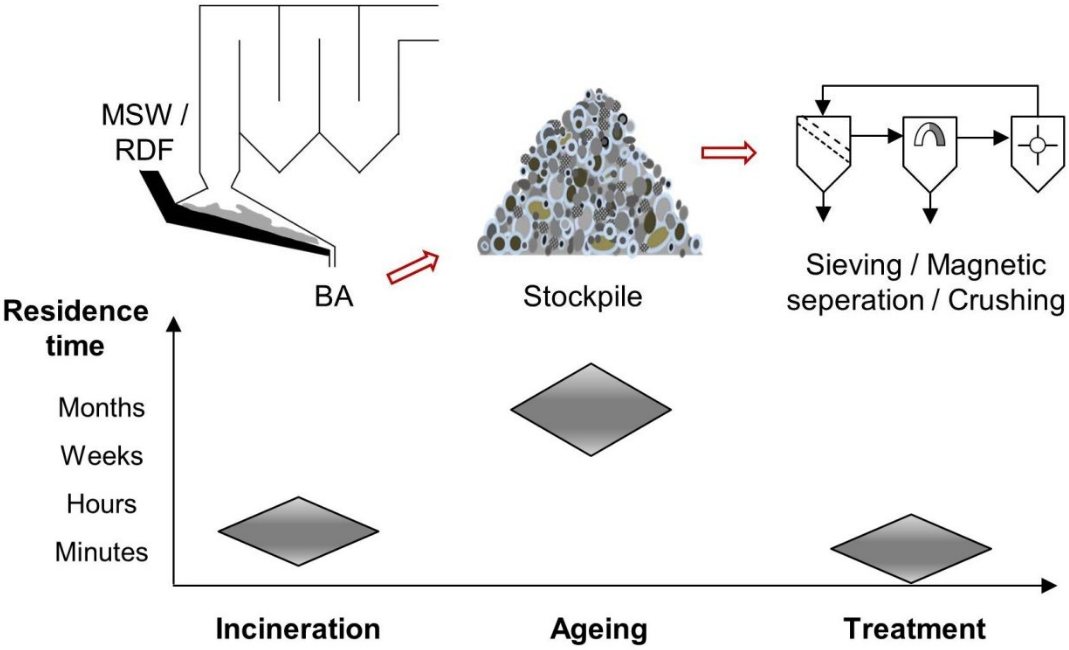

Figure 1.3 Typical material residence times during incineration, ageing of bottom ash (BA), and BA treatment.

1.7 Research design and applied methods

The BA used in this study was sampled from a grate-type refuse derived fuel incinerator located in central Germany. A total amount of about 2000 kg BA was used in the laboratory experiments. The fresh BA was characterised by X-ray powder diffraction (XRD), X-ray fluorescence (XRF) spectroscopy, and thermogravimetric analysis (TGA). To evaluate the carbonation performance standard batch leaching tests were performed at a liquid-to-solid ratio of 10 L kg^{-1} prior and after carbonation treatment. The filtrates were analysed by inductively coupled plasma–mass spectrometry regarding concentration of trace metals (Pb, Zn, Cu, Mo, Cr, V). The BA properties were screened over a period of three months. Results indicated that the material exhibits a pronounced temporal and spatial variability. In the research design this was considered using large samples of about 5 to 40 kg in the carbonation experiments.

Chapter 2 reports on a novel method to monitor and evaluate the progress of carbonation in both static and dynamic reactor systems equipped with an automated CO_2 supply at close to atmospheric pressure conditions. The method is based on following the pressure drop in the gas phase induced by the CO_2-uptake of BA and was benchmarked against carbonate contents as measured by thermogravimetric analysis. To gather information about the moisture conditions inside the reactor system and self-heating induced by the exothermal carbonation reaction, the relative humidity and temperature were logged. The obtained high-resolution pressure curves were also used to analyse the kinetics of carbonation.

The effect of mixing on carbonation efficiency was studied in more detail in Chapter 3. Therefore, carbonation experiments were conducted with and without agitation of the BA in a rotating drum batch reactor. Since carbonation performance was superior under dynamic conditions, the influence of drum operation conditions was evaluated. Effects of rotation speed and reactor fill level on the solid’s motion were cinematographically analysed. In addition, the effects of CO_2 concentration, fill level, and moisture on BA carbonation were investigated with respect to BA leachate properties. The CO_2 uptake was quantified according to the findings of Chapter 2. The self-heating described therein was considered in a heat-balance model that accounts for the exothermal carbonation reaction.

The results summarized in Chapter 3 were obtained in a batch system. The CO_2 supply was demand-driven by automated dosage at pre-defined set-points. However, thermal processes provide a continuous supply of CO_2. Therefore, Chapter 4 presents results obtained with a system where the BA was contacted with a synthetic exhaust gas in a rotating drum reactor under flow-through conditions. Different mixing tool designs and configurations were tested to enhance mixing while the specific CO_2 supply and reactor loading were varied. Carbonation performance was assessed by thermogravimetric analyses and the leaching behaviour of the treated BA.

As next step towards the implementation of the accelerated carbonation at an incinerator site a novel rotating drum reactor has been developed and tested as described in Chapter 5. The design considered the findings of Chapters 2 to 4 and was extended to allow for the supply of a hot and humid reactant gas. The set-up used in Chapter 4 was extended. Asides the flow-through of the gas also the BA could be continuously fed employing appropriate material dosage and discharge units. Electric balances were used to log the input and output mass flux for control of the residence time. Projected and experimental residence times were compared by mass balancing and by analysing the breakthrough curves of a tracer. Leachates and solid phase properties of the treated BA served to evaluate the carbonation performance.

Finally, in Chapter 6, the most important results of the study are summarized and their implications are discussed in the light of a future implementation of the accelerated carbonation process.

Chapter 2 A fast and simple method to monitor carbonation of MSWI bottom ash under static and dynamic conditions

Waste Management (2018) 78: 588−594.
DOI: 10.1016/j.wasman.2018.06.042

Co-authors: Christine Fröhlich, Tim Mansfeldt, Harald Weigand

Formatting and orthography of the manuscript is adapted to the dissertation style.

2.1 Abstract

Accelerated carbonation may be employed to improve the leaching behaviour and the geotechnical properties of MSWI bottom ash (BA). Here we report on a novel method to monitor and evaluate the progress of carbonation in both static and dynamic reactor systems. The method is based on following the pressure drop in the gas phase induced by the CO_2-uptake of BA and was benchmarked against carbonate contents as measured by thermogravimetry. Laboratory results demonstrated the serviceability and reproducibility of the method. Complementary logging of relative humidity and temperature showed constant moisture conditions and self-heating induced by the exothermal carbonation reaction, respectively. Under dynamic conditions BA carbonation was higher than in the static reactor. Consistently, the self-heating was more pronounced. After a reaction time of 120 minutes the pressure records indicated a CO_2-uptake of 1.5 g CO_2 /100 g BA (static tests) and of 2.6 g CO_2 /100 g BA (dynamic tests). The proposed method is suited to study carbonation processes at minimum analytical expense and integrates over the small-scale heterogeneity of BA.

Keywords: Bottom ash, alkaline waste, accelerated carbonation, carbon dioxide

2.2 Introduction

Bottom ash (BA) is the dominant solid residue generated in municipal solid waste incinerators and waste-to-energy plants. Worldwide, the installation of incineration capacities has increased (Santos et al., 2013) causing increasing quantities of BA. Disposal options for BA (landfilling or geotechnical reuse) depend on country-specific guidelines especially regarding the leachability of trace elements (Liu et al., 2015; Verbinnen et al., 2016).

Fresh BA contains highly reactive constituents and their transformation under ambient conditions has been referred to as the ageing of BA. One of the most important ageing processes is carbonation by atmospheric carbon dioxide (CO_2). Due to the presence of alkaline mineral phases (mainly $Ca(OH)_2$; Rendek et al., 2006) the pore water of BA acts as a CO_2-trap (Fernández Bertos et al., 2004b). The simplified carbonation reaction equation (2.1) shows that by CO_2-uptake $Ca(OH)_2$ is converted to $CaCO_3$ and alkalinity is consumed.

$$Ca(OH)_2 + CO_2 \rightarrow CaCO_3 + H_2O, \triangle H = -113 \text{ kJ/mol} \qquad \text{(Eq. 2.1)}$$

For a more detailed description of the reaction routes refer to Costa et al. (2007) and Pan (2012). Consumption of BA alkalinity by carbonation is beneficial since it reduces the leachability of amphoteric trace metals (Saffarzadeh et al., 2011) and thereby lowers disposal costs. For Germany, cost savings between 10 € and 45 € per metric tonne of BA have been estimated after improving the leacheate characteristics by carbonation (our own unpublished data). Carbonation may also improve the geotechnical properties of BA, e.g. by increasing the compressive strength and modulus of elasticity (Chimenos et al., 2005; Fernández Bertos et al., 2004b).

Under ambient conditions, carbonation is slow (Costa et al., 2007) and limited by the access of CO_2 requiring storage periods of up to several months (Astrup, 2007; Santos et al., 2013). Therefore, considerable efforts have been made to accelerate CO_2-uptake by increasing the CO_2 partial pressure under static and dynamic conditions.

In static laboratory-scale reactors a thin layer of BA is contacted with the CO_2 enriched gas phase without agitation of the solid. Such systems with flow-through supply of CO_2 have frequently been described (Arickx et al.,2006; Lin et al.,2015; Sakita and Nishimura,2015; Nam et al.,2012; Um et al.,2013; van Gerven et al.,2005). As an alternative approach, pressurized stainless-steel vessels with discontinuous gas supply operated under CO_2

partial pressures of $2 \cdot 10^2$ kPa to $1.7 \cdot 10^3$ kPa have been used by Baciocchi et al. (2010), Fernández Bertos et al. (2004a), Johnson (2000), and Rendek et al. (2006a).

In view of industrial scale applications dynamic reactor systems, e.g. rotating drums, have been suggested (Fernández Bertos et al., 2004b; Zingaretti et al., 2013). These simultaneously provide agitation, exposure to the reaction gas, and mixing. Rotating drum reactors have been tested under flow-through conditions and showed superior CO_2-uptake as compared with static reactor systems (Lombardi et al., 2016).

In practice, the management of BA ageing is solely based on whether or not leachate properties comply with legal values. A comprehensive and systematic development of appropriate methods for the accelerated carbonation of BA including quality control for CO_2-uptake is lacking. As a prerequisite these require a time-resolved monitoring of the process capable of integrating over the heterogeneity of BA.

In this study we tested the hypothesis that CO_2-uptake of BA can adequately be deduced from the pressure drop observed in closed reactor systems. This would spare classical analyses and provide a better understanding of processes. In addition, pressure monitoring integrates over the whole reactor loading which circumvents problems related to small-scale variability of BA. Quantification of CO_2-uptake from pressure data was first suggested by Sun et al. (2008) for air pollution control residues. However, their application was restricted to pressures >200 kPa. This is beyond practical conditions where exhaust gas from thermal processes is an available CO_2 source. Here, we expanded the approach to atmospheric pressure conditions to monitor and evaluate the progress of carbonation. The method is based on following the pressure drop in the gas phase induced by the CO_2-uptake of BA. Suitability was tested both in a static reactor system with manual CO_2-dosage and a rotating drum reactor with automated CO_2- supply.

2.3 Material and methods

2.3.1 Bottom ash sampling and characterisation

Freshly quenched BA was obtained from a grate-type refuse derived fuel incinerator located in central Germany. Annually, the incinerator handles 25,000 metric tons of sorted commercial waste residues providing 75,000 MWh to a district heating system. Total BA production amounts to 5,000 metric tons per year, approximately. The BA was sampled at the end of an apron conveyor which transports the material from the quenching tank to the collection containers. The sample was screened to remove the 11 mm oversize fraction (about 40%-wt. of the raw sample).

Table 2.1. Moisture content, loose bulk density, particle density and particle size distribution of fresh bottom ash.

Water content % wt.	Loose bulk density kg/L	Particle density kg/L	< 0.125 mm	0.125 - 1.00 mm	1.00 - 2.00 mm	2.00 - 4.00 mm	4.00 - 11.0 mm
			% wt.				
15.2	1.14	2.78	18.7	35.8	17.9	16.8	10.8

This considered findings by Lombardi et al. (2016) according to which the coarse material contributes little to the overall carbonation. Moisture content was determined gravimetrically after drying subsamples at 105 °C for 24 h (DIN EN 12880). The particle size-distribution was determined by sieving with stainless-steel screens (mesh size 0.125, 1, 2, and 4 mm) in conformity with DIN 18123. Substance density was obtained by pycnometry (EN 11508).

The loose bulk density of the fresh BA was determined by weighing a graduated cylinder holding 100 mL of the material. Table 2.1 summarizes the results. These are consistent with values reported elsewhere (Chimenos et al., 2005; Costa et al., 2007).

2.3.2 Reactor configuration

Figure 2.1 shows the experimental set-up for the accelerated carbonation under static conditions. Experiments were conducted in glass reaction vessels with a void volume of 1 L. Six vessels connected in series were equipped with piezoresistive pressure sensors (OxiTopTM, WTW, Weilheim, Germany) and sealed air-tightly.

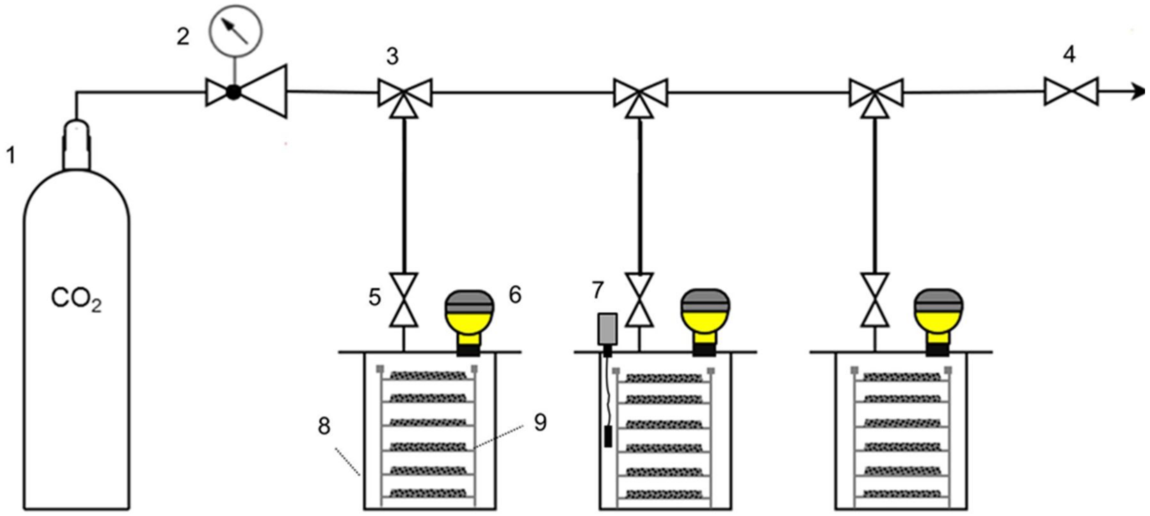

Figure 2.1 Set-up of the lab scale carbonation experiments under static conditions. (1) CO_2 supply; (2) ball valve with flow rate display; (3) 3-way valve; (4) exhaust gas; (5) 2-way valve; (6) OxiTop pressure sensor; (7) temperature and relative humidity sensor; (8) reaction vessel; (9) sample rack.

The OxiTop respirometry system is commonly used to monitor biological aerobic activity in water, soil, or waste (Ilyas et al., 2014; Rendek et al., 2006b). In the classical set-up, CO_2 evolved by respiration is trapped in NaOH causing a pressure drop in the vessel, which is proportional to O_2 consumption. In our set-up, the BA replaces the NaOH trap and the pressure course can be directly linked to the CO_2-uptake, i.e. to the progress and extent of carbonation.

For CO_2-supply, the vessels were connected to a gas cylinder (CO_2, N4.5). Throughout the experiment, we aimed at maintaining the differential pressure in the vessels between +7.5 kPa to -7.5 kPa relative to atmospheric pressure by opening the corresponding manual valves. Tests under dynamic conditions were conducted in a rotating drum reactor (Fig. 2.2) consisting of a PVC cylinder with a void volume of 71 L (internal diameter 0.3 m, length of 1 m). It was run on four rubber roller bearings attached to metal stand. Rotation was provided by tooth belt drive. The front-end covers of the reactor were fixed to the mantle by spring locks. This ensured fast opening and closure for reactor loading.

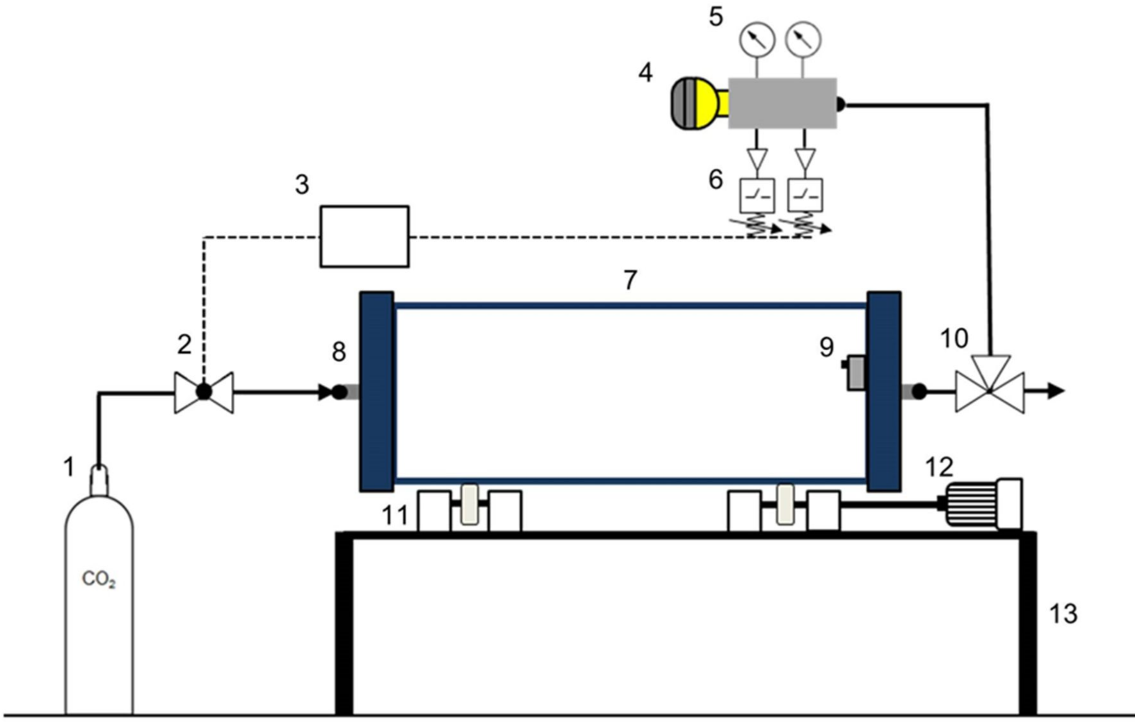

Figure 2.2 Set-up of the laboratory-scale carbonation experiments under dynamic conditions. (1) CO_2 gas cylinder; (2) 2-way magnetic valve; (3) relay (control unit); (4) slot for two piezoresistive pressure sensors; (5) pressure gauges for positive and negative pressure; (6) magnetic switches; (7) rotating drum; (8) rotating joints at the inlet and outlet of the reactor; (9) wireless temperature and relative humidity sensor; (10) 3-way valve; (11) drive roller; (12) electric motor; (13) substructure.

The CO_2-supply and the exhaust were attached to the front-end covers of the reactor via rotating joints. The supply-side was connected to a CO_2 pressure cylinder. Contrary to the static carbonation system, CO_2-dosage was automated using a relay-controlled magnetic valve connected to two magnetic switches. The lower and upper set-points for valve opening (start of CO_2-dosage) and closure (stop of CO_2-dosage) were –7.5 kPa and +7.5 kPa relative to atmospheric pressure, respectively.

The pressure course was logged at fixed intervals. Therefore, the dynamic reactor system was equipped with two separate piezoresistive pressure sensors operated in two logging periods of 0-30 minutes and 0-120 minutes (logging interval 10 seconds and 20 seconds, respectively). Temperature and relative humidity (RH) in the reaction vessels were recorded every minute using a wireless sensor (AREXX TSN-TH70E, RS Zwolle, The Netherlands) with tolerances of ± 1°C and ± 0.5 % RH. The difference between ambient and reactor temperature ($\triangle T$) served as an indicator of the self-heating induced by the carbonation.

2.3.3 Reactor preparation

For both, the static and dynamic carbonation, leak tests were performed by applying a vacuum of -30 kPa and monitoring the pressure for at least 30 minutes. To improve airtightness, all rubber seals were greased. The vessels were purged with CO_2 for 3 minutes employing volumetric flow rates of ~1 L/minute (static carbonation) and ~100 L/min (dynamic carbonation). Control measurements with a portable gas-analyser equipped with infrared sensors (Multitec ®540, SEWERIN, Gütersloh, Germany) confirmed that this purging time was sufficient to produce a pure CO_2 atmosphere.

For static carbonation, 110 g ± 0.5 g of the fresh BA were placed on sample racks (7 plains with an area of 7 cm x 7 cm) consisting of stainless-steel frames equipped with nylon flyscreens (Fig. 2.1). Each plain received a BA layer of 1 cm thickness, approximately. Subsequently, the racks were placed into the reaction vessels, which were immediately covered. For dynamic carbonation, reactor loading was carried out by removing the exhaust-side front cover. A total of 8 kg of BA was placed into a PVC half-pipe of 1 m length. Under continued purging, the half pipe was inserted into the reactor and emptied by turning. The spring-lock system ensured that reactor loading could be performed within 1 minute. To compensate CO_2 losses during loading the reactors were purged again for 2 minutes employing the above-named flow rates. After purging, the carbonation experiments were started.

2.3.4 Experiment design

A total of six static and three dynamic carbonation tests were conducted under a 100% CO_2 atmosphere. The dynamic reactor was operated under a constant rotation speed of 1.5 rpm. Taking into account the loose bulk density of BA (1.1 kg/L, Table 2.1) both the static and the dynamic tests were conducted at a volume to mass ratio of 9 L/kg. The fill-level (ratio of packed bed volume and void volume) for both reactors was 10%, approximately. All experiments were started at ambient temperature and terminated after 240 (static tests) and 120 minutes (dynamic tests). This time-scale suffices practical applications and has been recognised as adequate in terms of reaction rates (Fernández Bertos et al., 2004a; Lin et al., 2015). Reactor pressure, temperature, and RH as well leachate properties of BA and $CaCO_3$ contents were evaluated as dependent variables of the carbonation process.

2.3.5 Calculation of CO_2 uptake

The molar CO_2-uptake was determined by the pressure drop ($\Delta p_i = p_{i+1} - p_i$) between successive readings according to the universal gas equation, see equation (2.2):

$$\Delta n_{CO_2} = \sum_{i=1}^{z} \left(\frac{V}{R} \cdot \frac{\Delta p_i}{T_i} \right) \qquad \text{(Eq.2. 2)}$$

where Δn is the total molar quantity of CO_2 taken up, z is the number of logging intervals, V is the void volume of the reactor (m^3) corrected for the volume of the sample, T is the absolute temperature (K) of the gas phase and R is the universal gas constant (8.314 J/(mol K)). Integration was performed separately for each CO_2 dosage and uptake cycle ensuring positive values of Δp.

The specific CO_2-uptake ($\zeta_{Pressure}$, g CO_2 /100 g BA_{DM}) was obtained as the ratio of the mass of CO_2 (g), calculated by multiplying the molar CO_2-uptake with the molar mass of CO_2 (M_{CO_2}, 44.01 g/mol) and the reactor loading as dry mass of BA according to equation (2.3):

$$\zeta_{Pressure} = \frac{\Delta n_{CO_2} \cdot M_{CO_2}}{\text{Reactor loading (g } BA_{DM})} \cdot 100 \left(\frac{g}{100\ g} \right) \qquad \text{(Eq. 2.3)}$$

2.3.6 Analytical

Thermogravimetric analysis (TGA) is commonly employed to quantify carbonates (Costa et al., 2007; Fernández Bertos et al., 2004a; Um et al., 2013) and $Ca(OH)_2$ (Huntzinger et al., 2009; Rocca et al., 2013) in solid samples. Here, TGA was used as a benchmark of the CO_2-uptake as estimated from the pressure course. Therefore, approximately 20 g of BA_{DM} were ground in a planetary ball mill. The TGA was carried out using a thermobalance (TG 209 F1, Netzsch, Selb, Germany). Samples (~40 mg) were heated in corundum crucibles to 900°C at 20 °C/minute under a nitrogen atmosphere. The weight loss (WL, g CO_2/100 g BADM) due to carbonate decomposition was quantified according to equation (2.4):

$$\mathrm{WL} = \frac{\Delta m_{(480\text{ - }800\ ^\circ\mathrm{C})}\ (\mathrm{g})}{\text{Sample mass (g }\mathrm{BA_{DM}})} \cdot 100 \left(\frac{\mathrm{g}}{100\ \mathrm{g}}\right) \qquad \text{(Eq. 2.4)}$$

with △m(480 - 800 °C) as the mass loss observed between 480 °C and 800 °C.

The specific CO_2-uptake based on TGA (ζTG, g CO_2/100g BA_{DM}) was obtained from the difference in WL of fresh and carbonated samples according to equation (2.5):

$$\zeta_{\mathrm{TG}} = \frac{\text{WL carbonated BA} - \text{WL fresh BA}}{(1 - \text{WL carbonated BA})} \qquad \text{(Eq. 2.5)}$$

The $Ca(OH)_2$ content of the solid can be determined for the mass loss (△m(230 - 430 °C)) observed in the temperature window between 230 °C and 430 °C according to equation 2.6:

$$\mathrm{Ca(OH)_2} = \frac{\Delta m_{(230\text{ - }430\ ^\circ\mathrm{C})}\ (\mathrm{g})}{\text{Sample mass (g)}} \cdot 100 \left(\frac{\mathrm{g}}{100\ \mathrm{g}}\right) \cdot \left(\frac{M_{\mathrm{Ca(OH)_2}}}{M_{\mathrm{H_2O}}}\right) \qquad \text{(Eq. 2.6)}$$

with $M_{Ca(OH)_2}$ and M_{H_2O} as the molar mass of $Ca(OH)_2$ (74.10 g/mol) and H_2O (18.02 g/mol), respectively. Here, the $Ca(OH)_2$ content of fresh BA served as a proxy for the CO_2-uptake capacity and was quantified as 5.14 ± 0.53 g $Ca(OH)_2$ / 100 g BA_{DM} (three-fold determination) which corresponds to a CO_2-uptake capacity of 3.06 g CO_2 / 100 g BA_{DM}).

To evaluate the effect of carbonation on the leachability of BA, batch leaching tests were performed with fresh and carbonated samples at a liquid-to-solid ratio (L:S) of 10 according to EN 12457-2. The pH and electrical conductivity of fresh BA leachates were 12.6 and 11.60 mS/cm, respectively (n = 6).

2.4 Results and discussion

2.4.1 Static carbonation tests

The performance of the monitoring system was tested under static conditions in six experimental runs with a reactor loading of 110 g fresh BA exposed to a 100% CO_2 atmosphere. Complementary information about the reaction conditions was obtained by logging RH and temperature.

Figure 2.3 shows the time courses of RH, temperature, differential pressure and specific CO_2-uptake for a representative experimental run. The differential pressure followed a sawtooth pattern imposed by carbonation and its compensation by manual CO_2-dosage. The CO_2-uptake shows a steep initial increase (first 30 minutes) and then gradually levels off (Figure 2.3a). This is consistent with findings by Fernández Bertos et al. (2004a) and Um et al. (2013). After 120 minutes, a CO_2-uptake of 1.50 g CO_2/100 g BA_{DM} was attained which accounts for 86% of the final uptake (see Table 2.2).

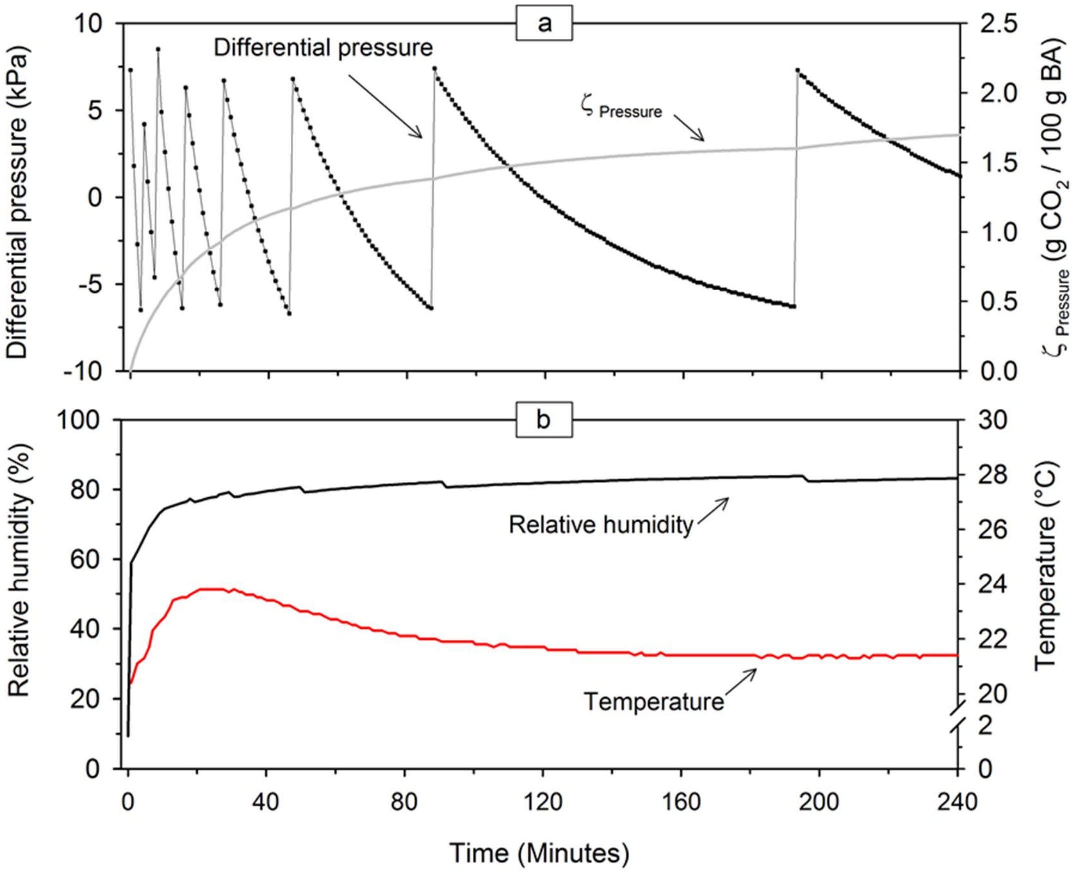

Figure 2.3 a) Differential pressure and CO_2 uptake ($\zeta_{Pressure}$) and b) temperature and relative humidity during static carbonation for a reactor loading of 0.11 kg (BA, bottom ash) and a 100 % CO_2 atmosphere.

Since carbonation is exothermic (cf. Eq. 2.1), self-heating of BA can be expected. Indeed, a temperature increase of up to 90 °C was reported for a BA mono landfill (Klein et al., 2001). Our data show that carbonation was accompanied by an initial temperature increase, which peaked at 24 °C after 20 minutes (Fig. 2.3b).

With ongoing carbonation, the temperature progressively dropped and returned to ambient conditions after about 160 minutes. Since temperature is a variable in the universal gas equation, self-heating affects the CO_2-uptake estimation. However, for the observed ΔT (3 - 4 °C) the effect is less than 1 % of the final CO_2-uptake. Thus, it seems acceptable to assume isothermal conditions when temperature logging is not viable.

Due to the use of moist BA (see Table 2.1) the RH increased rapidly (Fig. 2.3b) and constant values of 78% ± 2% were attained after 10 minutes, approximately. Small dents in the humidity course are attributed to intermittent CO_2-dosage whereby a small amount of dry gas was fed into the reactor.

Table 2.2 summarizes the CO_2-uptake of BA, the temperature increase and RH for the six experimental runs as well as pH and electrical conductivity determined in the leachates of the carbonated BA. Estimating the CO_2-uptake from the pressure drop shows satisfactory reproducibility (standard deviation: 0.09 g CO_2 / 100g BA_{DM}). As a benchmark for the calculated CO_2-uptake the increase in carbonate content was determined by TGA according to Eq. 5. It is apparent that the methods agree favourably. The leachate pH of carbonated BA was 12.2 compared to 12.6 in the leachates of the fresh BA (see Table 2.2). While some alkalinity was consumed pH is still buffered by $Ca(OH)_2$ (Dou et al., 2017). This is consistent with a CO_2-uptake in the order of 50% of carbonation capacity (cf. section 2.5). The electrical conductivity was considerably lowered compared to the fresh BA (5.6 mS/cm vs. 11.6 mS/cm), primarily due to neutralization of OH^-.

Table 2.2 Results of the static carbonation tests; CO_2-uptake of BA_{DM} (dry matter) after 240 minutes as obtained from the pressure course ($\zeta_{Pressure}$) and by thermogravimetric analysis (ζ_{TG}), temperature increase (ΔT), relative humidity (RH) as well as pH and electrical conductivity (EC) determined in batch leachates (n = 6).

	$\zeta_{Pressure}$	ζ_{TG}	ΔT	RH	pH	EC
	(g CO_2 / 100 g BA_{DM})		(°C)	(%)	(-)	(mS/cm)
Arithmetic mean	1.90	1.88	3.7	82.1	12.2	5.51
Standard deviation	0.09	0.18	0.3	0.7	0.1	0.34

2.4.2 Dynamic carbonation tests

Previous studies indicated that carbonation of alkaline materials may be enhanced under dynamic reaction conditions (Fernández Bertos et al., 2004a; Jiang et al., 2009; Lombardi et al., 2016). Therefore, the monitoring system was adapted to a rotating drum reactor. Dynamic carbonation tests were performed with a reactor loading of 8 kg of fresh BA exposed to a 100% CO_2 atmosphere in four replications. Figure 2.4 shows the temperature, RH, differential pressure, and CO_2-uptake for a representative run. Compared to the duration of the static tests (240 minutes) a shorter reaction time was chosen since most of the CO_2-uptake was expected to take place in 120 minutes.

The automated CO_2-supply yielded a more uniform sawtooth pattern compared to the manual CO_2-dosage. Under dynamic conditions self-heating (ΔT = 5 - 9 °C) was more pronounced and CO_2-uptake was higher (2.56 g CO_2/100 g BA_{DM}). This suggests that the solid's motion exposed internal surfaces susceptible to the mass exchange between BA and CO_2.

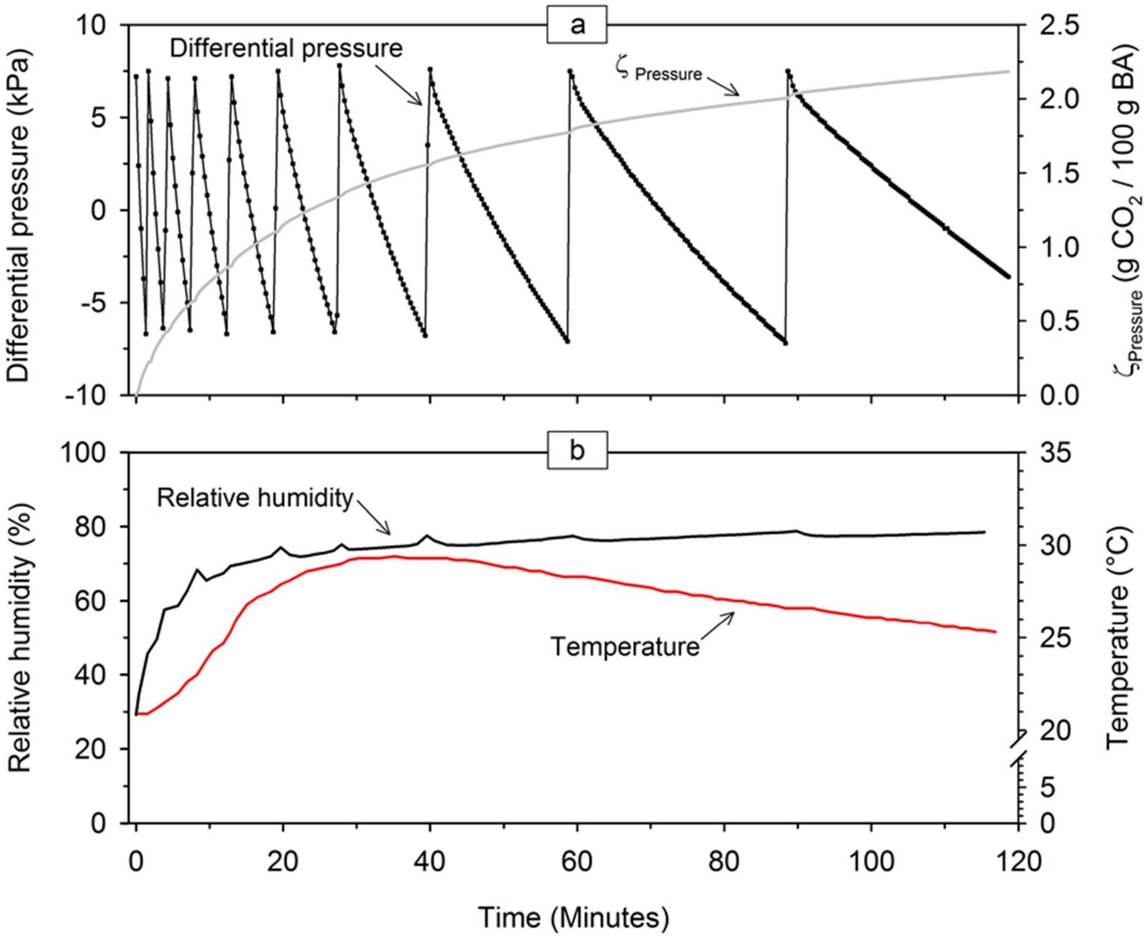

Figure 2.4 a) Differential pressure and CO_2 uptake ($\zeta_{Pressure}$) and b) temperature and relative humidity during dynamic carbonation for a reactor loading of 8 kg (BA, bottom ash) and a 100 % CO_2 atmosphere.

Both the temperature and the CO_2-uptake characteristic indicate that turnover could have been enhanced further by increasing the reaction time. Compared to static conditions the RH increase was slightly delayed owing to the specific material distribution within the reactors (static: thin layers of BA distributed over the planes of a rack; dynamic: moving bed). However, the equilibrium values of RH compare favourably for the two systems.

Table 2.3 summarizes the CO_2-uptake of BA, the temperature increase, RH for the four experimental runs as well as pH and electrical conductivity determined in the leachates of the carbonated BA. Results largely substantiate the findings for the static application. Yet, the CO_2-uptake as measured by TGA was higher than determined by the pressure drop and the data showed a stronger scatter. The first may be attributed to reactor preparation. As described in section 2.3, a purging time of two minutes is required to compensate CO_2 losses from the loading procedure. During purging, the CO_2-uptake cannot be monitored. Therefore a small initial part of the carbonation passes unnoticed. The pressure course of the first ten minutes reveals three dosage events. Thus, purging time correspond to one CO_2 dosage, approximately. Considering the total number of dosages (9-10) this accounts 10 % of the total CO_2-uptake. Uptake of CO_2 during purging may be prevented by initially covering the BA with a thin layer of sand. Therewith BA exposure to CO_2 would be postponed to the onset of reactor rotation after purging. The higher scatter of TGA data (standard deviation) may be an effect of sample heterogeneity. While estimation of CO_2-uptake from the pressure drop integrates over the whole reactor loading, TGA relies on the analysis of a small BA aliquot (sample mass: 20 g).

The leachate pH of BA carbonated under dynamic conditions was 11.4 and about 1 pH unit below the pH of the fresh BA. The electrical conductivity dropped from 11.6 to 4.1. The more pronounced effect of carbonation on leachate quality compared to the static conditions is in accordance with the higher carbonation turnover indicated by the CO_2-uptake and $\triangle T$.

Overall, also the results of the dynamic carbonation test suggest that our method is suited for the monitoring of accelerated carbonation, e.g. in processes studies aiming at optimized operating conditions. Since rotating drums have been suggested for accelerated carbonation, the presented dynamic system might be useful to study the effect of operating conditions to gather valuable information prior to scale-up.

Table 2.3 Results of the dynamic carbonation tests; CO_2-uptake of BA_{DM} (dry matter) after 120 minutes as obtained from the pressure course ($\zeta_{Pressure}$) and by thermogravimetric analysis (ζ_{TG}), temperature increase (ΔT), relative humidity (RH) as well as pH and electrical conductivity (EC) determined in batch leachates (n = 4).

	$\zeta_{Pressure}$	ζ_{TG}	ΔT	RH	pH	EC
	(g CO_2 / 100 g BA_{DM})		(°C)	(%)	(-)	(mS/cm)
Arithmetic mean	2.56	2.72	7.7	78	11.4	4.09
Standard deviation	0.09	0.21	1.3	1.9	0.2	0.09

2.4.3 Evaluation of carbonation kinetics

Previous studies have shown that carbonation kinetics of BA (Nam et al., 2012; Um et al., 2013) and air pollution control residues (Sun et al., 2008) can be adequately described by two solid-state kinetic models that were combined into Eq. (2.7) (Khawam and Flanagan, 2006):

$$1 - (1 - \alpha)^{1/3})^{n} = kt \qquad \text{(Eq. 2.7)}$$

with k as the rate constant, t as the reaction time, n as a (parametrizable) index of the rate determining step, and α as the conversion factor (carbonation turnover, α = 1 for full carbonation) according to Eq. (2.8).

$$\alpha = C_t/Ca(OH)_2 \qquad \text{(Eq. 2.8)}$$

with C_t as the specific molar amount of CO_2 taken up by BA at time t (mol/100 g BA_{DM}) and $Ca(OH)_2$ as the molar $Ca(OH)_2$ content of fresh BA (mol $Ca(OH)_2$/100g BA_{DM}). The latter was determined independently by TGA (see section 2.5).

By adapting the exponent n in Eq. (2.7), two kinetic models can be defined. For n = 1, Eq 2.7 represents a purely phase-boundary controlled reaction that applies to the initial stages of carbonation. For n = 2 Eq. 2.7 applies to a diffusion-limited reaction (Jander equation), where the rate-limiting step is diffusion through the growing layer of precipitated $CaCO_3$. The conformity between experimental data and the kinetic model was expressed by the correlation coefficients (R^2).

Figure 2.5 shows the converted experimental data of the carbonation tests (i.e. $\ln(1- (1 - \alpha)^{1/3})$ vs. ln(t). A relatively high R^2 value indicates that the model successfully describes the kinetics of carbonation. Fits of Eq. 2.7 to the converted data suggest that the reaction is phase-boundary controlled during the initial stages of accelerated carbonation ($\ln(t) < 3.6$) irrespective of static or dynamic conditions. With ongoing turnover, carbonation becomes controlled by diffusion through the product-layer. The transition between the two kinetic models is illustrated by the change of the slope for the plot of $\ln(1 - (1 - \alpha)^{1/3})$ vs. ln(t) (Fig. 2.5). The change in slope seems to be less pronounced under dynamic reaction conditions. This indicates that rate limitations by diffusion through a growing layer of precipitated $CaCO_3$ are less important when the solid is in motion (exposure of internal surfaces) corroborating the higher CO_2-uptake.

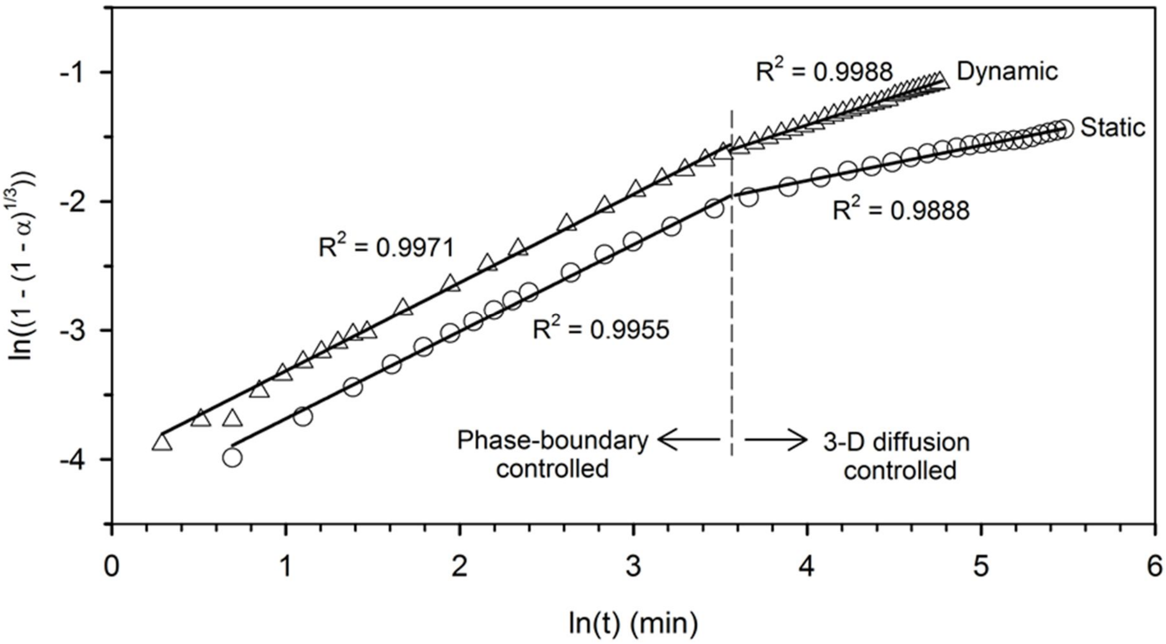

Figure 2.5 Evaluation of carbonation kinetics: $\ln(1-(1-\alpha)^{1/3})$ versus ln(t) for static and dynamic carbonation (R^2 = correlation coefficient).

2.5 Conclusions

Here we reported on a fast and simple method to quantify the carbonation of BA under static and dynamic conditions based on a monitoring of the pressure in the reaction vessel. Results demonstrate the serviceability and reproducibility of the approach as compared to the analytical quantification of carbonates. In combination with static carbonation set-ups, the method may be suited for a routine assessment of the CO_2-uptake capacities of BA and other alkaline materials. Specifically, the ability to follow the process online gives insight into carbonation kinetics (e.g. as influenced by operating conditions) without the need to vary the reaction time in separate runs and at minimum analytical expense. Evaluation of carbonation capacities may be particularly useful in the context of taking accelerated carbonation to the industrial scale. As a prerequisite, however, the laboratory findings presented here need to be verified on a pilot-scale.

2.6 Acknowledgement

This project (HA project no. 483/15-25) is funded in the framework of Hessen ModellProjekte, financed with funds of LOEWE – Landes-Offensive zur Entwicklung Wissenschaftlich-ökonomischer Exzellenz, Förderlinie 3: KMU-Verbundvorhaben (State Offensive for the Development of Scientific and Economic Excellence). We thank Mr Jürgen Henkel for technical assistance.

2.7 References

Arickx, S., van Gerven, T., Vandecasteele, C., 2006. Accelerated carbonation for treatment of MSWI bottom ash. J. Hazard. Mater., 137 (1), 235–243.

Astrup, T., 2007. Pretreatment and utilization of waste incineration bottom ashes: Danish experiences. Waste Manage., 27 (10), 1452–1457.

Baciocchi, R., Costa, G., Lategano, E., Marini, C., Polettini, A., Pomi, R., Postorino, P., Rocca, S., 2010. Accelerated carbonation of different size fractions of bottom ash from RDF incineration. Waste Manage., 30 (7), 1310–1317.

Chimenos, J.M., Fernández, A.I., Miralles, L., Rosell, J.R., Ezquerra, A.N., 2005. Change of mechanical properties during short-term natural weathering of MSWI bottom ash. Environ. Sci. Technol., 39 (19), 7725–7730..

Costa, G., Baciocchi, R., Polettini, A., Pomi, R., Hills, C.D., Carey, P.J., 2007. Current status and perspectives of accelerated carbonation processes on municipal waste combustion residues. Environ. Monit. Assess., 135 (1-3), 55–75. DIN 18123, 2011. Soil, investigation and testing - Determination of grain-size distribution. German standard methods.

DIN EN 11508, 2014. Soil quality - Determination of particle density. German version of European standard.

DIN EN 12880, 2001. Characterization of sludges - Determination of dry residue and water content. German version of European standard.

DIN EN 12457-2, 2003. Characterization of waste - Leaching; Compliance test for leaching of granular and sludges - Part 2. German version of European standard.

Dou, X., Ren, F., Nguyen, M.Q., Ahamed, A., Yin, K., Chan, W.P., Chang, V.W.-C., 2017. Review of MSWI bottom ash utilization from perspectives of collective characterization, treatment and existing application. Renew. Sust. Energ. Rev. 79, 24–38.

Fernández Bertos, M., Li, X., Simons, S.J.R., Hills, C.D., Carey, P.J., 2004a. Investigation of accelerated carbonation for the stabilisation of MSW incinerator ashes and the sequestration of CO_2. Green Chem., 6 (8), 428–436.

Fernández Bertos, M., Simons, S.J.R., Hills, C.D., Carey, P.J., 2004b. A review of accelerated carbonation technology in the treatment of cement-based materials and sequestration of CO_2. J. Hazard. Mater., 112 (3), 193–205..

Huntzinger, D.N., Gierke, J.S., Kawatra, S.K., Eisele, T.C., Sutter, L.L., 2009. Carbon dioxide sequestration in cement kiln dust through mineral carbonation. Environ. Sci. Technol., 43 (6), 1986–1992.

Ilyas, A., Lovat, E., Persson, K.M., 2014. Effects of substrate induced respiration on the stability of bottom ash in landfill cover environment. Waste Manage. Res., 32 (12), 1241–1246.

Jiang, J.-G., Du, X.-J., Chen, M.-Z., Zhang, C., 2009. Continuous CO_2 capture and MSWI fly ash stabilization, utilizing novel dynamic equipment. Environ. Pollut., 157 (11), 2933–2938.

Johnson, D.C., 2000. Accelerated carbonation of waste calcium silicate materials. SCI Lecture papers series (108).

Khawam, A., Flanagan, D.R., 2006. Solid-state kinetic models: Basics and mathematical fundamentals. J. Phys. Chem. B, 110 (35), 17315–17328.

Klein, R., Baumann, T., Kahapka, E., Niessner, R., 2001. Temperature development in a modern municipal solid waste incineration (MSWI) bottom ash landfill with regard to sustainable waste management. J. Hazard. Mater., 83 (3), 265–280.

Lin, W.Y., Heng, K.S., Sun, X., Wang, J.-Y., 2015. Accelerated carbonation of different size fractions of MSW IBA and the effect on leaching. Waste Manage., 41, 75–84.

Liu, A., Ren, F., Lin, W.Y., Wang, J.-Y., 2015. A review of municipal solid waste environmental standards with a focus on incinerator residues. Int. J. Sustain. Built Environ., 4 (2), 165–188.

Lombardi, L., Carnevale, E.A., Pecorini, I., 2016. Experimental evaluation of two different types of reactors for CO_2 removal from gaseous stream by bottom ash accelerated carbonation. Waste Manage., 58, 287–298.

Nam, S.-Y., Seo, J., Thriveni, T., Ahn, J.-W., 2012. Accelerated carbonation of municipal solid waste incineration bottom ash for CO_2 sequestration. Geosys. Eng. 15 (4), 305–311.

Pan, S.-Y., 2012. CO_2 capture by accelerated carbonation of alkaline wastes: A review on its principles and applications. Aerosol Air Qual. Res., 12, 770–791

Rendek, E., Ducom, G., Germain, P., 2006a. Carbon dioxide sequestration in municipal solid waste incinerator (MSWI) bottom ash. J. Hazard. Mater., 128 (1), 73–79.

Rendek, E., Ducom, G., Germain, P., 2006b. Influence of organic matter on municipal solid waste incinerator bottom ash carbonation. Chemosphere 64 (7), 1212–1218.

Rocca, S., van Zomeren, A., Costa, G., Dijkstra, J.J., Comans, R.N.J., Lombardi, F., 2013. Mechanisms contributing to the thermal analysis of waste incineration bottom ash and quantification of different carbon species. Waste Manage. 33 (2), 373–381.

Saffarzadeh, A., Shimaoka, T., Wei, Y., Gardner, K.H., Musselman, C.N., 2011. Impacts of natural weathering on the transformation/neoformation processes in landfilled MSWI bottom ash: A geoenvironmental perspective. Waste Manage., 31 (12), 2440–2454.

Sakita, S., Nishimura, K., 2015. Physical containment of municipal solid waste incineration bottom ash by accelerated carbonation. J. Mater. Cycles Waste Manage., 18 (4), 1–8.

Santos, R.M., Mertens, G., Salman, M., Cizer, Ö., van Gerven, T., 2013. Comparative study of ageing, heat treatment and accelerated carbonation for stabilization of municipal solid waste incineration bottom ash in view of reducing regulated heavy metal/metalloid leaching. J. Environ. Manage., 128, 807–821.

Sun, J., Bertos, M.F., Simons, S.J.R., 2008. Kinetic study of accelerated carbonation of municipal solid waste incinerator air pollution control residues for sequestration of flue gas CO_2. Energy Environ. Sci. 1 (3), 370–377.

Um, N., Nam, S.-Y., Ahn, J.-W., 2013. Effect of accelerated carbonation on the leaching behavior of Cr in municipal solid waste incinerator bottom ash and the carbonation kinetics. Mater. Trans., 54 (8), 1510–1516.

van Gerven, T., van Keer, E., Arickx, S., Jaspers, M., Wauters, G., Vandecasteele, C., 2005. Carbonation of MSWI-bottom ash to decrease heavy metal leaching, in view of recycling. Waste Manage., 25 (3), 291–300..

Verbinnen, B., Billen, P., van Caneghem, J., Vandecasteele, C., 2016. Recycling of MSWI bottom ash: A review of chemical barriers, engineering applications and treatment technologies. Waste Biomass. Valor., 4 (7), 695–709.

Zingaretti, D., Costa, G., Baciocchi, R., 2013. Assessment of the Energy Requirements for CO_2 storage by carbonation of industrial residues. Part 1: Definition of the process layout. Energy Procedia 37, 5850–5857.

Chapter 3 Accelerated carbonation of waste incineration bottom ash in a rotating drum batch reactor

Journal of Environmental Chemical Engineering (2018) 6: 5259-5268.
DOI: 10.1016/j.jece.2018.08.024

Co-authors: Kevin Schnabel, Tim Mansfeldt, Harald Weigand

Formatting and orthography of the manuscript is adapted to the dissertation style.

3.1 Abstract

Accelerated carbonation is known to improve the leaching behaviour and geotechnical properties of waste incineration bottom ash (BA). Regarding process implementation on the industrial scale dynamic reactor configurations may be particularly suited since they enhance the mass exchange between gas and solid. Here we evaluated the influence of fundamental parameters on accelerated carbonation of BA in a rotating drum batch reactor equipped with an automated CO_2 supply at close to atmospheric pressure conditions. Firstly, the effect of rotation speed and reactor fill level on the solids motion was studied. Secondly, the effects of CO_2-concentration, fill level, and moisture on BA carbonation were investigated. Evaluation was based on the observed CO_2 uptake, self-heating, and BA leachability. The bed behaviour of BA strongly differed from that of standard materials and was more affected by fill level than by rotation speed. The fill level was not a limiting factor for BA carbonation within the tested range (7-45 vol.-%). Both the CO_2 uptake rate and the final level of carbonation increased as the CO_2-concentration was raised from 15 to 75 vol.-%. A close relationship between CO_2 uptake and reactor temperature was confirmed by benchmarking a heat balance model against the carbonation enthalpy. Carbonated BA exhibited a strongly decreased mobility of Pb and Zn as compared to fresh BA. The leaching behaviour of BA could be improved such as to comply with the German landfill ordinance for non-hazardous waste.

Keywords: Bottom ash, accelerated carbonation, carbon dioxide, rotating drum

Graphical abstract

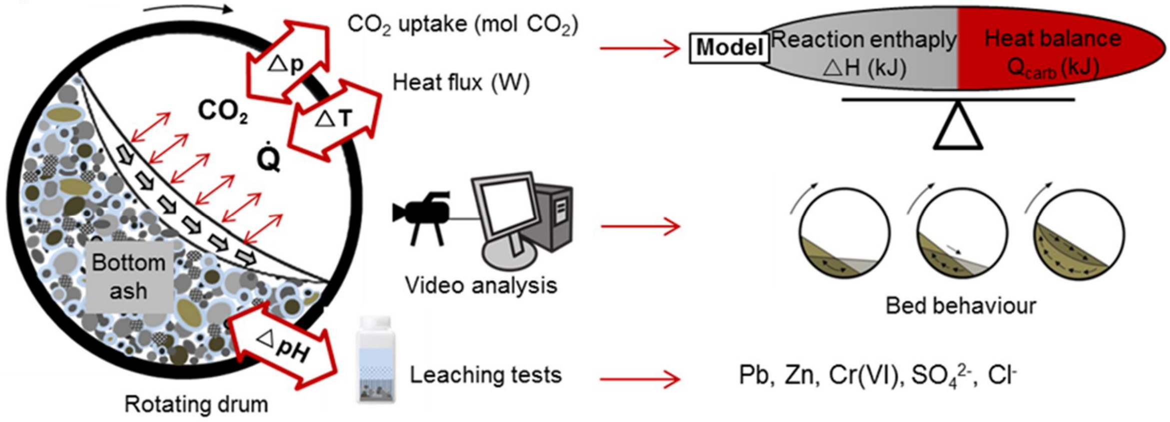

3.2 Introduction

Bottom ash (BA) is the dominant solid residue generated in municipal solid waste incinerators and waste-to-energy plants and amounts to between 20 and 30% of the original input (Sabbas et al., 2003). Fresh BA contains reactive alkaline constituents (mainly $CaO/Ca(OH)_2$) and exhibits a high leachability of trace metals (e.g. Pb, Zn, Cu). Ageing reduces the mobility of the aforementioned contaminants in BA and is commonly applied prior to geotechnical utilization or landfilling of the material (Dou et al., 2017). One of the most important ageing processes is carbonation by atmospheric carbon dioxide (CO_2), an irreversible gas/solid reaction mediated by pore water. Through this reaction $Ca(OH)_2$ is converted to $CaCO_3$ and alkalinity is consumed. Under ambient conditions carbonation is slow (Costa et al., 2007) and limited by the access of CO_2 (Arickx et al., 2006). Therefore, BA is typically stored in open stockpiles for several months (Astrup, 2007; Dou et al., 2017; Santos et al., 2013), periodically turned, and potentially watered. In recent years, efforts have been made to circumvent storage requirements especially in densely populated areas (Lin et al., 2015b) by accelerating the carbonation of BA under controlled conditions. This may be achieved in static reactor systems by exposing the material to CO_2 partial-pressures values of typically above 100 kPa (Baciocchi et al., 2010; Fernández Bertos et al., 2004a; Rendek et al., 2006) or passing CO_2 rich gas streams over thin layers of BA in climate chamber systems at ambient pressure (Lin et al., 2015a; Nam et al., 2012; Um et al., 2013).

As an alternative, dynamic reactor configurations, e.g. rotating drums, may be employed. In rotating drums the BA is mixed to improve the mass transfer between the gas and the solid (Fernández Bertos et al., 2004b; Zingaretti et al., 2013) yielding comparably higher CO_2 uptake rates (Brück et al., 2018; Lombardi et al., 2016). Beyond BA, rotating drums have proven useful for the accelerated carbonation of other alkaline residues like fly ash, biomass ash, and paper ash (Gunning et al., 2010; Łączny et al., 2015). Overall, the dynamic conditions prevailing in rotating drums seem favourable for the accelerated carbonation on the industrial scale. Yet, prior to the integration into the management of BA optimum drum operating conditions need to be identified.

Knowledge of the bed behaviour of BA under drum operation is crucial for the reactor layout. The radial motion determines the degree of material mixing and the rate of heat and mass transfer both inside the material bed and between the bed surface and the headspace (Ding et al., 2001b). Contrary to the bed behaviour of dry standard materials little is known about the motion of wet BA in rotating drums and its implications for accelerated carbonation.

Wetness of BA is a consequence of the quenching process applied at most waste incinerators and is, at the same time, a prerequisite for carbonation since the related reactions take place in the pore water (Costa et al., 2007). Excess moisture may, however, slow down carbonation due to the low diffusivity of CO_2 in water (Arickx et al., 2006). For freshly quenched BA, moisture contents of 20 to 46 wt.-% have been reported (Inkaew et al., 2016). The actual value of the critical moisture content may depend on the grain size distribution of BA and the reaction conditions (Lin et al., 2015b).

The exothermal carbonation reaction leads to a self-heating of BA (Hao et al., 2017). In principle, heating may feed-back into the rates of CO_2 and $Ca(OH)_2$-dissolution as well as carbonate precipitation (Costa et al., 2007; Pan, 2012). However, temperature effects on carbonation have so far only been investigated with external heating (Lin et al., 2015b; Nam et al., 2012; van Gerven et al., 2005) and a clear temperature optimum could not be identified.

A series of CO_2 sources have been suggested for the accelerated carbonation of BA including stack gas from waste incinerators (Nam et al., 2012; van Gerven et al., 2005), syngas from gasification processes (Zingaretti et al., 2014), biogas (Baciocchi et al., 2013; del Valle-Zermeño et al., 2015; Mostbauer et al., 2014) and landfill gas (Mostbauer et al., 2014). Depending on origin, the CO_2 concentration ranges from 5 to 70 vol.-%, yet a systematic study on the effect of CO_2 concentration on the accelerated carbonation at atmospheric pressure is lacking.

Most of the research has been devoted to individual aspects of accelerated carbonation under static conditions. Here, we aimed at providing a systematic insight into the accelerated carbonation of BA in a rotating drum. Firstly, the BA bed behaviour was studied as function of the rotation speed and reactor fill level. Secondly, a series of accelerated carbonation tests were performed at near atmospheric pressure employing an automated CO_2 supply. To identify optimum operating conditions the effects of reactor fill level, CO_2 concentration, and BA moisture were investigated. The experiments were evaluated in terms of CO_2 uptake by BA, self-heating, and leaching behaviour.

3.3 Theory: Radial motion of solids in rotating drums

Besides the rheological properties of the solid, the bed behaviour in rotating drums depends on rotation speed, drum diameter, fill level, and surface roughness of the drum (Liu et al., 2005; Zhu et al., 2008). For unbaffeled drums, i.e. reactors without mixing tools, six basic radial motion patterns have been recognized (Boateng, 2015; Henein et al., 1983) and denoted as slipping, slumping, rolling, cascading, cataracting and centrifuging with transitions in between (Henein et al., 1983). Regarding industrial applications of rotating drum reactors (Ding et al., 2001b; Mellmann et al., 2004) only the first three patterns (see Figure 3.1) are deemed relevant.

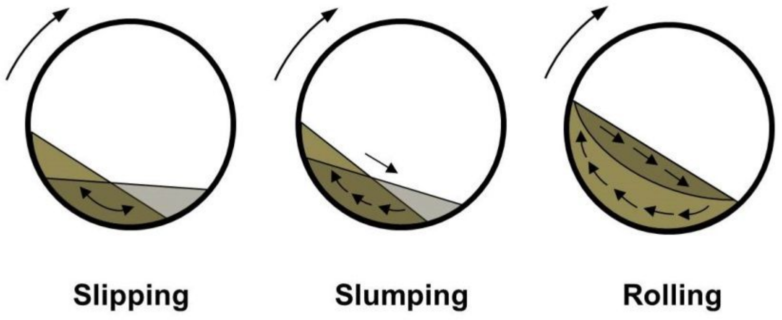

Figure 3.1 Schematic of selected modes of radial bed motion in rotating drums.

Slipping motion is likely to occur at slow rotation and at low friction between the solid and drum wall (Mellmann, 2001). Under these conditions the bulk material slips along the drum wall either permanently (‘sliding’) or alternatingly after exceeding a critical angle (‘surging’, see Figure 3.1). Since the solid bed moves essentially as a whole only little radial mixing happens.

By increasing the rotation speed the bed motion will typically move from slipping to slumping. Thereby, the rotating drum wall periodically lifts the whole bed until a segment of the shear wedge becomes unstable and slides down the slope (Boateng, 2015). Under slumping conditions a fractional movement of the bed interior is achieved. This causes a radial mixing component as a combined effect of mixing of wedges and mixing within wedges (Metcalfe et al., 1995).

If the rotation speed increases further a rolling flow regime develops. Rolling motion is characterized by continuous movement of a thin layer of solids over the inclined bed. Under these conditions mixing occurs in the so called ‘active layer’. Since the free surface is continuously renewed, mixing and heat exchange is expected to be more efficient in comparison to slumping or slipping flow (Boateng, 2015). However, contrary findings have also been reported (Ding et al., 2001a).

Bottom ash is a heterogeneous mixture of particles with diameters ranging from powder to coarse aggregates (Inkaew et al., 2016). Differences in particle size, shape or density may cause segregation (Chou et al., 2010) when the material is dry. However, seggregation may be inhibited in presence of a water phase (Chou et al., 2010; Yang and Hsiau, 2005). Bottom ash is usually a wet system since the majority of incinerators employ a wet deslagging (quenching step). It is well known that the bed motion of granular material in rotating drums becomes very complicated even when just a small amount of liquid is added (Chou et al., 2010; Nase et al., 2001). Water forms a liquid bridge between grains that increase cohesion forces which in turn affects the solid motion (Chou and Hsiau, 2011).

3.4 Material and methods

3.4.1 Bottom ash sampling and characterisation

The experiments were carried out over a time period of 10 weeks. For logistic reasons and to prevent BA ageing during long storage times the BA was collected at two different occasions. The material was obtained from a grate-type refuse derived fuel incinerator located in central Germany. For details of the plant refer to (Brück et al., 2018). Two samples comprising 200 kg (BA sample 1) and 400 kg (BA sample 2) were taken from the roofed temporary storage pile. The BA was manually passed through an 11 mm sieve and the oversize grain was discarded. This was done since the coarse fraction of BA (i) is rather uncritical in terms of contaminant leaching and (ii) contributes little to carbonation. The samples were stored in air-tight clamping ring drums until used in the experiments.

Moisture content was determined gravimetrically after drying subsamples at 105 °C for 24 h. The loose bulk density of the fresh BA was determined by weighing a graduated cylinder holding 100 mL of the material. The $Ca(OH)_2$ content of the BA was determined by thermogravimetric analysis (TGA) from the weight loss caused by decomposition of $Ca(OH)_2$ between 380 °C and 480 °C employing a thermobalance [TG 209 F1, Netzsch, Selb, Germany]. Therefore, approximately 20 g of dry BA were ground in a planetary ball mill. Samples were heated in corundum crucibles to 900°C at 20 °C/minute under a nitrogen atmosphere.

Table 3.1 summarizes BA properties. While the moisture content and bulk density were almost identical for both samples a higher $Ca(OH)_2$ content was found for sample 2.

Table 3.1 Properties of BA sample 1 and 2 (replications: n=5 for sample 1 and n=10 for sample 2).

Sample Nr. (quantity)	1 (200 kg)			2 (400 kg)		
	Min	Mean	Max	Min	Mean	Max
Moisture (wt.-%)	13.3	15.3	17.9	13.5	14.7	17.3
Loose bulk density (kg/L)	0.96	1.06	1.14	0.95	1.04	1.12
$Ca(OH)_2$ (wt.-%)	2.38	2.59	2.84	2.88	3.40	4.48

3.4.2 Experimental setup

The experiments were conducted in a rotating drum reactor (diameter: 0.3 m, length: 1.0 m) equipped with an automated CO_2 supply system. To adjust the initial CO_2 concentration the reactor was purged before (3 min), during (1 min) and after (2 min) reactor loading. To provide CO_2 concentrations lower than 100 % compressed air and CO_2 gas (N4.5) were mixed using a gas mixing station [Gmix HiTec Zang GmbH, Herzogenrath, Germany].

For reactor loading, the required amount of BA was filled into PVC half-pipes of 1 m length. Under continued purging the front end cover of the reactor was removed. The halfpipes were then inserted into the reactor and quickly emptied by turning. Thereafter, the reactor was closed and pressure logging was initiated. CO_2 supply was automated using a relay-controlled magnetic valve connected to two magnetic switches. The valve was connected to a CO_2 pressure cylinder and the reactor was operated between pre-defined pressure set-points (-7.5 kPa and +7.5 kPa relative to atmospheric pressure, respectively) by opening and closing CO_2 supply. Carbonation of BA was quantified from the logged pressure course and specified as the CO_2 uptake by 100 g dry matter of BA (BA_{DM}). For a detailed description refer to (Brück et al., 2018).

Temperature and relative humidity inside the reactor as well as the ambient temperature were recorded every minute using wireless sensors [AREXX TSN-TH70E, RS Zwolle, The Netherlands] with tolerances of ± 1°C and ± 0.5 % RH. The self-heating of BA induced by the exothermic carbonation reaction was monitored by the differential temperature ($\triangle T$). The latter is defined as the difference between reactor temperature (T_{in}) and ambient temperature (T_{amb}). For comparisons among the experimental runs also the maximum differential temperature ($\triangle T_{max}$) was calculated as the difference between the maximum reactor temperature and T_{amb}.

3.4.3 Characterization of the radial mixing of BA

Bed motion in rotating drums affects heat and mass transfer and follows characteristic patterns depending on reactor operation (Mellmann, 2001). The bed behaviour was cinematographically analysed. Therefore the rear end of the reactor was equipped with a transparent acrylic glass plate and the bed motion was recorded with a video camera [Logitech c920 HD, resolution 1,920 x 1,080 pixels] while the reactor was completely encased and illuminated with three diffusor lamps.

The bed behaviour was studied under varied rotation speed and fill level employing BA sample 1. A first test series was conducted with fill levels as aimed at in the accelerated carbonation experiments (see section 3.4) applying seven different rotation rates between 0.4 to 8.0 rpm. In a second test series specific rotation rates and fill levels were chosen to identify the transitions between types of solid motion. The solid motion was recorded for at least two minutes for each combination of reactor loading and rotation rate. The videos were visually analysed in terms of the mode of transversal bed motion (slipping, slumping, rolling, or transitional). Prior to all runs the BA was replaced to circumvent changes of the rheological properties due to, e.g., granulation or crushing of BA aggregates.

3.4.4 Accelerated carbonation tests

The accelerated carbonation of BA was studied under varied operation conditions with respect to (i) reactor fill level under static (without rotation) and dynamic conditions (with rotation), (ii) CO_2 concentration and (iii) initial BA moisture. Table 3.2 gives a summary of the experimental conditions and operating parameters. A total reaction time of 120 minutes was chosen since this time scale has been recognized as adequate in terms of reaction rates (Brück et al., 2018; Fernández Bertos et al., 2004a; Lin et al., 2015a). Based on the findings of the bed behaviour study (see section 3.3) all carbonation experiments were conducted at a rotation speed of 1.2 rpm.

The effect of the CO_2 level on carbonation was tested with five concentrations of 15, 35, 55, 75, and 100 vol.-% CO_2 with a constant reactor loading of 8 kg BA. Considering the specific bulk density of the material this corresponded to a fill level of 11 vol.-%.

In a further set of experiments the influence of the reactor fill level was studied with reactor loadings of 5, 8, 10, 15, 20, and 30 kg of BA. This corresponded to reactor fill levels of 7, 11, 14, 21, 28, and 42 vol.-%, respectively. To pinpoint the effect of bed motion the tests were carried out under both static (without rotation) and dynamic conditions (with rotation) at a fixed CO_2 concentration of 55 vol.-%.

The effect of BA moisture on carbonation was tested under dynamic conditions. The initial moisture of BA was raised by adding water to give moisture contents of 15, 18, 21, 24, and 27 wt.-%. Therefore, the BA was loaded into a concrete mixer and thoroughly mixed with the appropriate amount of water for 1 minute and soaked in a closed clamping ring drum for 12 h. The mass of wet BA used in all experiments was adjusted such as to correspond to a uniform loading of 12.9 kg. The CO_2 concentration was 55 vol.-%.

Upon completion of experiments the BA was taken out of the reactor and manually homogenized prior to conduction of leaching tests.

Table 3.2 Experimental conditions of BA carbonation test series in a rotating drum.

Parameter	Test series 1	Test series 2	Test series 3
CO_2 concentration (vol.-%)	15, 35, 55, 75, 100	55	55
Fill level (vol.-%)	11	7, 11, 14, 21, 28, 41	21
Rotation speed (rpm)	1.2	0 and 1.2	1.2
BA sample Nr. (-)*1	1	2	2
BA moisture (wt.-%)	15	15	15, 18, 21, 24, 27

*1 see also Table 3.1

3.4.5 Analytical methods

Batch leaching tests were performed at a liquid-to-solid ratio (L:S) of 10 according to EN 12457-2. Tests were run as duplicates for reactor loadings of up to 15 kg and as quadruplicates for higher loadings. All leachates were immediately analysed for pH and electrical conductivity (EC). The leachates were then passed through 0.45 µm membrane filter (cellulose acetate) and divided into two aliquots. One aliquot was analysed by ion chromatography [Metrohm 861 Advanced Compact IC with a Metrosep A Supp 5 column and a conductivity detector] for Cl^- and SO_4^{2-} as bulk anions. Hexavalent Cr was determined using the 1,5-diphenyl-carbohydrazide method and the magenta-coloured complex was photometrically analysed at a wavelength of 550 nm. The other aliquot was acidified with nitric acid to pH < 2 for element analysis. Zinc (Zn) and Lead (Pb) were determined by atomic absorption spectrometry [AAnalyst 100, Perkin Elmer].

3.4.6 Heat balance of BA carbonation

Since carbonation is exothermic the temperature development inside the reactor should be closely related to the CO_2 uptake of BA. Provided that carbonation of $Ca(OH)_2$ (see reaction 1) is the only reaction generating heat, the total heat ($\triangle H$) can be calculated by multiplying the standard enthalpy of the carbonation reaction ($\triangle H_{carb}$, Eq, 3.1) with the molar CO_2 uptake estimated from the pressure course.

$$Ca(OH)_2 + CO_2 \rightarrow CaCO_3 + H_2O,\ \triangle H_{carb} = -113\ kJ/mol \qquad \text{(Eq. 3.1)}$$

As an alternative approach a simple model was developed to calculate the heat release on the basis of measured temperatures (reactor and environment), heat capacities, and heat transfer through the reactor wall.

The reactor was assumed to be perfectly mixed (see Figure 3.2) implying thermal equilibrium between the gas phase, the wet BA, and the reactor wall.

The model considers the heat stored in the entire reactor (including the wet BA) and the heat flux to the environment ($\dot{Q}$, Eq. 3.2) driven by the gradient between internal temperature (T_{in}) and the ambient temperature (T_{amb}).

$$\dot{Q} = k \cdot A \cdot (T_{in} - T_{amb}) \qquad \text{(Eq. 3.2}$$

where A is the wall area (1,1 m²) and k the heat transfer coefficient ($W \cdot m^{-2} \cdot K^{-1}$).

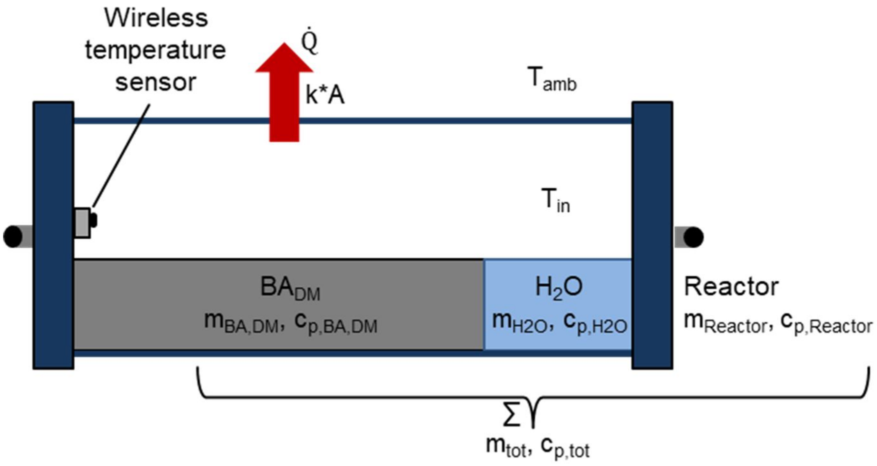

Figure 3.2 Schematic of the heat balance model of the rotating drum reactor (abbreviations explained in the text).

The heat release by carbonation (Q_{Carb}) is then defined as the stored heat and the integral of $\dot{Q}$ over time according to Eq. 3.3. The prior was calculated using the total system mass (m_{tot}), the mass-weighted heat capacity of the system ($c_{p,tot}$), and initial (t = 0 min) and final temperatures (t = 120 min) observed in the experiments. The integral of $\dot{Q}$ was obtained by numerical integration of Eq. 3.2 over the reaction time (see Figure S3.1).

$$Q_{carb} = m_{tot} \cdot c_{p,tot} \cdot \left(T_{in,t=120\,min} - T_{in,t=0min}\right) + \int_{t=0\,min}^{t=120\,min} \left(\dot{Q}\right) \cdot dt \qquad \text{(Eq. 3.3)}$$

All parameters of the model were independently determined. The reactor and the ambient temperatures (T_{in} and T_{amb}, respectively) were logged. The mass of dry BA ($m_{BA,DM}$) and the corresponding mass of water (m_{H2O}) were known for each test configuration. The mass of the reactor ($m_{reactor}$ = 17.6 kg) was determined by weighing. The total system mass m_{tot} was obtained as the sum of $m_{BA,DM}$ + m_{H2O} + $m_{reactor}$. The total heat capacity of the system $c_{p,tot}$ was calculated as the mass-weighted average of the heat capacities of BA ($c_{p,BA,DM}$ of 0.8 $kJ*kg^{-1}*K^{-1}$ (Hao et al., 2017), water ($c_{p,H2O}$ of 4.18 $kJ*kg^{-1}*K^{-1}$) and the reactor material (PVC, $c_{p,Reactor}$ of 0.85 $kJ*kg^{-1}*K^{-1}$ Domininghaus et al., 2012). The heat capacity of the gas phase was neglected due to its low absolute value (m_{gas} = <<1 kg and $c_{p,gas}$=~0.85 $kJ*kg^{-1}*K^{-1}$).
To determine k, a constant heat source was placed inside the reactor. The source was run with varying heating power (30 W, 65 W, 100 W) to provide a defined heat flux ($\dot{Q}$) until T_{in} was constant. The resulting T_{in} at equilibrium was in the range of 32 - 42 °C. Based on duplicate measurements for each heating power k was obtained by re-arranging equation (3.2) and averaged to k_{mean} = 4.6 $W*m^{-2}*K^{-1}$ (standard deviation: 0.8 $W*m^{-2}*K^{-1}$). Using a constant k implies that there is no relevant variation of conditions with influence on k. This is justified

since the model does not consider internal heat transfer but only the heat flux to the environment from a completely mixed thermally equilibrated system. The model (including the numerical value of k) was experimentally validated using a reference material. Therefore, defined amounts (8, 15, 23 kg) of quartz gravel were heated to 50°C and 70 °C in an oven for 24 h and then immediately loaded into the reactor. Subsequently, reactor rotation was started (1.2 rpm) and T_{in} and T_{amb} were logged for 120 min. The heat input via the quartz gravel was then compared to the sum of stored heat and integral heat flux as calculated by the model yielding satisfactory agreement (see Figure S3.2).

3.5 Results and discussion

3.5.1 Bed behaviour of BA

The bed behaviour of BA encoded in accordance with section 3.3 is shown in Figure 3.3. From the video analyses the bed motion of wet BA was predominantly identified as slipping or slumping. Additionally, slipping/slumping and slumping/rolling transitions were identified. Slipping predominated at fill levels below 18 vol.-% irrespective of rotation speed. A slipping/slumping transition occurred at fill levels between 18 % and 21 % when rotation speed was below 6.5 rpm. At higher rotation speed (8 rpm), a direct transition between slipping and rolling was observed.

For fill levels above 21 % slumping predominated, unless the rotation speed was higher than 6 rpm where bed motion changed to the slumping/rolling transition. Note that no pure rolling was identified under the test conditions indicating that BA behaves like a highly cohesive material (Chou and Hsiau, 2011; Yang and Hsiau, 2005). Overall, the bed behaviour of BA contrasts that of standard materials like sand and gravel for which the onset of slumping/rolling is typically found at rotation speeds below 2 rpm and at fill levels lower than 20 % (Henein et al., 1983; Mellmann, 2001).

The videos were further analysed in terms of the slipping and slumping frequencies as a function of rotation speed and fill level (see Figure S3.3 and Figure S3.4). For comparison and to pinpoint the effect of moisture a dry BA sample was also studied. While the slumping frequency of dry BA was similar to gravel, wet BA showed less frequent slipping or slumping. Furthermore, axial segregation (alternating bandings of fine and coarse BA particles) was observed for dry BA after 30 rotations, approximately. For wet BA segregation did not occur and bed behaviour was less sensitive to rotation speed. These findings may explain the low significance of the rotation speed on CO_2 removal performance of a rotating drum reactor reported by Lombardi et al. (2016). Overall, our findings suggest that the bed behaviour of wet BA is primarily controlled by the reactor fill level. Therefore a slow rotation speed of 1.2 rpm was chosen for all accelerated carbonation experiments.

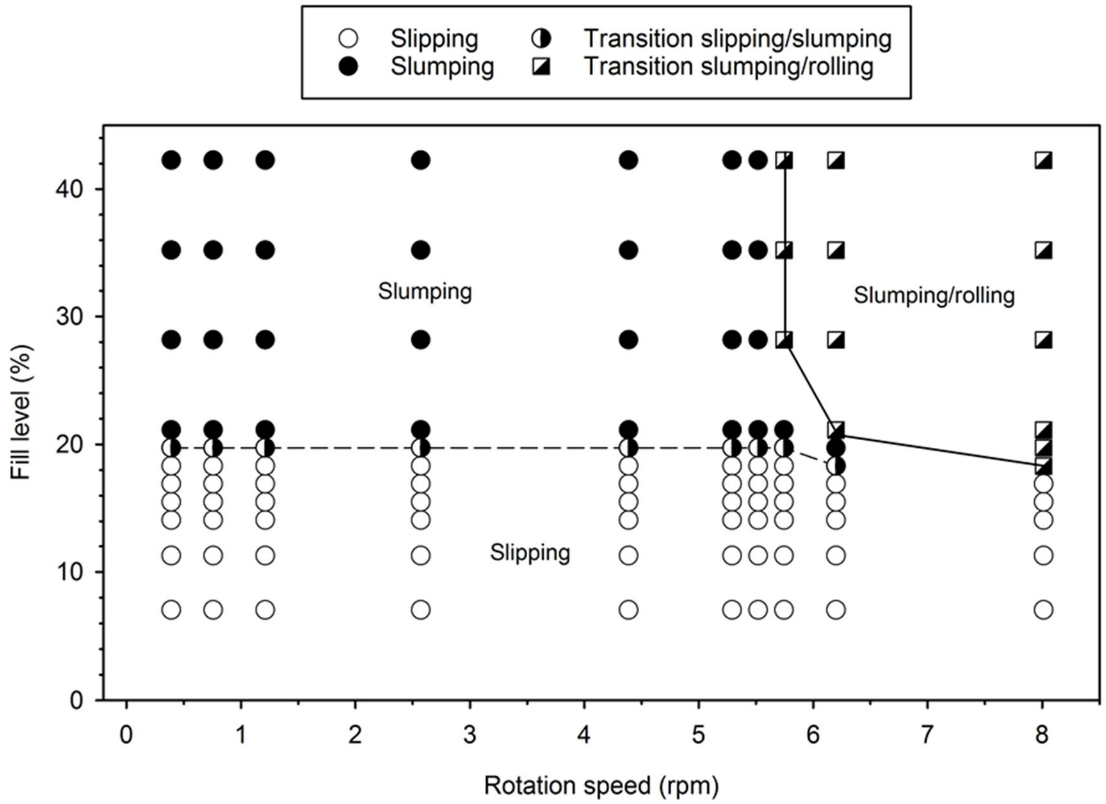

Figure 3.3 Bed behaviour of wet BA in a rotating drum reactor (diameter: 0.3 m, length: 1 m) as obtained by video analysis.

3.5.2 CO_2 uptake and self-heating of BA as affected by operating conditions

Effect of CO_2 concentration

According to the law of mass action carbonation should be enhanced by increasing the CO_2 partial pressure. Here we evaluated the effect at five different CO_2 concentrations (15, 35, 55, 75 and 100 vol.-%). Figure 3.4 shows the observed time courses of CO_2 uptake and $\triangle$T. Both the CO_2 uptake rate and the final level of carbonation increased as the CO_2 concentration increased from 15 to 75 vol.-%. For CO_2 concentrations >15 vol.-% the carbonation increased rapidly during the first 30 minutes and slowed down with ongoing reaction. The highest final CO_2 uptake of 2.39 g CO_2/100 g BA_{DM} was found at 75 vol.-% CO_2 and no further increase was found at 100 vol.-% CO_2 in spite of a higher initial uptake rate.

Hampered carbonation at high CO_2 concentrations was also observed in static carbonation studies (Nam et al., 2012; Sun et al., 2008). The authors concluded that this was due to inhibition of CO_2 diffusion through carbonates precipitated on the BA surface. Under static conditions, this effect occurred at CO_2 concentrations >20 vol.-%. In our dynamic carbonation tests it was shifted >75 vol.-%. Since the bed motion causes friction among BA aggregates, surfaces are continuously renewed and diffusion through a growing layer of precipitated $CaCO_3$ seems less important.

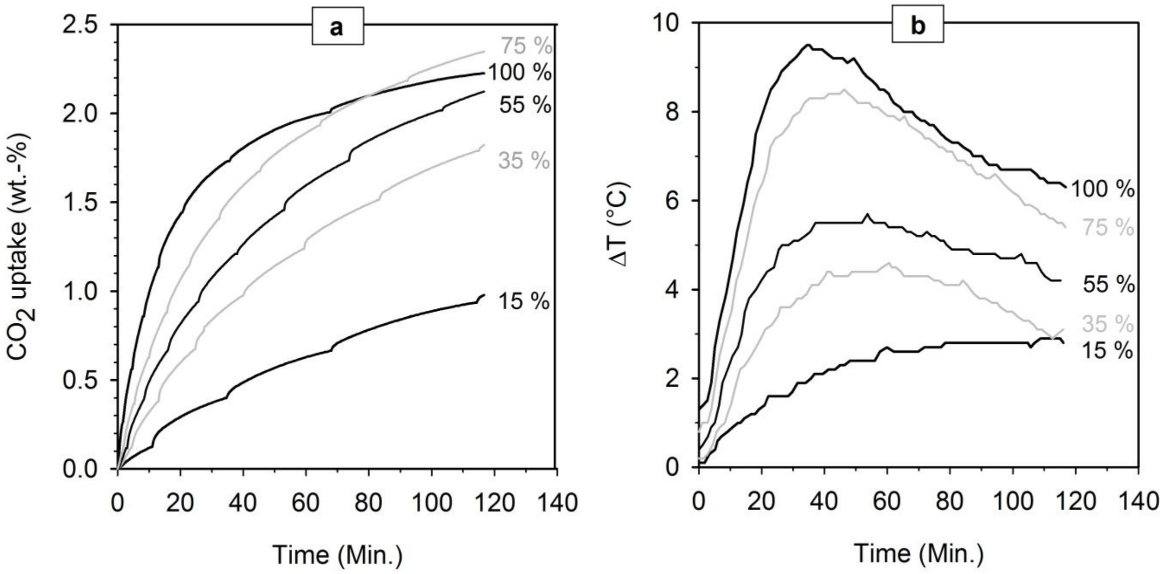

Figure 3.4 Progress of BA carbonation at different CO_2 concentrations as reflected by CO_2 uptake (a) and self-heating (b) where △T denotes the difference between reactor temperature and ambient temperature. Experiments were conducted at a reactor loading of 8 kg (fill level: 11 %) and a rotation speed of 1.2 rpm.

Carbonation was accompanied by a temperature increase of 2 to 10 °C relative to ambient conditions. As expected from the thermodynamics of the carbonation reaction, △T increased with CO_2 uptake (see Figure 3.4b). At 15 vol.-% CO_2 the temperature increased slowly during the first 80 minutes and then levelled off indicating lower but ongoing turnover. This contrasts the findings for higher CO_2 concentrations where △T peaked between 30 to 60 minutes and decreased again until the end of the experiment (120 minutes).

To check whether self-heating was solely due to carbonation two control experiments were conducted. In the first, a pure N_2 atmosphere was adjusted to inhibit carbonation as well as a potential aerobic biodegradation of unburnt matter. In the second, a pure O_2 atmosphere was applied to account for self-heating by corrosion and/or aerobic biodegradation reactions. Under neither condition a temperature increase was observed suggesting that self-heating was due to carbonation, only.

Effect of Reactor Fill Level

The fill level is crucial for a future development of the rotating drum reactor towards a continuously fed system as it determines the BA residence time at a given throughput. Recently, Lombardi et al. (2016) tested the CO_2 removal from a gas stream in a rotating drum using BA as an absorbent and found that performance was best at low fill levels. However, results from section 4.1 indicated that even at low rotation high fill levels may be beneficial for carbonation by promoting the transition from sliding to slumping bed motion. Therefore, we systematically tested the carbonation performance over a fill level range between 7 and 42 vol.-% applying rotation rates of 0 rpm (static conditions) and 1.2 rpm (dynamic conditions). Figure 3.5a shows the corresponding specific CO_2 uptakes after a reaction time of 120 minutes. Overall, higher CO_2 uptakes were attained under dynamic conditions.

Under static conditions the CO_2 uptake linearly decreased with fill level, indicating that the access of CO_2 may have been hampered by the increasing BA layer thickness. Under dynamic conditions, CO_2 uptake was less limited. The highest CO_2 uptakes were found for fill levels between 7 - 15 vol.-% (slipping bed motion) while turnover was somewhat reduced at fill levels exceeding 15 vol.-% (slumping bed motion). These findings contrast with results of Boateng (2015) and indicate that in our system the actual BA layer thickness is more decisive for carbonation performance than the type of bed motion. A clear benefit of reactor rotation is recognized from the results obtained at high fill levels since the differences of CO_2 uptake between the static and the dynamic system increased. Due to the solid's motion internal surfaces susceptible to the mass exchange between BA and CO_2 are exposed and limitations due to layer thickness are overcome.

Figure 3.5b shows the $\triangle T_{max}$ values after 120 min of accelerated carbonation. In accordance with higher CO_2-uptakes the values of $\triangle T_{max}$ were higher under dynamic than under static conditions. For the former $\triangle T_{max}$ showed a roughly linear increase with fill level due to the higher amount of BA available for carbonation. Under static conditions $\triangle T_{max}$ peaked at fill levels between 20 – 30 % and decreased for a fill level of 42 vol.-%.

Since the automated CO_2 dosage provides a quasi-infinite source of CO_2 reaction turnover is limited by the amount of BA present in each experimental run. Thus, $\triangle T_{max}$ relates to the absolute CO_2 uptake of the system rather that to the specific CO_2 uptake per unit weight of BA. In our dynamic experiments the total CO_2 uptake was roughly linear with reactor loading (as was $\triangle T_{max}$) and increased from approximately 100 g CO_2 at 7 % fill level to 550 g CO_2 at 42 % fill level (see Figure S3.5). Under static conditions, the absolute uptake levelled-off to approximately 250 g CO_2 at fill levels of 21 % and above.

Overall, under dynamic conditions reactor loading does not seem to be a limiting factor for BA carbonation. Although slightly reduced, carbonation performance was satisfactory even at fill levels above 20%. This is encouraging in terms of the treatment capacities of potential full-scale applications.

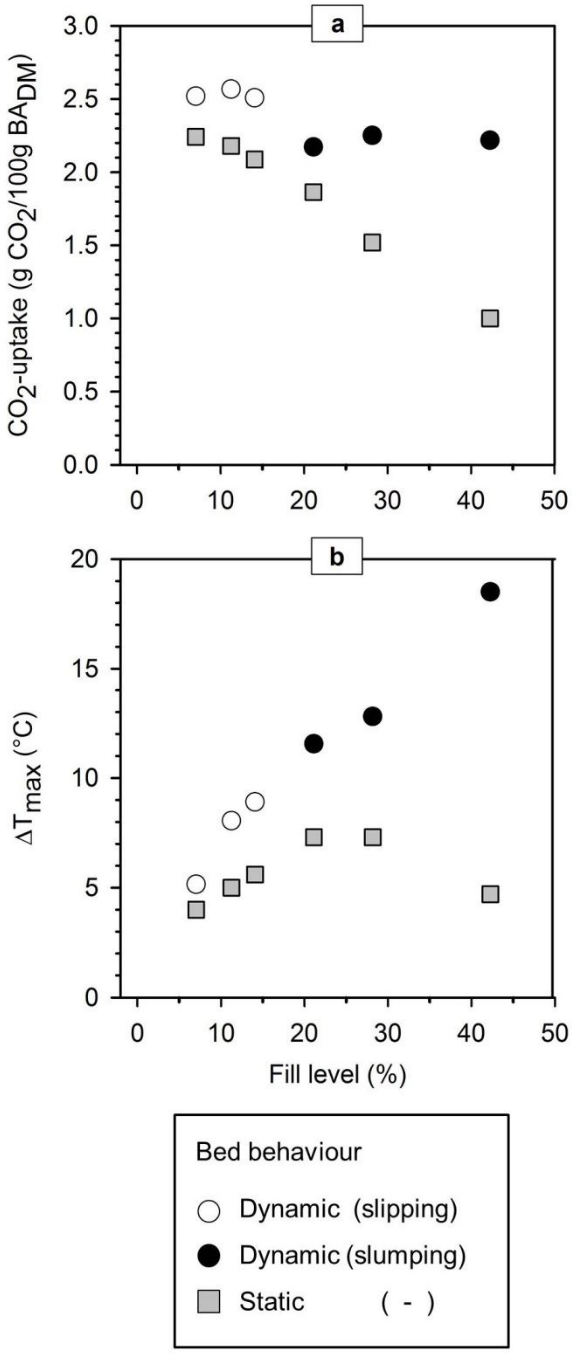

Figure 3.5 Effect of reactor fill level on CO_2 uptake (a) and $\triangle T_{max}$ (b) under dynamic (1.2 rpm) and static conditions (0 rpm) where $\triangle T_{max}$ is the maximum difference between reactor temperature and ambient temperature. Experiments were conducted at a CO_2 concentration of 55 vol.-%. For classification of bed motion cf. Figure 3.3.

Effect of BA Moisture

The moisture content of BA is critical in that sufficient water must be present for carbonation to occur, but not as much as to fill pores and slow down the access of CO_2. To identify a possible moisture optimum, water was added to the material to increase the moisture contents from 15% to 18%, 21%, 24%, and 27%. Figure 3.6 shows the observed CO_2 uptake along with the corresponding values of $\triangle T_{max}$.

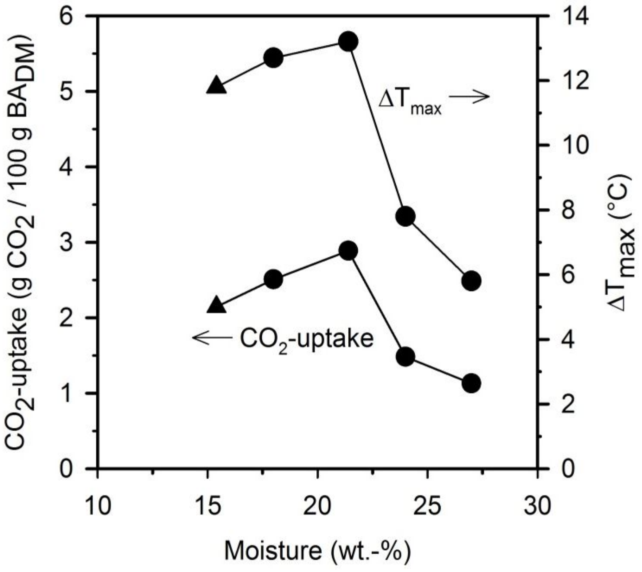

Figure 3.6 Effect of BA moisture on CO_2 uptake and $\triangle T_{max}$ (maximum difference between reactor temperature and ambient temperature). Experiments were conducted at a reactor fill level of 21 %, a rotation speed of 1.2 rpm, and a CO_2 concentration of 55 Vol.-%.

As BA moisture was increased from its native value to 21%, the CO_2 uptake and $\triangle T_{max}$ increased slightly to 2.89 g CO_2/100 g BA_{DM} and 13.2 °C, respectively. It appears that the addition of small amounts of water may enhance the carbonation under dynamic conditions. For moisture contents of 24% and above both the CO_2 uptake and $\triangle T_{max}$ dropped sharply. These findings are consistent with results of Lin et al. (Lin et al., 2015b) and it is likely that excess intergranular water limited the diffusion of CO_2 (Rendek et al., 2006).

For the tested BA (1-3 days of storage in a roofed pile, grain size <10 mm) a moisture content of 20 wt.-% seems advisable for maximum CO_2 uptake. However, water addition is not a perquisite given that the CO_2 uptake was only slightly smaller for BA at its inherent moisture. On the other hand, excess water should be avoided underlining the benefit of a proper drainage after BA quenching.

3.5.3 Heat balance

As indicated in the previous sections the development of reactor temperature is closely related to the carbonation reaction and may possibly serve as a process performance indicator. In this regard a heat-balance model was set up as described in section 3.6. Based on the measured temperatures the heat stored in the reactor as well as the integrated heat flux to the environment were calculated and combined to Q_{Carb}. This was compared to the theoretical reaction heat $\triangle H$, as obtained from the CO_2 uptake using Eq. 1 (see Figure 3.7).

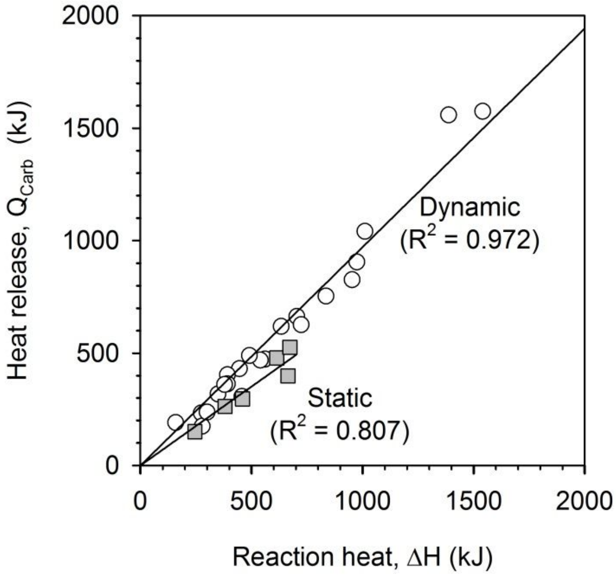

Figure 3.7 Comparison of BA self-heating under static and dynamic conditions as derived from the reaction enthalpy (△H) and from the heat-balance model (Q_{Carb}).

For the dynamic carbonation tests the slope of the regression line in Figure 3.7 is close to unity indicating excellent agreement between the heat balance and the reaction enthalpy. Therefore, the assumption of thermal equilibrium in a perfectly mixed system satisfactorily applies to the rotating drum reactor. Furthermore, the good agreement of △H with Q_{Carb} confirms that carbonation was the dominant heat source underpinning the results obtained under pure O_2 and N_2 atmospheres (see section 4.2.1).

Contrasting the findings for the rotating drum, under static conditions the values of Q_{Carb} were systematically lower than the values of △H (slope of regression line = 0.8). Apparently, the unmixed solid was not in equilibrium with the gas phase and the model assumptions did not apply.

Overall, the outlined close relation of both heat values, △H and Q_{Carb}, may serve to evaluate the progress of carbonation. The reactor temperature may therefore be used as a monitoring parameter for the accelerated carbonation of BA in rotating drum batch reactors.

3.5.4 Leaching behaviour of fresh and carbonated BA

The leaching behaviour of BA determines the disposal options (landfilling or geotechnical reuse) depending on country-specific guidelines. To assess the effect of accelerated carbonation on the mobility of BA constituents, batch leaching tests were performed with both the fresh and carbonated BA. Figure 3.8 shows the results including the German waste acceptance criteria (WAC) for landfill classes (LC) 0, 1, and 2, where applicable.

The leachates largely support different performances of the static and dynamic carbonation systems. According to an independent two-sample t-test the differences were highly significant for pH, EC, and Zn ($p \leq 0.001$). The leachate pH (Figure 3.8a) decreased from 12.5 to 11.7 and 12.1 for the dynamic and the static tests, respectively. This is attributed to the consumption of alkalinity (mainly related to $Ca(OH)_2$) by BA carbonation. Carbonation also caused a considerable reduction of EC (see Figure 3.8b) compared to the control indicating that the leachates were depleted in mobile charged constituents, most importantly in OH^-. Both pH and EC decreased with increasing CO_2 uptake (see Figures 3.4, 3.5, and 3.6). This also holds for the carbonation experiments conducted at varied CO_2 concentration and moisture (see Figure S3.6).

Regarding trace metals, the leachability of Pb and Zn from BA is particularly relevant (Costa et al., 2007; Fernández Bertos et al., 2004a). Most frequently, a carbonation-induced immobilisation has been reported (Arickx et al., 2006; Sakita and Nishimura, 2015) although mobilising effects were also observed (Todorovic and Ecke, 2006; van Gerven et al., 2005). Our results show that for fresh BA the leachate concentration of Pb was way above the LC 2 WAC while Zn exceeded the LC 0 WAC. Overall, the leachate values characterized fresh BA as a hazardous waste.

In the carbonated BA, Zn and Pb were substantially immobilized since leachate concentrations dropped by at least one order of magnitude compared to fresh BA. Chemically, contaminant immobilization may have been due to precipitation as (hydroxy-)carbonates (Fernández Bertos et al., 2004b) or to the pH-driven leachability decrease of $Zn(OH)_2$ and $Pb(OH)_2$ (Chimenos et al., 2000)). In addition, leachability may have been decreased due to physical containment via formation of a carbonate layer on the surface of BA (Sakita and Nishimura, 2015) or by enhanced adsorption of Pb and Zn (Chaspoul et al., 2008; Oehmig et al., 2015; Yao et al., 2012). The above-named processes are associated with primary and secondary mineral reactions and may overlap (Yin et al., 2017).

In accordance with pH and EC, the immobilisation of Zn and Pb was more pronounced under dynamic conditions. Irrespective of the fill level, leachate concentrations were below WAC for LC 0 and LC 2, respectively, classifying the carbonated BA as a non-hazardous waste. Under static conditions the leachate concentration of Zn and especially Pb increased with increasing fill level which in turn is consistent with the reduced CO_2 uptake.

Several authors (Rendek et al., 2006; Um et al., 2013; van Gerven et al., 2005) have shown that also the leaching of the Cr(VI) oxoanion is affected by carbonation. In our experiments the concentration of Cr(VI) in the leachates of both the fresh and carbonated BA was below the detection limit of 50 µg/L which is equivalent to the LC 0 WAC.

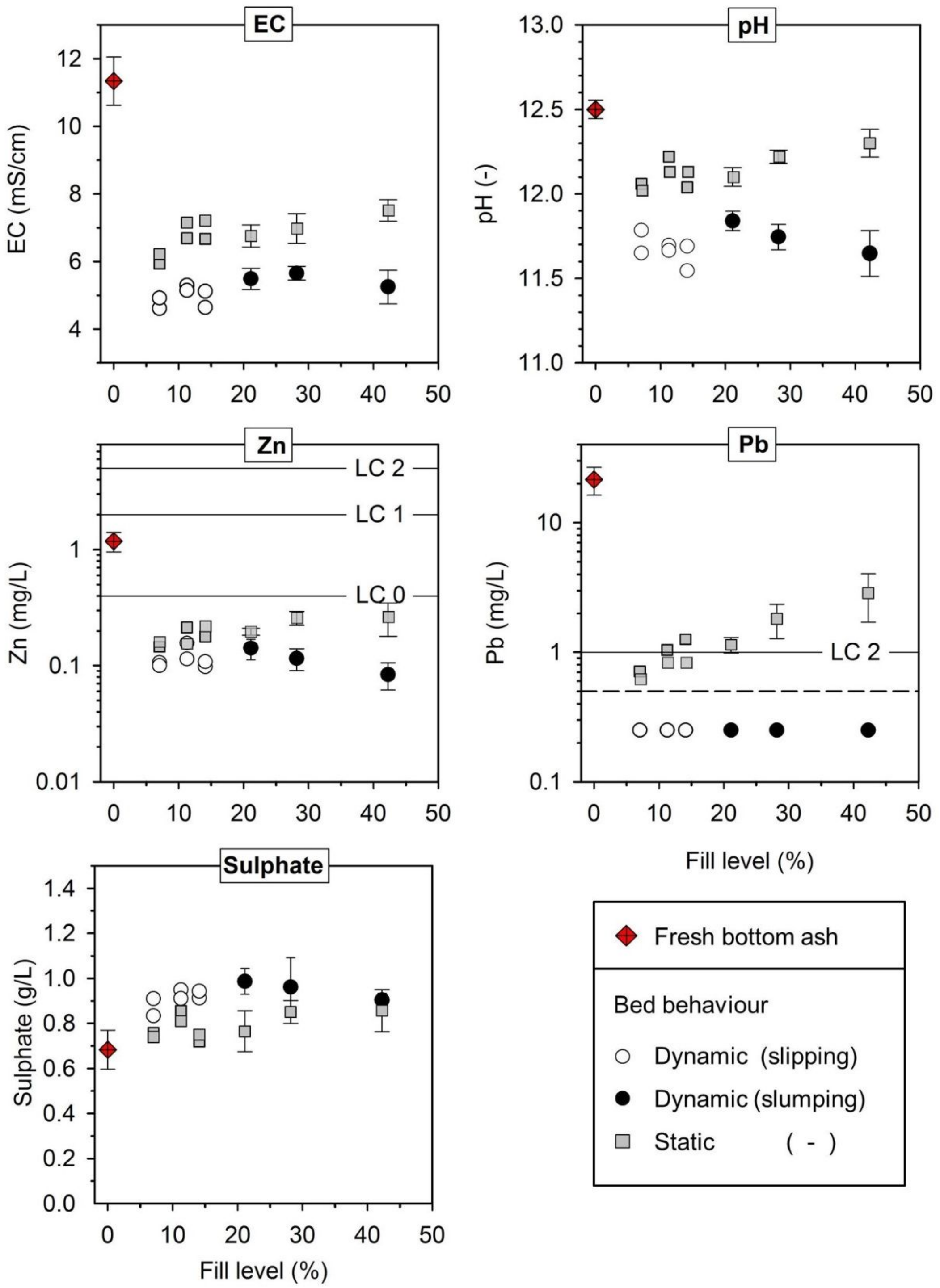

Figure 3.8 Leachate properties of fresh BA and BA carbonated under dynamic (1.2 rpm) and static conditions (0 rpm). Experiments were performed in a rotating drum reactor at varied fill level and a CO_2 concentration of 55 %. Error bars: Standard deviation for fill levels >20 % (n = 8 and n = 4 for fresh and carbonated BA, respectively); solid lines: German waste acceptance criteria for landfill class (LC) 0, 1, and 2; broken line: Limit of quantitation for Pb by AAS. For classification of bed motion cf. Figure 3.3.

Sulphate and chloride are two bulk anions in the BA leachate (Yin et al., 2017). The leachability of sulphate is virtually pH-independent when controlled by the solubility of gypsum, barite or monosulphate (Dijkstra et al., 2006; Rocca et al., 2012). Sulphate-substituted ettringite may however cause a pH-dependent leaching since at pH below 10.5 ettringite becomes unstable (Chrysochoou and Dermatas, 2006). The mean leachate concentration of sulphate for fresh BA was 683 mg/L (Standard deviation: ±87 mg/L).

In carbonated samples, the sulphate concentration increased relative to fresh BA, especially when carbonation was performed under dynamic conditions where a stronger pH-drop was observed. This is in accordance with previous investigations (Bertos et al., 2004; Chimenos et al., 2000) where increased SO_4^{2-}-leaching was explained by the decomposition of ettringite (Fernández Bertos et al., 2004b; Polettini and Pomi, 2004). In our experiments despite the observed gain in sulphate concentrations of up to 300 mg/L the LC 1 WAC of 2000 mg/L was not exceeded. Therefore, carbonation-induced sulphate mobilization did not outweigh the beneficial effects observed for Zn and Pb.

Leachate concentrations of chloride for fresh BA were in the range of 800 - 900 mg/L (below the LC 1 WAC of 1500 mg/L) and did not exhibit any clear tendency (data not shown).

Overall, carbonation improved the leachate quality of BA (decrease in trace metal release, lower pH and EC). While the leachate values classify fresh BA as a hazardous waste carbonated BA complies with the WACs of non-hazardous waste.

3.6 Conclusions

Dynamic reactor systems may be suited for the accelerated carbonation of BA on the industrial scale. This study aimed at two central aspects of BA carbonation in a rotating drum batch reactor: the bed behaviour and the influence of operating conditions on the carbonation performance as judged by CO_2 uptake, temperature evolution and leachate quality.

Slipping and slumping were identified as the dominant patterns of bed motion within the range of test conditions (fill level: 7 – 42 %, rotation speed: 0.4 – 8 rpm) and the bed behaviour of BA broadly differed from that of dry standard materials. The results from this study may be used to attain desired bed behaviour by selecting an appropriate combination of fill level and rotation speed.

Regarding operating conditions of the rotating drum, the effects of fill level, CO_2 concentration, and BA moisture on carbonation performance were tested. Compared to a static system, CO_2 uptake was superior under dynamic conditions even at fill levels exceeding 20 %. This is consistent with the improved mass transfer imposed by BA mixing.

Both the CO_2 uptake rate and the final level of carbonation increased as the CO_2 concentration was increased from 15 to 75 vol. %. A modest uptake inhibition was observed at 100 vol.-% CO_2, only. This suggests that under dynamic conditions a broad range of exhaust gases are suitable as a CO_2 source for the carbonation process.

The optimum moisture content for the tested BA (sieve fraction: <10 mm) is 21 wt.-%. This is roughly in the range of the native moisture content of BA after storage in a roofed pile for 1 to 3 days. Excess moisture contents (>24 wt.-%), which can be found directly after the quenching process, should be avoided.

Due to the exothermal carbonation reaction a close relationship exists between CO_2 uptake and the reactor temperature. This was confirmed by a heat balance model. Based on measured temperatures the heat content of the reactor and the flux to the environment were calculated and benchmarked against the reaction enthalpy. Under dynamic conditions excellent agreement was observed indicating that carbonation is, indeed, the most important heat-generating reaction. Thus, temperature monitoring may be an alternative way of evaluating the carbonation performance in rotating drum batch reactors.

Accelerated carbonation yielded a strong decrease of the leachability of Pb and Zn from BA but was not able to reduce leachate concentrations of chloride and sulphate. Under dynamic conditions the leaching behaviour of BA could be improved such as to comply with the German waste acceptance criteria for landfilling the material as a non-hazardous waste.

3.7 Acknowledgement

This project (HA project no. 483/15-25) was supported in the framework of Hessen ModellProjekte financed with funds of LOEWE – Landes-Offensive zur Entwicklung Wissenschaftlich-ökonomischer Exzellenz, Förderlinie 3: KMU-Verbundvorhaben (State Offensive for the Development of Scientific and Economic Excellence). We thank Svenja Vogt, Raphael Gissel and Marcel Pingsmann for their support during the experiments.

3.8 References

Arickx, S., van Gerven, T., Vandecasteele, C., 2006. Accelerated carbonation for treatment of MSWI bottom ash. Journal of Hazardous Materials 137, 235–243.

Astrup, T., 2007. Pretreatment and utilization of waste incineration bottom ashes: Danish experiences. Waste Management 27, 1452–1457.

Baciocchi, R., Carnevale, E., Corti, A., Costa, G., Lombardi, L., Olivieri, T., Zanchi, L., Zingaretti, D., 2013. Innovative process for biogas upgrading with CO2 storage: Results from pilot plant operation. Biomass and Energy 53, 128–137.

Baciocchi, R., Costa, G., Lategano, E., Marini, C., Polettini, A., Pomi, R., Postorino, P., Rocca, S., 2010. Accelerated carbonation of different size fractions of bottom ash from RDF incineration. Waste Management 30, 1310–1317.

Bertos, M.F., X. Li, R. Simons, S.J., D. Hills, C., J. Carey, P., 2004. Investigation of accelerated carbonation for the stabilisation of MSW incinerator ashes and the sequestration of CO_2. Green Chemistry 6, 428–436.

Boateng, A.A., 2015. Rotary Kilns: Transport Phenomena and Transport Processes. Butterworth-Heinemann, Oxford.

Brück, F., Fröhlich, C., Mansfeldt, T., Weigand, H., 2018. A fast and simple method to monitor carbonation of MSWI bottom ash under static and dynamic conditions. Waste Management 78, 588–594.

Chaspoul, F.R., Le Droguene, M.F., Barban, G., Rose, J.C., Gallice, P.M., 2008. A role for adsorption in lead leachability from MSWI bottom ASH. Waste Management 28, 1324–1330.

Chimenos, J.M., Fernández, A.I., Nadal, R., Espiell, F., 2000. Short-term natural weathering of MSWI bottom ash. Journal of Hazardous Materials 79, 287–299.

Chou, S.H., Hsiau, S.S., 2011. Experimental analysis of the dynamic properties of wet granular matter in a rotating drum. Powder Technology 214, 491–499.

Chou, S.H., Liao, C.C., Hsiau, S.S., 2010. An experimental study on the effect of liquid content and viscosity on particle segregation in a rotating drum. Powder Technology 201, 266–272.

Chrysochoou, M., Dermatas, D., 2006. Evaluation of ettringite and hydrocalumite formation for heavy metal immobilization: Literature review and experimental study. Journal of Hazardous Materials 136, 20–33..

Costa, G., Baciocchi, R., Polettini, A., Pomi, R., Hills, C.D., Carey, P.J., 2007. Current status and perspectives of accelerated carbonation processes on municipal waste combustion residues. Environmental Monitoring and Assessment 135, 55–75.

del Valle-Zermeño, R., Romero-Güiza, M.S., Chimenos, J.M., Formosa, J., Mata-Alvarez, J., Astals, S., 2015. Biogas upgrading using MSWI bottom ash: An integrated municipal solid waste management. Renewable Energy 80, 184–189..

Dijkstra, J.J., Van der Sloot, Hans A., Comans, R.N.J., 2006. The leaching of major and trace elements from MSWI bottom ash as a function of pH and time. Applied Geochemistry 21, 335–351.

Ding, Y.L., Forster, R.N., Seville, J. P. K, Parker, D.J., 2001a. Some aspects of heat transfer in rolling mode rotating drums operated at low to medium temperatures. Powder Technology 121, 168–181.

Ding, Y.L., Seville, J.P.K., Forster, R., Parker, D.J., 2001b. Solids motion in rolling mode rotating drums operated at low to medium rotational speeds. Chemical Engineering Science 56, 1769–1780.

Domininghaus, H., Elsner, P., Eyerer, P., Hirth, T., 2012. Kunststoffe: Eigenschaften und Anwendungen. Springer, Berlin, Heidelberg,

Dou, X., Ren, F., Nguyen, M.Q., Ahamed, A., Yin, K., Chan, W.P., Chang, V.W.-C., 2017. Review of MSWI bottom ash utilization from perspectives of collective characterization, treatment and existing application. Renewable and Sustainable Energy Reviews 79, 24–38.

Fernández Bertos, M., Li, X., Simons, S.J.R., Hills, C.D., Carey, P.J., 2004a. Investigation of accelerated carbonation for the stabilisation of MSW incinerator ashes and the sequestration of CO_2. Green Chemistry 6, 428–436.

Fernández Bertos, M., Simons, S.J.R., Hills, C.D., Carey, P.J., 2004b. A review of accelerated carbonation technology in the treatment of cement-based materials and sequestration of CO_2. Journal of Hazardous Materials 112, 193–205.

Gunning, P.J., Hills, C.D., Carey, P.J., 2010. Accelerated carbonation treatment of industrial wastes. Waste Management 30, 1081–1090.

Hao, Z., Sun, M., Ducoste, J.J., Benson, C.H., Luettich, S., Castaldi, M.J., Barlaz, M.A., 2017. Heat Generation and Accumulation in Municipal Solid Waste Landfills. Environmental Science and Technology 51, 12434–12442.

Henein, H., Brimacombe, J.K., Watkinson, A.P., 1983. Experimental study of transverse bed motion in rotary kilns. MTB 14, 191–205.

Inkaew, K., Saffarzadeh, A., Shimaoka, T., 2016. Modeling the formation of the quench product in municipal solid waste incineration (MSWI) bottom ash. Waste management 52, 159–168.

Łączny, J.M., Iwaszenko, S., Gogola, K., Bajerski, A., Janoszek, T., Klupa, A., Cempa-Balewicz, M., 2015. Study on the possibilities of treatment of combustion by-products from fluidized bed boilers into a product devoid of free calcium oxide. Journal of Sustainable Mining 14, 164–172.

Lin, W.Y., Heng, K.S., Sun, X., Wang, J.-Y., 2015a. Accelerated carbonation of different size fractions of MSW IBA and the effect on leaching. Waste Management 41, 75–84.

Lin, W.Y., Heng, K.S., Sun, X., Wang, J.-Y., 2015b. Influence of moisture content and temperature on degree of carbonation and the effect on Cu and Cr leaching from incineration bottom ash. Waste Management 43, 264–272.

Liu, P.Y., Yang, R.Y., Yu, A.B., 2013. DEM study of the transverse mixing of wet particles in rotating drums. Chemical Engineering Science 86, 99–107.

Liu, X.Y., Specht, E., Mellmann, J., 2005. Slumping–rolling transition of granular solids in rotary kilns. Chemical Engineering Science 60, 3629–3636.

Lombardi, L., Carnevale, E.A., Pecorini, I., 2016. Experimental evaluation of two different types of reactors for CO_2 removal from gaseous stream by bottom ash accelerated carbonation. Waste Management 58, 287–298.

Mellmann, J., 2001. The transverse motion of solids in rotating cylinders—forms of motion and transition behavior. Powder Technology 118, 251–270.

Mellmann, J., Specht, E., Liu, X., 2004. Prediction of rolling bed motion in rotating cylinders. American Institute of Chemical Engineers Journal. 50, 2783–2793.

Metcalfe, G., Shinbrot, T., McCarthy, J.J., Ottino, J.M., 1995. Avalanche mixing of granular solids. Nature 374, 39–41.

Mostbauer, P., Lombardi, L., Olivieri, T., Lenz, S., 2014. Pilot scale evaluation of the BABIU process – Upgrading of landfill gas or biogas with the use of MSWI bottom ash. Waste Management 34, 125–133.

Nam, S.-Y., Seo, J., Thriveni, T., Ahn, J.-W., 2012. Accelerated carbonation of municipal solid waste incineration bottom ash for CO 2 sequestration. Geosystem Engineering 15, 305–311.

Nase, S.T., Vargas, W.L., Abatan, A.A., McCarthy, J.J., 2001. Discrete characterization tools for cohesive granular material. Powder Technology 116, 214–223.

Oehmig, W.N., Roessler, J.G., Zhang, J., Townsend, T.G., 2015. Effect of ferrous metal presence on lead leaching in municipal waste incineration bottom ashes. Journal of Hazardous Materials 283, 500–506.

Pan, S.-Y., 2012. CO_2 Capture by Accelerated Carbonation of Alkaline Wastes: A Review on Its Principles and Applications. Aerosol Air Quality Research 12, 770–791.

Polettini, A., Pomi, R., 2004. The leaching behavior of incinerator bottom ash as affected by accelerated ageing. Journal of Hazardous Materials 113, 209–215.

Rendek, E., Ducom, G., Germain, P., 2006. Carbon dioxide sequestration in municipal solid waste incinerator (MSWI) bottom ash. Journal of Hazardous Materials 128, 73–79.

Rocca, S., van Zomeren, A., Costa, G., Dijkstra, J.J., Comans, R.N.J., Lombardi, F., 2012. Characterisation of major component leaching and buffering capacity of RDF incineration and gasification bottom ash in relation to reuse or disposal scenarios. Waste Management 32, 759–768.

Sabbas, T., Polettini, A., Pomi, R., Astrup, T., Hjelmar, O., Mostbauer, P., Cappai, G., Magel, G., Salhofer, S., Speiser, C., Heuss-Assbichler, S., Klein, R., Lechner, P., 2003. Management of municipal solid waste incineration residues. Waste Management 23, 61–88.

Sakita, S., Nishimura, K., 2015. Physical containment of municipal solid waste incineration bottom ash by accelerated carbonation. Journal of Material Cycles and Waste Management 18, 1–8.

Santos, R.M., Mertens, G., Salman, M., Cizer, Ö., van Gerven, T., 2013. Comparative study of ageing, heat treatment and accelerated carbonation for stabilization of municipal solid waste incineration bottom ash in view of reducing regulated heavy metal/metalloid leaching. Journal of Environmental Management 128, 807–821..

Sun, J., Bertos, M.F., Simons, S.J.R., 2008. Kinetic study of accelerated carbonation of municipal solid waste incinerator air pollution control residues for sequestration of flue gas CO_2. Energy Environmental Science 1, 370–377.

Todorovic, J., Ecke, H., 2006. Treatment of MSWI Residues for Utilization as Secondary Construction Minerals: A Review of Methods. Minerals and Energy - Raw Materials Report 20, 45–59.

Um, N., Nam, S.-Y., Ahn, J.-W., 2013. Effect of Accelerated Carbonation on the Leaching Behavior of Cr in Municipal Solid Waste Incinerator Bottom Ash and the Carbonation Kinetics. Materials Transactions 54, 1510–1516.

van Gerven, T., van Keer, E., Arickx, S., Jaspers, M., Wauters, G., Vandecasteele, C., 2005. Carbonation of MSWI-bottom ash to decrease heavy metal leaching, in view of recycling. Waste Management 25, 291–300.

Yang, W.-L., Hsiau, S.-S., 2005. Wet granular materials in sheared flows. Chemical Engineering Science 60, 4265–4274.

Yao, J., Li, W.-B., Kong, Q., Xia, F., Shen, D.-S., 2012. Effect of weathering on the mobility of zinc in municipal solid waste incinerator bottom ash. Fuel 93, 99–104.

Yin, K., Chan, W.P., Dou, X., Ren, F., Chang, V.W.-C., 2017. Measurements, factor analysis and modeling of element leaching from incineration bottom ashes for quantitative component effects. Journal of Cleaner Production 165, 477–490..

Zhu, H.P., Zhou, Z.Y., Yang, R.Y., Yu, A.B., 2008. Discrete particle simulation of particulate systems: A review of major applications and findings. Chemical Engineering Science 63, 5728–5770.

Zingaretti, D., Costa, G., Baciocchi, R., 2013. Assessment of the Energy Requirements for CO_2 Storage by Carbonation of Industrial Residues. Part 1: Definition of the Process Layout. Energy Procedia 37, 5850–5857.

Zingaretti, D., Costa, G., Baciocchi, R., 2014. Assessment of Accelerated Carbonation Processes for CO_2 Storage Using Alkaline Industrial Residues. Industrial Engineering Chemical Research 53, 9311–9324.

3.9 Supplementary material

3.9.1 Heat balance of BA carbonation

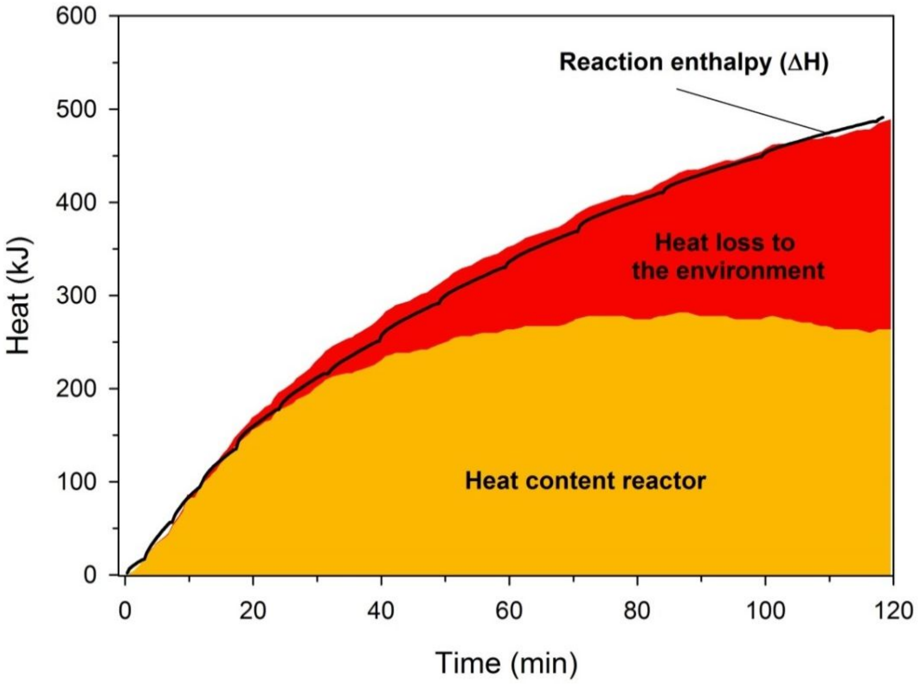

Figure S3.1 Heat balance for a selected experimental run, temporal course of heat storage in the reactor, the heat loss to the environment, and the carbonation enthalpy (△H). Experiment conducted at a reactor fill level of 21 % (BA sample 2, moisture content 24 wt.-%), a rotation speed of 1.2 rpm, and a CO_2 concentration of 55 Vol.-%.

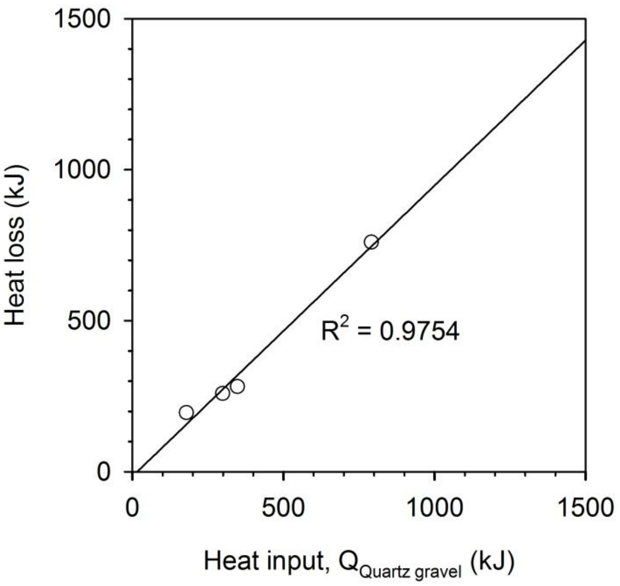

Figure S3.2 Validation of the heat-balance model. Defined quantities of heated quartz gravel were filled into the reactor (heat input) and the cumulative heat loss was calculated from the measured temperatures (heat balance).

3.9.2 Solid motion of bottom ash

For both the wet and dry bottom ash (BA) the slipping frequency increased with rotation speed (see Figure S3.3). The concave characteristic demonstrates that this effect is most pronounced at low rotation speeds. For wet BA a slipping motion was observed throughout. For dry BA a sliding motion was observed when rotation speed was above 4 rpm and slipping frequency was higher than for wet BA. This suggests that moisture increased the friction between the BA bed and the drum wall. A similar effect was observed by Liu et al. (Liu et al., 2013) who found that the mixing rate for wet particles was largely unaffected by the rotation speed.

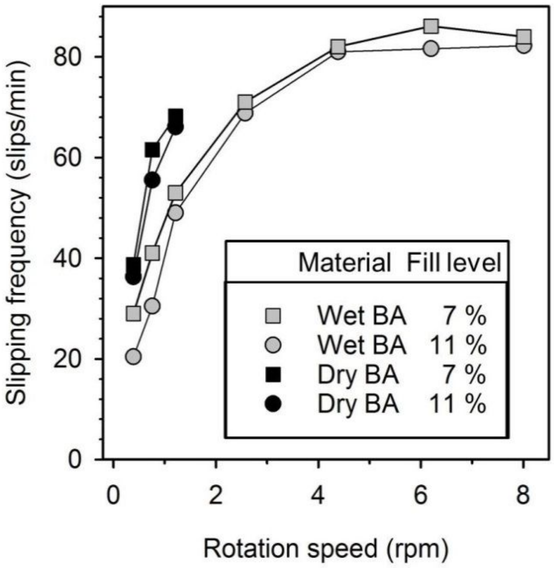

Figure S3.3 Slipping frequency of wet and dry BA as a function of rotation speed.

Figure S3.4 shows the slumping frequencies for fresh and dry BA as compared to literature data for sand and gravel (Henein et al., 1983). For both, fresh and dry BA, the slumping frequencies increased with increasing rotation speed. Higher slumping frequencies and a stronger dependence on the rotation speed were found for dry BA. The fill level had a minor impact on the slumping frequency. Even though BA comprises a heterogeneous mixture of powder like particles to coarse aggregates (e.g. gravel) the slumping frequency pattern of dry BA compares favourably to that of gravel.

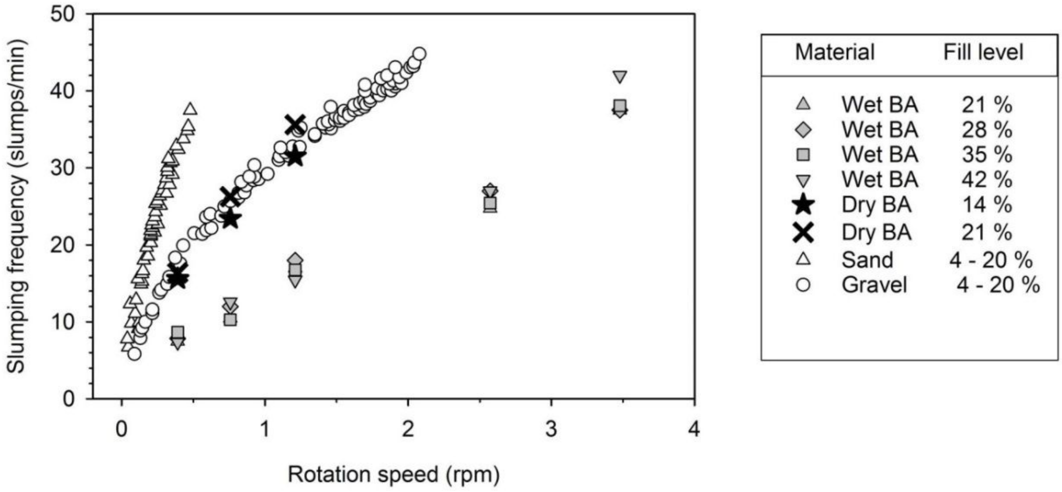

Figure S3.4 Slumping frequency as a function of rotation speed for wet and dry BA compared to sand and gravel as extracted from Henein et al. (1983).

3.9.3 Effect of reactor fill level

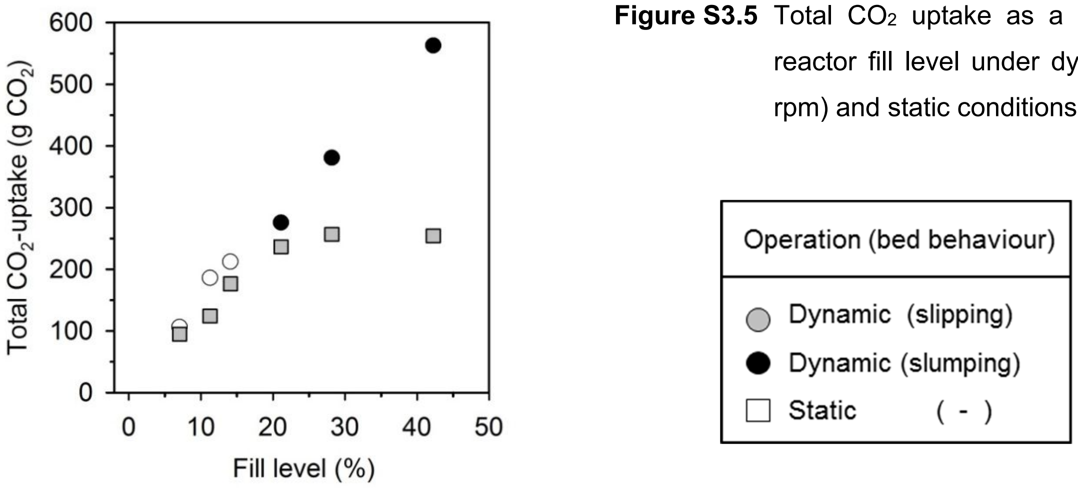

Figure S3.5 Total CO_2 uptake as a function of reactor fill level under dynamic (1.2 rpm) and static conditions (0 rpm).

3.9.4 Leaching behaviour of fresh and carbonated BA

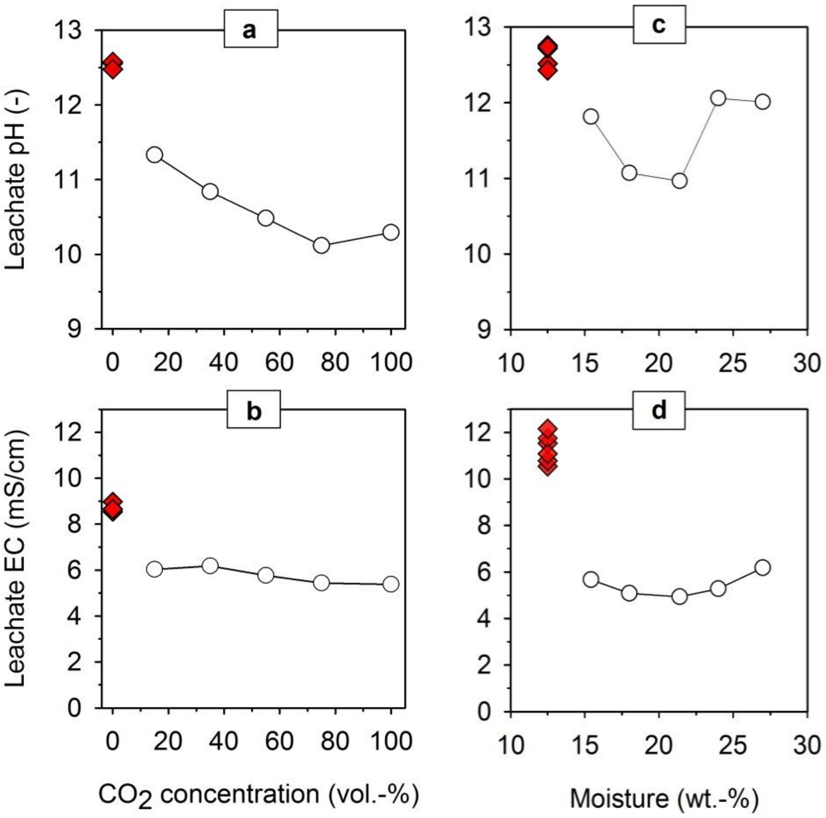

Figure S3.6 Comparion of leachate pH and EC of fresh (diamonds) and carboanted (circles) BA as a function of CO_2 concentration (a, b) and moisture content (c, d).

References Supplementary Material

Liu, P.Y., Yang, R.Y. and Yu, A.B. DEM study of the transverse mixing of wet particles in rotating drums, *Chemical Engineering Science*, vol. 86, pp. 99–107, 2013.

Henein, H. Brimacombe, J. K. and Watkinson, A. P. Experimental study of transverse bed motion in rotary kilns, *Metallurgical Transactions B*, vol. 14, no. 2, pp. 191–205, 1983.

Chapter 4 Flow-through carbonation of waste incinerator bottom ash in a rotating drum batch reactor: role of specific CO_2 supply, mixing tools and fill level

Journal of Environmental Chemical Engineering (2019) 7: 102975
DOI: 10.1016/j.jece.2019.102975

Co-authors: Tim Mansfeldt, Harald Weigand

Formatting and orthography of the manuscript is adapted to the dissertation style.

4.1 Abstract

Bottom ashes (BA) constitute the dominant solid residue of municipal solid waste incineration. Ageing of BA over a period of several months is known to reduce the reactivity and leachability of critical trace metals via carbonation by atmospheric CO_2. This process may be accelerated by contacting the material with CO_2-rich exhaust gas in rotating drum reactors. In this study, we investigated carbonation of BA under dynamic conditions with continuous feed of the reactant gas. This is of particular interest for the integration of the process with the management of BA at incinerator sites. The effects of specific CO_2 supply, mixing tools, and reactor loadings on process performance were assessed by the leaching behaviour of the treated BA. The experiments were performed in a rotating drum. Overall, carbonation improved the leachate quality of BA. Leachate values characterized the reactor output as a non-hazardous waste when the specific CO_2 supply was above 100 g CO_2 per kg BA. The reaction could be accelerated to around 100 minutes and was enhanced by the use of mixing tools. Of the configurations tested, a perforated mixing cage performed best even at fill levels of up to 50 %. This set-up was also least prone to the formation of BA incrustations.

Keywords: Incineration; CO_2 capture; rotating drum; bottom ash; accelerated carbonation; leaching

4.2 Introduction

It has long since been recognized that the ageing of bottom ash (BA) generated during municipal solid waste incineration is beneficial to its leaching behaviour. Ageing takes place when this highly reactive alkaline and typically moist waste is in contact with the ambient air. Moisture contents of 15 to 25 wt.-% are due to the quenching applied at most waste incinerators and provide the pore water necessary for the majority of ageing reactions (Costa et al., 2007). During ageing, the access of oxygen promotes the formation of Fe- and Al-(hydr)oxides as prominent adsorbents for environmentally relevant trace metals (Chaspoul et al., 2008; Oehmig et al., 2015). Concomitantly, the access of carbon dioxide (CO_2) leads to the carbonation of the material. This denotes the process where $Ca(OH)_2$ formed from CaO during quenching reacts with CO_2 and converts to $CaCO_3$. Thereby BA alkalinity is consumed and the pH drops, which in turn lowers the leachability of amphoteric trace metals like Pb, Zn and Cu (Saffarzadeh et al., 2011).

On the one hand, the benefit of ageing-induced contaminant immobilisation rests with lower landfilling costs. This is due to the fact that the waste acceptance criteria specific to each landfill class are predominantly determined on a leachability basis. On the other hand, also reuse options of BA, e.g. as substitute aggregates in civil engineering are favoured by ageing (Xuan et al., 2018; Di Gianfilippo et al., 2018; Lynn et al., 2017). Therefore, a series of national guidelines in Europe demand that BA is aged over a period of 3 to 6 months prior to final disposal or reuse (Blanc et al., 2019; Nørgaard et al., 2019; Dou et al., 2017).

Passive BA ageing over these timescales requires adequate storage installations at the incinerator sites as well as machinery and manpower for periodic turning (Blanc et al., 2018). Thus, a number of researchers have addressed the question of how the ageing of BA and other alkaline waste materials (e.g. air pollution control residues) can be accelerated. Methods investigated to this end include static reactor systems where the material is exposed to CO_2 partial pressures typically above 100 kPa (Baciocchi et al., 2010; Fernández Bertos et al., 2004a; Rendek et al., 2006) or where CO_2-rich gas streams are passed over thin layers of the solid at ambient pressure (Sakita et al., 2015; Lin et al., 2015a; Um et al., 2013).

Although the scientific literature reveals substantial progress in accelerated BA carbonation, to the best of our knowledge a full-scale implementation has not been documented. This would ideally include a thorough mixing of BA to promote the CO_2 uptake from a CO_2-rich exhaust gas stream and a reactor system ideally operated under flow-through conditions in terms of both, gas and BA. Such a system could be implemented in a rotating drum reactor with a throughput synchronized with the generation of BA (Fernández Bertos et al., 2004b; Zingaretti et al., 2013). Rotating drums simultaneously provide agitation and mixing. Thereby the mass transfer between the gas and the solid is enhanced and the CO_2 uptake rate is increased (Brück et al., 2018b; Lombardi et al., 2016). The pattern of bed motion in rotating drums generally depends on the rheological properties of the solid, rotation speed, drum diameter, fill level and surface roughness of the drum wall (Liu et al., 2005). So far only rotating drums without any mixing tools have been tested for CO_2 uptake from the gas phase (Brück et al., 2018b; Łączny et al., 2015; Lombardi et al., 2016). However, several studies in other application fields indicated that mixing tools could improve the performance of rotating drums regarding the exchange between the solid and the gas (Fung and Mitchell, 1995; Jiang et al., 2011). Therefore, mixing tool design and configuration should be considered with respect to accelerated carbonation.

A series of exhaust gases have been successfully tested as CO_2 sources for BA carbonation. One obvious option is to use incineration exhaust gas, which normally contains around 10% CO_2 (Costa et al., 2007), since it is available in large quantities and generated at the same location as the BA. The amount of CO_2 supplied per unit mass of BA should be adequate to achieve a proper CO_2 uptake within a reasonable reaction time. In view of full-scale applications, the latter should be ideally below 2 h. The CO_2-uptake levels reported for this reaction time frame range from 5 to 35 g CO_2 per kg BA (Brück et al., 2018a; Lin et al., 2015b; Sakita and Nishimura, 2015; Um et al., 2013).

Under flow through conditions, the specific CO_2 supply is determined by the CO_2 concentration in the reactant gas, its volumetric flow rate, the residence time of the BA in the reactor and the reactor loading. While CO_2 concentration and flow rate are fixed depending on the source of the reactant gas, BA residence time and reactor loading are important process parameters for BA carbonation in a rotating drum. Residence time and reactor loading determine the reactor throughput (i.e. the feed rate of BA) and the corresponding values need to be identified prior to the full-scale implementation of enhanced BA carbonation.

Three successive test series were conducted to identify the effects of (i) specific CO_2 supply, (ii) mixing tool configuration, and (iii) reactor loading on accelerated carbonation. In the first series a broad range of specific CO_2 supplies (5 to 210 g CO_2/kg BA) was tested and evaluated. In the second test series, five different mixing configurations were studied. These comprised four different designs, namely the plain drum, two arrangements of lifter plates, a mixing shaft and a perforated mixing cage. In the third test series, the reactor loading was varied over a range of 8 to 40 kg. The effect of operating conditions on carbonation performance was assessed by the leaching behaviour of the treated BA in terms of hydrochemical parameters and regulated contaminants.

4.3 Material and methods

4.3.1 Bottom ash sampling

The BA was sampled at a grate-type refuse derived fuel incinerator located in central Germany. For details of the plant refer to (Brück et al., 2018a). For logistic reasons and to circumvent long storage times the BA was collected at three distinct occasions. Samples of about 200 kg were taken from a roofed temporary storage pile. The BA was manually passed through an 11 mm sieve and the oversize grain was discarded. This was done since the coarse fraction of BA is rather uncritical in terms of contaminant leaching and contributes little to carbonation. The samples were stored in air-tight clamping ring drums for a maximum of 14 d before used in the experiments.

4.3.2 Experimental setup

The experiments were conducted in a rotating drum reactor (see Figure 4.1). The reactor was a polyvinyl chloride cylinder (diameter 0.3 m; length 1 m). It was mounted on six rubber rollers attached to metal stand and rotated by an electric motor at a rate of 2.5 rpm. The BA was agitated by the rotary motion and was exposed to an adjustable flux of synthetic exhaust gas. The gas was produced from pure CO_2 (N4.5) and synthetic air employing a gas mixing station [Gmix, HighTec Zang, Herzogenrath, Germany]. Gas supply and exhaust tubes were connected to the reactor via rotating joints. The front-end covers of the reactor were fixed to the mantle by spring locks. This ensured fast opening and closure for reactor loading and sampling. In some experiments, the exhaust was passed through a flow-through cell to monitor the gas temperature. Values were recorded every minute using a wireless sensor [AREXX TSN-TH70E, RS Zwolle, The Netherlands] with a tolerance of ± 1°C.

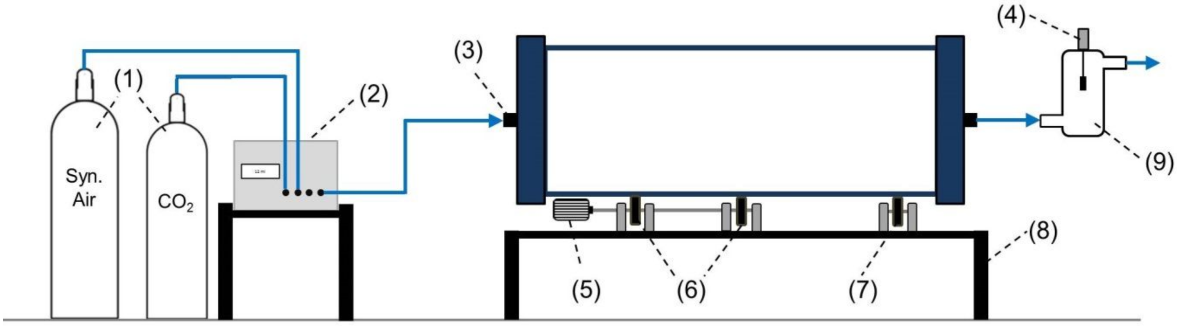

Figure 4.1 Experimental set-up. (1) Gas cylinders; (2) gas mixing station; (3) end cover with rotating joint (4) wireless temperature sensor; (5) electric motor; (6) drive rollers; (7) track rollers; (8) substructure; (9) flow-through cell.

The mixing of BA influences the mass exchange between the solid and the gas phase and thereby affects the rate of BA carbonation (Brück et al., 2018a; Brück et al., 2018b). Varied sets of mixing tools were evaluated in terms of carbonation performance (see Figure 4.2). Mixing tool configuration (MTC) 1 consisted of an axial cross-shaped mixing shaft with 20 perforated baffles. MTC 2 and 3 denote a configuration of 3 and 12 straight plates (width: 0.3 m, length: 0.06 m), respectively. These served as lifters and were mounted perpendicularly on the inner drum wall. In the MTC 2 the three plates were spread along the length of the reactor with an offset of 90 degrees. In the MTC 3 the 12 plates were arranged in 3 x 4 groups. MTC 4 denotes the plain drum. For MTC 5 a mixing cage (Length: 0.95 m, diameter: 0.25 m) made out of a PVC pipe was used. A tumbling motion of the cage resulted from the fact that its diameter was lower than the reactor diameter. The cage was perforated by 18 elongated gaps (0.4 x 0.05 m) to provide material lifting.

To study the effect of the MTCs on the pattern of bed motion, the reactor was equipped with a transparent acrylic glass plate and the bed behaviour was cinematographically analysed as described in Brück et al. (2018b). For MTC 5 the mode of transversal bed motion (slipping, slumping, rolling, or transitional) was outlined in a bed behaviour diagram.

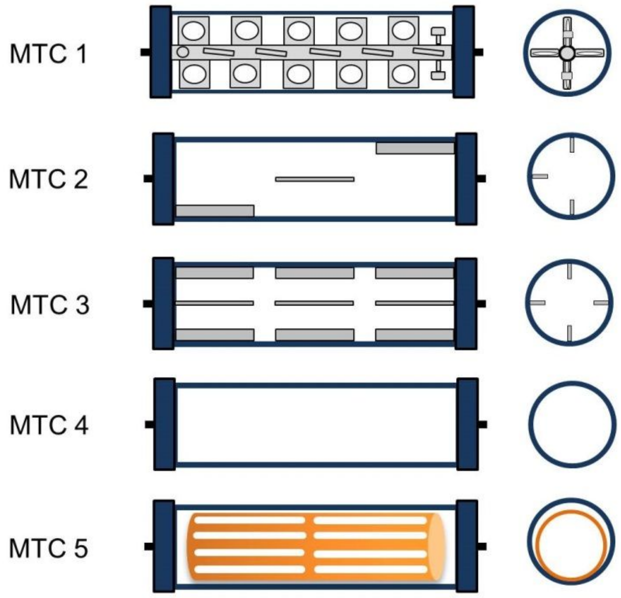

Figure 4.2 Schematic of the mixing tool configurations (MTCs) 1 - 5 in longitudinal and cross-sectional view. MTC 1: axial mixing shaft with 20 perforated baffles; MTC 2: 3 lifter plates (L = 30 cm, H = 6 cm); MTC 3: 12 lifter plates (L = 30 cm, H = 6 cm); MTC 4: plain drum; MTC 5: perforated mixing cage.

4.3.3 Accelerated carbonation tests

The accelerated carbonation of BA under flow-through conditions was tested in three distinct sets of experiments. Table 4.1 summarizes the experimental conditions and operation parameters. Carbonation performance was evaluated in terms of the leaching behaviour of BA. Therefore, upon completion of experiments the BA was taken out of the reactor and manually homogenized prior to the conduction of leaching tests as described in section 2.4.

The first set of experiments served to evaluate BA carbonation under systematic variation of (i) reactor loading (4, 6, 8 kg fresh BA), (ii) gas flow rate ($\dot{V}$; 20, 40, 60 L/min) and (iii) reaction time (t_R; 20, 60, 100 min) in a total of 27 runs. The CO_2 concentration (c_{CO_2}) of the synthetic exhaust gas was adjusted to 6.7 vol.-%. This corresponds to the CO_2 concentration of a gas-powered co-generation plant available at the site which in perspective may be used as a reactant gas source for a full scale application of the accelerated carbonation process. The variation of the parameter values (i)-(iii) yielded a specific CO_2 supply (ε_{CO_2}) in the range of 7 - 210 g CO_2/kg BA and was calculated according to equation 4.1:

$$\varepsilon_{CO_2} = \frac{\dot{V} \cdot \frac{c_{CO_2}}{100\ \%} \cdot t_R \cdot M_{CO_2}}{V_m \cdot m_{BA}} \qquad \text{(Eq. 4.1)}$$

where M_{CO_2} is the molar mass of CO_2 (44.01 g/mol), V_m is the molar volume of an ideal gas at 25 °C (24.465 L/mol), and m_{BA} is the dry mass of BA (kg) loaded into the reactor. Test series 1 was conducted using MTC 1.

In the second set of experiments the effect of different MTCs (see Figure 4.2) on carbonation was tested. Based on the findings of test series 1, the gas flow rate $\dot{V}$, reactor loading m_{BA} and reaction time t_R were set to 60 L/min, 8 kg, and 100 minutes, respectively. This yielded a ε_{CO_2} of 100 g CO_2/kg BA.

In the third set of experiments the influence of the reactor loading on carbonation was studied. The experiments were conducted with reactor loadings ranging from 8 to 40 kg fresh BA, while the MTC and ε_{CO_2} were identical to test series 2. Considering the loose bulk density of the material (1.11 kg/L) the reactor loading corresponded to a fill level range of 10 to 50 vol.-%. By adjusting the CO_2 concentration in the reactant gas we maintained a constant ε_{CO_2} of 100 g CO_2/kg BA.

Table 4.1 Conditions of BA carbonation test series 1 to 3 conducted in a rotating drum reactor.

Parameter	Test series 1	Test series 2	Test series 3
c_{CO_2} (vol.-%)	6.7	6.7	6.7 - 33.5
$\dot{V}$ (L/min)	20/40/60	60	60
Reactor loading (kg BA)	4/6/8	8	8/10/15/20/30/35/40
Reaction time (min)	20/60/100	100	100
ε_{CO_2} (g CO_2/kg BA)	7 - 210	100	100
Rotation speed (rpm)	2.5	2.5	2.5
BA sample Nr. (-)	1	2	3
Mixing tool configuration (-)	MTC 1	MTC 1 - 5	MTC 5

4.3.4 Analytical

The moisture content of the BA was determined gravimetrically after drying subsamples at 105 °C for 24 h. The loose bulk density was determined by weighing a graduated cylinder holding 100 mL of the material. The bulk chemical composition of the BA was measured by X-ray fluorescence (XRF) spectroscopy [Spectroscout ES, Spectro Analytical Instruments GmbH, Kleve, Germany] with a detection limit of ~0.01 wt.-%. Results are summarized in the supplementary material (Table S4.1).

To evaluate the carbonation performance, batch leaching tests were performed at a liquid-to-solid ratio (L:S) of 10 L kg^{-1}. Therefore, 1 L of de-ionized water was added to a BA equivalent of 100 g of dry matter and agitated on an end-over-end shaker for 24 h according to EN 12457-2. To assess the suitability of the carbonated BA for a geotechnical reuse, an up-stream percolation test was performed in accordance with the draft of the German Ordinance on Secondary Construction Materials in conjunction with the standard method DIN 19528. The sample was taken from a selected run of test series 1 (loading: 8 kg, reaction time: 100 min, volumetric flux: 40 L/min) and run against an uncarbonated control (fresh BA). The percolation tests were conducted in plexiglass columns with a void volume of 2 L at the prescribed contact time of 5 h and observing the final L:S ratio of 2 L kg^{-1}. A detailed description of the experimental conditions can be found in the supplement.

All leachates were immediately analysed for pH and electrical conductivity (EC). The leachates were then passed through 0.45 µm membrane filter (cellulose acetate) and acidified with concentrated nitric acid (suprapur) to pH <2 for element analysis. The concentrations of Cu, Pb, Zn, Ba, V, Sb, Cr and Mo were measured by inductively coupled plasma–mass spectrometry [ICP-MS, X-Series II, Thermo Scientific: Dreieich, Germany]. Leachate aliquots of the column percolation tests were analysed for Cl^- and SO_4^{2-} as bulk anions by ion chromatography [Metrohm 861 Advanced Compact IC with a Metrosep A Supp 5 column and a conductivity detector].

The $Ca(OH)_2$ and $CaCO_3$ content of the BA was determined by thermogravimetric analysis (TGA) using a thermobalance [TG 209 F1, Netzsch, Selb, Germany]. Therefore, approximately 20 g of dry BA were ground in a planetary ball mill [Pulverisette 6, Fritsch GmbH, Idar-Oberstein, Germany]. Samples were heated in corundum crucibles to 900°C at 20 °C/minute under a nitrogen atmosphere. The thermal decomposition of $Ca(OH)_2$ to CaO and H_2O as well as the decomposition of $CaCO_3$ to CaO and CO_2 yielded a specific weight loss in the temperature window between 380 °C to 480 °C and 480 °C to 900 °C, respectively. The specific weight loss was then used to calculate the content of $Ca(OH)_2$ and $CaCO_3$ of the sample.

4.4 Results and discussion

4.4.1 Effect of specific CO_2 supply on carbonation performance

To assess the effect of accelerated carbonation on the mobility of BA constituents, batch leaching tests were performed with both the fresh and carbonated BA. Figure 4.3 shows the leachate pH, EC and trace metal concentrations as a function of ε_{CO_2}. The latter integrates all varied parameters of the experiment into a single variable (see Equation 1).

Leachate pH and EC dropped markedly for ε_{CO_2} of up to 50 g CO_2/kg BA, whereas further increases of ε_{CO_2} yielded less pronounced effects. The decrease in leachate pH is consistent with the consumption of BA alkalinity (mainly related to the dissolution of $Ca(OH)_2$) by carbonation. The EC drop indicates that in addition the leachates were depleted in mobile charged constituents, most prominently in OH^- and possibly in Ca^{2+} which is consumed in the carbonation reaction and precipitates as $CaCO_3$. Carbonation of the treated BA was independently confirmed by TGA, which indicated a consumption of $Ca(OH)_2$ and a generation of $CaCO_3$.

The leachates of the fresh BA characterize the material as a hazardous waste. This is due to Pb concentrations way above the German waste acceptance criterion (WAC) for landfill class (LC) 2, whereas Cu and Zn exceeded the LC 1 and LC 0 WAC, respectively.

In the carbonated BA, these amphoteric metals were substantially immobilized. This is consistent with previous findings (Brück et al., 2018b; Chimenos et al., 2000; Fernández Bertos et al., 2004a; Wei et al., 2011). Leachates of the carbonated BA were depleted in Pb and Zn by up to two orders of magnitude and in Cu by at least one order of magnitude as compared to fresh BA. For ε_{CO_2} in excess of 100 g CO_2/kg BA the Pb concentrations in the leachates were below 200 µg/L, classifying the carbonated BA as a non-hazardous waste, altogether. Previous studies with BA from the same incinerator indicated a CO_2 uptake between 20 and 30 g CO_2/ kg BA, which is also in accordance with findings reported by other authors (Rendek et al., 2006; Sakita and Nishimura, 2015; Um et al., 2013). This carbonation level was also confirmed by the TGA performed with the sample carbonated at a reactor loading of 8 kg, a volumetric gas flow of 40 L/min, and a reaction time of 100 min. The CO_2 uptake of 21.4 g CO_2/kg BA as determined by TGA of the carbonated material is far lower than the specific CO_2 supply to the reactor (100 g CO_2/kg BA). Thus, the CO_2 mass transfer under flow-through conditions was incomplete and residual CO_2 remained in the exhaust.

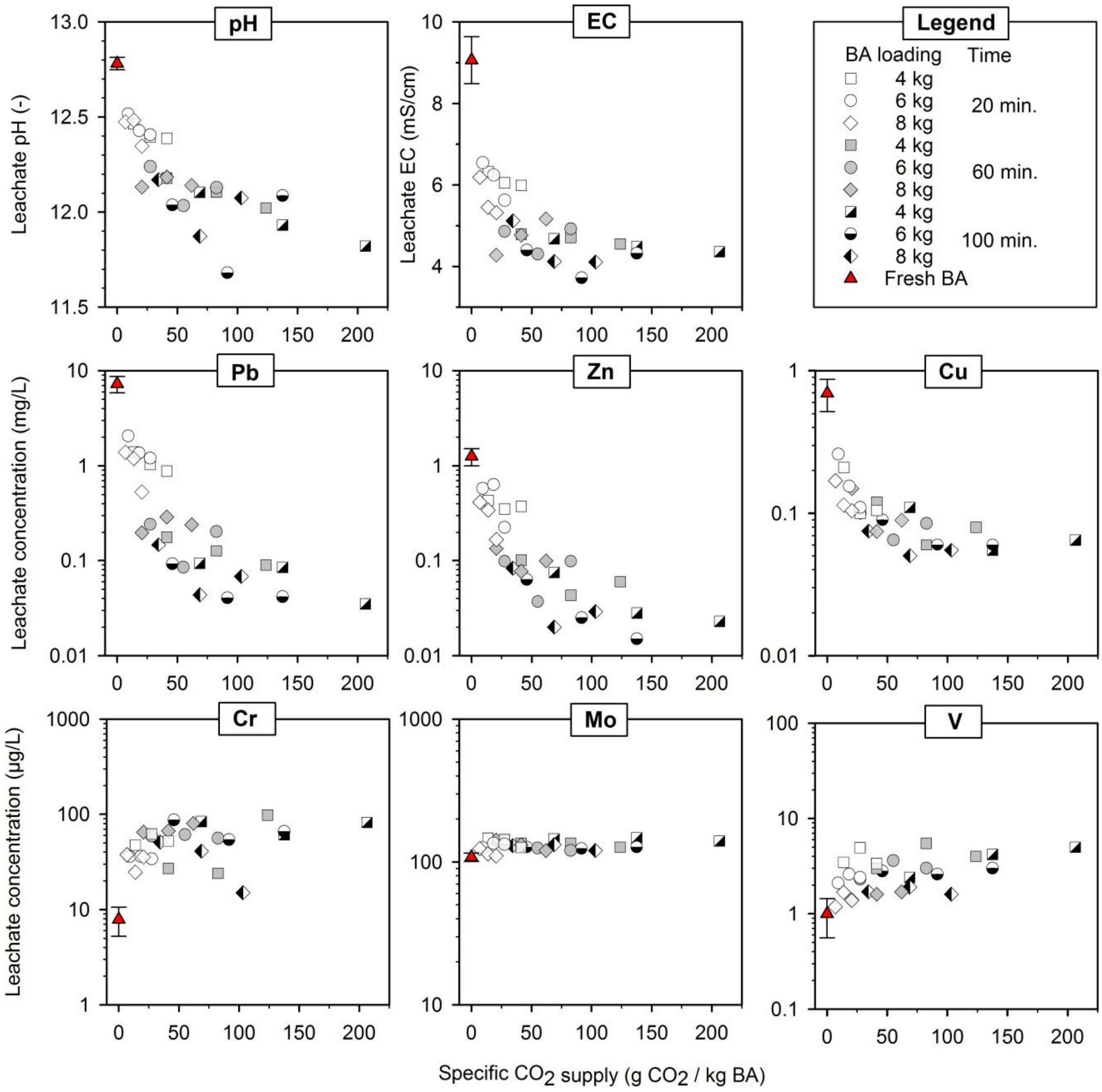

Figure 4.3 Leachate properties of fresh and carbonated BA as a function of specific CO_2-supply. Experiments were performed at a CO_2 concentration of 6.7 vol.-% in a rotating drum reactor at varied reactor loadings, volumetric flow rates and reaction times (see Table 4.1). Error bars: Standard deviation for fresh BA (n = 6). EC = electric conductivity.

Under alkaline conditions, Cr, Mo, and V are predominantly present as chromate, molybdate and vanadate, i.e. as oxyanions. The concentration-vs.-ε_{CO_2} characteristic of these differed greatly from that of the amphoteric metals. Contrary to the latter, leachate concentrations of Cr, Mo and V were higher in the carbonated BA than in the fresh BA (see Figure 4.3). Carbonation-induced mobilisation was most pronounced for Cr and least pronounced for Mo.

Despite the adverse effect of carbonation on the mobility of oxyanions the leachate concentrations of Cr and Mo remained below the German LC 1 WAC of 300 µg/L for both. No such comparison can be made for V since the German Landfill Ordinance does not include a pertinent WAC. Overall the mobilization of oxyanions did not outweigh the beneficial effects observed for amphoteric metals.

It is beyond the scope of this study to provide a mechanistic understanding of the immobilizing and mobilizing effects of BA carbonation. Yet it is evident, that the amphoteric trace metals show a concentration-vs.-ε_{CO_2} characteristic very similar to the development of pH. Indeed, Wei et al. (Wei et al., 2011) concluded that the immobilization of amphoteric metals in carbonated BA is primarily due to the pH-drop. Coefficients of determination (R^2) of Pb, Zn and Cu vs. pH are between 0.62 to 0.90 and largely support this (see Figure S4.1). In addition, physical containment by carbonates precipitated on the surface of BA aggregates may have contributed to lowered leachability (Sakita and Nishimura, 2015) and adsorption to newly formed mineral phases may also be important (Dijkstra et al., 2006; Meima and Comans, 1999; Yao et al., 2012). The mobility of the oxyanions has been described as primarily controlled by dissolution/precipitation reactions (Cornelis et al., 2008) possibly in conjunction with sulphate substitution in ettringite or ettringite-like phases (Alam et al., 2019; Marchese and Genon, 2009).

In view of a geotechnical reuse option of carbonated BA the leachability was complementarily studied in the upstream percolation test described in the draft of the German Ordinance on Secondary Construction Materials. The leachate levels of the carbonated BA fully complied with the so-called material values of class 2 waste incinerator BA, allowing for their utilization as e.g. road basement material, backfilling. Such potential applications have been previously addressed by (del Valle-Zermeño et al., 2014; Le et al., 2018). For more detailed results, please refer to the supplement (see Table S4.1).

Overall, carbonation improved the leachate quality of BA (decrease in amphoteric trace metal release, lower pH and EC). While the leachate values classified fresh BA as a hazardous waste, the carbonated BA complied with the WACs for the landfilling as a non-hazardous waste. Potentially it would also be suited for geotechnical reuse since it complies with the corresponding material values of the draft ordinance. When carbonation is performed under flow through conditions, the specific CO_2 supply should be 100 g CO_2 / kg BA or higher, although care should be taken in view of a carbonation-induced mobilization of oxyanions.

4.4.2 Effect of mixing tools on carbonation performance

We evaluated the effect of enhanced mixing on carbonation under five mixing tool configurations (MTCs). Based on the results shown in section 3.1 the ε_{CO_2} was kept constant at 100 g CO_2/kg BA (see Table 4.1). This value was sufficient to achieve the desired decrease in leachate pH and immobilisation of critical trace metals and avoided exceedingly high concentrations of oxyanions in the leachate. Again, carbonation performance at varied MTC was assessed by the leachate properties of carbonated vs. fresh BA as well as the $Ca(OH)_2$-content of the solid (see Figure 4.4).

For MTC 3 and 4, the leachate pH and EC decreased only slightly compared to the fresh BA. Thus, only little portlandite was consumed which is in line with the relatively high $Ca(OH)_2$ content of the carbonated BA. In accordance with the slightly decreased leachate pH in the carbonated BA, concentrations of amphoteric trace metals were still high. While carbonation was sufficient to decrease leachate concentrations of and Zn and Cu below WAC for LC 0 and LC 1 (0.4 mg/L and 0.5 mg/L), Pb leachate of the carbonated material were still above the LC2 WAC (1 mg/L).

For MTCs 1, 2, and 5 the leachate pH and EC as well as $Ca(OH)_2$ content notably decreased as compared to the control. Leachate pH values below 12 are in line with the consumption of $Ca(OH)_2$ and a significant immobilisation of amphoteric trace metals. Here, Zn and Cu were both below WAC LC 0 and Pb below LC 1 WAC, again classifying the carbonated BA as a non-hazardous waste.

Results in section 3.1 pointed to a carbonation-induced mobilization of oxyanions as a result of proceeding carbonation. This is confirmed by the results of test series 2 where leachate concentrations of oxyanions also increased relative to the control. Mobilisation was most significant for V (up to 15 times higher) and lowest for Mo. For the latter rather no effect was observed for MTC 1-4, whereas MTC 5 gave leachate values two times higher than the control. As in test series 1, the leachate concentrations of Cr and Mo remained below the WAC for LC 1.

Overall, the evaluation of the leaching behaviour showed that carbonation performance was affected by the MTC, indicating that adequate mixing is beneficial for accelerated carbonation in a rotating drum reactor. Overall, MTC 1, 2 and 5 showed superior carbonation performance than MTC 3 and 4.

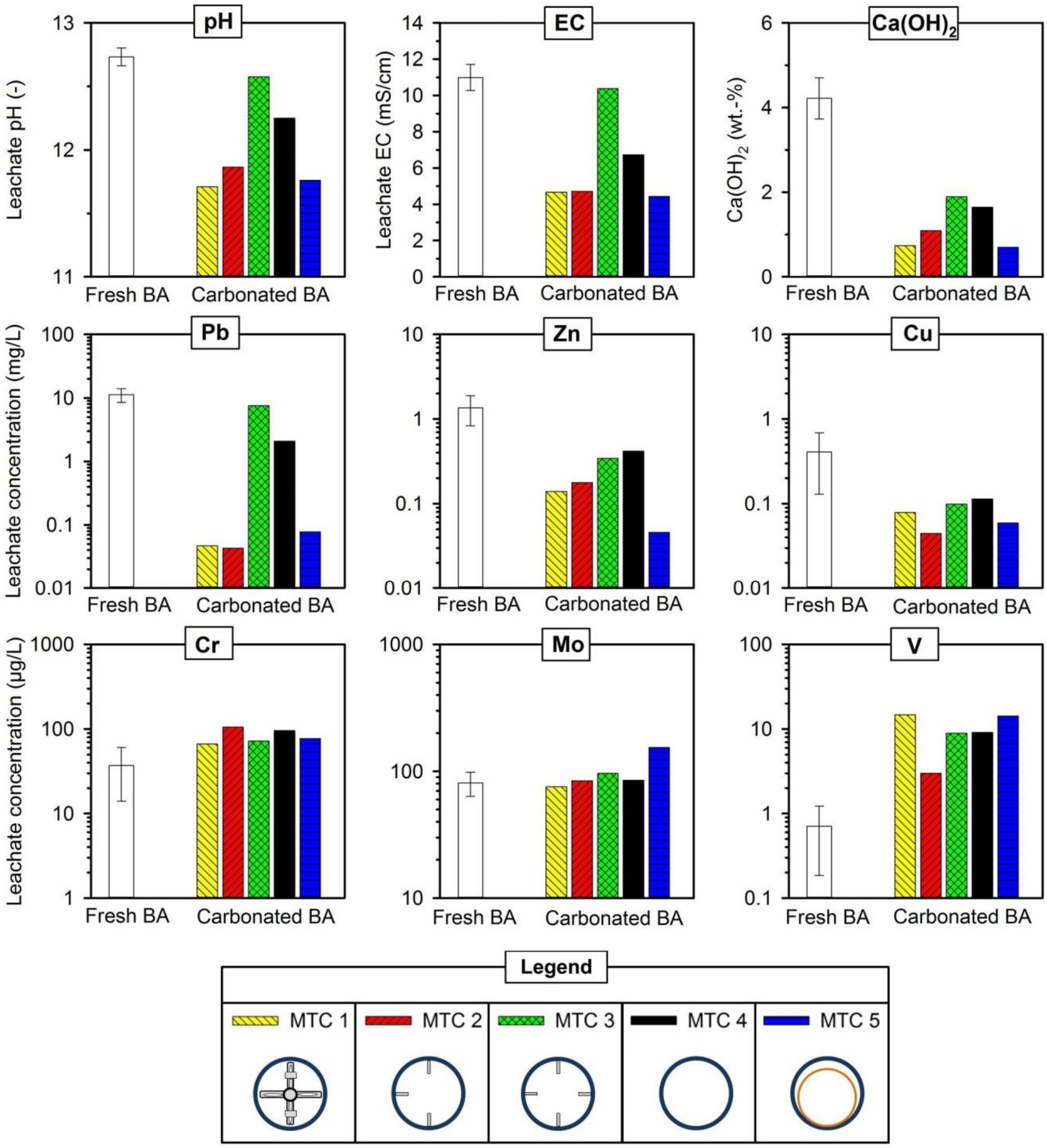

Figure 4.4 Leachate properties and $Ca(OH)_2$-contents of fresh and carbonated BA under varied mixing tool configurations. Experiments were performed at a CO_2 concentration of 6.7 vol.-% in a rotating drum reactor with a reactor loading of 8 kg BA, volumetric flow rate of 40 L/min and a reaction time of 100 min yielding a specific CO_2 supply of 100 g CO_2 per kg BA (see Table 4.1). Error bars: Standard deviation for fresh BA (n = 6).

Since carbonation is exothermic, self-heating of BA occurs. In a closed reactor system, we previously found a temperature increase of up to 14 °C (Brück et al., 2018b). A heat balance model revealed that the degree of self-heating correlates with carbonation intensity. Under the flow-through conditions applied here, the reactor is cooled by the continuous gas stream. To test whether still a self-heating is detectable, the exhaust gas temperature was monitored during the runs with MTC 2, 4, and 5 (see Figure 4.5). Indeed, compared to the closed reactor system the self- heating was lower. Starting from virtually the same temperature at the beginning of the experiment, the exhaust gas temperature increased during the first 50 min of the experiment. The achieved exhaust maximum gas temperature (T_{max}) increased in the order MTC 4 (plain drum; T_{max} = 22.8 °C), MTC 2 (three lifter plates; T_{max} = 23.6 °C), MTC 5 (mixing cage; T_{max} = 24.4 °C). Final exhaust gas temperatures followed the same order. Thus, the observed self-heating is in line with the order of carbonation performance as judged by the leachate pH and EC as well as the $Ca(OH)_2$ contents (see Figure 4.4). Temperatures peaked earliest for MTC 5 and latest for MTC 4. Thus, the use of mixing tools not only enhanced total turnover (as indicated by peak temperatures and final temperatures) but also increased the rate of carbonation (as indicated by the corresponding times-to-peak). In view of residence times under full-scale conditions the latter finding is of particular importance.

Overall, the results of test series 2 indicate that adequately designed mixing tools enhance BA carbonation in rotating drums. This is due to a modified bed motion where inter-particle mixing is enhanced over free surface flow (Jiang et al., 2011).

A possible draw-back of mixing tools is that they may promote the formation of BA incrustations which in turn would cause costs for periodic maintenance. This issue was addressed by the video analyses of bed motion and reactor inspections conducted after each run of test series 2. Bed motion in the plain drum represents the basic pattern, which was modified by the mixing tools. Therefore, in the following the results of MTC 4 will be discussed, first.

For the plain drum (MTC 4) a slipping bed motion prevailed. This is in accordance with the bed behaviour characteristic shown in a previous study for the same BA and reactor (Brück et al., 2018b).

In the plain drum, the bed slipped after exceeding a critical inclination due to reactor rotation. Since a slipping bed moves essentially as a whole, only little radial mixing happens (Boateng, 2015). Thus, in absence of mixing tools, carbonation under flow-through conditions is rather restricted to the upper layer of the BA bed. Patchy incrustations remained on the reactor mantle after a reaction time of 100 minutes and required moderate mechanical force for removal.

A slipping bed motion also prevailed with three lifter plates mounted on the drum wall (MTC 2) but the bed was periodically disturbed by plates’ passage. In consequence, material from the lower bed region was lifted and thrown back to the bed surface. This bed motion favoured BA carbonation (as corroborated by the leachates and the self-heating, see Figure 4.4 and 4.5). Incrustations were found both on the reactor mantle itself and the lifter plates, most prominently along the mantle contact path.

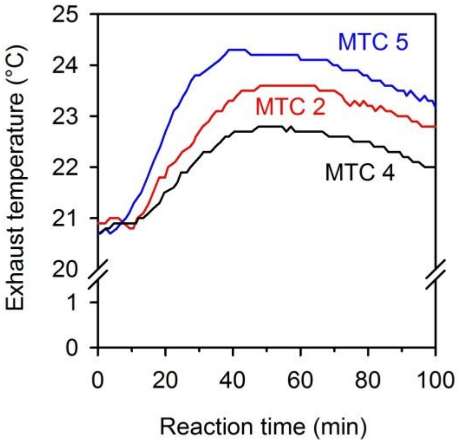

Figure 4.5 Time courses of reactor exhaust temperature during accelerated carbonation in a rotating drum reactor for mixing tool configurations (MTC) 2, 4 and 5.

Increasing the number of plates to 12 arranged in 3 x 4 groups (MTC 3) did not favour carbonation over MTC 2 in terms of pH, EC, and $Ca(OH)_2$. Indeed, MTC 3 performed worst of all mixing tool configurations. This was surprising since MTC 3 is commonly used in other applications of rotating drums (Bongo Njeng, A. S. et al., 2015; Kalamdhad et al., 2012; Mitchell et al., 2006). Therefore, poor performance of MTC 3 may be related to the rheological properties of wet BA. Specifically, we observed that slipping was almost entirely inhibited with MTC 3. This may have promoted BA incrustations (see Figure S4.3). As a consequence, mixing was impaired, which in turn may have hampered CO_2 access to the BA as compared to the use of only 3 lifter plates (MTC 2).

Axially located mixing tools are known for their high mixing quality (Ottino and Lueptow, 2008). This was confirmed by the satisfactory carbonation performance achieved with MTC 1. During the experiments we observed that the passage of the perforated baffles evoked a high degree of agitation. No incrustations on the reactor mantle were observed. However, incrustations formed on the mixing shaft itself (see Figure S4.2). In practical applications these would require periodical cleaning to maintain the functionality.

In contrast to MTC 1 - 3 the perforated mixing cage (MTC 5) does not comprise mounted plates or baffles. Carbonation was enhanced (strongest drop in pH, EC, and $Ca(OH)_2$ contents). As revealed by video analysis, this mixing tool yielded an alternating slipping/slumping bed motion. Slumping prevailed when the cage rotated synchronously with the drum. Compared to slipping, slumping favours bed mixing (Lim et al., 2003; Metcalfe et al., 1995) and may therefore also enhance carbonation. Time by time the cage (and the BA) slipped along the reactor mantle against the direction of rotation (asynchronous rotation). This had a cleaning effect on the reactor mantle and incrustations observed after a reaction time of 100 minutes were minimal as compared to the other MTCs.

Results of test series 2 suggest that MTC 1, 2 and 5 are suitable for the accelerated carbonation of BA in a rotating drum batch reactor operated under flow-through conditions.

Compared to the configuration without mixing tools, amphoteric metal levels in the leachate were decreased and safely met the WAC for LC1. With the perforated mixing cage (MTC 5) the reactor was least prone to formation of BA incrustations. Therefore, this configuration seems particularly suited.

4.4.3 Effect of reactor loading on accelerated carbonation

The reactor loading is crucial for a future development of the rotating drum reactor towards a full-scale application. This is due to the fact that the reactor loading in conjunction with the residence time determines the BA throughput. Therefore, in test series 3 we systematically tested the carbonation performance over a reactor loading between 8 and 40 kg corresponding to fill levels of 10 to 50 vol.-%. For all experiments MTC 5 was used since it both enhanced carbonation and prevented formation of BA incrustations. Calling back to test series 1, a specific CO_2 supply of 100 g CO_2/kg BA was maintained by increasing the CO_2 concentration of the feed proportionally to reactor loading (see Eq. 4.1 and Table 4.1). Figure 4.6 shows the leachate pH, EC and concentration of trace metals as a function of reactor loading against the untreated control.

Overall, accelerated carbonation achieved a significant improvement of the leachate quality across the entire range of reactor loadings. Increasing the reactor loading from 8 kg to 15 kg caused a pronounced drop in leachate pH, EC and concentration of amphoteric metals. For reactor loadings above 15 kg the carbonation effect remained roughly unchanged. This suggests that high fill levels do not impair CO_2 uptake as long as the CO_2 supply is adapted.

This effect may be due to the dependence of bed motion on the reactor loading. Figure 4.7a and b show the bed behaviour as a function of rotation speed and reactor loading as well as the slipping and slumping frequency. We previously reported that in the absence of mixing tools, the bed motion of BA changes from slipping to slumping when the reactor loading exceeds 15 kg, approximately. With the mixing cage, the transition from slipping to slumping was shifted to reactor loadings <8 kg and a broad field of transitional slipping/slumping bed motion was identified. Transitional slipping/slumping bed motion also dominated for the rotation rate of 2.5 rpm used in the carbonation experiments. Pure slumping was observed for a reactor loading of 30 kg BA (see Figure 4.7a).

Video analyses showed that the slipping frequency decreased with fill level while the slumping frequency increased (see Figure 4.7b). Since a slumping bed motion generally yields a better mixing than slipping, the access of CO_2 to the BA may be enhanced and carbonation performance should increase. This indicates that a rotating drum reactor equipped with an adequate mixing tool can be operated at fill levels of up to 50 vol.-%, provided that the specific CO_2 supply is adjusted accordingly. Alongside an increase in CO_2 concentration this could potentially be done by increasing the reaction time.

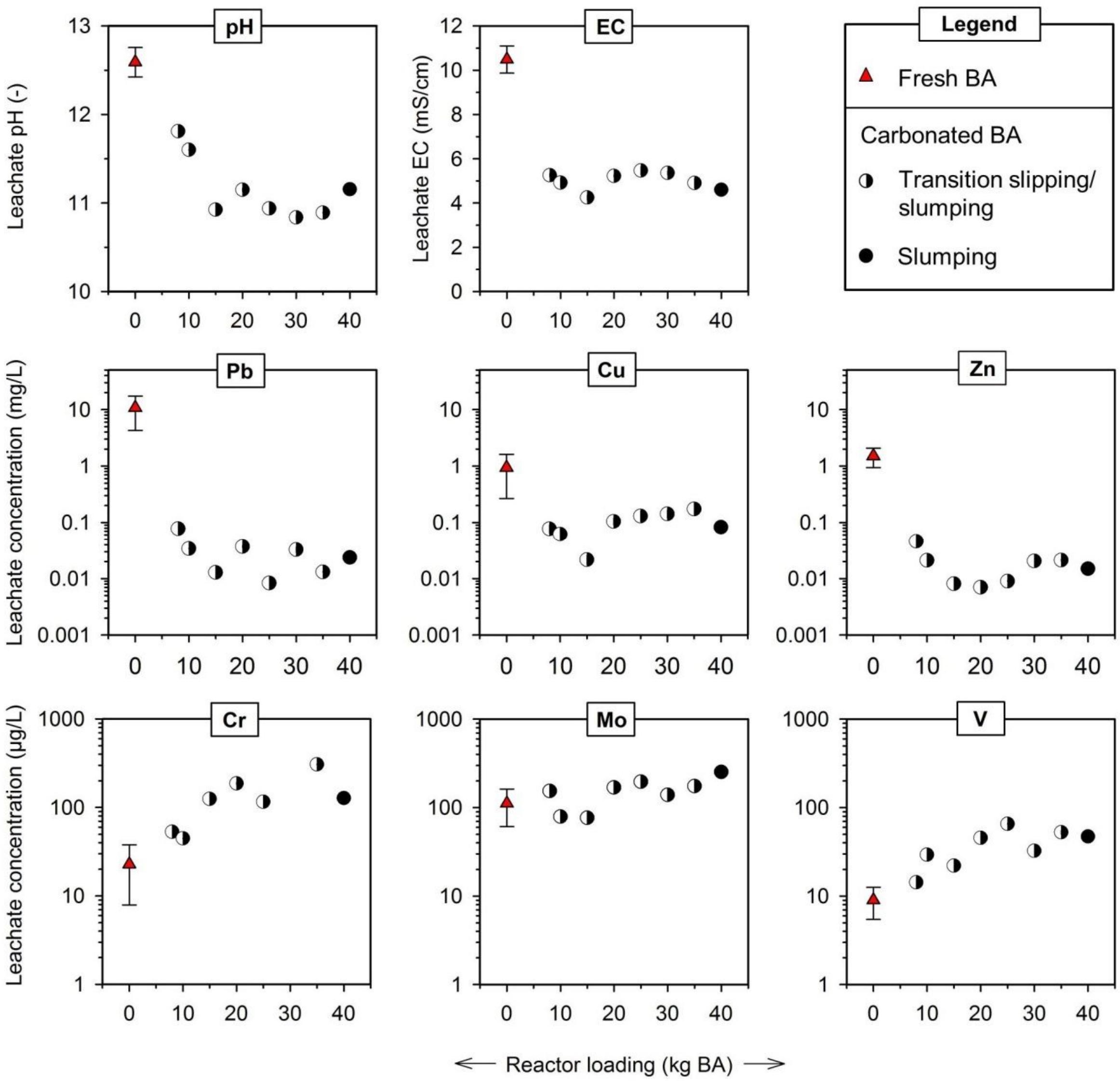

Figure 4.6 Leachate properties of fresh and carbonated BA at varied reactor loading and a specific CO_2 supply of 100 g CO_2/kg BA (see Table 4.1). Symbols: red triangle = fresh BA (error bars: Standard deviation for n = 6); circles = carbonated BA.

Again, a mobilisation effect was observed for oxyanion forming elements, especially for Cr and V. In the experiments discussed in the previous sections the mobilisation effect was uncritical in terms of compliance with the German WACs for the LC 1. At high fill levels, however, Cr leaching in the carbonated material may become critical as it partially exceeded 0.3 mg/l. This is in line with the observed strong pH-drop. Obviously, the identification of a proper end point is crucial to achieve the desired immobilisation of critical amphoteric metals and at the same time prevent an excessive mobilisation of oxyanion forming elements.

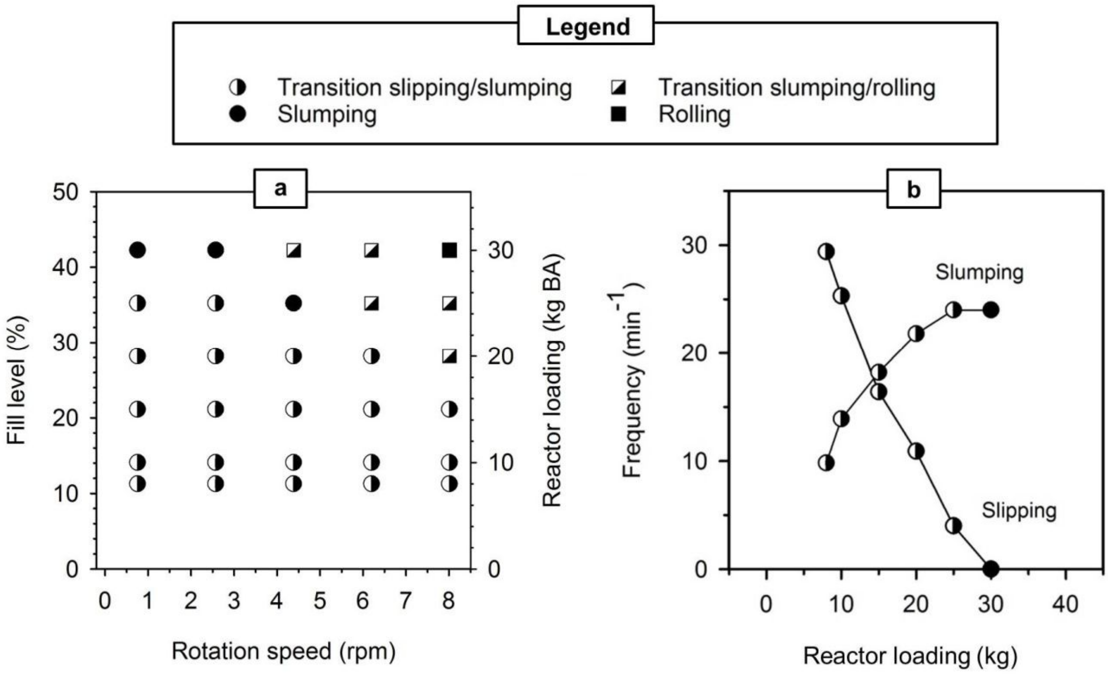

Figure 4.7 (a) Bed behaviour of BA as a function of rotation speed and fill level; (b) slipping/slumping frequencies as a function of reactor loading at 2.5 rpm.

4.5 Conclusions

In this study a rotating drum reactor was successfully used for the accelerated carbonation of BA. For reactor loadings of up to 8 kg reaction times could be cut to 100 minutes employing a specific CO_2 supply of 100 g CO_2/kg BA. The treated material complied with the German WAC for class I landfills and was suited for geotechnical reuse. The concentration of critical trace metals - in particular Pb and Zn - dropped by up to two orders of magnitude. By contrast, a moderate mobilisation was observed for the oxyanions Cr, Mo and V. This, however, did not outweigh the beneficial effects observed for the amphoteric metals. Carbonation in a rotating drum reactor can be enhanced by the use of specific mixing tools. This is attributed to the modified bed motion and, hence, increased mixing rate. Particular attention should be paid to a possible formation of incrustations during long-term use. In this context, the use of a perforated mixing cage was quite encouraging and its design aspects should be considered in more detail.

With the mixing cage, carbonation performance slightly increased with reactor loadings of up to 15 kg and remained stable for reactor loadings between 15 and 40 kg. This may have been due to the promotion of a slumping over a slipping bed behaviour.

Overall, the rotating drum reactor concept appears promising for the full-scale treatment of BA in terms of high reactor loadings in combination with relatively short residence times. Yet, in a full-scale operation the reactor throughput would ideally have to be synchronized with the rate of BA generation. This issue is addressed in ongoing work.

4.6 Acknowledgements

This project (HA project no. 483/15-25) was supported in the framework of Hessen ModellProjekte financed with funds of LOEWE – Landes-Offensive zur Entwicklung Wissenschaftlich-ökonomischer Exzellenz, Förderlinie 3: KMU-Verbundvorhaben (State Offensive for the Development of Scientific and Economic Excellence). We thank Tobias Brenne and Tim Hoberg for their support during the experiments.

4.7 References

Alam, Q., Schollbach, K., van Hoek, C.; van der Laan, S., Wolf, T.de, ;Brouwers, H.J.H. 2019. In-depth mineralogical quantification of MSWI bottom ash phases and their association with potentially toxic elements. Waste Manage. 87, 1–12.

Baciocchi, R., Costa, G., Lategano, E., Marini, C., Polettini, A., Pomi, R., Postorino, P., Rocca, S., 2010. Accelerated carbonation of different size fractions of bottom ash from RDF incineration. Waste Manage. 30 (7), 1310–1317.

Blanc, D., Gonzalez, L., Lupsea-Toader, M., Brauer, C. de, 2018. Mineralogical evolution and leaching behaviour of a heap of bottom ash as a function of time: Influence on its valorization. Waste Biomass Valor. 32 (1-2), 1–11.

Boateng, A.A., 2015. Rotary Kilns: Transport Phenomena and Transport Processes, second ed. Butterworth-Heinemann, Oxford.

Bongo Njeng, A. S., Vitu, S., Clausse, M., Dirion, J.-L., Debacq, M., 2015. Effect of lifter shape and operating parameters on the flow of materials in a pilot rotary kiln: Part I. Experimental RTD and axial dispersion study. Powder Techn. 269, 554–565.

Brück, F., Fröhlich, C., Mansfeldt, T., Weigand, H., 2018 a. A fast and simple method to monitor carbonation of MSWI bottom ash under static and dynamic conditions. Waste Manage. 78, 588–594.

Brück, F., Schnabel, K., Mansfeldt, T., Weigand, H., 2018 b. Accelerated carbonation of waste incinerator bottom ash in a rotating drum batch reactor. J. Environ. Chem. Eng. 6 (4), 5259–5268.

Chaspoul, F.R., Le Droguene, M.F., Barban, G., Rose, J.C., Gallice, P.M., 2008. A role for adsorption in lead leachability from MSWI bottom ash. Waste Manage. 28 (8), 1324–1330.

Chimenos, J.M., Fernández, A.I., Nadal, R., Espiell, F., 2000. Short-term natural weathering of MSWI bottom ash. J. Hazard. Mater. 79 (3), 287–299.

Cornelis, G., Johnson, C.A., van Gerven, T., Vandecasteele, C., 2008. Leaching mechanisms of oxyanionic metalloid and metal species in alkaline solid wastes: A review. Appl. Geochem. 23 (5), 955–976.

Costa, G., Baciocchi, R., Polettini, A., Pomi, R., Hills, C.D., Carey, P.J., 2007. Current status and perspectives of accelerated carbonation processes on municipal waste combustion residues. Environ. Monit. Assess. 135 (1-3), 55–75.

del Valle-Zermeño, R., Formosa, J., Prieto, M., Nadal, R., Niubó, M., Chimenos, J.M., 2014. Pilot-scale road subbase made with granular material formulated with MSWI bottom ash and stabilized APC fly ash: Environmental impact assessment. J. Hazard. Mater. 266, 132–140.

Di Gianfilippo, M., Hyks, J., Verginelli, I., Costa, G., Hjelmar, O., Lombardi, F., 2018. Leaching behaviour of incineration bottom ash in a reuse scenario: 12years-field data vs. lab test results. Waste Manage. 73, 367–380.

Dijkstra, J.J., Van der Sloot, Hans A., Comans, R.N.J., 2006 a. The leaching of major and trace elements from MSWI bottom ash as a function of pH and time. Appl. Geochem. 21 (2), 335–351.

DIN 19528 - German Institute for Standardization: Leaching of solid materials - Percolation method for the joint examination of the leaching behaviour of inorganic and organic substances. Beuth Verlag GmbH, Berlin

Dou, X., Ren, F., Nguyen, M.Q., Ahamed, A., Yin, K., Chan, W.P., Chang, V.W.-C., 2017. Review of MSWI bottom ash utilization from perspectives of collective characterization, treatment and existing application. Renew. Sustain. Energy Rev. 79 , 24–38.

EN 12457-2, 2003 Characterization of waste - Leaching; Compliance test for leaching of granular and sludges - Part 2. German version of European standard. Beuth Verlag GmbH, Berlin

Fernández Bertos, M., Li, X., Simons, S.J.R., Hills, C.D., Carey, P.J., 2004 a. Investigation of accelerated carbonation for the stabilisation of MSW incinerator ashes and the sequestration of CO_2. Green Chem. 6 (8), 428–436.

Fernández Bertos, M., Simons, S.J.R., Hills, C.D., Carey, P.J., 2004 b. A review of accelerated carbonation technology in the treatment of cement-based materials and sequestration of CO_2. J. Hazard. Mater. 112 (3), 193–205.

Fung, C.J., Mitchell, D.A., 1995. Baffles increase performance of solid-state fermentation in rotating drum bioreactors. Biotechnol. Tech. 9 (4), 295–298.

Jiang, M., Zhao, Y., Liu, G., Zheng, J., 2011. Enhancing mixing of particles by baffles in a rotating drum mixer. Particuology 9 (3), 270–278.

Kalamdhad, A.S., Khwairakpam, M., Kazmi, A.A., 2012. Drum composting of municipal solid waste. Environ. Technol. 33 (1-3), 299–306.

Łączny, J.M., Iwaszenko, S., Gogola, K., Bajerski, A., Janoszek, T., Klupa, A., Cempa-Balewicz, M., 2015. Study on the possibilities of treatment of combustion by-products from fluidized bed boilers into a product devoid of free calcium oxide. J. Sustain. Min.14 (4), 164–172.

Le, N.H., Razakamanantsoa, A., Nguyen, M.-L., van Phan, T., Dao, P.-L., Nguyen, D.H., 2018. Evaluation of physicochemical and hydromechanical properties of MSWI bottom ash for road construction. Waste Manage. 80, 168–174.

Lim, S.-Y., Davidson, J.F., Forster, R.N., Parker, D.J., Scott, D.M., Seville, J. P. K, 2003. Avalanching of granular material in a horizontal slowly rotating cylinder: PEPT studies. Powder Techn. 138, 25–30.

Lin, W.Y., Heng, K.S., Sun, X., Wang, J.-Y., 2015 a. Accelerated carbonation of different size fractions of MSW IBA and the effect on leaching. Waste Manage. 41, 75–84.

Lin, W.Y., Heng, K.S., Sun, X., Wang, J.-Y., 2015 b. Influence of moisture content and temperature on degree of carbonation and the effect on Cu and Cr leaching from incineration bottom ash. Waste Manage. 43, 264–272.

Liu, X.Y., Specht, E., Mellmann, J., 2005. Slumping–rolling transition of granular solids in rotary kilns. Chem. Eng. Sci. 60 (13), 3629–3636.

Lombardi, L., Carnevale, E.A., Pecorini, I., 2016. Experimental evaluation of two different types of reactors for CO_2 removal from gaseous stream by bottom ash accelerated carbonation. Waste Manage. 58, 287–298.

Lynn, C. J., Ghataora, G. S., Dhir Obe, R.K. 2017. Municipal incinerated bottom ash (MIBA) characteristics and potential for use in road pavements. Int. J. Pavment. Res. Eng. Technol. 10 (2), 185–201.

Marchese, F., Genon, G., 2009. Full scale tests of short-term municipal solid waste incineration bottom ash weathering before landfill disposal. Am. J. Environ. Sci. 5 (4), 570–577.

Meima, J.A., Comans, R.N.J., 1999. The leaching of trace elements from municipal solid waste incinerator bottom ash at different stages of weathering. Appl. Geochem. 14 (2), 159–171.

Metcalfe, G., Shinbrot, T., McCarthy, J.J., Ottino, J.M., 1995. Avalanche mixing of granular solids. Nature 374 (6517), 39–41.

Mitchell, D.A., Stuart, D.M., Hardin, M.T., Krieger, N., 2006. Group III: Rotating-drum and stirred-drum bioreactors, in: Mitchell, D.A., Berovic, M., Krieger, N. (Eds.), Solid-state fermentation bioreactors: fundamentals of design and operation. Springer Berlin, pp. 95–114.

Nørgaard, K.P., Hyks, J., Mulvad, J.K., Frederiksen, J.O., Hjelmar, O. 2019. Optimizing large-scale ageing of municipal solid waste incinerator bottom ash prior to the advanced metal recovery. Phase I: Monitoring of temperature, moisture content, and CO_2 level. Waste Mange. 85, 95–105.

Oehmig, W.N., Roessler, J.G., Zhang, J., Townsend, T.G., 2015. Effect of ferrous metal presence on lead leaching in municipal waste incineration bottom ashes. J. Hazard. Mat. 283, 500–506.

Ottino, J.M., Lueptow, R.M., 2008. On mixing and demixing. Science 319 (5865), 912–913.

Rendek, E., Ducom, G., Germain, P., 2006. Carbon dioxide sequestration in municipal solid waste incinerator (MSWI) bottom ash. J. Hazard. Mat. 128 (1), 73–79.

Saffarzadeh, A., Shimaoka, T., Wei, Y., Gardner, K.H., Musselman, C.N., 2011. Impacts of natural weathering on the transformation/neoformation processes in landfilled MSWI bottom ash: A geoenvironmental perspective. Waste Manage. 31 (12), 2440–2454.

Sakita, S., Nishimura, K., 2015. Physical containment of municipal solid waste incineration bottom ash by accelerated carbonation. J. Mater. Cycles Waste Manage. 18 (4), 1–8.

Um, N., Nam, S.-Y., Ahn, J.-W., 2013. Effect of accelerated carbonation on the leaching behavior of Cr in municipal solid waste incinerator bottom ash and the carbonation kinetics. Mater. Trans. 54 (8), 1510–1516.

Wei, Y., Shimaoka, T., Saffarzadeh, A., Takahashi, F., 2011. Mineralogical characterization of municipal solid waste incineration bottom ash with an emphasis on heavy metal-bearing phases. J. Hazard. Mater. 187 (1-3), 534–543.

Xuan, D., Tang, P., Poon, C.S. 2018. Limitations and quality upgrading techniques for utilization of MSW incineration bottom ash in engineering applications – A review. Constr. Build. Mater. 190, 1091–1102.

Yao, J., Li, W.-B., Kong, Q., Xia, F., Shen, D.-S., 2012. Effect of weathering on the mobility of zinc in municipal solid waste incinerator bottom ash. Fuel 93, 99–104.

Zingaretti, D., Costa, G., Baciocchi, R., 2013. Assessment of the energy requirements for CO_2 storage by carbonation of industrial residues. Part 1: Definition of the Process Layout. Energy Procedia 37, 5850–5857.

4.8 Supplementary material

4.8.1 Bottom ash characteristics

Table S4.1 Physical properties and elemental composition of BA sample 1-3.

	Sample 1	Sample 2	Sample 3
Bulk density [kg/L]	1.06 (0.07)	1.04 (0.05)	1.05 (0.02)
Moisture content [wt.-%]	23.8 (1.2)	23.7 (0.7)	21.4 (1.3)
Major components [g/100 g]			
Ca	25.6	24.3	23.9
Si	12.6	12.9	12.5
Al	3.5	3.9	3.2
S	3.8	2.9	4.2
Fe	2.8	2.6	3.0
Na	1.2	1.6	1.7
Ti	1.2	1.4	1.5
Mg	1.4	1.3	1.3
Cl	1.7	1.3	1.3
K	0.5	0.5	0.5
Trace elements [mg/kg]			
Cu	3,902	2,596	2,190
Zn	3,140	3,847	3,377
Ba	3,713	3,506	3,173
Pb	1,853	2,204	1,909
Cr	833	692	669
V	548	566	501
Sb	133	119	115
Mo	24	25	35

4.8.2 Leachate concentrations vs. leachate pH

Complementary to the representation of the leachate concentration as a function of the specific CO_2 supply given in Figure 4.3 the leachate concentration (logarithmic scale) is here plotted against the leachate pH in Figure S4.1.

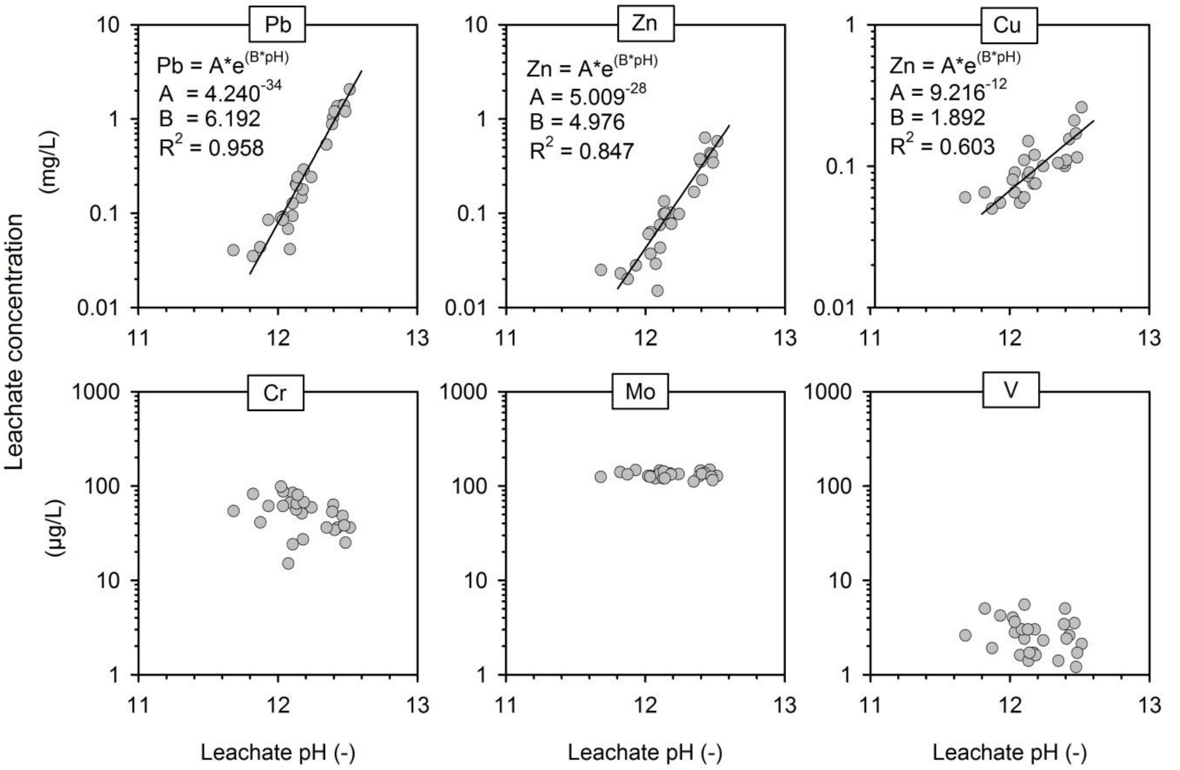

Figure S4.1 pH-dependent metal leaching from carbonated bottom ash. Nonlinear regression was performed by applying a single exponential function with two parameters (A,B). R^2 = correlation coefficient. Probability values were <0.0001, throughout.

4.8.3 Evaluation of BA carbonation with regard to its geotechnical reuse

According to the draft of the German Ordinance on Secondary Construction Materials (OSCM) column leachates of BA need to comply with the so-called material values if a geotechnical reuse is intended. The ordinance differentiates between class 1, 2 and 3 bottom ashes based on their leaching behaviour. The higher the leachate levels the more restricted is a geotechnical reuse of the waste (e. g. observation of a minimum distance to groundwater). To assess a possible reuse option comparative column leaching tests were performed for fresh and carbonated BA. Leaching tests were performed in accordance with the standard method DIN 19528 in plexiglass columns (height 30 cm, inner diameter 9 cm). The columns were gradually packed with approximately 3.2 kg of wet BA by applying a vibrating plate. A geotextile pre-filter was placed at the top and bottom of the packed beds. Before starting the test, the column was saturated with deionized water within 2 h. After the saturation phase, the pump was set to a flow rate of 225 mL/h to provide the prescribed contact time of 5 h. The samples were taken from the column effluent after the percolate mass was twice the mass of packed bed (L:S of 2 L kg^{-1}).

The leachate properties are shown in Table S4.1. The results largely support the batch leaching tests. In the carbonated column the pH and amphoteric metal (Pb, Zn, Cu) concentrations were substantially lower compared to the untreated control. A slight mobilisation of oxyanion forming elements (Cr, V and Mo) was also observed. Overall, the accelerated carbonation gave column leachate concentrations that comply with the material values of class 2 BA of the German OSCM. Thus, the output of the accelerated carbonation is suitable for high quality geotechnical reuse.

Table S4.2 Results of column leaching tests for fresh and carbonated BA from test series 1 (reactor loading: 8 kg, CO_2 concentration: 6.7 vol.-%, volumetric gas flow: 40 L/min, reaction time: 100 min) and material values of the German ordinance on secondary construction materials (draft).

Parameter		Column leachate		Material values		
		Fresh BA	Carbonated BA	Class 1	Class 2	Class 3
pH	(-)	12.4	11.4	7 - 13	7 - 13	7 - 13
EC	(mS/cm)	17.56	11.8	2.0	12.5	12.5
Pb	(mg/L)	5.05	0.04	n.r.	n.r.	n.r.
Zn	(mg/L)	0.52	0.01	n.r.	n.r.	n.r.
Cu	(mg/L)	0.20	0.01	≤0.11	≤1.0	≤2.0
Ba	(mg/L)	0.70	0.32	n.r.	n.r.	n.r.
Cr	(µg/L)	2.0	26.0	≤150	≤460	≤600
Mo	(µg/L)	270	340	≤55	≤400	≤1000
V	(µg/L)	2.1	7.0	≤55	≤150	≤200
Chloride	(mg/L)	3628	3614	≤160	≤5000	≤5000
Sulphate	(mg/L)	216	273	≤820	≤3000	≤3000

n.r. not regulated

4.8.4 Use of mixing tools for accelerated carbonation

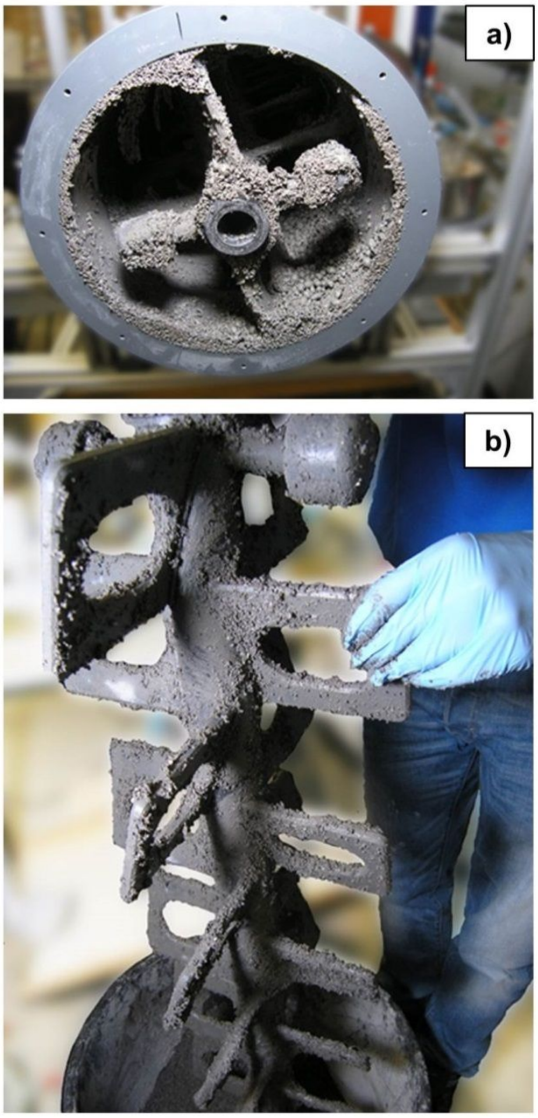

Figure S4.2 Mixing shaft (MTC1) as fixed in the rotating drum reactor (a) and dismantling (b).

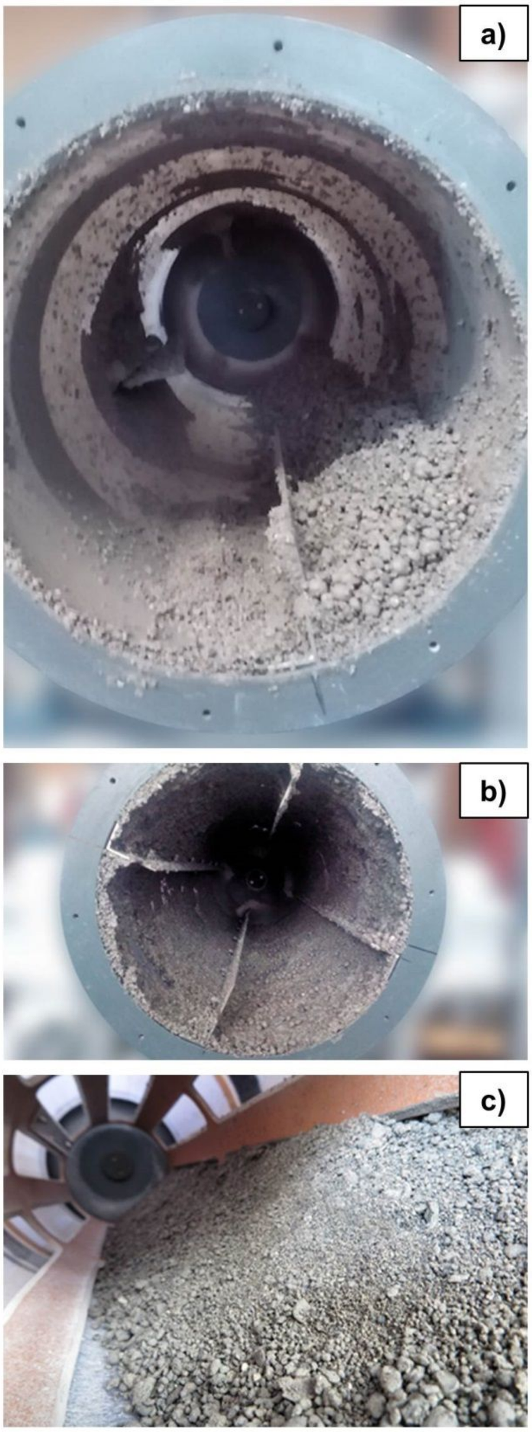

Figure S4.3 View into the rotating drum with MTCs 2 (a) and 3 (b) and 5 (c).

4.8.5 Thermogravimetric analyses

The weight loss (△m) during heating to 900 °C was divided into three temperature windows. Thereby △m is ascribed to individual temperature-dependent processes:

$\triangle m_1$ (20 - 390 °C):	release of free and weakly bound water (Gonzalez et al., 2017), e.g. from hydrocalumite (260 - 280 °C, Vieille et al., 2003) and gypsum (110 - 180 °C, Huntzinger et al., 2009),
$\triangle m_2$ (390 - 490 °C):	decomposition of $Ca(OH)_2$ (400 - 450 °C Galan et al., 2012; Rocca et al., 2013),
$\triangle m_3$ (490 - 750 °C):	decomposition of carbonate ($CaCO_3$) (Rocca et al., 2013).

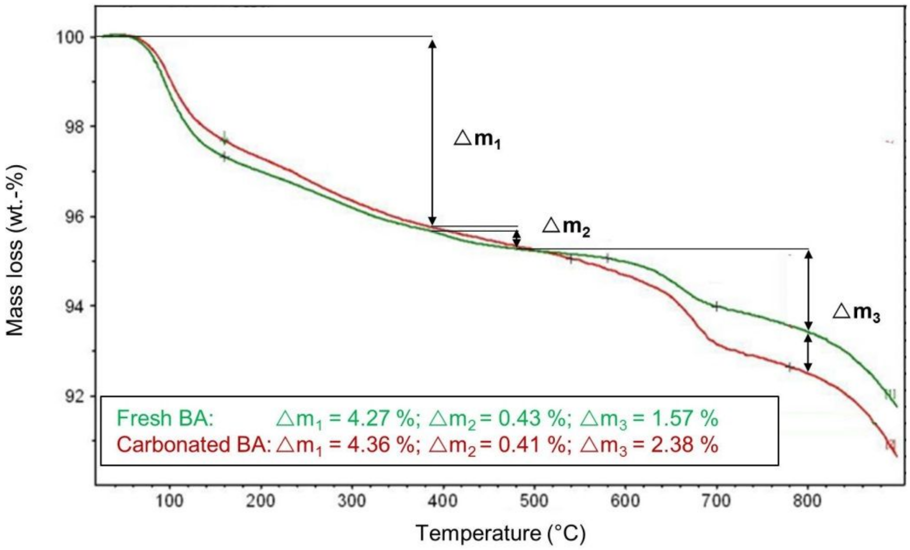

Figure S4.4 Thermogravimetric analysis of fresh and carbonated bottom ash (selected sample of test series 1). For the classification of the indicated mass losses ($\triangle m_{1-3}$) see explanation in the text.

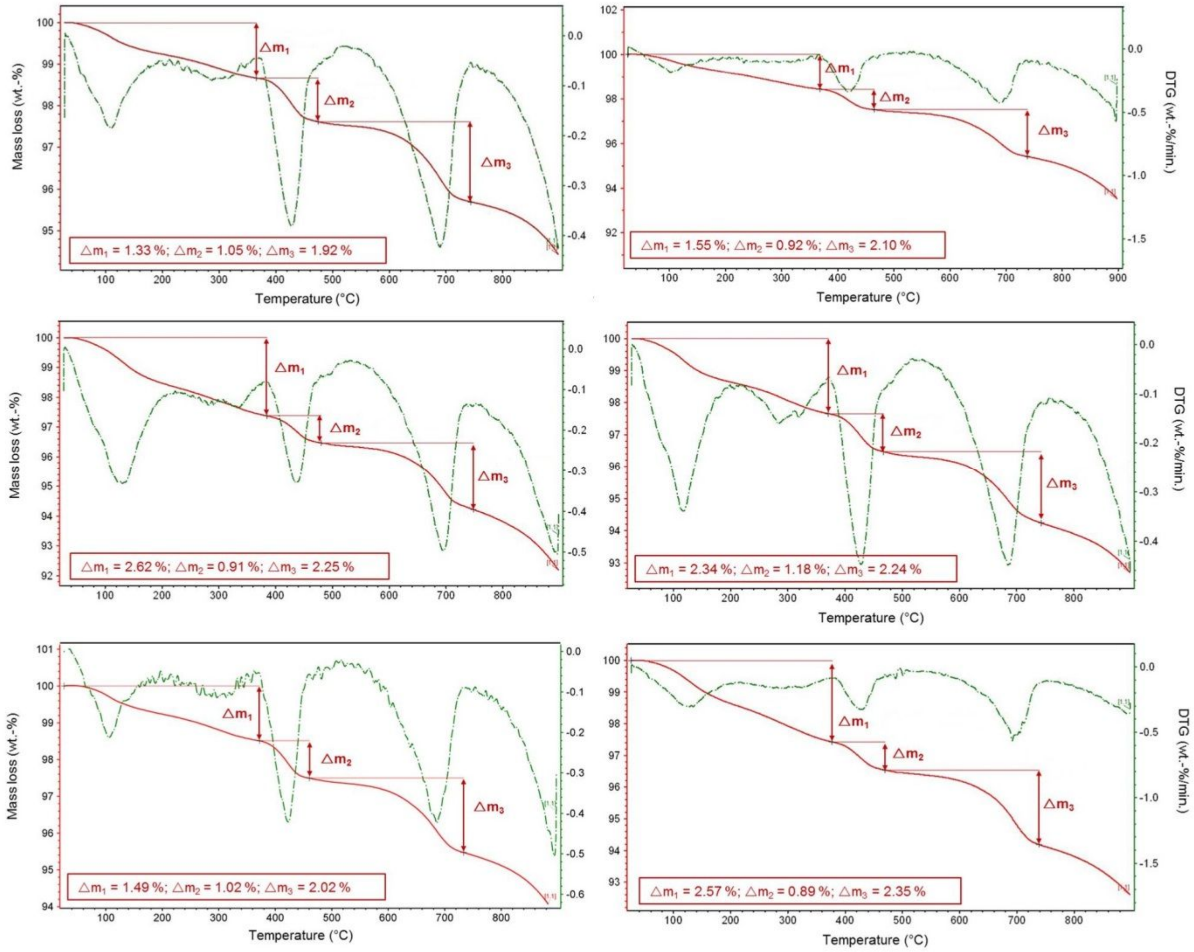

Figure S4.5 Thermogravimetric analysis of fresh bottom ash. For the classification of the indicated mass losses (△m) see explanation in the text.

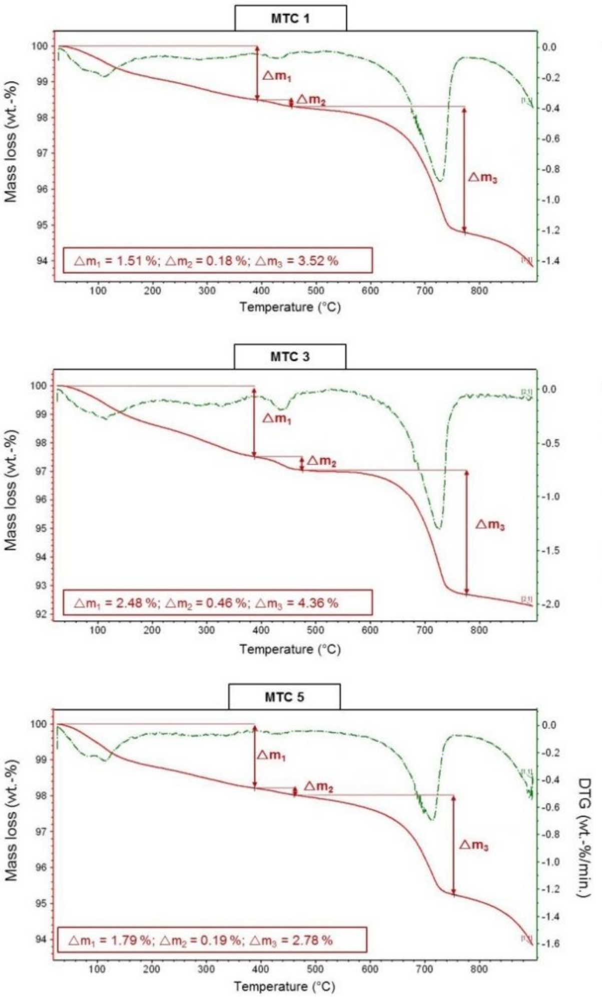

Figure S4.6 Thermogravimetric analysis of carbonated bottom ash under varied mixing tool configurations (MTC). For the classification of the indicated mass losses (△m) see explanation in the text.

References Supplementary Material

Galan, I., Andrade, C., Castellote, M., 2012. Thermogravimetrical analysis for monitoring carbonation of cementitious materials. Journal of Thermal Analysis and Calorimetry 110, 309–319. 10.1007/s10973-012-2466-4.

Gonzalez, M.L., Blanc, D., Brauer, C. de, 2017. Multi-Analytical Approach and Geochemical Modeling for Mineral Trace Element Speciation in MSWI Bottom-Ash. Waste and Biomass Valorization. 10.1007/s12649-017-0075-y.

Huntzinger, D.N., Gierke, J.S., Kawatra, S.K., Eisele, T.C., Sutter, L.L., 2009. Carbon Dioxide Sequestration in Cement Kiln Dust through Mineral Carbonation. Environ. Sci. Technol. 43, 1986–1992. 10.1021/es802910z.

OSCM, Verordnung über Anforderungen an den Einbau von mineralischen Ersatzbaustoffen in technische Bauwerke (Ersatzbaustoffverordnung – ErsatzbaustoffV) (a recent draft piece of legislation prepared by German government) version of February 2017

Rocca, S., van Zomeren, A., Costa, G., Dijkstra, J.J., Comans, R.N.J., Lombardi, F., 2013. Mechanisms contributing to the thermal analysis of waste incineration bottom ash and quantification of different carbon species. Waste Manag 33, 373–381. 10.1016/j.wasman.2012.11.004.

Vieille, L., Rousselot, I., Leroux, F., Besse, J.-P., Taviot-Guého, C., 2003. Hydrocalumite and Its Polymer Derivatives. 1. Reversible Thermal Behavior of Friedel's Salt: A Direct Observation by Means of High-Temperature in Situ Powder X-ray Diffraction. Chem. Mater. 15, 4361–4368. 10.1021/cm031069j.

Chapter 5 Continuous-feed carbonation of waste incinerator bottom ash in a rotating drum reactor

Waste Management (2019) 99: 135−145

Co-authors: Kristian Ufer, Tim Mansfeldt, Harald Weigand

Formatting and orthography of the manuscript is adapted to the dissertation style.

5.1 Abstract

Carbonation is a key process in the aging of waste incinerator bottom ash (BA). The reaction with CO_2 decreases the BA alkalinity and lowers the leachability of amphoteric trace metals. Passive ageing over several months is usually performed in intermittently mixed BA heaps. Here we aimed at accelerating the process in a rotating drum reactor continuously fed with the BA and the reactant gas (10 vol.-% CO_2, volumetric flow rate 60 L/min). In one test, the gas was heated and humidified. Since carbonation depends on the specific CO_2-supply, experiments were conducted at varied BA residence time (60, 80, and 100 min). Residence time was calculated by mass balancing and confirmed by the breakthrough time of two tracers. Leachates and solid phase properties of the treated BA served to evaluate the carbonation performance. The residence time of BA could be adequately controlled by the reactor loading and feed rate. A residence time of 80 min was sufficient to reduce the BA leachability such as to comply with the German regulatory standards for non-hazardous waste, whereas the untreated BA was hazardous waste. Decreased alkalinity was indicated by lower leachate pH and $Ca(OH)_2$ contents of the BA as compared to the input. Leachate concentrations of amphoteric trace metals (Pb, Zn, Cu) decreased by at least one order of magnitude while oxyanions became slightly more mobile upon carbonation. In view of relatively short residence times and stable process performance, the rotating drum reactor seems promising for a full-scale implementation of BA carbonation.

Keywords: Waste incineration residue, accelerated carbonation, CO_2 capture, rotating drum, ageing

5.2 Introduction

The ageing of waste incinerator bottom ash (BA) is beneficial to its leaching behaviour. Ageing takes place when this highly reactive alkaline and typically moist waste is in contact with the ambient air. Access of oxygen causes the formation of Fe- and Al-(hydr)oxides as prominent adsorbents for environmentally relevant trace metals (Chaspoul et al., 2008; Oehmig et al., 2015). Concomitant exposure to carbon dioxide (CO_2) causes the conversion of $Ca(OH)_2$ to $CaCO_3$. Thereby, BA alkalinity is consumed and the pH drops, which in turn lowers the leachability of amphoteric trace metals like Pb, Zn, and Cu (Arickx et al., 2010; Saffarzadeh et al., 2011).

A series of national guidelines demand that BA is aged over a period of 3 to 6 months prior to landfilling or geotechnical utilization (Astrup, 2007; Dou et al., 2017; Gori et al., 2011; Holm and Simon, 2016; Santos et al., 2013). Passive ageing over these timescales requires adequate storage installations at the incinerator sites as well as machinery and manpower for periodic turning (Blanc et al., 2018). Thus, a number of researchers have addressed the question of how the ageing of BA and other alkaline waste materials (e.g., air pollution control residues) can be accelerated.

Approaches investigated to this end include static reactor systems where the material is exposed to CO_2 partial pressures typically above 100 kPa (Baciocchi et al., 2010; Fernández Bertos et al., 2004a; Rendek et al., 2006) or where CO_2-rich gas streams are passed over thin layers of the solid at ambient pressure (Lin et al., 2015a; Nam et al., 2012; Um et al., 2013). In view of practical applications, it may be advisable to implement the accelerated carbonation in rotating drum reactor systems (Fernández Bertos et al., 2004b; Zingaretti et al., 2013). These reactors simultaneously provide agitation and mixing of the material. Thereby, the mass transfer between the gas and the solid is enhanced (Tan and Chen, 2006) and the CO_2 uptake rate is increased (Brück et al., 2018b; Lombardi et al., 2016).

Several gases have been tested as CO_2 sources for BA carbonation. One obvious option is to use the incinerator exhaust. After passing through a heat exchanger the exhaust is typically hot (112 °C), moist (relative humidity, RH: 21 %) and contains around 10 vol.-% CO_2 (Arickx et al., 2006; Rendek et al., 2006), and it is available in large quantities at the same location where the BA is generated. However, the effects of gas properties such as temperature and moisture have not been extensively examined up to now. Under static conditions Arickx et al. (2006) found a decrease in carbonation efficiency due to the condensation of water vapour on the BA surface.

So far, carbonation in rotating drums has only been tested under batch conditions (Brück et al., 2018b; Łączny et al., 2015; Librandi et al., 2017; Lombardi et al., 2016). In full scale applications, continuously operated reactor systems may be preferable since, therewith, the treatment may be synchronized to the BA generation. Depending on the nature of the involved reactions, the transition from batch to continuous processes can be challenging (Calabrese and Pissavini, 2011). However, some specifics of BA carbonation may favour the implementation into a continuous process. These include the facts that carbonation is enhanced by mixing, that the reaction is exothermic (Brück et al., 2018b), and that carbonation kinetics of the Ca-oxide phases present in BA are rather fast (Brück et al., 2018a). Since carbonation may be accompanied by an undesirable mobilisation of oxyanions if CO_2 uptake is excessively high (Costa et al., 2007, Brück et al., 2019) control of the BA residence time in a continuously fed system is deemed crucial.

Here we investigated the use of a rotating drum reactor continuously fed with both the reactant gas and the BA. The reactor design allowed for the supply of a hot and moist reactant gas. An adjustable slide at the reactor discharge served to control the reactor fill level while the feed rate was adjusted by a voltage-controlled feed screw. The BA residence time was obtained by mass balancing and compared to the residence time distribution as judged from tracer experiments. Carbonation performance was assessed by the BA leaching behaviour as well as the solid phase contents of $Ca(OH)_2$ and $CaCO_3$ of the treated BA.

5.3 Materials and methods

5.3.1 Bottom ash sampling

The BA was sampled from a grate-type refuse derived fuel incinerator located in central Germany. For details of the plant refer to (Brück et al., 2018a). A sample of about 500 kg BA was taken from a roofed temporary storage pile. The material was manually passed through a 10 mm mesh size sieve and the oversize grain was discarded. This was done since the coarse fraction of BA (i) is rather uncritical in terms of contaminant leaching and (ii) contributes little to carbonation. The sample was stored in air-tight clamping ring drums before used in the experiments. Prior to each experiment, the appropriate amount of BA was filled into a concrete mixer and homogenized. From this, two samples were then taken to characterize the input of each experiment.

5.3.2 Analytical methods

The moisture of the BA was determined gravimetrically after drying sample aliquots at 105 °C for 24 h (EN 12880). The loose bulk density was determined by weighing a graduated cylinder holding 100 mL of the material.

For characterisation of the solid phase, approximately 20 g of dry BA were ground in a planetary ball mill [Pulverisette 6, Fritsch GmbH, Idar-Oberstein, Germany]. The contents of $Ca(OH)_2$ and $CaCO_3$ were determined by thermogravimetric analysis (TGA) using a thermobalance [TG 209 F1, Netzsch, Selb, Germany]. Samples were heated in corundum crucibles to 900°C at 20 °C/minute under a nitrogen atmosphere. The contents of $Ca(OH)_2$ and $CaCO_3$ were calculated from the weight loss in specific temperature ranges. The weight loss between 380 °C and 480 °C relates to the decomposition of hydrates and the concomitant release of water vapour, whereas the weight change between 480 °C and 900 °C is due to the decomposition of carbonates and the release of CO_2.

The total organic carbon content (TOC) was determined with a CNS analyser [Vario EL, Elementar, Langenselbold, Germany].

The concentration of trace element, as well as major anions and cations was determined in aqueous batch leachates according to EN 12457-4 obtained at a liquid-to-solid ratio of 10 L kg^{-1}. The suspensions were agitated for 24 h on an end-over-end shaker. All samples were immediately analysed for pH and electrical conductivity (EC). The leachates were then passed through 0.45 µm membrane filters (cellulose acetate) and divided into two aliquots. One aliquot was analysed for anions (Cl^- and SO_4^{2-}) and cations (Ca^{2+}, Mg^{2+} and Na^+) by ion chromatography [Metrohm 861 Advanced Compact IC with a Metrosep A Supp 5 column]. The other aliquot was acidified with nitric acid to pH <2 for the detection of Cu, Pb, Zn, Ba, V, Sb, Cr, and Mo by inductively coupled plasma–mass spectrometry [ICP-MS, X-Series II, Thermo Scientific, Dreieich, Germany].

The bulk chemical composition of fresh BA samples was measured by X-ray fluorescence (XRF) spectroscopy [Spectroscout ES, Spectro Analytical Instruments GmbH, Kleve, Germany] with a detection limit of ~0.01 wt.-%. The X-ray diffraction (XRD) patterns were recorded using a PANalytical X'Pert PRO MPD Θ-Θ diffractometer (Cu-Kα radiation generated at 40 kV and 30 mA), equipped with a variable divergence slit (20 mm irradiated length), primary and secondary soller, Scientific X´Celerator detector (active length 0.59°), and a sample changer (sample diameter 28 mm). The samples were investigated from 2° to 85° 2Θ with a step size of 0.0167° for 2Θ and a total measuring time of 24 min. The back-loading technique was used for specimen preparation. Phase identification was conducted with reference to patterns in the PDF-2 database of the International Center for Diffraction Data (ICDD), released in 2009.

To pinpoint possible carbonation-induced changes in the particle size distribution of the BA untreated and carbonated BA were subjected to particle size analysis. . Therefore, dry sample aliquots of 1 kg were passed through stainless steel mesh screens with openings of 1, 2, 4, 8, and 10 mm.

5.3.3 Experimental Setup

Reactor equipment. The experiments were conducted in a rotating drum reactor continuously fed with both the reactant gas and the BA (see Figure 5.1). The drum was a thermally insulated stainless steel cylinder (diameter 0.3 m; length: 1.5 m) with a void volume of 106 L. It was run on four roller bearings attached to a substructure. Both front covers of the reactor were made of transparent polycarbonate and rigidly coupled to the substructure. A chain drive served to rotate the reactor against the front covers within gas-tight v-seal rings at 2.5 rpm, throughout. To enhance mixing, the drum was equipped with three straight plates (width: 0.3 m, length: 0.06 m) mounted perpendicularly on the inner drum wall as described in Brück et al. (2019).

Reactant gas. The gas was produced from pure CO_2 (N4.5) and synthetic air employing a gas mixing station [Gmix, HighTec Zang, Herzogenrath, Germany]. For optional temperature adjustment, the gas could be led through a temperature-regulated heating tube with a WRW-200 control unit [Winkler GmbH, Heidelberg, Germany]. This was used in combination with a humidifier unit consisting of a water-filled washing bottle and a heating device [Rettberg GmbH, Göttingen, Germany].

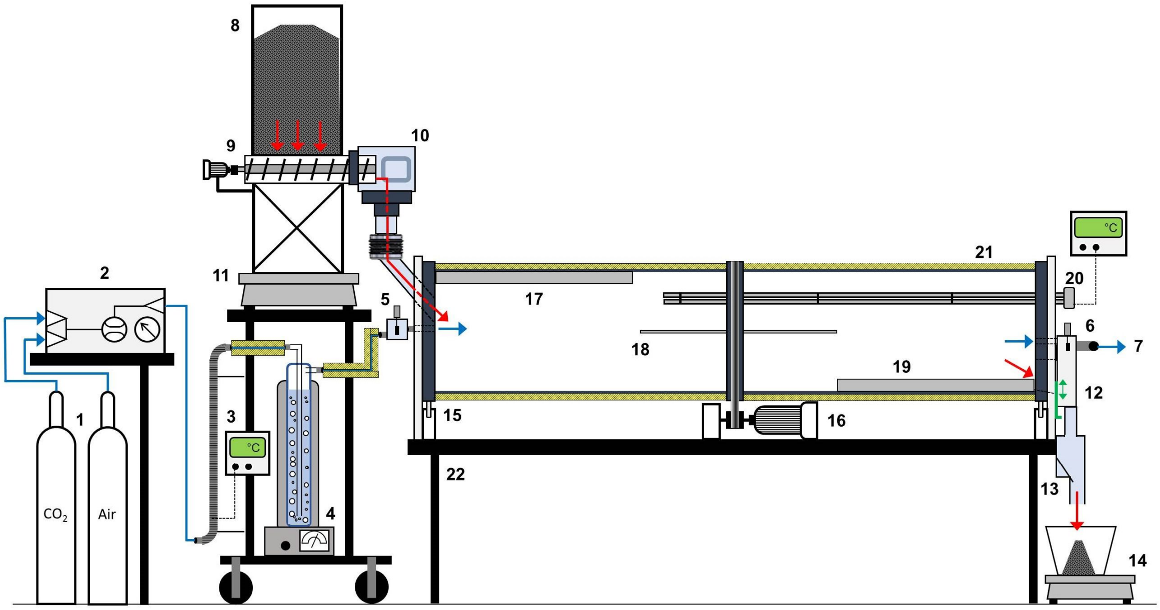

Figure 5.1. Set-up of the carbonation plant.
Reactant gas (blue arrows): (1) Gas cylinders; (2) gas mixing station; (3) heating tube with temperature controller; (4) gas humidifier; (5,6) flow-through cell with wire-less temperature and relative humidity sensors; (7) gas outlet.
Bottom ash feeding system (red arrows): (8) hopper; (9) feed screw; (10) by-pass for tracer application; (11) electric scale; (12) adjustable slide as exit dam; (13) gas-solid separator; (14) electric scale with sampling vessel.
Reactor equipment: (15) roller; (16) electric motor for reactor rotation; (17-19) lifter plates; (20) heating element; (21) insulation; (22) substructure.

At both, the gas inlet and outlet, the temperature (T_{in} and T_{out}) and relative humidity (RH_{in} and RH_{out}) were monitored. The values of both parameters were recorded every minute using wireless sensors [AREXX TSN-TH70E, RS Zwolle, The Netherlands] with tolerances of ± 1°C and ± 0.5 % RH. In the experiment with the heated reactant gas, the reactor was additionally equipped with a 2000 W temperature-controlled heating element of 1.2 m length [Nüga, Georgensgmünd, Germany, control unit WRW-100, Winkler GmbH] to compensate a potential heat-loss over the reactor mantle.

Bottom ash feeding system. The feeding system for BA was a combination of a hopper and an electrically driven feed screw. The hopper served for BA storage and was manually supplied with an adequate mass of BA prior to each experiment. The feed screw delivered the BA to a chute leading to the reactor inlet. According to preliminary tests, the input mass flow of BA was a linear function of the operating voltage (2 to 24 V, see Figure S5.1). An adjustable metal slide was installed at the discharge end of the reactor for fill level control. This served to slow down the BA discharge and thereby increase the fill level under continuous feed conditions depending on the position of the slide (Karra and Fuerstenau, 1977). The ejected BA was collected and the exhaust gas was led to a fume hood.

Both the input and output mass flows ($\dot{M}_{in}$ and $\dot{M}_{out}$, kg/min) were monitored. This was done by placing the feed unit as well as the collection vessel on electrical scales [DE 300K5DL and FCB30K1, Kern & Sohn, Balingen-Frommen, Germany] with resolutions of ± 0.005 kg and ± 0.001 kg, respectively. Weights were logged every minute and served to calculate the current reactor loading (M_R, kg) as well as $\dot{M}_{In}$ and $\dot{M}_{Out}$.

5.3.4 Experimental

The accelerated carbonation of BA under continuous-feed conditions was tested in a total of five experimental runs. Table 5.1 summarizes the operation parameters. By applying a defined mass flow rate ($\dot{M}$, kg/min) and with a known M_R, the residence time (τ, min) can be calculated according to Eq. 5.1

$$\tau = \frac{M_R}{\dot{M}}, \qquad \text{(Eq. 5.1)}$$

Under steady-state conditions ($\dot{M} = \dot{M}_{In} = \dot{M}_{Out}$, M_R = const.) the residence time for each experiment (τ_{MB}) was derived from the mass balance using the recorded M_{In} and M_{Out}. Experiment 1 was started with an empty reactor. All other experiments were started with a pre-filled reactor by adding M_R. Prefilling served to shorten the time necessary to reach steady state conditions with respect to BA mass flow. Steady-state conditions were reached 30 minutes after starting the feed, approximately. This was defined as equivalence of $\dot{M}_{In}$ and $\dot{M}_{Out}$ with a tolerance of ± 0.01 kg/min over at least 10 min accepting a variation of M_R of ± 0.25 kg. After attaining steady-state, the tracer was added to the BA feed and the gas supply was switched on. The reactor discharge was continuously collected in sealable vessels for allotted intervals (for a detailed description of the sampling procedure see section 5.3.5). Samples were homogenized and analysed as described in section 5.3.2.

Experiments 2 to 4 served to specify the residence time distribution in tracer tests and to evaluate BA carbonation under systematic variation of τ by applying three targeted mass flows (see Table 5.1). The CO_2 concentration was 10 vol.-% and the gas flow rate ($\dot{V}$) was 60 L/min.

Experiment 5 included a step-change of the reactant gas properties. For the first 140 minutes ($t/\tau = 1.8$) the reactant gas supply was identical to the one adopted in experiments 1 through 4. Then, the input was switched to the conditioned gas with a temperature of 55 °C and a RH of 30 % and the experiment was continued for another 100 minutes. The values of temperature and relative humidity were chosen in close agreement with the exhaust of the combined heat and power (CHP) plant available at the site where a large-scale carbonation trial is planned.

Table 5.1 Conditions of BA carbonation in a continuously fed rotating drum reactor.

Parameter	Experiment		
	1	2 / 3 / 4	5
Reactant gas properties			
CO_2 (vol.-%)	10	10	10
$\dot{V}$ (L/min)	60	60	60
Temperature (°C)	20 - 22	20 - 22	55
Relative humidity (%)	<10	<10	30
Reactor settings			
τ (min)	$f(\dot{M})$	60 / 80 / 100	80
Fill level (vol.-%)	$f(\dot{M})$	14	14
M_R (kg)	$f(\dot{M})$	15	15
$\dot{M}$ (kg/min)	0.30	0.25 / 0.19 / 0.15	0.19
Feed screw voltage (V)	13.1	11.1 / 8.8 / 7.2	8.8

5.3.5 Tracer experiments

In a continuously fed system, the residence time of solid particles is not constant but follows a distribution. To quantify the residence time distribution, tracer experiments were performed. The tracers were pulse-injected in the by-pass behind the feeding screw after the reactor had reached steady-state conditions with respect to mass flow. Polystyrene (PS) balls with a diameter between 2 and 5 mm and sodium chloride (NaCl) were used as particulate and conductivity tracers, respectively. We anticipated that the PS balls would stick to the wet surface of the BA particles and be co-transported through the reactor. Preliminary tests indicated that a total of 600 PS balls provided a clear response signal at the reactor discharge. The use of PS balls as a tracer in carbonation experiments is new. Therefore, we decided to cross-check results with a more commonly used tracer by adding 50 g of NaCl to the tracer batch.

At the reactor discharge, samples were collected in allotted intervals by replacing the collection vessel. The sampling intervals were 2, 5 and, 10 min with the shortest interval located around the expected tracer breakthrough ($t/\tau = 1.0$) to maximize the signal resolution. Aliquots of the discharge samples (50 g) were used for the determination of moisture. The dry material was preserved for the analysis of solid phase properties. Another 50 g aliquots were used in rapid leaching tests (RT) to determine the breakthrough behaviour of NaCl. Therefore, the solid samples were filled into beakers and 500 ml of distilled water were added. The suspensions were then intensively stirred for 15 min. Subsequently the electric conductivity (referred to as EC_{RT} in the following) was measured with a conductivity probe using the EC as a proxy for the NaCl concentration. Every second sample of the reactor discharge was subjected to a regular batch leaching test according to EN 12457-4. Both leachates (RT and regular batch test) were analysed in terms of the number of PS balls released to the supernatant. All remaining sample material was also mixed with water and the upwelled PS balls were counted.

The evolution of the PS tracer signal was used to derive the residence time distribution (E(t), E-curve). Since $\dot{M}$ was constant for each experiment, E(t) is given as the actual tracer signal N divided by the total tracer input using Eq. 5.2.

$$E(t) = \frac{N(\Delta t_i)}{N_0} \qquad \text{(Eq. 5.2)}$$

where N_0 is the total number of PS balls injected. The cumulative residence time distribution function F(t) (=F-curve) was obtained by integrating E(t) over time (Eq. 5.3).

$$F(t) = \int_0^\infty E(t_i)\,dt \approx \sum_{i=1}^{I} E(t_i)\,dt \qquad \text{(Eq. 5.3)}$$

where I is the total number of sampling intervals.

The mean residence time (tm) is the first moment of the residence time distribution E(t) and was obtained graphically from the intersection of the F-curve with the horizontal line corresponding to F(t)/N0 = 0.5 (centre of mass). The variance of the residence time (σ2) was calculated using equation 4. It is the second moment of the E(t) function and a measure of its spread around tm (Bongo Njeng et al., 2014).

$$\sigma^2 = \int_0^\infty (t-t_m)^2 E(t)\,dt \approx \sum_{i=1}^{I} \left(t_i - t_m\right)^2 E(t_i)\,dt \qquad \text{(Eq. 5.4)}$$

The axial dispersion of the tracer in the rotating drum reactor was modelled using the values of t_m and σ^2, according to Eq. 5.5 (Sherritt et al., 2003).

$$E(t) = \frac{1}{2}\sqrt{\frac{Pe}{\pi \cdot t_m \cdot t}}\exp\left\{-\frac{Pe(t_m - t)^2}{4 \cdot t_m \cdot t}\right\} \qquad \text{(Eq. 5.5)}$$

where Pe is the dimensionless Péclet number obtained from the variance of the residence time ($Pe = 2/\sigma^2$).

5.4 Results and discussion

5.4.1 Bottom ash characterisation

All of the following data refer to the grain size fraction 0 - 11 mm. The BA sample used in the experiments had a mean moisture content of 17.3 wt.-% (±1.5 wt.-%) and a loose bulk density of 1.0 kg/L (±0.05 wt.-%). Table 5.2 shows the elemental composition. The major components of the BA were Ca and Si followed by Al, S, and Fe. Regarding trace elements, considerable levels of Cu and Zn were found. This largely matches results reported previously for BA from municipal solid waste incinerators, e.g., (Wiles, 1996). The high Ca content of 24.2 wt.-% is similar to data for BA from refuse-derived fuel incineration (Rocca et al., 2012). Especially the trace elements revealed considerably high standard deviations (for Cu: ±57.5 %). This points to (small-scale) variability of the BA composition, which was addressed in the experiments by using high reactor loadings of 15 kg (experiments 2 through 5). The mean TOC-value of 0.9 wt.-% (±0.2 wt.-%) indicates that the combustion was quite complete.

Part of the Ca in the fresh BA was present as $Ca(OH)_2$ as indicated independently by the TGA and XRD-results (see diffractogram Figure S5.2). According to TGA data, the average $Ca(OH)_2$ content was 3.1 wt.-%; this suggests a considerable carbonation potential. Besides $Ca(OH)_2$, mineral phases identified by XRD included quartz (SiO_2), calcite ($CaCO_3$; also confirmed by TGA), anhydrite ($CaSO_4$) and gehlenite ($Ca_2Al_2SiO_7$). This agrees with previous findings (Baciocchi et al., 2010; Inkaew et al., 2016; Yang et al., 2014).

Hydrotalcite ($Mg_6Al_2[(OH)_{16}|CO_3]_4 \cdot H_2O$) was also identified. This naturally occurring layered double hydroxide (Ohtsubo et al., 2004) is known for its potential role as an anion scavenger (Châtelet et al., 1996; Palmer et al., 2009). Trace levels of ettringite ($Ca_6Al_2[(OH)_{12}|(SO_4)_3] \cdot 26H_2O$), larnite ($Ca_2SiO_4$), cristobalite ($SiO_2$) and magnesioferrite ($Mg(Fe^{3+})_2O_4$) were also identified by XRD.

The leaching behaviour of selected solid phase components as assessed in batch leaching tests is summarized in Table 5.3. Leachability was calculated as the ratio of the released mass and the total content of the corresponding element. Batch leachates of the fresh BA were alkaline and rich in charged mobile constituents as indicated by the high EC.

Table 5.2. Elemental composition of the BA (n = 5). Data are given as arithmetic mean ± standard deviation (s.d.).

Major components		Trace elements	
Mean (±s.d.) [g/100 g]		Mean (±s.d.) [mg/kg]	
Ca	24.2 (1.0)	Cu	5,170 (2,970)
Si	12.9 (0.7)	Zn	4,030 (932)
Al	3.5 (0.3)	Ba	3,850 (519)
S	3.2 (0.7)	Pb	1,650 (410)
Fe	2.9 (0.2)	Cr	807 (145)
Na	1.6 (0.2)	V	545 (51)
Ti	1.4 (0.1)	Sb	112 (13)
Mg	1.3 (0.1)	Mo	34 (13)
Cl	1.3 (0.2)		
C_{org}[a]	0.9 (0.2)		

[a] analyzed as TOC

High leachate pH and Ca concentrations agree with the identified $Ca(OH)_2$ content. In addition, notable concentrations of Cl^- and SO_4^{2-} were found in the leachate. The high mobility of Cl^- points to the presence of readily available alkali salts in BA (e.g. NaCl, $CaCl_2$) (Hyks et al., 2009; Wiles, 1996). Sulfate concentrations may in turn have been the result of ettringite and anhydrite dissolution (Dijkstra et al., 2006; Hyks et al., 2009; Rocca et al., 2012). Regarding trace elements, high leachate concentrations were found for Pb, Zn, and Cu. Among the amphoteric trace metals Pb showed the highest leachability. The Pb leachate concentration was eight times higher than the German waste acceptance criterion (WAC) for landfill class (LC) 2 (1.0 mg/L). Consequently, the fresh BA is classified as a hazardous waste. Zinc and Cu concentrations were both below LC 2 but exceeded LC 0 and 1, respectively.

Under alkaline conditions, Cr, Mo, Sb and V are predominantly present as chromate, molybdate, antimonate, and vanadate, i.e. as oxyanions. A surprisingly high leachability of Mo was found for fresh BA. Molybdenum was also the only oxyanion-forming element exceeding the limit value for LC 0 (50 µg/L). No such comparison can be made for V since the German Landfill Ordinance does not include a pertinent WAC.

Table 5.3. Leachate concentrations and leachability of major components and trace elements of the fresh BA; data as arithmetic mean ± standard deviation (s.d.).

		Average concentration (±s.d.)	Leachability [a] (%)
pH	(-)	12.7 (0.1)	-
EC	(mS/cm)	9.4 (0.8)	-
Ca	(mg/L)	1,330 (140)	5.5
Na	(mg/L)	116 (14)	7.3
Mg	(mg/L)	33 (1)	2.5
S	(mg/L)	200 (96)	2.1
Cl	(mg/L)	497 (67)	38
Pb	(µg/L)	8,300 (4,700)	5.0
Zn	(µg/L)	800 (217)	0.2
Cu	(µg/L)	558 (303)	0.1
Ba	(µg/L)	586 (213)	0.2
Mo	(µg/L)	74.4 (10.5)	25
Cr	(µg/L)	13.5 (4.9)	0.2
V	(µg/L)	5.7 (0.7)	0.1
Sb	(µg/L)	2.0 (1.5)	0.2

[a] leachability = (leached mass of element/ total mass of element in the sample) ·100

5.4.2 Control of BA residence time

In experiment 1 the reactor was run with an open discharge. Under these conditions, the experimental residence time τ_{MB} was below 30 min (see Table 5.4). This value is too low for a sufficient degree of BA carbonation (Brück et al., 2019). Increasing the residence time to the range of 60 to 120 min would require a modification of either the reactor (e.g. size, discharge geometry) or a lower feed rate. The latter is disadvantageous in terms of throughput. Therefore, we opted to use an adjustable slide at the reactor discharge in all further experiments. The residence times τ were 60, 80 and 100 min (Table 5.1). The mass balance yielded τ_{MB} values of 60.3 min, 80.2 min, and 102.0 min, respectively. This excellent agreement of τ and τ_{MB} indicates that at constant rotation speed the feed rate and M_R could be adequately controlled via the voltage vs. $\dot{M}_{In}$ characteristic and the position of the adjustable slide.

In experiments 2, 3, and 4 the residence time distribution was assessed by analysing the breakthrough behaviour of two tracers, namely PS balls as a particulate tracer and NaCl as a conductivity tracer.

Figure 5.2 shows the cumulative tracer signal for PS balls (F-curve, left) and the corresponding residence time distribution (E-curve, right). The centres of mass of the F-curves {F(t) = 0.5} are indicated by a dashed line. The obtained mean residence time (t_m) agreed well with τ_{MB} for experiment 1, 3 and 4 whereas in experiment 2 the tracer breakthrough occurred 7.4 min earlier than expected. Additional results obtained by the analysis of the residence time distribution are summarized in Table 5.4.

The F-curves are largely symmetric and the corresponding centres of mass are in good agreement with τ_{MB} indicating that the PS balls behaved as an inert tracer. The maxima of the normalized tracer concentrations showed a recovery of more than 80%.

Table 5.4 Results of the tracer experiments.

		Experiment No.			
		1	2	3	4
t_m	(min)	26.0	52.9	76.0	107.0
t_m/τ_{exp}	(-)	1.00	0.88	0.95	1.05
σ^2	(min²)	30.2	134.1	324.2	486.0
σ	(min)	5.5	11.6	18.0	22.0
σ/t_m	(-)	0.21	0.22	0.24	0.21

Both the incomplete tracer recoveries and the partial deviation of t_m and τ_{exp} may be due to the existence of dead zones, i.e. of inaccessible reactor space. Yet, considering that the movement of BA through the reactor has a chaotic component (mixing and/or segregation), the results of the tracer experiments are very satisfactory.

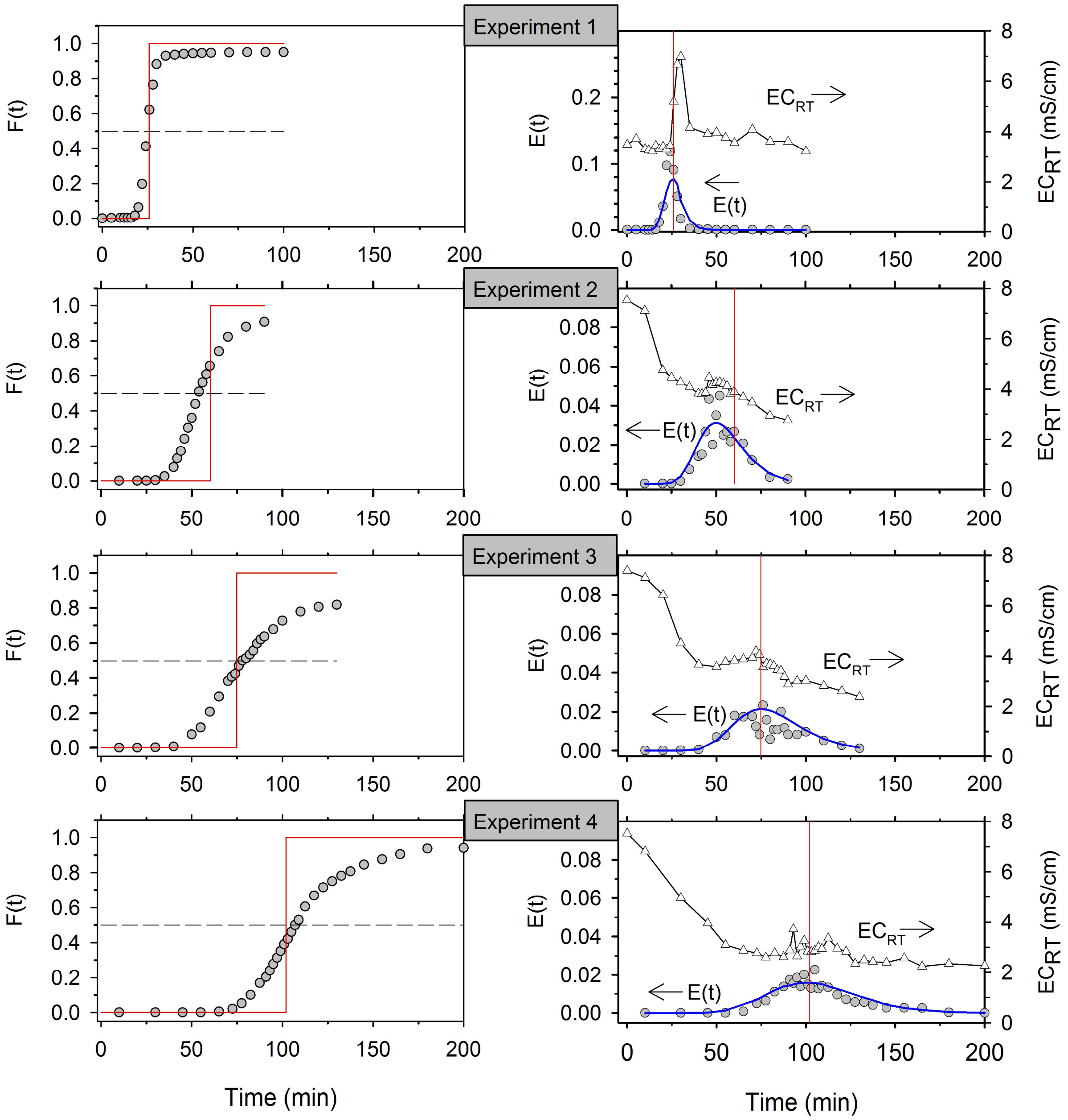

Figure 5.2 Tracer response signals for experiment 1 through 4 given as F(t) and E(t) for the particle tracer (polystyrene) and evolution of the NaCl tracer represented as the leachate electric conductivity (EC_{RT}). For F(t) and E(t) the red lines denote the experimental residence time (τ_{MB}) as derived from the mass balance. Blue solid lines along with the E(t) values are the results of the axial dispersion model (Eq. 5).

A relatively high spread around t_m was observed. With decreasing $\dot{M}$ (i.e. with increasing τ_{MB}) the E-curves spread and flattened corresponding to increasing σ^2 values, while the relative variance of residence time (σ/t_m) remained in a narrow range from 0.21 to 0.24 (see Table 5.4). This is consistent with an increasing longitudinal dispersion (σ^2) as a function of mean residence time.

The evolution of the electrical conductivity (ECRT) is the result of two overlapping processes, i.e. the gradual decrease of EC caused by BA carbonation (see section 3.3) and the break-through of the salt tracer. The tracer signal was expected to appear as a secondary maximum. This was the case in experiments 2 and 3. In experiment 4, no clear peak could be discerned, which is consistent with the high degree of dispersion. Indeed, in experiments 2 and 3 the position of the secondary maxima compared favourably with the peak times of the PS tracer. This indicates that both tracers, despite their differing properties, were adequate to describe the axial transport behaviour of BA.

3.3 Effect of residence time on carbonation performance

During reactor start-up the reactant gas stream was switched off. It was only turned on after a steady state had been reached. Thus, the exposure time of BA to CO_2 increased with experiment duration until the reaction time $t = \tau_{MB}$. Kinetics of carbonation may therefore potentially be reflected in the differences among experiments 2, 3, and 4 (variation of τ_{MB}) as well as within each experiment for reaction times $t < \tau_{MB}$.

To obtain a measure of the carbonation performance, the reactor discharge (carbonated BA) was sampled and subjected to batch leaching tests. Additionally, TG analyses on the solid samples were performed to gain insight into the evolution of $CaCO_3$ and $Ca(OH)_2$ contents. Since the residence time in experiment 1 (open discharge) was below the pursued range (60 - 120 min) carbonation performance was expectedly insufficient and will therefore not be discussed here (see Figure S5.3).

Figure 5.3 shows the temporal evolution of the outlet gas properties as well as selected solution and solid phase properties for experiments 2 to 4.

In all experiments, an initial temperature increase was observed with a peak at 24 °C after around 40 to 50 minutes. With prolonged carbonation the temperature gradually decreased but remained between 2 and 3 °C above ambient conditions. Overall, self-heating by the exothermal carbonation reaction was far lower than observed for BA carbonation under batch conditions (Brück et al., 2018b). This is due to reactor cooling by the gas stream and by the continuous BA feed. Since the BA was moist, the RH of the outlet gas increased rapidly in all experiments and nearly constant values of 94% ± 2% were attained after 25 minutes, approximately.

Regarding leachate properties, similar temporal trends were obtained in experiments 2 through 4. The leachate pH decreased from 12.7 (fresh BA) to 12.2, 12.0, and 11.7, for experiment 2 to 4, respectively. This is attributed to the consumption of alkalinity (mainly related to $Ca(OH)_2$) by BA carbonation (Brück et al., 2019; Marchese and Genon, 2009).

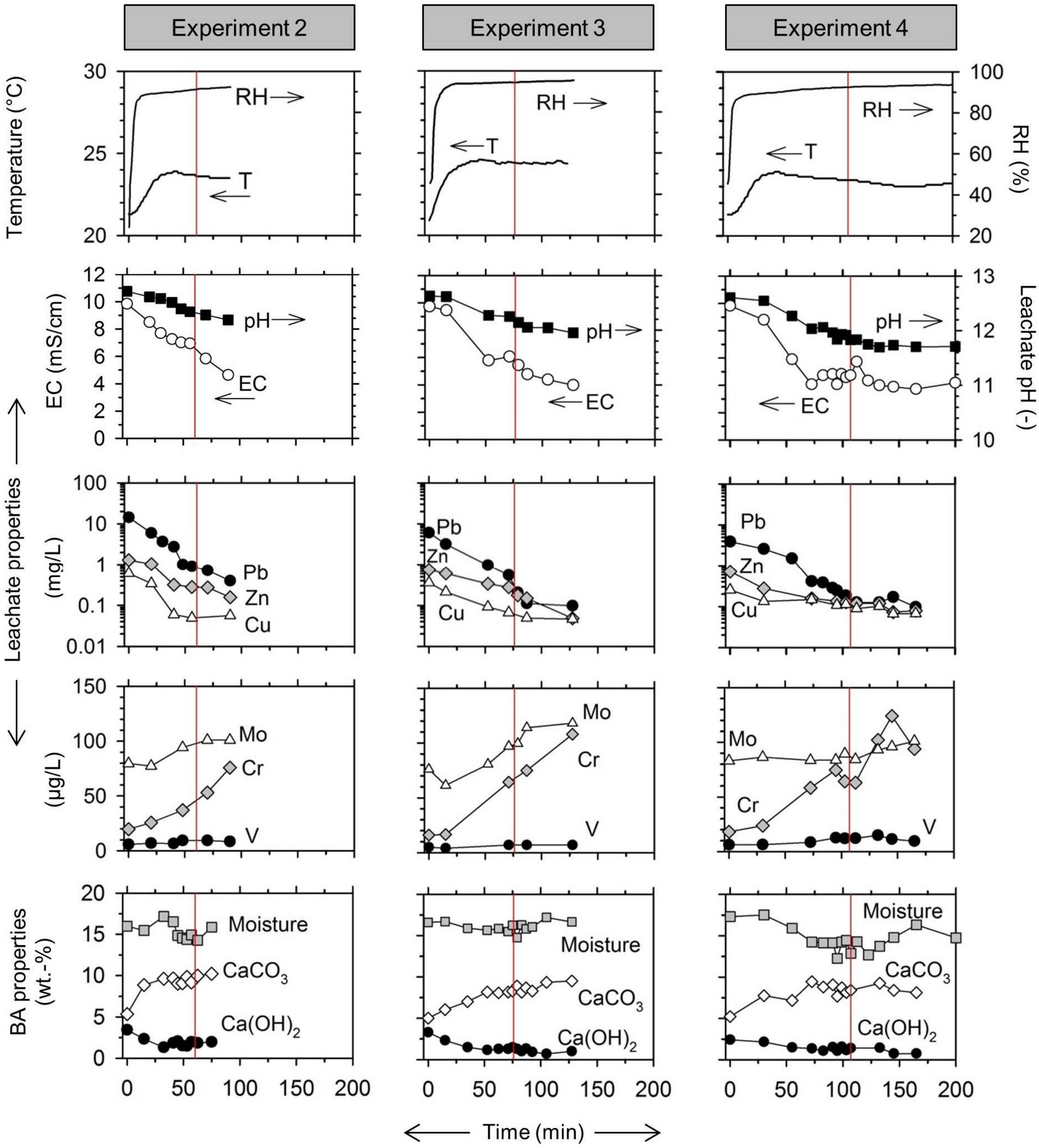

Figure 5.3 Results of carbonation experiments 2 to 4 performed at different residence times determined by the mass flow. Evolution of temperature and relative humidity (RH) in the gas outlet as well as selected parameters determined in aqueous batch extracts and solid phase samples; vertical line: residence time (τ_{MB}) obtained by mass balance. Values at experimental time zero represent leachate values of the fresh BA.

The longer the residence time, the lower was the final pH. In either experiment, the pH decreased over time due to proceeding carbonation, indicating that residence time is, indeed, a critical factor for BA carbonation. A similar trend was observed for the leachate EC which dropped from around 10 mS/cm (fresh BA) to 4.6, 3.6, and 3.9 mS/cm, in experiments 2 to 4, respectively. Thus, the leachates became increasingly depleted in mobile charged constituents (most prominently Ca^{2+} and OH^{-}) with increasing CO_2 uptake.

In parallel to the drop in pH and EC, the leachate concentration of amphoteric metals (Pb, Zn, Cu) decreased by at least one order of magnitude as compared to fresh BA.

Immobilization of amphoteric trace metals is primarily attributed to the pH-drop induced by the carbonation reaction (Wei et al., 2011) and is consistent with previous findings by (Brück et al., 2018b; Chimenos et al., 2000; Fernández Bertos et al., 2004a; Wei et al., 2011).

For fresh BA, the average leachate concentrations of Cu and Pb were above the German WAC for LC 0 and LC 2, respectively, classifying the material as a hazardous waste. At the end of experiment 2 the leachate concentration of Cu was below the limit values for LC 0 (inert waste) but the Pb concentration still exceeded the WAC for LC 1. For experiment 3 the final leachate concentrations of Pb, Zn, and Cu were below LC 0. The same holds for experiment 4 except for Pb which was slightly above LC 0. Overall, leaching behaviour for amphoteric metals largely improved upon carbonation.

It is well known that the pH dependent leaching of oxyanions differs greatly from that of amphoteric metals (Cornelis et al., 2008). This was also confirmed in our leaching tests. As an example Figure 5.3 shows the leachate values of Cr, Mo and V for the treated material and the fresh BA. Antimony leaching was in the range of the values for V (< 10 µg/L) and is shown as a separate figure in the supplement section (Figure S5.4). Compared to the untreated material (time zero in Fig. 5.3) carbonation-induced mobilisation was highest for Cr and Sb and lowest for Mo and V.

The enhanced mobility of oxyanions as a consequence of BA ageing has been attributed to dissolution (Johnson et al., 1999) and/or desorption processes (Piantone et al., 2004). Hydrotalcite and ettringite as potentially involved phases were identified in our XRD analysis (see section 5.4.1). Calcium antimonate and calcium molybdate have been suggested to control the dissolution-controlled leaching of Sb and Mo (Verbinnen et al., 2016; Simon and Holm, 2019). Carbonation could potentially promote their leaching by decreasing the Ca level in solution (Simon and Holm, 2019). Chromium, Mo and Sb may also be hosted by ettringite when they substitute sulphate in the crystal lattice (Marchese and Genon, 2009; van Gerven et al., 2005). In this case, carbonation may enhance oxyanion leaching by lowering the pH and thereby promote ettringite decomposition (Chrysochoou and Dermatas, 2006; Costa et al., 2007).

Hydrotalcite has been recognized as a potential sorbent for SO_4^{2-} and CrO_4^{2-} (Châtelet et al., 1996; Lazaridis and Asouhidou, 2003) and could potentially release these elements into solution when the BA is aged due to the limited stability range of Hydrotalcite (Tamura et al., 2006). Iron(hydr)oxides have frequently been recognized to impact oxyanion leaching (Meima and Comans, 1999). In our system, oxyanion sorption to iron(hydr)oxides may have been favoured by the carbonation-induced pH decrease (Cornelis et al., 2008). Yet, a net mobilisation was observed.

It was beyond the scope of this study to elucidate the underlying - and most probably overlapping – processes of oxyanion mobilization. From the practical viewpoint, their enhanced leaching is clearly an adverse effect of BA carbonation. However, the leachate concentrations of Cr and Mo remained below the German LC 1 WAC of 300 µg/L, throughout. The incomplete carbonation and, hence, limited CO_2 uptake may have prevented excessive leaching of oxyanions and particularly that of Sb. Overall, the beneficial immobilization of amphoteric metals was not outweighed by the mobilization of oxyanions.

Although the exhaust gas showed a higher RH than the input, the BA moisture content did not change in a clear manner and non-systematic variations are rather attributed to the heterogeneity of the material than to the treatment.

The TGA results confirm the occurrence of the two basic carbonation reactions: (i) neutralisation of $Ca(OH)_2$ by CO_2 and (ii) formation of $CaCO_3$. The increase in $CaCO_3$ content corresponded to CO_2 uptakes between 3.7 to 4.9 wt.-%. The $Ca(OH)_2$ contents decreased from 2.5 wt.-% to 1.9, 0.9, and 0.7 wt.-% in experiments 2, 3, and 4, respectively. Thus, in none of the experiments $Ca(OH)_2$ was fully converted to $CaCO_3$.

It should be noted that TGA was performed with ground material. This makes $Ca(OH)_2$ contained in the core of the grains analytically accessible. The batch leachates summarized in Figure 5.3 were performed with unground samples. This may explain why the pH decreased to values below 12 in experiment 4 in spite of detectable amounts $Ca(OH)_2$.

5.4.3 Effect of reactant gas properties on carbonation performance

Results of the previous sections indicated that a mean residence time of 80 min (experiment 3) was sufficient to achieve the desired immobilisation of critical trace metals (below the WAC for LC1). The conversion of fresh BA to a non-hazardous waste was achieved with a dry reactant gas at a temperature of 22 °C. However, the stack gas of most thermal processes can be expected to be moist and hot.

To simulate this under conditions feasible in a laboratory set-up, we tested the effect of the reactant gas properties on carbonation performance with a residence time τ of 80 min employing a preconditioned reactant gas with a temperature of 55 °C and a RH of 30%. Results are shown in Figure 5.4.

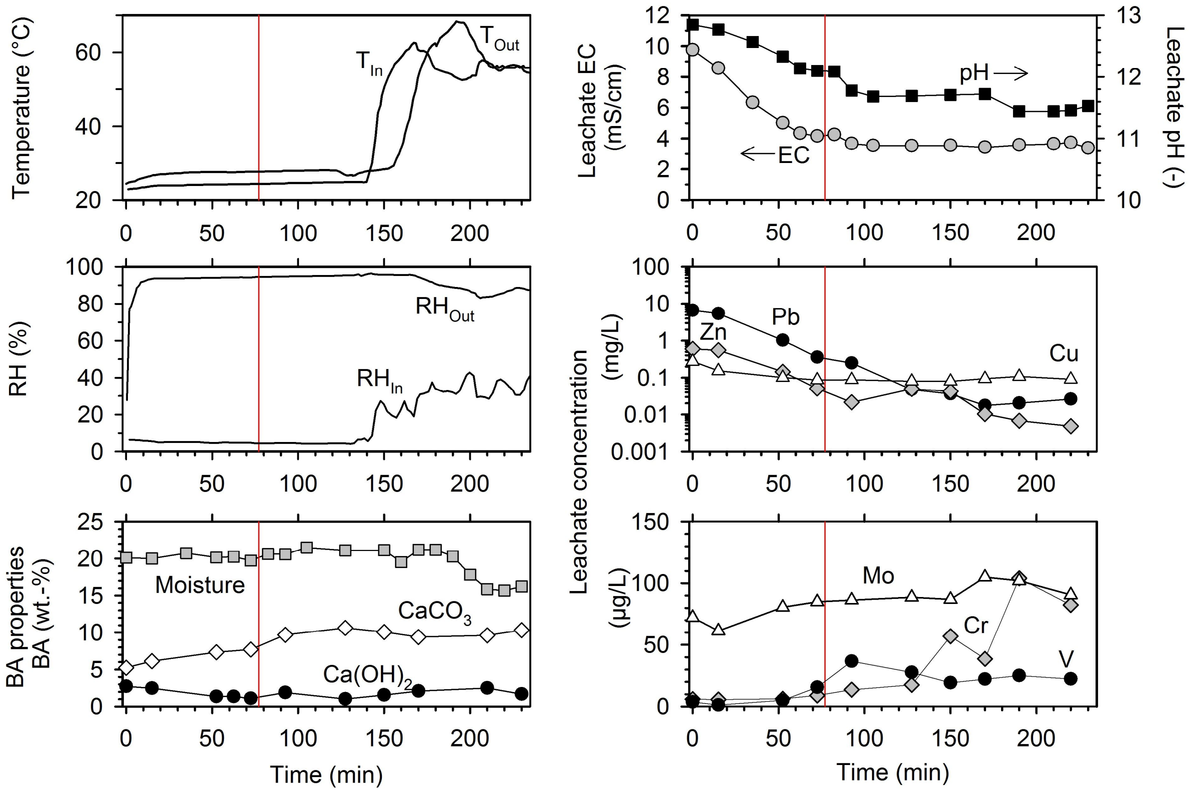

Figure 5.4 Results of carbonation experiment 5 performed with a dry reactant gas at ambient temperature (0 - 140 min) switched to a pre-heated humidified reactant gas (140 - 230 min; T = 50 °C, RH = 30 %). Evolution of gas properties and of selected parameters as determined in aqueous batch extracts and solid phase samples; vertical red line: residence time (τ_{MB}) as derived from the mass balance.

The feed of the moist and hot reactant gas was initiated after 140 min. At this point carbonation was at steady state with respect to leachate EC, pH, concentration of amphoteric metals, and conversion of $Ca(OH)_2$ to $CaCO_3$, while the leachate concentration of oxyanions was still increasing. Upon the step change of input gas quality T_{in} increased quickly to about 60 °C. With a slight delay, T_{out} increased to approximately 70 °C and finally, both temperatures stabilized at around 55 °C. Synchronous to the increase of T_{in}, RH_{in} increased to values of around 30%.

Contrary to the increase of T_{out}, the RH_{out} decreased. This can be explained by the temperature dependence of water vapour saturation. For the observed change of gas properties in the outlet gas, the absolute humidity increased by a factor of 3 to 4 (from 23 g/m^3 to 83 g/m^3).

Apparently, in our case the vapour uptake was limited by the evaporation from the wet BA, thereby explaining the decrease of RH_{out}.

As a result of the step change of the reactant gas properties, the moisture content of discharged BA decreased by about 5 wt.-%. This is in line with a temperature-driven increase of moisture output via the reactant gas. A similar trend was observed by (Lin et al., 2015b) during static carbonation experiments at a temperature of 50 °C. The authors concluded that, depending on the conditions, a loss or gain of moisture content during carbonation would have a significant impact on the carbonation efficiency on the industrial scale.Our results show that the increased temperature and humidity did not affect the carbonation performance as judged by the BA content of $CaCO_3$ and $Ca(OH)_2$ as well as the leachate EC and concentration of Cu, Mo and V.

A modest beneficial effect was observed for Pb and Zn since the leachate concentration decreased slightly as compared to the levels attained before the step change in reactant gas properties. This went along with a decrease of the leachate pH. Overall, carbonation was sufficient to decrease leachate concentrations of Zn and Cu below WAC for LC 0. For Pb the leachate concentration was below the WAC for LC 1 and dropped further below the WAC for LC 0 with the treatment at increased reactant gas temperature and moisture.

Compared to experiments 2 to 4 (gas temperature 22 °C) the higher gas temperature enhanced the carbonation-induced mobilization of Cr. This is contrary to findings by van Gerven et al. (2005) who found that Cr leaching was lowered by increasing the treatment temperature from ambient to 50 °C. However, despite the slight mobilization observed for both elements here their concentrations were still far below the WAC for LC 1.

From the findings in this section we conclude that the stack gas of a thermal process may be suited for the accelerated carbonation of BA as long as the initial moisture content of BA is within its optimum range (between 15 – 22 wt.-%, Brück et al., 2018b). However, it should be noted that the volumetric flow rate of the gas might be larger under real life conditions, which would probably enhance the observed drying effect. Therefore, particular attention should be given to the gas-to-solid ratio for carbonation (in this study: 200 - 400 L/kg). The latter may not just depend on the reactant gas properties (CO_2 concentration, temperature, moisture) but also on the characteristics of the BA (alkalinity, moisture content).

Along with the improvement of the leaching behaviour of waste incineration BA carbonation in the rotating drum reactor also initiated granulation of the BA. This is substantiated by the particle size distributions of the untreated and the carbonated BA (see Figure S5.5). The granulation effect increased slightly with residence time and virtually vanished at the elevated temperatures prevailing in experiment 5. A similar effect was observed for steel slag by (Librandi et al., 2017). Overall, the rotating drum reactor provides an opportunity to combine carbonation and granulation in a single treatment step to improve both the chemical and physical properties of BA. Obtaining a granulated product with a specific size-distribution could be beneficial in terms product handling and geotechnical reuse (Gunning et al., 2009). However, if a high temperature exhaust gas is used additional water might be required to support granulation.

5.5 Conclusions

In this study we reported on the accelerated carbonation of BA in a rotating drum reactor operated under continuous-feed of both the reactant gas and the BA.

The use of a movable slide at the reactor discharge in conjunction with an adjustable feed rate of the solid allowed for a control of the BA residence time. Mass balance results agreed well with the first moment of the residence time distribution derived from tracer experiments. The reactor was supplied with reactant gas with 10 vol-% CO_2 at a flow rate of 60 L/min. Under these conditions a residence time of 80 min was enough to improve the BA leachate quality such as to comply with the regulatory standards for non-hazardous waste.

With increasing residence time, the leachate pH and $Ca(OH)_2$ content of the BA dropped. Leachate concentrations of amphoteric trace metals (Pb, Zn, Cu) decreased by at least one order of magnitude. Oxyanion forming elements (Cr, Mo, V and Sb), however, became more mobile upon carbonation. Thus, the degree of carbonation should be carefully chosen to minimize this side effect. To this end, control of the residence time is particularly useful.

Increasing the temperature and moisture of the reactant gas to resemble properties of a typical CHP-plant induced a BA drying of about 5 wt.-% but only slightly affected the carbonation performance. This finding is encouraging since stack gas is one of the readily available CO_2 sources for accelerated carbonation.

Overall, the rotating drum reactor concept appears promising for the full-scale implementation of BA carbonation in terms of relatively short residence times and stable performance. Yet, in a full-scale operation, the reactor throughput would ideally have to be synchronized with the rate of BA generation. This issue is addressed in ongoing work directed towards the operation of a continuously-fed pilot-scale reactor.

5.6 Acknowledgement

This project (HA project no. 483/15-25) was supported in the framework of Hessen ModellProjekte financed with funds of LOEWE – Landes-Offensive zur Entwicklung Wissenschaftlich-ökonomischer Exzellenz, Förderlinie 3: KMU-Verbundvorhaben (State Offensive for the Development of Scientific and Economic Excellence). We thank Tim Hoberg and Jürgen Henkel for their support during the experiments.

5.7 References

Arickx, S., Borger, V. de, van Gerven, T., Vandecasteele, C., 2010. Effect of carbonation on the leaching of organic carbon and of copper from MSWI bottom ash. Waste Manage. 30, 1296–1302.

Arickx, S., van Gerven, T., Vandecasteele, C., 2006. Accelerated carbonation for treatment of MSWI bottom ash. J. Hazard. Mater. 137 (1), 235–243.

Astrup, T., 2007. Pretreatment and utilization of waste incineration bottom ashes: Danish experiences. Waste Manage. 27, 1452–1457..

Baciocchi, R., Costa, G., Lategano, E., Marini, C., Polettini, A., Pomi, R., Postorino, P., Rocca, S., 2010. Accelerated carbonation of different size fractions of bottom ash from RDF incineration. Waste Manage. 30, 1310–1317.

Bongo Njeng, A. S., Vitu, S., Clausse, M., Dirion, J.-L., Debacq, M., 2014. Effect of lifter shape and operating parameters on the flow of materials in a pilot rotary kiln: Part II. Experimental hold-up and mean residence time modelling. Powder Techn. 269, 566–576.

Brück, F., Fröhlich, C., Mansfeldt, T., Weigand, H., 2018a. A fast and simple method to monitor carbonation of MSWI bottom ash under static and dynamic conditions. Waste Manage. 78, 588–594.

Brück, F., Schnabel, K., Mansfeldt, T., Weigand, H., 2018b. Accelerated carbonation of waste incinerator bottom ash in a rotating drum batch reactor. J. Environ. Chem. Eng. 6, 5259–5268.

Brück, F., Mansfeldt, T., Weigand, H., 2019. Flow-through carbonation of waste incinerator bottom ash in a rotating drum batch reactor: Role of specific CO_2 supply, mixing tools and fill level. J. Environ. Chem. Eng. (accepted manuscript), 102975.

Calabrese, G.S., Pissavini, S., 2011. From batch to continuous flow processing in chemicals manufacturing. AIChE Journal 57, 828–834. 10.1002/aic.12598

Chaspoul, F.R., Le Droguene, M.F., Barban, G., Rose, J.C., Gallice, P.M., 2008. A role for adsorption in lead leachability from MSWI bottom ASH. Waste Manage. 28, 1324–1330. 10.1016/j.wasman.2007.07.005.

Châtelet, L., Bottero, J.Y., Yvon, J., Bouchelaghem, A., 1996. Competition between monovalent and divalent anions for calcined and uncalcined hydrotalcite: Anion exchange and adsorption sites. Colloid Surface A 111, 167–175.

Chimenos, J.M., Fernández, A.I., Nadal, R., Espiell, F., 2000. Short-term natural weathering of MSWI bottom ash. J. Hazard. Mater. 79, 287–299.

Chrysochoou, M., Dermatas, D., 2006. Evaluation of ettringite and hydrocalumite formation for heavy metal immobilization: Literature review and experimental study. J. Hazard. Mater. 136, 20–33.

Costa, G., Baciocchi, R., Polettini, A., Pomi, R., Hills, C.D., Carey, P.J., 2007. Current status and perspectives of accelerated carbonation processes on municipal waste combustion residues. Environ. Monit. Assess. 135, 55–75.

Dijkstra, J.J., Van der Sloot, Hans A., Comans, R.N.J., 2006. The leaching of major and trace elements from MSWI bottom ash as a function of pH and time. Appl. Geochem. 21, 335–351.

Dou, X., Ren, F., Nguyen, M.Q., Ahamed, A., Yin, K., Chan, W.P., Chang, V.W.-C., 2017. Review of MSWI bottom ash utilization from perspectives of collective characterization, treatment and existing application. Renew. Sust. Energ. Rev. 79, 24–38.

Fernández Bertos, M., Li, X., Simons, S.J.R., Hills, C.D., Carey, P.J., 2004a. Investigation of accelerated carbonation for the stabilisation of MSW incinerator ashes and the sequestration of CO_2. Green Chem., 6, 428–436.

Fernández Bertos, M., Simons, S.J.R., Hills, C.D., Carey, P.J., 2004b. A review of accelerated carbonation technology in the treatment of cement-based materials and sequestration of CO2. J. Hazard. Mater. 112, 193–205.

Gori, M., Bergfeldt, B., Pfrang-Stotz, G., Reichelt, J., Sirini, P., 2011. Effect of short-term natural weathering on MSWI and wood waste bottom ash leaching behaviour. J. Hazard. Mater. 189, 435–443..

Gunning, P.J., Hills, C.D., Carey, P.J., 2009. Production of lightweight aggregate from industrial waste and carbon dioxide. Waste Manage. 29, 2722–2728.

Holm, O., Simon, F.-G., 2016. Innovative treatment trains of bottom ash (BA) from municipal solid waste incineration (MSWI) in Germany. Waste Manage. 59, 229–236.

Hyks, J., Astrup, T., Christensen, T.H., 2009. Leaching from MSWI bottom ash: evaluation of non-equilibrium in column percolation experiments. Waste Manage. 29, 522–529.

Inkaew, K., Saffarzadeh, A., Shimaoka, T., 2016. Modeling the formation of the quench product in municipal solid waste incineration (MSWI) bottom ash. Waste Manage. 52, 159–168.

Johnson, C.A., Kaeppeli, M., Brandenberger, S., Ulrich, A., Baumann, W., 1999. Hydrological and geochemical factors affecting leachate composition in municipal solid waste incinerator bottom ash: Part II. The geochemistry of leachate from Landfill Lostorf, Switzerland. J. Contam. Hydrol. 40, 239–259.

Karra, V.K., Fuerstenau, D.W., 1977. Material transport in a continuous rotary drum. Effect of discharge plate geometry. Powder Techn. 16, 23–28. 10.1016/0032-5910(77)85017-1

Łączny, J.M., Iwaszenko, S., Gogola, K., Bajerski, A., Janoszek, T., Klupa, A., Cempa-Balewicz, M., 2015. Study on the possibilities of treatment of combustion by-products from fluidized bed boilers into a product devoid of free calcium oxide. J. Sustain. Min. 14, 164–172.

Lazaridis, N.K., Asouhidou, D.D., 2003. Kinetics of sorptive removal of chromium(VI) from aqueous solutions by calcined Mg–Al–CO3 hydrotalcite. Water Res. 37, 2875–2882.

Librandi, P., Costa, G., Souza, A.C.B.d., Stendardo, S., Luna, A.S., Baciocchi, R., 2017. Carbonation of Steel Slag: Testing of the Wet Route in a Pilot-scale Reactor. Energy Proced. 114, 5381–5392.

Lin, W.Y., Heng, K.S., Sun, X., Wang, J.-Y., 2015a. Accelerated carbonation of different size fractions of MSW IBA and the effect on leaching. Waste Manage. 41, 75–84.

Lin, W.Y., Heng, K.S., Sun, X., Wang, J.-Y., 2015b. Influence of moisture content and temperature on degree of carbonation and the effect on Cu and Cr leaching from incineration bottom ash. Waste Manage. 43, 264–272.

Lombardi, L., Carnevale, E.A., Pecorini, I., 2016. Experimental evaluation of two different types of reactors for CO2 removal from gaseous stream by bottom ash accelerated carbonation. Waste Manage. 58, 287–298.

Marchese, F., Genon, G., 2009. Full scale tests of short-term municipal solid waste incineration bottom ash weathering before landfill disposal. American J. Environ. Sci. 5, 570–577.

Meima, J.A., Comans, R.N.J., 1999. The leaching of trace elements from municipal solid waste incinerator bottom ash at different stages of weathering. Applied Geochem. 14, 159–171. 10.1016/S0883-2927(98)00047-X

Nam, S.-Y., Seo, J., Thriveni, T., Ahn, J.-W., 2012. Accelerated carbonation of municipal solid waste incineration bottom ash for CO2 sequestration. Geosystem Eng. 15, 305–311.

Oehmig, W.N., Roessler, J.G., Zhang, J., Townsend, T.G., 2015. Effect of ferrous metal presence on lead leaching in municipal waste incineration bottom ashes. J. Hazard. Mater. 283, 500–506.

Ohtsubo, M., Li, L.Y., Yamaoka, S., Higashi, T., 2004. Leachability of metals from municipal solid waste fly-ash and bottom-ashes at different pH, in: Yong, R.N., Thomas, H.R. (Eds.), Geoenvironmental Engineering, Integrated Management of Groundwater and Contaminated Land. Thomas Telford, Michigan, pp. 283–291.

Palmer, S., Frost, R., Nguyen, T., 2009. Hydrotalcites and their role in coordination of anions in Bayer liquors: Anion binding in layered double hydroxides. Coord. Chem. Rev., 253, 250–267.

Piantone, P., Bodénan, F., Chatelet-Snidaro, L., 2004. Mineralogical study of secondary mineral phases from weathered MSWI bottom ash: implications for the modelling and trapping of heavy metals. Appl. Geochem. 19, 1891–1904. 10.1016/j.apgeochem.2004.05.006

Rendek, E., Ducom, G., Germain, P., 2006. Carbon dioxide sequestration in municipal solid waste incinerator (MSWI) bottom ash. J. Hazard. Mater. 128, 73–79.

Rocca, S., van Zomeren, A., Costa, G., Dijkstra, J.J., Comans, R.N.J., Lombardi, F., 2012. Characterisation of major component leaching and buffering capacity of RDF incineration and gasification bottom ash in relation to reuse or disposal scenarios. Waste Manage. 32, 759–768.

Saffarzadeh, A., Shimaoka, T., Wei, Y., Gardner, K.H., Musselman, C.N., 2011. Impacts of natural weathering on the transformation/neoformation processes in landfilled MSWI bottom ash: A geoenvironmental perspective. Waste Manage. 31, 2440–2454.

Santos, R.M., Mertens, G., Salman, M., Cizer, Ö., van Gerven, T., 2013. Comparative study of ageing, heat treatment and accelerated carbonation for stabilization of municipal solid waste incineration bottom ash in view of reducing regulated heavy metal/metalloid leaching. J. Environ. Manage. 128, 807–821.

Sherritt, R.G., Chaouki, J., Mehrotra, A.K., Behie, L.A., 2003. Axial dispersion in the three-dimensional mixing of particles in a rotating drum reactor. Chem. Eng. Sci. 58, 401–415.

Simon, F.-G., Holm, O., Kalbe, U., 2019. Antimon in Rostaschen aus der Müll-verbrennung - Auslaugverhalten und Rückschlüsse für die Aufbereitung. In: Thiel, S., Thome-Kozmiensky, E., Pretz, T., Senk, D. G., Wotruba, H., Mineralische Nebenproduckte und Abfälle 6, Aschen, Schlacken und Baurestmassen, TK Verlag, Nietweder, Germany, pp. 148–164.

Tamura, H., Chiba, J., Ito, M., Takeda, T., Kikkawa, S., Mawatari, Y., Tabata, M., 2006. Formation of hydrotalcite in aqueous solutions and intercalation of ATP by anion exchange. J. Colloid Interface Sci. 300, 648–654.10.1016/j.jcis.2006.04.007

Tan, C.-S., Chen, J.-E., 2006. Absorption of carbon dioxide with piperazine and its mixtures in a rotating packed bed. Sep. Purif. Technol. 49, 174–180.

Um, N., Nam, S.-Y., Ahn, J.-W., 2013. Effect of accelerated carbonation on the leaching behavior of Cr in municipal solid waste incinerator bottom ash and the carbonation kinetics. Mater. Trans. 54, 1510–1516.

van Gerven, T., van Keer, E., Arickx, S., Jaspers, M., Wauters, G., Vandecasteele, C., 2005. Carbonation of MSWI-bottom ash to decrease heavy metal leaching, in view of recycling. Waste Manage. 25, 291–300.

Verbinnen, B., Billen, P., van Caneghem, J., Vandecasteele, C., 2016. Recycling of MSWI Bottom Ash: A Review of Chemical Barriers, Engineering Applications and Treatment Technologies. Waste Biomass Valor. 4, 695–709. 10.1007/s12649-016-9704-0

Wei, Y., Shimaoka, T., Saffarzadeh, A., Takahashi, F., 2011. Mineralogical characterization of municipal solid waste incineration bottom ash with an emphasis on heavy metal-bearing phases. J. Hazard. Mater. 187, 534–543.

Wiles, C.C., 1996. Municipal solid waste combustion ash: State-of-the-knowledge: Municipal Waste Incineration. J. Hazard. Mater. 47, 325–344.

Yang, S., Saffarzadeh, A., Shimaoka, T., Kawano, T., 2014. Existence of Cl in municipal solid waste incineration bottom ash and dechlorination effect of thermal treatment. J. Hazard. Mater. 267, 214–220.

Zingaretti, D., Costa, G., Baciocchi, R., 2013. Assessment of the energy requirements for CO_2 storage by carbonation of industrial residues. Part 1: definition of the process layout. Energy Proced. 37, 5850–5857.

5.8 Supplementary material

5.8.1 Preliminary tests

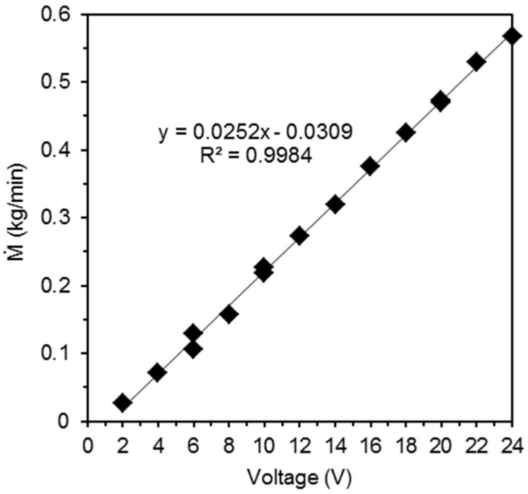

Figure S5.1 Resulting mass flow (Ṁ) of BA as function of the operating voltage of the feed screw.

5.8.2 X-ray diffraction

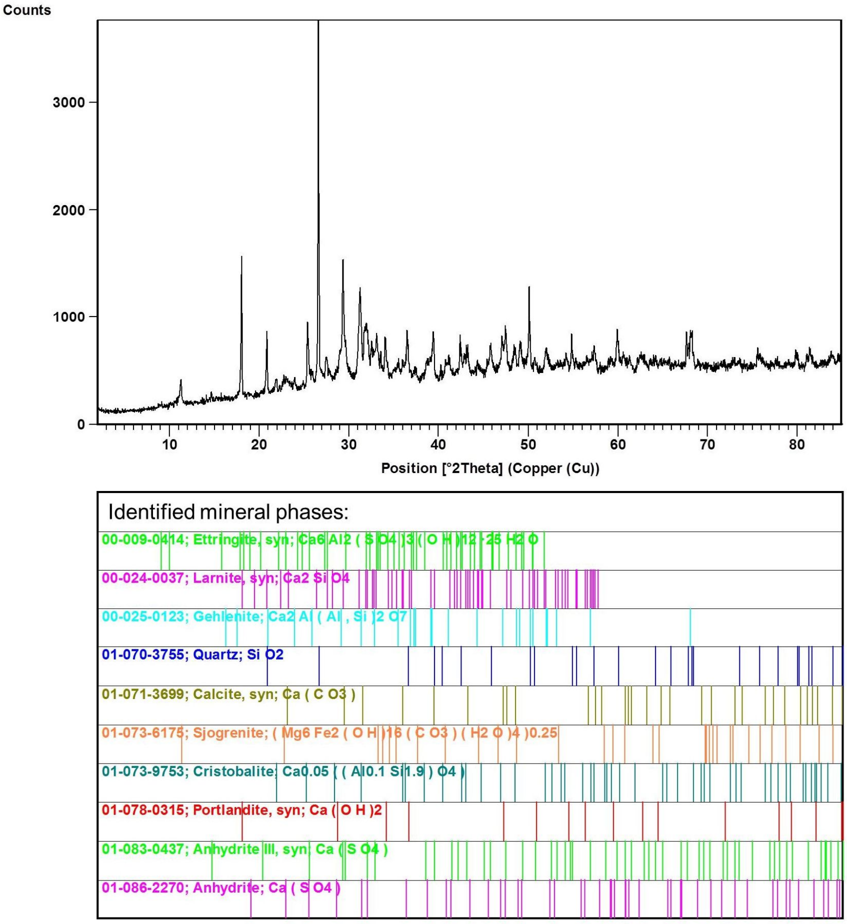

Figure S5.2 Analysis of mineral components of the fresh bottom ash by X-ray diffraction. Main and minor components: quartz, calcite, portlandite, hydrotalcite and anhydrite. Trace components: gehlenite, ettringite, larnite, cristobalite and sjogrenite.

5.8.3 Results of accelerated carbonation experiment 1

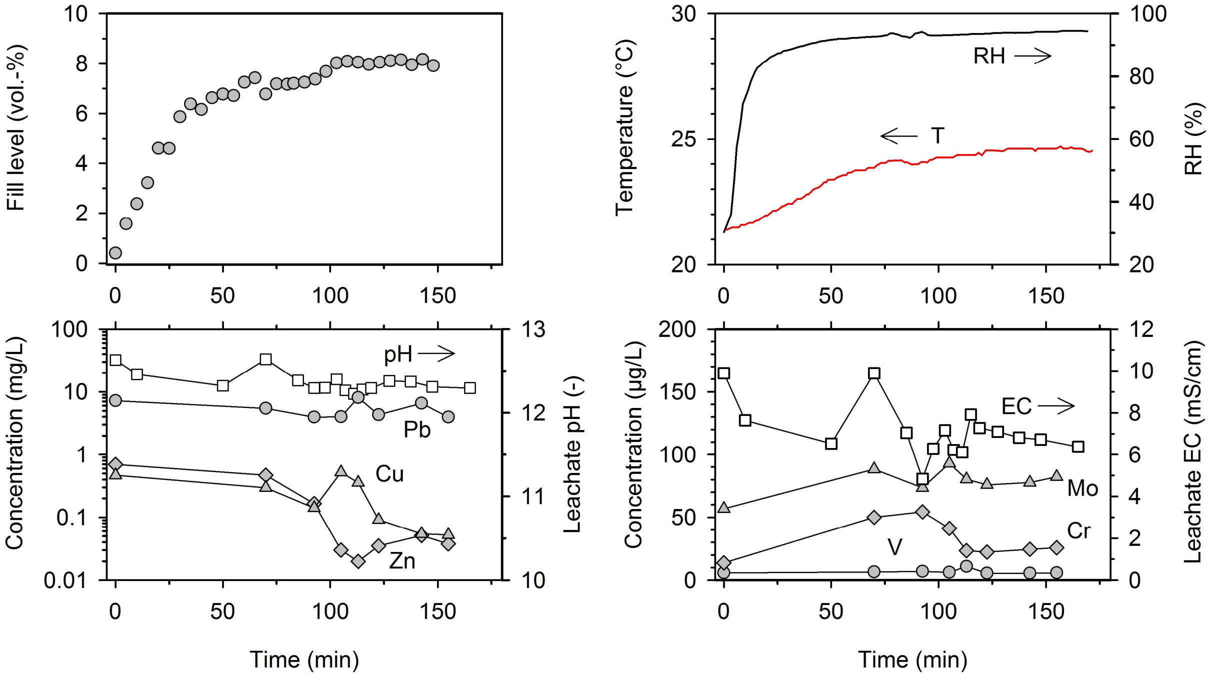

Figure S5.3. Results of experiment 1 with open reactor outlet, mass flow rate: 0.30 kg/min, rotation speed: 2.5 rpm, CO_2 concentration: 10 vol.-%, exhaust gas temperature (T): 21 °C and relative humidity (RH): <10 %. Tracer pulse was injected at time (t) = 70 min.

5.8.4 Antimony leaching results for experiment 2 - 4

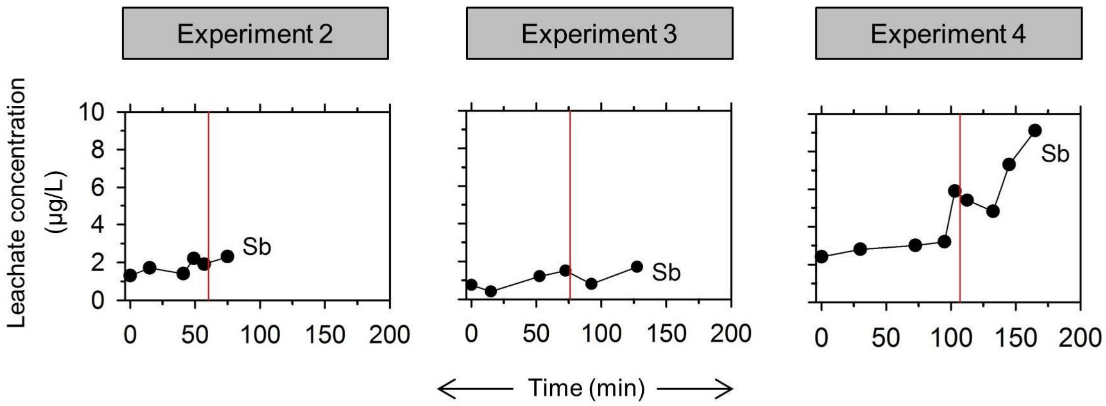

Figure S5.4. Results of carbonation experiments 2 to 4 performed at different residence times determined by the mass flow. Evolution of Sb concentration in aqueous batch extracts; vertical line: experimental residence time (τ_{MB}) obtained by mass balance. Values at experimental time zero represent leachate values of the fresh BA.

5.8.5 Results of the sieve analysis

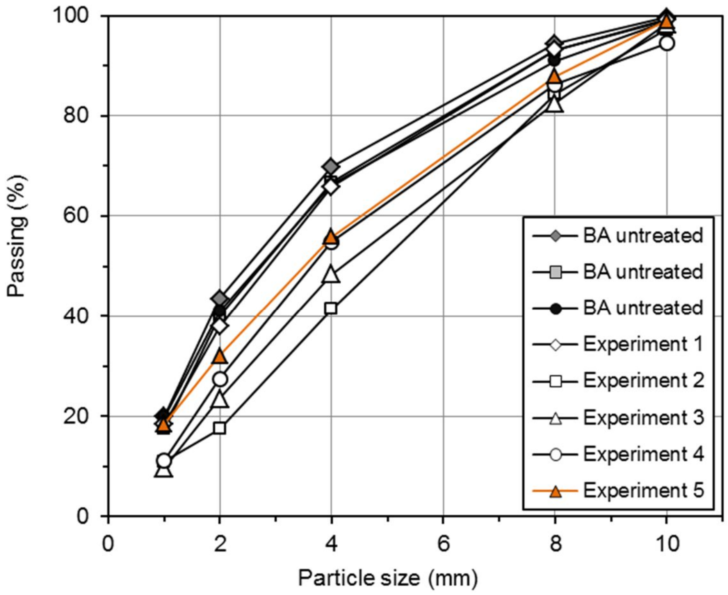

Figure S5.5. The cumulative particle size distribution of the untreated BA and the carbonated BA of experiment 1-5.

Chapter 6 Comprehensive discussion

6.1 Discussion

The current practice of BA ageing requires a large quantity of space, time and appropriate measures to control the process. A recent study by Blanc et al. (2018) indicated problems provoked by a lack of process control under industrial scale conditions. A promising approach to overcoming the problems is the accelerated carbonation of BA, which is a controlled enhancement of the natural ageing. However, practical applicability of reactor systems for accelerated carbonation developed so far remains beyond reach since they do not allow for the necessary throughput.

This thesis aimed at delineating both the technical set-up and the operation parameters suited for process integration of accelerated carbonation of BA at incinerator sites. This included the development of a screening technique (Chapter 2) to evaluate the progress of carbonation as well as a stepwise transfer of the reactor into a continuously fed system (Chapter 3 to 5). Table 6.1 summarizes the reactor concepts for accelerated carbonation developed and tested in this thesis.

The major findings regarding the objectives a) to e) of this thesis will be discussed in the following.

Table 6.1 Development steps and reactor concepts for accelerated carbonation of bottom ash (BA) developed and tested in this thesis.

Reactor scheme	Operating mode	Reaction gas supply	Corresponding chapter
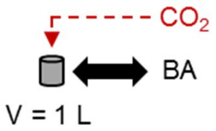	Batch	Manual dosage	2
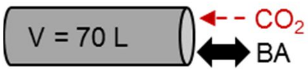	Batch	Automated dosage	2, 3
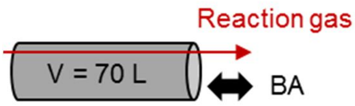	Batch	Flow-through	4
	Continuous	Flow-through	5

Objective a)

Develop a monitoring system to evaluate the progress of carbonation under static and dynamic conditions

Two alternative approaches may be used to evaluate the effects of BA carbonation: i) changes in (batch or column) leachate characteristics like pH, concentration of major components or critical trace metals and ii) alterations of the solid phase composition either by simply following the weight gain or by more sophisticated methods to resolve changes of specific mineral phases, e.g. by XRD or TGA, usually applied to small sample aliquots. While the analysis of leachates and the solid phase are usually time-consuming and require specific instrumentation, the gravimetric approach is error-prone, e.g. due to changes of the moisture content of BA during accelerated carbonation (Lin et al., 2015b).

An alternative approach was first applied in carbonation experiments conducted in pressurized reactors (Sun et al., 2008). Since the CO_2 consumption in a closed system is directly related to the carbonation reaction, the resulting pressure drop can be converted to the CO_2 quantity absorbed by the solid sample. However, applications described hitherto were restricted to pressures >200 kPa, which is beyond practical conditions (Fernández Bertos et al., 2004b).

Here, a simple method was developed and tested under static and dynamic conditions to quantify the CO_2-uptake by the pressure drop at atmospheric pressure (see Figure 6.1). Results demonstrated the serviceability and reproducibility of the approach as compared to the analytical quantification of carbonates by TGA. The monitoring system renders classical analyses unnecessary and integrates over the whole reactor loading which circumvents problems related to the small-scale heterogeneity of BA. In combination with static carbonation set-ups, the method may be suited for a routine assessment of the CO_2 uptake capacities of BA and other alkaline materials, e.g. in the context of carbon capture and storage. This may be particularly useful in the context of taking accelerated carbonation to the full scale.

The ability to follow carbonation online may contribute to a better process understanding. It could be shown that the experimental data was suited to quantify the carbonation kinetics at minimum analytical expense and without the need to vary the reaction time in separate runs.

Additional information was obtained by monitoring the temperature and relative humidity of the gaseous phase during the CO_2 uptake by BA. Due to the exothermic carbonation reaction the temperature increased by up to 10 °C.

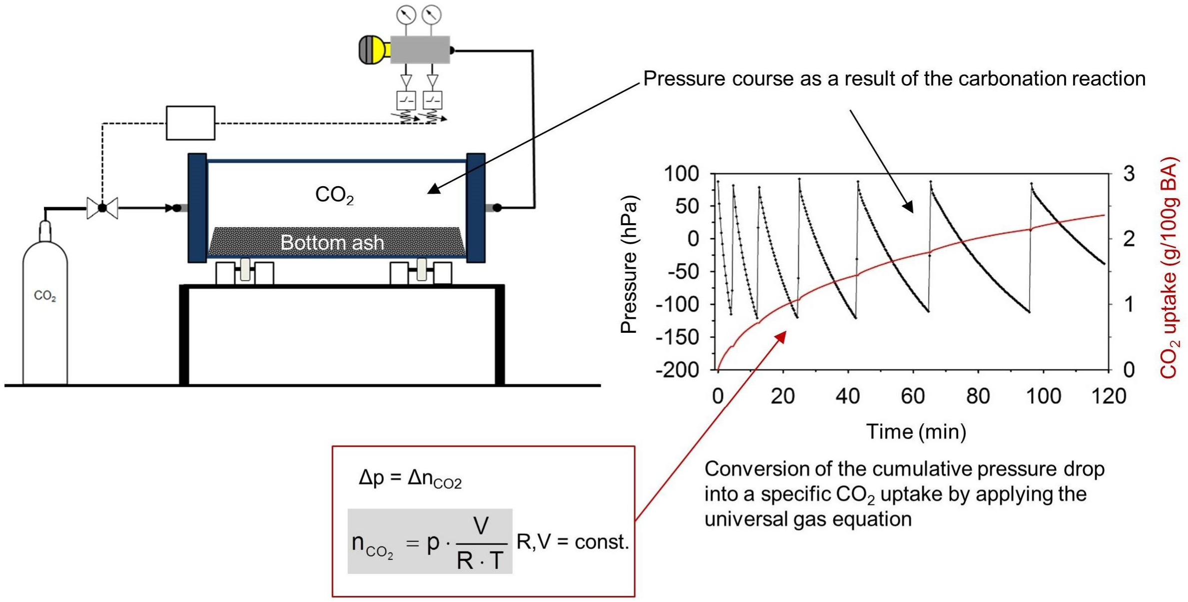

Figure 6.1 Schematic of the automated monitoring method for accelerated carbonation at near atmospheric pressure; the CO_2 uptake is quantified by integrating the pressure drop (△p) over time and apllying the universal gas equation (eq. 2.2).

The time course of self-heating matched with the CO_2 uptake and based on measured temperatures the heat content of the reactor and the flux to the environment were calculated and benchmarked against the reaction enthalpy. Excellent agreement demonstrated that, indeed, carbonation is the most important heat-generating reaction. Thus, temperature monitoring may be an alternative way of evaluating the carbonation performance.

Results presented in chapter 3 showed that the monitoring system may also be used in dynamic reactor setups where the BA is mixed to enhance the CO_2-uptake, e.g. in rotating drum reactors. Such systems are promising for practical applications, and fast and simple methods to follow the carbonation reaction are extremely useful to identify optimal operation conditions.

Objective b)

Evaluate the benefits of mixing and agitation for the accelerated carbonation

The first indications of the beneficial effect of dynamic conditions on BA carbonation were given by (Palitzsch et al., 1999). Subsequently (Fernández Bertos et al., 2004a) showed that the reaction velocity was two to three times higher when the BA was continuously shaken. In this thesis, BA carbonation under dynamic conditions was systematically investigated. First, a static (packed bed) and a dynamic reactor type (rotating drum) were directly compared, using identical volume-to-mass ratios but different layer thicknesses (static: 1 cm, dynamic: 3 -12 cm) (Chapter 2). Higher CO_2-uptake, self-heating and reaction velocities were found under dynamic conditions evoked by the rotation of the reactor.

The effect of the turning motion was studied in more detail in Chapter 3, where static and dynamic experiments were performed in the same reactor with or without rotation. The comparison was made across a broad range of reactor fill levels 7 - 42 vol.-% to investigate the effect of the BA layer thickness on carbonation. Under static conditions, the carbonation performance decreased with increasing fill level. In contrast, carbonation was superior under dynamic conditions even at fill levels exceeding 20 vol.-%. Under dynamic conditions the leaching behaviour of BA could be improved such as to comply with the German waste acceptance criteria for a landfilling of the material as a non-hazardous waste.

Overall, mixing and agitation are beneficial for BA carbonation. Within the tested range of reactor loadings, the layer thickness does not seem to be a limiting factor for the carbonation of BA when the drum is rotated (see Figure 6.2).

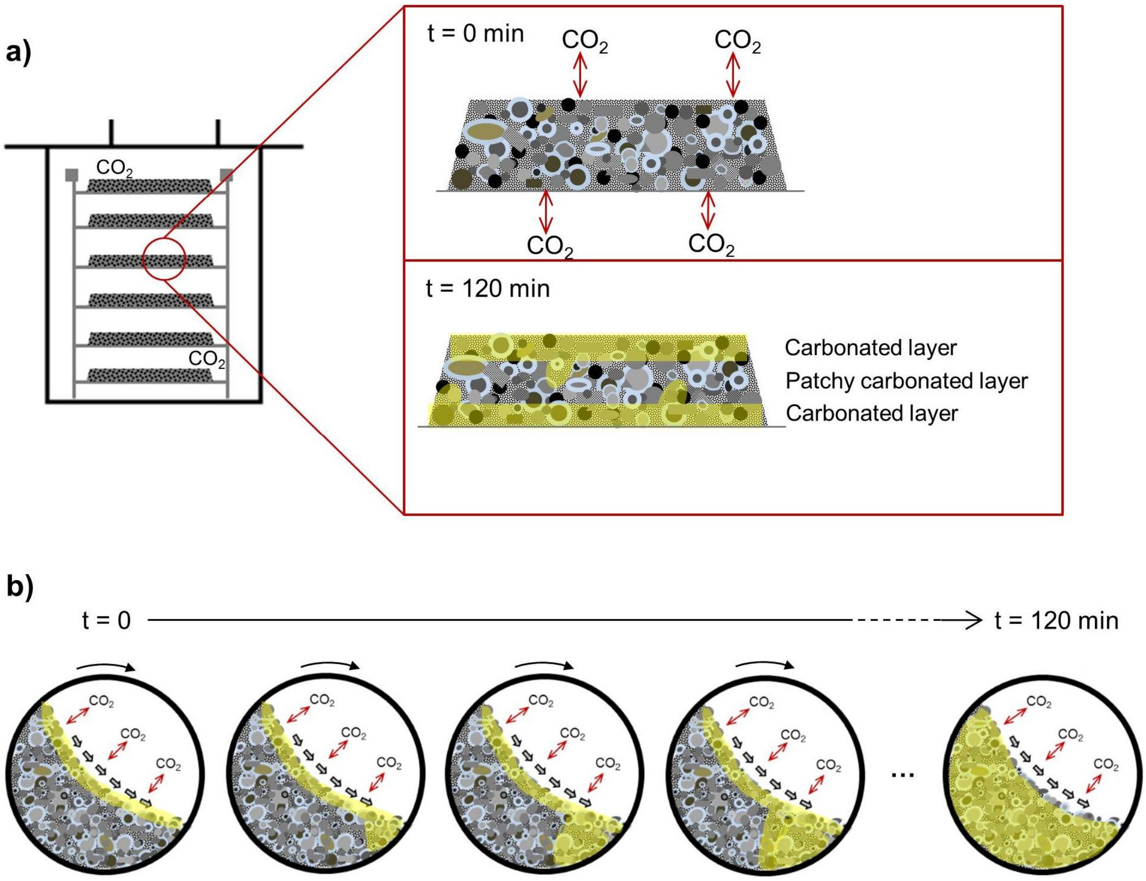

Figure 6.2 Illustration of the progress of BA carbonation in a static reactor (a) and a dynamic reactor (b) over time (t).

Objective c)

Study the bed behaviour of BA in rotating drum reactors

Recently, dynamic reactors (e.g. granulators, rotating drums) have successfully been tested for the accelerated carbonation of moist BA, FA and steel slag (Łączny et al., 2015; Librandi et al., 2019; Librandi et al., 2017; Morone et al., 2014). However, very little is known about how the motion of these materials is affected by the operating conditions, like fill level and rotation speed of the reactor. The radial motion is crucial for the reactor layout since it determines the degree of material mixing and the rate of heat and mass transfer both inside the material bed and between the bed surface and the headspace (Ding et al., 2001). With respect to objective (c) the effects of rotation speed, reactor fill level (chapter 3), and mixing tools (chapter 4) on the solids motion were studied. The bed behaviour of BA was tested both under moist and dry conditions and was compared to that of standard materials (sand and gravel).

In the plain drum without mixing tools dry BA behaved similarly to gravel in terms of slumping frequency and tended to segregate (i.e. to form alternating bandings of fine and coarse BA particles) after 30 rotations, approximately. In contrast, moist BA showed less frequent slipping or slumping and thereby a less dynamic behaviour than dry BA. This may be compensated by an increased thickness of the flowing layer (Chou et al., 2011), whereby a larger amount of material participates in the mixing process. No segregation was observed for moist BA which is deemed beneficial for the carbonation process, since segregation hampers the mass transfer between the gas and the solid. Thus, moisture may not only be a prerequisite for the carbonation reaction but may also be beneficial to the rheological behaviour of BA in rotating drums.

Video analyses revealed that over the range of tested rotation speeds and fill levels the bed motion of moist BA was predominantly characterized by slipping or slumping. Slipping occurred at fill levels below 18 vol.-% irrespective of rotation speed while for fill levels >18 vol.-% either a slumping or a transitional slumping/rolling bed motion were identified. Compared to standard materials, the onset of slumping/rolling was shifted towards higher fill levels and rotation speeds. Since slumping improves radial mixing, these results may be used to attain desired bed behaviour by a combination of fill level and rotation speed. With respect to the adjustment of BA residence times in a projected continuous feed operation, reactor fill level is a key parameter. The findings with respect to objective (c) show that fill levels of up to 42 vol.-% are feasible (and even beneficial to substrate mixing) as long as the CO_2-supply is not a limiting factor.

Besides the enhancing effect on mixing, the solid's motion may also evoke particle granulation (Librandi et al., 2017; Morone et al., 2014). Indeed, rotating drums are extensively used in many industries for granulation (Rodrigues et al., 2017; Wang and Cameron, 2002). Obtaining a granulated product with a specific size-distribution might be beneficial in terms product handling and geotechnical reuse (Gunning et al., 2009). As reported in Chapter 5, BA tended to granulate during carbonation without the addition of a binder (see Figure S5.4). Thus, the rotating drum reactor provides an opportunity to combine carbonation and granulation in a single treatment step to improve both, the chemical and physical properties of BA.

Objective d)

> *Investigate the effect of process conditions and reactor design on carbonation performance*

Rotating drums have long since been used in multiple engineering applications (Demagh et al., 2012). The following operation conditions have been identified as being of particular importance: rotation speed and fill level of the drum, properties of the reactant material and gas, and the design of mixing tools. These aspects were studied in detail in chapters 3 and 4 and findings are outlined in the following paragraphs.

Rotation speed

For processes comprising a gas-solid reaction, the rotation rate of the drum is, generally, deemed an important process variable (Stuart et al., 1999; Zhang et al., 2012) as it imposes a radial motion on the solid. However, Lombardi et al. (2016) recently tested the CO_2 removal from a gas stream in a rotating drum using BA as an absorbent and found that the rotation speed had a low significance on the CO_2 removal performance. This is in line with the findings presented in chapter 3 where the bed behaviour of BA showed a low sensitivity to rotation speed within the tested range (< 10 rpm). Since slow rotation is typically applied in industrial applications (Pichtel, 2014; Specht and Becker, 2014) throughout this study the rotation speed was kept below 3 rpm for carbonation experiments.

BA moisture

Wetness of BA is a consequence of the quenching process applied at most waste incinerators and is, at the same time, a prerequisite for carbonation since the related reactions take place in the pore water (Pan, 2012). Depending on ash characteristics and quenching procedures the moisture contents of BA can vary considerably (Costa et al., 2007). In chapter 3, the optimum moisture content for the tested BA (sieve fraction: <10 mm) was found to be 21 wt.-% as judged by the CO_2 uptake. This is roughly in the range of the typical moisture content of BA after storage in a roofed pile for 1 to 3 days. Excess moisture (>24 wt.-%), which can be found directly after the quenching process, caused a lower CO_2 uptake and should therefore be avoided.

CO_2 concentration

The use of waste gas streams as the CO_2 source in accelerated carbonation has been suggested by (Marzi et al., 2004). Depending on origin, their CO_2 concentration ranges from 5 to 70 vol.-%. However, a systematic study on the effect of CO_2 concentration on the accelerated carbonation at atmospheric pressure is lacking. As demonstrated in Chapter 3 both the CO_2 uptake rate and the final level of carbonation increased as the CO_2 concentration was raised from 15 to 75 vol.-%. The latter is in accordance with the law of mass action. However, a modest uptake inhibition was observed at 100 vol.-% CO_2. Under static conditions, carbonation was hampered at CO_2 concentrations exceeding 20 vol.-% (Nam et al., 2012; Sun et al., 2008). The authors concluded that this was due to inhibition of CO_2 diffusion through carbonates precipitated on the BA surface and the formation of calcite coatings has been documented, repeatedly (Brett et al., 2018; Ruiz-Agudo et al., 2013; Sakita and Nishimura, 2015). Under the dynamic test conditions used here, uptake inhibition was shifted to CO_2 concentrations of >75 vol.-% (see Figure 3.4). This may be attributed to the bed motion which causes friction among BA aggregates, whereby surfaces are continuously renewed and diffusion through a growing layer of precipitated $CaCO_3$ becomes less important. Overall, the findings suggest that under dynamic conditions a broad range of exhaust gases are suitable as a CO_2 source for the carbonation process. If available, the process can be accelerated by using CO_2 rich waste streams.

Reaction time

As outlined in the introduction, short reaction times favour the integration of accelerated carbonation procedures into the management of BA incinerator sites (see Figure 1.2). Experiments described in Chapter 3 were run in a closed reactor with an automated CO_2 dosage system. Reaction times of 120 minutes were sufficient to achieve high CO_2 uptakes and significantly improve the leachate quality of BA. In chapter 4 the reaction time was focused in more detail under flow-through conditions. These are particularly relevant in view of a full-scale implementation of the accelerated carbonation since most CO_2 waste gas streams are generated continuously. Under the tested conditions, reaction times could be cut to 100 minutes employing a specific CO_2 supply of 100 g CO_2/kg BA.

Fill level

In many applications of rotating drum reactors, the material bed only occupies a small part of the cross section and typical fill levels are between 10 to 20 vol.-% (Helmrich and Schügerl, 1979; Specht and Becker, 2014). As outlined in chapter 3, the fill level is of outstanding importance for the bed motion of BA. This is due to the fact that with increasing fill level the bed motion changes from slipping to slumping thereby favouring the mixing process. Thus, dynamic BA carbonation is not hampered by high fill levels exceeding 20 vol.% (see Figure 3.5). This is encouraging in terms of the treatment capacities in potential full-scale applications and may have been a consequence of the use of mixing tools (Chapter 4). Their beneficial effects on carbonation will be discussed next.

Reactor design: mixing tools

Mixing tools have proven to promote heat transfer and mixing in rotating drums and manifold designs and configurations exist (e.g. straight lifter plates or baffles mounted on the inner drum wall, axially located mixing tools) (Lee and Choi, 2013; Marsh et al., 2000; Ottino and Lueptow, 2008). In Chapter 4, five different mixing tool configurations including the plain drum were studied with respect to their effect on carbonation. The results indicated that carbonation can be enhanced by different mixing tool configurations, namely three single plates, an axially located mixing tool and a mixing cage. Selection of tools should, however, also consider a possible formation of incrustations during long-term use since these would require periodical cleaning to maintain the functionality causing additional costs for maintenance. Except for the mixing cage, BA incrustations formed either on the reactor mantle or on the mixing tools themselves. Similar effects were also recognized during the carbonation of steel slag in a rotating drum equipped with plates (Figure 1 (b), Librandi et al., 2017). The perforated mixing cage largely prevented the formation of incrustations even at fill levels of up to 50 %. In addition, it favoured a slumping over a slipping bed motion. Since, at present there are no references in the scientific literature regarding this type of mixing tool future research should focus on specific design aspects, like the number and geometry of the elongated gaps and the weight-to-diameter ratio.

Objective e)

Develop a continuous-fed operating reactor with adjustable BA residence time

So far, carbonation in rotating drums has only been tested under batch conditions (Łączny et al., 2015; Librandi et al., 2017 and 2019; Lombardi et al., 2016). In full scale applications, continuously operated reactor systems may be preferable since, therewith, the treatment may be synchronized to the BA generation (see Figure 1.3). Depending on the nature of the involved reactions the transition from batch to continuous processes can be challenging (Calabrese and Pissavini, 2011). However, some specifics of BA carbonation may favour the implementation into a continuous process. These include the facts that carbonation is favoured by mixing (Chapters 2 and 3), is an exothermic reaction (Chapter 3) that follows relatively fast kinetics (Chapter 2) and may be accompanied by an undesirable mobilisation of oxyanions if CO_2 uptake is excessively high (Chapters 3 and 4). Taking advantage of the above-named specifics in a continuously fed system requires that the residence time of BA is adequately controlled.

Continuously operated rotating drums are commonly used for the processing of granular materials in the mineral, ceramic, cement, metallurgical, chemical, pharmaceutical, food, and waste treatment industries (Abouzeid and Fuerstenau, 2010; Abouzeid et al., 1974; Liu et al., 2009; Sullivan et al., 1927). However, process design is mostly empirical (Sherritt et al., 2003). Furthermore, wet granular materials have been seldomly addressed.

Building on the knowledge gained from Chapters 2 to 4, a rotating drum reactor was developed for the operation under continuous-feed of both the reactant gas and the BA. Most importantly, this required the integration of a dosage system for BA. The decisive factor in this respect was to keep the effective shear force low to avoid altering the rheological properties of BA. This was achieved with a voltage-controlled dosage screw (see Figure S5.1). Furthermore, a movable slide was used at the reactor discharge to control the reactor hold up (resident mass of BA) following the observations by Karra and Fuerstenau (1977) and both the feed and the discharge unit were weighted for mass balancing purposes.

The serviceability of these layout solutions were demonstrated by the excellent agreement of projected and experimentally verified BA residence times. Tracer breakthrough curves demonstrated that the longitudinal transport of BA agrees well with the axial dispersion model for non-segregating particulate material. The reactor was supplied with reactant gas with 10 vol-% CO_2 at a flow rate of 60 L/min. Under these conditions a residence time of about 75 min was enough to improve the BA leachate quality such as to comply with the regulatory standards for non-hazardous waste. Regarding the immobilization of the amphoteric metals and the partial mobilization of oxyanions the results shown in Chapters 2 through 4 were confirmed under continuous feed conditions. Due to the effective control of residence time both effects can be balanced out.

In view of the properties of real-world exhaust gases and their use for BA carbonation, Chapter 5 included a run with a hot and moist reactant gas. Effects of this are largely unexplored in the scientific literature. Results demonstrated that using a hot and moist gas only slightly affected the carbonation performance. This finding is encouraging since most waste gas streams are typically moist and hot (e.g. stack gas from WtE plants, Tang et al., 2015).

Overall, the rotating drum reactor concept appears promising for the full-scale implementation of BA carbonation in terms of relatively short residence times and stable performance. Yet, in a full-scale operation, the reactor throughput would ideally have to be synchronized with the rate of BA generation, requiring a reactor scale-up.

6.2 Conclusion and outlook

The experimental work of this thesis was centred on the improvement of the leaching behaviour of waste incinerator bottom ash by accelerating its carbonation. As outlined in Chapter 1, accelerated carbonation is of economic and environmental interest when the time-scale of treatment can be synchronized to the rate of bottom ash generation. To this end, first, a simple and robust method to quantify the CO_2 uptake was developed, second, the reactor system was transferred from a static jar test to a rotating drum reactor, third, the mode of reactor operation was shifted batch to flow-though and, ultimately, to continuous-feed.

The results obtained along this path unequivocally demonstrated that the accelerated carbonation of waste incinerator bottom ash can, indeed, be synchronized to its generation rate. The reaction could be accelerated to around 100 minutes. The leachate properties characterized the carbonated material as a non-hazardous waste. This is due to the fact that the mobility of amphoteric metals (Pb, Cu, Zn) was reduced by up to three orders of magnitude. This would allow for a disposal on a class 1 landfill. In addition to landfilling the carbonated material was also studied under the perspective its geotechnical utilization. Based on the draft of the German Ordinance on Secondary Construction Materials, column and batch leaching test results show that carbonated bottom ash complies with the regulatory standards of a secondary construction material categorized as HMVA-1. For such materials a series of applications exist, including the use as road subbases, sound barriers, parking lot and bike path groundings. Therefore, the accelerated carbonation of bottom ash provides a material that is both suited for the cost-effective disposal on a lower landfill class and for the potential generation of revenues from if geotechnical use. These applications involve the benefit of substituting geogenic aggregates and thereby conserving natural resources.

Other than the amphoteric metals, oxyanions like Cr, Mo and V became more mobile upon carbonation. Although this side effect did not outweigh the benefits it would need to be considered in a full-scale application. This may be done in a multidimensional optimization where carbonation is not taken to the maximum CO_2 uptake but balanced for a minimization of the side effect. To this end, control of bottom ash residence time in the reactor and the knowledge of the carbonation kinetics are mandatory. Both aspects have been extensively addressed in this thesis and can now contribute to promote accelerated carbonation of BA as an industrial process.

It was beyond the scope of the work presented here to delineate the scale-up of the accelerated carbonation process. Yet, in the meantime, a series of semi-full scale experiments have been conducted (see. Figure 6.3). Results of these corroborated the findings obtained from the laboratory test. Therefore, the implementation of the process is in sight as soon as the draft Ordinance on Secondary Construction Materials is approved.

Figure 6.3 Semi-full scale reactor for continuous-fed carbonation of BA utilising the exhaust gas of a cogeneration plant (combined heat and power) as the CO_2 source.

Chapter 7 References

References for Chapter 1 and 6.

Abdulmatin, A., Tangchirapat, W., Jaturapitakkul, C., 2018. An investigation of bottom ash as a pozzolanic material. Construction and Building Materials 186, 155–162.

Abouzeid, A.-Z.M., Fuerstenau, D.W., 2010. Flow of non-homogeneous particulates in rotating drums. KONA Powder and Particle Journal 28, 155–166.

Abouzeid, A. -Z. M. A., Mika, T.S., Sastry, K.V., Fuerstenau, D.W., 1974. The influence of operating variables on the residence time distribution for material transport in a continuous rotary drum. Powder Technology 10, 273–288.

Allegrini, E., Vadenbo, C., Boldrin, A., Astrup, T.F., 2015. Life cycle assessment of resource recovery from municipal solid waste incineration bottom ash. Journal of Environmental Management 151, 132–143.

Al-Rawas, A.A., Wahid Hago, A., Taha, R., Al-Kharousi, K., 2005. Use of incinerator ash as a replacement for cement and sand in cement mortars. Building and Environment 40, 1261–1266.

Alwast, H., Riemann, A., Oktober / 2010. Verbesserungen der umweltrelevanten Qualitäten von Schlacken aus Abfallverbrennungsanlagen: Texte 50/2010. Umweltbundesamt, Dessau-Roßlau.

Arickx, S., Borger, V. de, van Gerven, T., Vandecasteele, C., 2010. Effect of carbonation on the leaching of organic carbon and of copper from MSWI bottom ash. Waste Management 30, 1296–1302.

Arickx, S., van Gerven, T., Vandecasteele, C., 2006. Accelerated carbonation for treatment of MSWI bottom ash. Journal of Hazardous Materials 137, 235–243.

Astrup, T., 2007. Pretreatment and utilization of waste incineration bottom ashes: Danish experiences. Waste Management 27, 1452–1457.

Astrup, T., Dijkstra, J.J., Comans, R.N.J., Van der Sloot, Hans A., Christensen, T.H., 2006. Geochemical modeling of leaching from MSWI Air-Pollution-Control residues. Environmental Science & Technology 40, 3551–3557.

Baciocchi, R., Carnevale, E., Corti, A., Costa, G., Lombardi, L., Olivieri, T., Zanchi, L., Zingaretti, D., 2013. Innovative process for biogas upgrading with CO_2 storage: Results from pilot plant operation. Biomass & Bioenergy 53, 128–137.

Baciocchi, R., Costa, G., Lategano, E., Marini, C., Polettini, A., Pomi, R., Postorino, P., Rocca, S., 2010. Accelerated carbonation of different size fractions of bottom ash from RDF incineration. Waste Management 30, 1310–1317.

Barberio, G., Buttol, P., Masoni, P., Scalbi, S., Andreola, F., Barbieri, L., Lancellotti, I., 2010. Use of Incinerator Bottom Ash for Frit Production. Journal of Industrial Ecology 14, 200–216.

Bayuseno, A.P., Schmahl, W.W., 2010. Understanding the chemical and mineralogical properties of the inorganic portion of MSWI bottom ash. Waste Management 30, 1509–1520.

Bendz, D., Tüchsen, P.L., Christensen, T.H., 2007. The dissolution kinetics of major elements in municipal solid waste incineration bottom ash particles. Journal of Contaminant Hydrology 94, 178–194.

Bertolini, L., Carsana, M., Cassago, D., Quadrio Curzio, A., Collepardi, M., 2004. MSWI ashes as mineral additions in concrete. Cement and Concrete Research 34, 1899–1906.

Bertos, M.F., X. Li, R. Simons, S.J., D. Hills, C., J. Carey, P., 2004. Investigation of accelerated carbonation for the stabilisation of MSW incinerator ashes and the sequestration of CO_2. Green Chemistry 6, 428–436.

Bilitewski, B., Härdtle, G., 2013. Abfallwirtschaft: Handbuch für Praxis und Lehre, Springer Vieweg, Berlin. p. 354.

Blanc, D., Gonzalez, L., Lupsea-Toader, M., Brauer, C. de, 2018. Mineralogical evolution and leaching behaviour of a heap of bottom ash as a function of time: Influence on its valorization. Waste and Biomass Valorization 32, 2517–2527.

Bobicki, E.R., Liu, Q., Xu, Z., Zeng, H., 2012. Carbon capture and storage using alkaline industrial wastes. Progress in Energy and Combustion Science 38, 302–320.

Bodor, M., Santos, R.M., van Gerven, T., Vlad, M., 2013. Recent developments and perspectives on the treatment of industrial wastes by mineral carbonation - a review. Central European Journal of Engineering 3, 566–584.

Bourtsalas, A., Vandeperre, L.J., Grimes, S.M., Themelis, N., Cheeseman, C.R., 2015. Production of pyroxene ceramics from the fine fraction of incinerator bottom ash. Waste management 45, 217–225.

Brett, B., Weigand, H., Fröhlich, P., 2018. Mineralische Reststoffe als Ersatzbaustoffe. Chemie in unserer Zeit 52, 322–328.

Bruder-Hubscher, V., Lagarde, F., Leroy, M.J.F., Coughanowr, C., Enguehard, F., 2002. Application of a sequential extraction procedure to study the release of elements from municipal solid waste incineration bottom ash. Analytica Chimica Acta 451, 285–295.

Calabrese, G.S., Pissavini, S., 2011. From batch to continuous flow processing in chemicals manufacturing. AIChE Journal 57, 828–834.

Caprai, V., Lazaro, A., Brouwers, H.J.H., 2019. Waterglass impregnation of municipal solid waste incineration bottom ash applied as sand replacement in mortars. Waste Management 86, 87–96.

CEWEP: Confederation of European Waste-to-Energy Plants, 2017. Bottom ash Factsheet. http://www.cewep.eu/2017/09/08/bottom-ash-factsheet/ (accessed 05 March 2019).

Chandler, A.J., Eighmy, T.T., Hartlen, J., Hjelmar, O., Kosson, D.S., Sawell, S.E., van der Sloot, H.A., Vehlow, J., 1997. Municipal solid waste incinerator residues. Elsevier, Amsterdam.

Chaspoul, F.R., Le Droguene, M.F., Barban, G., Rose, J.C., Gallice, P.M., 2008. A role for adsorption in lead leachability from MSWI bottom ash. Waste management 28, 1324–1330.

Chimenos, J.M., Fernández, A.I., Miralles, L., Rosell, J.R., Ezquerra, A.N., 2005. Change of mechanical properties during short-term natural weathering of MSWI bottom ash. Environmental Science & Technology 39, 7725–7730.

Chimenos, J.M., Fernández, A.I., Miralles, L., Segarra, M., Espiell, F., 2003. Short-term natural weathering of MSWI bottom ash as a function of particle size. Waste Management 23, 887–895.

Chimenos, J.M., Fernández, A.I., Nadal, R., Espiell, F., 2000. Short-term natural weathering of MSWI bottom ash. Journal of Hazardous Materials 79, 287–299.

Chimenos, J.M., Segarra, M., Fernández, M.A., Espiell, F., 1999. Characterization of the bottom ash in municipal solid waste incinerator. Journal of Hazardous Materials 64, 211–222.

Chou, S.H., Liao, C.C., Hsiau, S.S., 2011. The effect of interstitial fluid viscosity on particle segregation in a slurry rotating drum. Physics of Fluids 23, 83301.

Cornelis, G., Johnson, C.A., van Gerven, T., Vandecasteele, C., 2008. Leaching mechanisms of oxyanionic metalloid and metal species in alkaline solid wastes: A review. Applied Geochemistry 23, 955–976.

Costa, G., Baciocchi, R., Polettini, A., Pomi, R., Hills, C.D., Carey, P.J., 2007. Current status and perspectives of accelerated carbonation processes on municipal waste combustion residues. Environmental Monitoring and Assessment 135, 55–75.

Cucchiella, F., D'Adamo, I., Gastaldi, M., 2017. Sustainable waste management: Waste to energy plant as an alternative to landfill. Energy Conversion and Management 131, 18–31.

del Valle-Zermeño, R., Gómez-Manrique, J., Giro-Paloma, J., Formosa, J., Chimenos, J.M., 2017. Material characterization of the MSWI bottom ash as a function of particle size. Effects of glass recycling over time. The Science of the Total Environment 581-582, 897–905.

del Valle-Zermeño, R., Romero-Güiza, M.S., Chimenos, J.M., Formosa, J., Mata-Alvarez, J., Astals, S., 2015. Biogas upgrading using MSWI bottom ash: An integrated municipal solid waste management. Renewable Energy 80, 184–189.

Demagh, Y., Ben Moussa, H., Lachi, M., Noui, S., Bordja, L., 2012. Surface particle motions in rotating cylinders: Validation and similarity for an industrial scale kiln. Powder Technology 224, 260–272.

Di Gianfilippo, M., Costa, G., Verginelli, I., Gavasci, R., Lombardi, F., 2016. Analysis and interpretation of the leaching behaviour of waste thermal treatment bottom ash by batch and column tests. Waste management 56, 216–228.

Di Gianfilippo, M., Hyks, J., Verginelli, I., Costa, G., Hjelmar, O., Lombardi, F., 2018. Leaching behaviour of incineration bottom ash in a reuse scenario: 12years-field data vs. lab test results. Waste management 73, 367–380.

Dijkstra, J.J., Meeussen, J.C.L., Van der Sloot, Hans A., Comans, R.N.J., 2008. A consistent geochemical modelling approach for the leaching and reactive transport of major and trace elements in MSWI bottom ash. Applied Geochemistry 23, 1544–1562.

Dijkstra, J.J., Van der Sloot, Hans A., Comans, R.N.J., 2006. The leaching of major and trace elements from MSWI bottom ash as a function of pH and time. Applied Geochemistry 21, 335–351.

Ding, Y.L., Seville, J.P.K., Forster, R., Parker, D.J., 2001. Solids motion in rolling mode rotating drums operated at low to medium rotational speeds. Chemical Engineering Science 56, 1769–1780.

Döing, M., 2017. Energie aus Abfall stark nachgefragt. VDI Umwelt Magazin 6, 18–19.

Dou, X., Ren, F., Nguyen, M.Q., Ahamed, A., Yin, K., Chan, W.P., Chang, V.W.-C., 2017. Review of MSWI bottom ash utilization from perspectives of collective characterization, treatment and existing application. Renewable and Sustainable Energy Reviews 79, 24–38.

Ecke, H., Aberg, A., 2006. Quantification of the effects of environmental leaching factors on emissions from bottom ash in road construction. The Science of the total Environment 362, 42–49.

Eighmy, T.T., Eusden Jr., J.D., Marsella, K., Hogan, J., Domingo, D., Krzanowski, J.E., Stämpfli, D., 1994. Particle Petrogenesis and Speciation of Elements in MSW incineration Bottom Ashes, in: J.J.J.M. Goumans, H.A. van der Sloot and Th.G. Aalbers (Ed.), Studies in Environmental Science : Environmental Aspects of Construction with Waste Materials Proceeding of the International Conference on Environmental Implications of Construction Materials and Technology Developments, Volume 60. Elsevier, pp. 111–136.

Essington, M.E., 2004. Soil and Water Chemistry: An Integrative Approach. CRC, Boca Raton, Fla., London.

ErsatzbaustoffV, 2017. Verordnung über Anforderungen an den Einbau von mineralischen Ersatzbaustoffen in technische Bauwerke (Ersatzbaustoffverordnung) (a recent draft piece of legislation prepared by German government) version of February 2017

Eusden, J.D., Eighmy, T.T., Hockert, K., Holland, E., Marsella, K., 1999. Petrogenesis of municipal solid waste combustion bottom ash. Applied Geochemistry 14, 1073–1091.

Fernández Bertos, M., Li, X., Simons, S.J.R., Hills, C.D., Carey, P.J., 2004a. Investigation of accelerated carbonation for the stabilisation of MSW incinerator ashes and the sequestration of CO_2. Green Chem 6, 428–436.

Fernández Bertos, M., Simons, S.J.R., Hills, C.D., Carey, P.J., 2004b. A review of accelerated carbonation technology in the treatment of cement-based materials and sequestration of CO_2. Journal of Hazardous Materials 112, 193–205.

Fléhoc, C., Girard, J.-P., Piantone, P., Bodénan, F., 2006. Stable isotope evidence for the atmospheric origin of CO_2 involved in carbonation of MSWI bottom ash. Applied Geochemistry 21, 2037–2048.

Förstner, U., 2012. Umweltschutztechnik, 8th ed. Springer, Berlin. p. 353.

Freyssinet, P., Piantone, P., Azaroual, M., Itard, Y., Clozel-Leloup, B., Guyonnet, D., Baubron, J.C., 2002. Chemical changes and leachate mass balance of municipal solid waste bottom ash submitted to weathering. Waste Management 22, 159–172.

Fujimori, E., Minamoto, K., Iwata, S., Chiba, K., Haraguchi, H., 2004. Enrichment of elements in industrial waste incineration bottom ashes obtained from three different types of incinerators, as studied by ICP-AES and ICP-MS: Journal of Material Cycles and Waste Management 6, 73–79.

Giordano, P.M., Behel, A.D., Lawrence, J.E., Soileau, J.M., Bradford, B.N., 1983. Mobility in soil and plant availability of metals derived from incinerated municipal refuse. Environmental science & technology 17, 193–198.

Gori, M., Bergfeldt, B., Pfrang-Stotz, G., Reichelt, J., Sirini, P., 2011. Effect of short-term natural weathering on MSWI and wood waste bottom ash leaching behaviour. Journal of Hazardous Materials 189, 435–443.

Gunning, P.J., Hills, C.D., Carey, P.J., 2009. Production of lightweight aggregate from industrial waste and carbon dioxide. Waste management 29, 2722–2728.

Han, G.-C., Um, N.-I., You, K.-S., Cho, H.-C., Ahn, J.-W., 2009. Change of mineral phases in carbonation reaction of MSWI bottom ash. Geosystem Engineering 12, 5–8.

Hao, Z., Sun, M., Ducoste, J.J., Benson, C.H., Luettich, S., Castaldi, M.J., Barlaz, M.A., 2017. Heat generation and accumulation in municipal solid waste landfills. Environmental Science & Technology 51, 12434–12442.

Helmrich, H., Schügerl, K., 1979. Drehrohrreaktoren in der Chemietechnik. Chemie Ingenieur Technik 51, 771–778.

Heuss-Aßbichler, S., Magel, G., Fehr, K.T., 2010. Abiotic hydrogen production in fresh and altered MSWI-residues: Texture and microstructure investigation. Waste Management 30, 1871–1880.

Hirner, A.V., Rehage, H., Sulkowski, M., 2000. Umweltgeochemie: Herkunft, Mobilität und Analyse von Schadstoffen in der Pedosphäre. Steinkopff, Darmstadt.

Hjelmar, O., Holm, J., Crillesen, K., 2007. Utilisation of MSWI bottom ash as sub-base in road construction: First results from a large-scale test site. Journal of Hazardous Materials 139, 471–480.

Holm, O., Simon, F.-G., 2016. Innovative treatment trains of bottom ash (BA) from municipal solid waste incineration (MSWI) in Germany. Waste management 59, 229–236

Hoornweg, D., Bhada-Tata, P., Kennedy, C., 2013. Environment: Waste production must peak this century. Nature 502, 615–617.

Hoornweg, D., Bhada-Tata, P., Kennedy, C., 2015. Peak waste: When is it likely to occur? Journal of Industrial Ecology 19, 117–128.

Huber, H., Jaros, M., Lechner, P., 1996. Emissionsverhalten von MVA-Schlacke nach künstlicher Alterung: Endbericht. BOKU, Wien.

Huber, H., Jaros, M., Lechner, P., 1998. Langfristiges Emissionsverhalten von MVA-Schlacke. Wasser & Boden 50, 14–18.

Hyks, J., Astrup, T., Christensen, T.H., 2009. Leaching from MSWI bottom ash: evaluation of non-equilibrium in column percolation experiments. Waste management 29, 522–529.

Inkaew, K., Saffarzadeh, A., Shimaoka, T., 2016. Modeling the formation of the quench product in municipal solid waste incineration (MSWI) bottom ash. Waste management 52, 159–168.

Johnson, C.A., Brandenberger, S., Baccini, P., 1995. Acid neutralizing capacity of municipal waste incinerator bottom ash. Environmental Science & Technology 29, 142–147.

Johnson, C.A., Furrer, G., 2002. Influence of biodegradation processes on the duration of $CaCO_3$ as a pH buffer in municipal solid waste incinerator bottom ash. Environmental Science & Technology 36, 215–220.

Johnson, C.A., Kaeppeli, M., Brandenberger, S., Ulrich, A., Baumann, W., 1999. Hydrological and geochemical factors affecting leachate composition in municipal solid waste incinerator bottom ash: Part II. The geochemistry of leachate from Landfill Lostorf, Switzerland. Journal of Contaminant Hydrology 40, 239–259.

Karak, T., Bhagat, R.M., Bhattacharyya, P., 2012. Municipal solid waste generation, composition, and management: The world scenario. Critical Reviews in Environmental Science and Technology 42, 1509–1630.

Karamalidis, A.K., Dzombak, D.A., 2011. Surface Complexation Modeling: Gibbsite. John Wiley & sons, Hoboken (USA).

Karra, V.K., Fuerstenau, D.W., 1977. Material transport in a continuous rotary drum. Effect of discharge plate geometry. Powder Technology 16, 23–28.

Kashef-Haghighi, S., Ghoshal, S., 2013. Physico–Chemical Processes Limiting CO_2 Uptake in Concrete during Accelerated Carbonation Curing. Industrial & Engineering Chemistry Research 52 (16), 5529–5537.

Kersten, M., Christoph Moor, H., Johnson, C.A., 1997. Speciation of trace metals in leachate from a MSWI bottom ash landfill. Applied Geochemistry 12, 675–683.

Keulen, A., van Zomeren, A., Harpe, P., Aarnink, W., Simons, H.A.E., Brouwers, H.J.H., 2016. High performance of treated and washed MSWI bottom ash granulates as natural aggregate replacement within earth-moist concrete. Waste management 49, 83–95.

Kim, S.-Y., Tanaka, N., Matsuto, T., 2002. Solubility and adsorption characteristics of Pb in leachate from MSW incinerator bottom ash. Waste Management & Research 20, 373–381.

Kirby, C.S., Rimstidt, J.D., 1993. Mineralogy and surface properties of municipal solid waste ash. Environmental Science & Technology 27, 652–660.

Klemm, W.A., Berger, R.L., 1972. Accelerated curing of cementitious systems by carbon dioxide. Cement and Concrete Research 2 (5), 567–576.

Knorr, W., Frede, M., Hutzinger, O., Marb, C., Mathews, W., Rössert, M., Rommel, W., Ruckdeschel, W., Swerev, M., Tränkler, J., Vierle, O., 1999. Rückstände aus der Müllverbrennung: Chancen für eine stoffliche Verwertung von Aschen und Schlacken. Erich Schmidt, Berlin, p. 258.

Köster, R., Vehlow, J., 2002. Verwertung von Schlacken aus der Abfallverbrennung: Geochemische Wechselwirkungen zwischen Wasser und Reststoffen. Chemie in unserer Zeit 36, 82–89.

Kuo, W.-T., Liu, C.-C., Su, D.-S., 2013. Use of washed municipal solid waste incinerator bottom ash in pervious concrete. Cement and Concrete Composites 37, 328–335.

Łączny, J.M., Iwaszenko, S., Gogola, K., Bajerski, A., Janoszek, T., Klupa, A., Cempa-Balewicz, M., 2015. Study on the possibilities of treatment of combustion by-products from fluidized bed boilers into a product devoid of free calcium oxide. Journal of Sustainable Mining 14, 164–172.

Lam, C.H.K., Ip, A.W.M., Barford, J.P., McKay, G., 2010. Use of incineration MSW ash: A review. Sustainability 2, 1943–1968.

Lange, L.C., Hills, C.D., Poole, A.B., 1996. The effect of accelerated carbonation on the properties of cement-solidified waste forms. Waste Management 16, 757–763.

Le, N.H., Razakamanantsoa, A., Nguyen, M.-L., van Phan, T., Dao, P.-L., Nguyen, D.H., 2018. Evaluation of physicochemical and hydromechanical properties of MSWI bottom ash for road construction. Waste Management 80, 168–174.

Lee, H., Choi, S., 2013. Lifter design for enhanced heat transfer in a rotary kiln reactor. Journal of Mechanical Science and Technology 27, 3191–3197.

Librandi, P., Costa, G., Souza, A.C.B.d., Stendardo, S., Luna, A.S., Baciocchi, R., 2017. Carbonation of steel slag: Testing of the wet route in a pilot-scale reactor. Energy Procedia 114, 5381–5392.

Librandi, P., Costa, G., Stendardo, S., Baciocchi, R., 2019. Carbonation of BOF slag in a rotary kiln reactor in view of the scale-up of the wet route process. Environmental Progress & Sustainable Energy 47, 3308.

Lim, M., Han, G.-C., Ahn, J.-W., You, K.-S., 2010. Environmental remediation and conversion of carbon dioxide (CO_2) into useful green products by accelerated carbonation technology. International Journal of Environmental Research and Public Health 7, 203–228.

Lin, C.-L., Weng, M.-C., Chang, C.-H., 2012. Effect of incinerator bottom-ash composition on the mechanical behavior of backfill material. Journal of Environmental Management 113, 377–382.

Lin, W.Y., Heng, K.S., Sun, X., Wang, J.-Y., 2015a. Accelerated carbonation of different size fractions of MSW IBA and the effect on leaching. Waste Management 41, 75–84.

Lin, W.Y., Heng, K.S., Sun, X., Wang, J.-Y., 2015b. Influence of moisture content and temperature on degree of carbonation and the effect on Cu and Cr leaching from incineration bottom ash. Waste Management 43, 264–272.

Liu, A., Ren, F., Lin, W.Y., Wang, J.-Y., 2015. A review of municipal solid waste environmental standards with a focus on incinerator residues. International Journal of Sustainable Built Environment 4, 165–188.

Liu, X.Y., Zhang, J., Specht, E., Shi, Y.C., Herz, F., 2009. Analytical solution for the axial solid transport in rotary kilns. Chemical Engineering Science 64, 428–431.

Lombardi, L., Carnevale, E., Corti, A., 2015. A review of technologies and performances of thermal treatment systems for energy recovery from waste. Waste Management 37, 26–44.

Lombardi, L., Carnevale, E.A., Pecorini, I., 2016. Experimental evaluation of two different types of reactors for CO_2 removal from gaseous stream by bottom ash accelerated carbonation. Waste management 58, 287–298.

Lynn, C.J., Ghataora, G.S., Dhir OBE, R.K., 2017. Municipal incinerated bottom ash (MIBA) characteristics and potential for use in road pavements. International Journal of Pavement Research and Technology 10, 185–201.

Makarichi, L., Jutidamrongphan, W., Techato, K.-a., 2018. The evolution of waste-to-energy incineration: A review. Renewable and Sustainable Energy Reviews 91, 812–821.

Marsh, A.J., Stuart, D.M., Mitchell, D.A., Howes, T., 2000. Characterizing mixing in a rotating drum bioreactor for solid-state fermentation. Biotechnology Letters 22, 473–477.

Martens, H., 2011. Recyclingtechnik: Fachbuch für Lehre und Praxis. Spektrum, Akad. Verl, Heidelberg.

Marzi, T., Palitzsch, S., Beckmann, R., Kümmel, R., Beard, A., Keldenrich, K., 1998. Wirkungsmechanismen bei der Alterung von Müllverbrennungsaschen. Müll und Abfall, 316–322.

Marzi, T., Palitzsch, S., Kümmel, R., Pellens, J., Bleeker, P., 2004. Künstliche Alterung von Rostaschen aus der thermischen Abfallbehandlung: Ein Test im großtechnischen Maßstab zur Immobilisierung von Schwermetallen durch Behandlung mit Kohlendioxid, Müll und Abfall 1, 23–30.

Meima, J.A., Comans, R.N.J., 1997. Geochemical Modeling of Weathering Reactions in Municipal Solid Waste Incinerator Bottom Ash. Environmental Science & Technology 31, 1269–1276.

Meima, J.A., Comans, R.N.J., 1998. Application of surface complexation/precipitation modeling to contaminant leaching from weathered municipal solid waste incinerator bottom ash. Environmental Science & Technology 32, 688–693.

Meima, J.A., Comans, R.N.J., 1999. The leaching of trace elements from municipal solid waste incinerator bottom ash at different stages of weathering. Applied Geochemistry 14, 159–171.

Meima, J.A., van Zomeren, A., Comans, R.N.J., 1999. Complexation of Cu with dissolved organic carbon in municipal solid waste incinerator bottom ash leachates. Environmental Science & Technology 33, 1424–1429.

Morone, M., Costa, G., Polettini, A., Pomi, R., Baciocchi, R., 2014. Valorization of steel slag by a combined carbonation and granulation treatment: Accelerated Carbonation for Environmental and Materials Engineering. Minerals Engineering 59, 82–90.

Mostbauer, P., Lenz, S., Lechner, P., 2008. Mswi bottom ash for upgrading of biogas and landfill gas. Environmental Technology 29, 757–764.

Mostbauer, P., Lombardi, L., Olivieri, T., Lenz, S., 2014. Pilot scale evaluation of the BABIU process – Upgrading of landfill gas or biogas with the use of MSWI bottom ash. Waste Management 34, 125–133.

Nam, S.-Y., Seo, J., Thriveni, T., Ahn, J.-W., 2012. Accelerated carbonation of municipal solid waste incineration bottom ash for CO_2 sequestration. Geosystem Engineering 15, 305–311.

Nørgaard, K.P., Hyks, J., Mulvad, J.K., Frederiksen, J.O., Hjelmar, O., 2019. Optimizing large-scale ageing of municipal solid waste incinerator bottom ash prior to the advanced metal recovery: Phase I: Monitoring of temperature, moisture content, and CO_2 level. Waste Management 85, 95–105.

Oehmig, W.N., Roessler, J.G., Zhang, J., Townsend, T.G., 2015. Effect of ferrous metal presence on lead leaching in municipal waste incineration bottom ashes. Journal of Hazardous Materials 283, 500–506.

Ottino, J.M., Lueptow, R.M., 2008. Materials Science: On mixing and demixing. Science 319, 912–913.

Palitzsch, S., Marzi, T., Beckmann, R., Kümmel, R., Dohmann, J., 1999. Künstliche Alterung – ein wirtschaftlicher Weg zur Verringerung der Schwermetallfreisetzung aus Müllverbrennungsaschen. Müll und Abfall 3, 129–136.

Pan, S.-Y., 2012. CO_2 capture by accelerated carbonation of alkaline wastes: A review on its principles and applications. Aerosol and Air Quality Research.

Pfrang-Stotz, G., Schneider, J., 1995. Comparative studies of waste incineration bottom ashes from various grate and firing systems, conducted with respect to mineralogical and geochemical methods of examination. Waste Management & Research 13, 273–292.

Piantone, P., Bodénan, F., Chatelet-Snidaro, L., 2004. Mineralogical study of secondary mineral phases from weathered MSWI bottom ash: implications for the modelling and trapping of heavy metals. Applied Geochemistry 19, 1891–1904.

Pichtel, J., 2014. Waste Management Practices: Municipal, Hazardous, and Industrial, Second Edition. Taylor & Francis.

Polettini, A., Pomi, R., 2004. The leaching behavior of incinerator bottom ash as affected by accelerated ageing. Journal of Hazardous Materials 113, 209–215.

Quicker, P., 2017. Verbrennungsrückstände, in: Kurth, P., Oexle, A., Faulstich, M. (Eds.), Praxishandbuch der Kreislauf- und Rohstoffwirtschaft. Springer Fachmedien Wiesbaden, pp. 661–689.

Rendek, E., Ducom, G., Germain, P., 2006. Carbon dioxide sequestration in municipal solid waste incinerator (MSWI) bottom ash. Journal of Hazardous Materials 128, 73–79.

Rendek, E., Ducom, G., Germain, P., 2007. Influence of waste input and combustion technology on MSWI bottom ash quality. Waste management 27, 1403–1407.

Rettenberger, G., 2017. Deponien, in: Kurth, P., Oexle, A., Faulstich, M. (Eds.), Praxishandbuch der Kreislauf- und Rohstoffwirtschaft. Springer Fachmedien Wiesbaden, pp. 709–731.

Rocca, S., van Zomeren, A., Costa, G., Dijkstra, J.J., Comans, R.N.J., Lombardi, F., 2012. Characterisation of major component leaching and buffering capacity of RDF incineration and gasification bottom ash in relation to reuse or disposal scenarios. Waste Management 32, 759–768.

Rodrigues, R.F., Leite, S.R., Santos, D.A., Barrozo, M.A.S., 2017. Drum granulation of single super phosphate fertilizer: Effect of process variables and optimization. Powder Technology 321, 251–258.

Ruiz-Agudo, E., Kudłacz, K., Putnis, C.V., Putnis, A., Rodriguez-Navarro, C., 2013. Dissolution and carbonation of Portlandite [Ca(OH)2] single crystals. Environmental Science & Technology 47, 11342–11349.

Sabbas, T., Polettini, A., Pomi, R., Astrup, T., Hjelmar, O., Mostbauer, P., Cappai, G., Magel, G., Salhofer, S., Speiser, C., Heuss-Assbichler, S., Klein, R., Lechner, P., 2003. Management of municipal solid waste incineration residues. Waste Management 23, 61–88.

Saffarzadeh, A., Shimaoka, T., Wei, Y., Gardner, K.H., Musselman, C.N., 2011. Impacts of natural weathering on the transformation/neoformation processes in landfilled MSWI bottom ash: A geoenvironmental perspective. Waste Management 31, 2440–2454.

Sakita, S., Nishimura, K., 2015. Physical containment of municipal solid waste incineration bottom ash by accelerated carbonation. Journal of Material Cycles and Waste Management 18, 1–8.

Salminen, J., Prausnitz, J., 2007. Carbon dioxide in chemical processes, in: Letcher, T.M. (Ed.), Development and Applications in Solubility. RSC Pub, pp. 327–345.

Santos, R.M., Mertens, G., Salman, M., Cizer, Ö., van Gerven, T., 2013. Comparative study of ageing, heat treatment and accelerated carbonation for stabilization of municipal solid waste incineration bottom ash in view of reducing regulated heavy metal/metalloid leaching. Journal of Environmental Management 128, 807–821.

Saqib, N., Bäckström, M., 2015. Distribution and leaching characteristics of trace elements in ashes as a function of different waste fuels and incineration technologies. Journal of Environmental Sciences 36, 9–21.

Schreurs, J.P.G.M., van der Sloot, H.A., Hendriks, C., 2000. Verification of laboratory–field leaching behavior of coal fly ash and MSWI bottom ash as a road base material. Waste Management 20, 193–201.

Seifert, H., Vehlow, J., 2017. Thermische Verfahren, in: Kranert, M. (Ed.), Einführung in die Kreislaufwirtschaft. Planung - Recht - Verfahren, 5th ed. Springer Vieweg, Wiesbaden, pp. 423–470.

Sherritt, R.G., Chaouki, J., Mehrotra, A.K., Behie, L.A., 2003. Axial dispersion in the three-dimensional mixing of particles in a rotating drum reactor. Chemical Engineering Science 58, 401–415.

Shi, D., Wang, P., Xu, X., Gu, L., Li, L., Ma, H., Hu, C., 2018. Effect of source-classified collection of municipal solid waste on heavy metals and pozzolanic properties of incineration residues. International Journal of Environmental Research 12, 661–670.

Song, G.-J., Kim, K.-H., Seo, Y.-C., Kim, S.-C., 2004. Characteristics of ashes from different locations at the MSW incinerator equipped with various air pollution control devices. Waste Management 24, 99–106.

Sormunen, L.A., Kaartinen, T., Rantsi, R., 2018. MSWI BA treated with Advanced Dry Recovery: A field scale study on materials’ leaching properties. International Journal of Sustainable Engineering 34, 1–11.

Specht, E., Becker, F.H., 2014. Thermischer Apparatebau und Industrieöfen: K2 Drehrohröfen, in: Grote, K.-H., Feldhusen, J. (Eds.), Dubbel. Taschenbuch für den Maschinenbau, 24th ed. Springer Berlin, pp. 690–699.

Speiser, C., Baumann, T., Niessner, R., 2000. Morphological and chemical characterization of calcium-hydrate phases formed in alteration processes of deposited municipal solid waste incinerator bottom ash. Environmental Science & Technology 34, 5030–5037.

Speiser, C., Baumann, T., Niessner, R., 2001. Characterization of municipal solid waste incineration (MSWI) bottom ash by scanning electron microscopy and quantitative energy dispersive X-ray microanalysis (SEM/EDX). Fresenius' journal of analytical chemistry 370, 752–759.

Stegemann, J.A., Schneider, J., 1991. Leaching Potential of Municipal Haste Incinerator Bottom ASH as a Function of Particle Size Distribution, in: Goumans, J.J.J.M., van der Sloot, H.A., Aalbers, T.G. (Eds.), Waste materials in construction. Proceedings of the International Conference on Environmental Implications of Construction with Waste Materials, Maastricht, the Netherlands, 10-14 November 1991, vol. 48. Elsevier; New York, USA, pp. 135–143.

Stuart, D.M., Mitchell, D.A., Johns, M.R., Litster, J.D., 1999. Solid-state fermentation in rotating drum bioreactors: operating variables affect performance through their effects on transport phenomena. Biotechnology and Bioengineering 63, 383–391.

Sullivan, J.D., Maier, C.G., Ralston, O.C., 1927. Passage of solid particles through rotary cylindrical kilns. Technical Paper 384, 1-42.

Sun, J., Bertos, M.F., Simons, S.J.R., 2008. Kinetic study of accelerated carbonation of municipal solid waste incinerator air pollution control residues for sequestration of flue gas CO_2. Energy & Environmental Science 1, 370–377.

Tang, P., Florea, M.V.A., Spiesz, P., Brouwers, H.J.H., 2015. Characteristics and application potential of municipal solid waste incineration (MSWI) bottom ashes from two waste-to-energy plants. Construction and Building Materials 83, 77–94.

Todorovic, J., Ecke, H., 2006. Demobilisation of critical contaminants in four typical waste-to-energy ashes by carbonation. Waste Management 26, 430–441.

Um, N., Nam, S.-Y., Ahn, J.-W., 2013. Effect of accelerated carbonation on the leaching behavior of Cr in municipal solid waste incinerator bottom ash and the carbonation kinetics. Materials Transactions 54, 1510–1516.

van Gerven, T., Moors, J., Dutré, V., Vandecasteele, C., 2004. Effect of CO_2 on leaching from a cement-stabilized MSWI fly ash. Cement and Concrete Research 34, 1103–1109.

van Gerven, T., van Keer, E., Arickx, S., Jaspers, M., Wauters, G., Vandecasteele, C., 2005. Carbonation of MSWI-bottom ash to decrease heavy metal leaching, in view of recycling. Waste Management 25, 291–300.

Vehlow, J., Seifert, H., December/2012. Report for IEA Bioenergy Task36 Topic 5 Management of Residues from Energy Recovery by Thermal Waste -to-Energy Systems and Quality Standards, Karlsruhe.

Verbinnen, B., Billen, P., van Caneghem, J., Vandecasteele, C., 2016. Recycling of MSWI bottom ash: A review of chemical barriers, engineering applications and treatment technologies. Waste and Biomass Valorization 4, 695–709.

Wang, F.Y., Cameron, I.T., 2002. Review and future directions in the modelling and control of continuous drum granulation. Powder Technology 124, 238–253.

Wei, Y., Saffarzadeh, A., Shimaoka, T., Zhao, C., Peng, X., Gao, J., 2014. Geoenvironmental weathering/deterioration of landfilled MSWI-BA glass. Journal of hazardous materials 278, 610–619.

Wei, Y., Shimaoka, T., Saffarzadeh, A., Takahashi, F., 2011. Mineralogical characterization of municipal solid waste incineration bottom ash with an emphasis on heavy metal-bearing phases. Journal of Hazardous Materials 187, 534–543.

Wiles, C.C., 1996. Municipal solid waste combustion ash: State-of-the-knowledge: Municipal waste incineration. Journal of Hazardous Materials 47, 325–344.

Williams, P.T., 2013. Waste treatment and disposal. John Wiley & Sons, Hoboken (USA).

Xuan, D., Tang, P., Poon, C.S., 2018. Limitations and quality upgrading techniques for utilization of MSW incineration bottom ash in engineering applications – A review. Construction and Building Materials 190, 1091–1102.

Yang, S., Saffarzadeh, A., Shimaoka, T., Kawano, T., 2014. Existence of Cl in municipal solid waste incineration bottom ash and dechlorination effect of thermal treatment. Journal of Hazardous Materials 267, 214–220.

Yin, K., Chan, W.P., Dou, X., Ren, F., Chang, V.W.-C., 2017. Measurements, factor analysis and modeling of element leaching from incineration bottom ashes for quantitative component effects. Journal of Cleaner Production 165, 477–490.

You, G.-S., Ahn, J.-W., Han, G.-C., Cho, H.-C., 2006. Neutralizing capacity of bottom ash from municipal solid waste incineration of different particle size: Korean Journal of Chemical Engineering 23, 237–240.

Zacho, K.O., Mosgaard, M., Riisgaard, H., 2018. Capturing uncaptured values — A Danish case study on municipal preparation for reuse and recycling of waste. Resources, Conservation and Recycling 136, 297–305.

Zevenbergen, C., Comans, R.N.J., 1994. Geochemical factors controlling the mobilization of major elements during weathering of MSWI bottom ash, in: J.J.J.M. Goumans, H.A. van der Sloot and Th.G. Aalbers (Ed.), Studies in Environmental Science : Environmental Aspects of Construction with Waste Materials Proceeding of the International Conference on Environmental Implications of Construction Materials and Technology Developments, Volume 60. Elsevier, pp. 179–194.

Zevenbergen, C., van Reeuwijk, L.P., Bradley, J.P., Bloemen, P., Comans, R.N.J., 1996. Mechanism and conditions of clay formation during natural weathering of MSWI bottom ash. Clays and Clay Minerals 44, 546.

Zhang, H., He, P.-J., Shao, L.-M., Li, X.-J., 2008. Leaching behavior of heavy metals from municipal solid waste incineration bottom ash and its geochemical modeling. Journal of Material Cycles and Waste Management 10, 7–13.

Zhang, Q., Wang, Z., Wen, S., Liu, G., Wu, X., Cong, W., 2012. Gas-liquid mass transfer characteristics in a rotating-drum bioreactor. Chemical Engineering & Technology 35, 1842–1848.

Zingaretti, D., Costa, G., Baciocchi, R., 2013. Assessment of the energy requirements for CO_2 storage by carbonation of industrial residues. Part 1: Definition of the process layout. Energy Procedia 37, 5850–5857.

Zingaretti, D., Costa, G., Baciocchi, R., 2014. Assessment of accelerated carbonation processes for CO_2 storage using alkaline industrial residues. Industrial & Engineering Chemistry Research 53, 9311–9324.

Zwahr, H., 2005. MV-Schlacke – mehr als nur ein ungeliebter Baustoff? Müll und Abfall 3, 114–122.

Eigenbeteiligung an den Veröffentlichungen

1. **Brück F**., Fröhlich C., Mansfeldt T., Weigand H., 2018. A fast and simple method to monitor carbonation of MSWI bottom ash under static and dynamic conditions. Waste Management, 78: 588–594.
   DOI:10.1016/j.wasman.2018.06.042
   Erhebung der Daten im Labor: 95%
   Auswertung und Interpretation: 95%
   Verfassen der Publikation: 90%

2. **Brück F**., Schnabel K., Mansfeldt T., Weigand H., 2018. Accelerated carbonation of waste incinerator bottom ash in a rotating drum batch reactor. Journal of Environmental Chemical Engineering, 6: 5259-5268.
   DOI: 10.1016/j.jece.2018.08.024
   Erhebung der Daten im Labor: 90%
   Auswertung und Interpretation: 90%
   Verfassen der Publikation: 85%

3. **Brück F**., Mansfeldt T., Weigand H., 2019. Flow-through carbonation of waste incinerator bottom ash in a rotating drum batch reactor: role of specific CO_2 supply, mixing tools and fill level. Journal of Environmental Chemical Engineering, 7: 102975
   DOI: 10.1016/j.jece.2019.102975
   Erhebung der Daten im Labor: 70%
   Auswertung und Interpretation: 90%
   Verfassen der Publikation: 95%

4. **Brück F**., Ufer K., Mansfeldt T., Weigand H., Continuous-feed carbonation of waste incinerator bottom ash in a rotating drum reactor, Waste Management, 99: 135−145.
   Erhebung der Daten im Labor: 75 %
   Auswertung und Interpretation: 95%
   Verfassen der Publikation: 90%

Giessen, Mai 2019 Felix Benjamin Brück

Erklärung

Ich versichere, dass ich die von mir vorgelegte Dissertation selbständig angefertigt, die benutzten Quellen und Hilfsmittel vollständig angegeben und die Stellen der Arbeit − einschließlich Tabellen, Karten und Abbildungen −, die anderen Werken im Wortlaut oder dem Sinn nach entnommen sind, in jedem Einzelfall als Entlehnung kenntlich gemacht habe; dass diese Dissertation noch keiner anderen Fakultät oder Universität zur Prüfung vorgelegen hat; dass sie −abgesehen von unten angegebenen Teilpublikationen −noch nicht veröffentlicht worden ist, sowie, dass ich eine solche Veröffentlichung vor Abschluss des Promotionsverfahrens nicht vornehmen werde. Die Bestimmungen der Promotionsordnung sind mir bekannt. Die von mir vorgelegte Dissertation ist von Prof. Dr. Tim Mansfeldt betreut worden.

[1] Brück F., Fröhlich C., Mansfeldt T., Weigand H., 2018. A fast and simple method to monitor carbonation of MSWI bottom ash under static and dynamic conditions. Waste Management, 78: 588–594.

[2] Brück F., Schnabel K., Mansfeldt T., Weigand H., 2018. Accelerated carbonation of waste incinerator bottom ash in a rotating drum batch reactor. Journal of Environmental Chemical Engineering, 6: 5259-5268.

[3] Brück F., Mansfeldt T., Weigand H., 2019. Flow-through carbonation of waste incinerator bottom ash in a rotating drum batch reactor: role of specific CO_2 supply, mixing tools and fill level. Journal of Environmental Chemical Engineering, 7: 102975

[4] Brück F., Ufer K., Mansfeldt T., Weigand H., Continuous-feed carbonation of waste incinerator bottom ash in a rotating drum reactor. Waste Management, 99: 135−145.

Giessen, Mai 2019 Felix Benjamin Brück